DOCTOR OF PHILOSOPHY

Analysis of the diverse antibacterial strategies used by Serratia marcescens Db10

Gerc, Amy

Award date:
2014

Analysis of the diverse antibacterial strategies used by *Serratia marcescens* Db10

Amy J. Gerc

Division of Molecular Microbiology

College of Life Sciences

University of Dundee

2014

A thesis submitted in partial fulfilment of the requirements for the degree of Doctor of Philosophy

Table of contents

List of figures

List of tables

List of abbreviations

ABC transporter	ATP-binding cassette transporters
ACP domain	acyl carrier protein domain
A domain	adenylation domain
Amp	ampicillin
APS	ammonium persulphate
AT domain	acyltransferase domain
ATP	adenosine triphosphate
bp	base pair(s)
cDNA	complementary DNA
C domain	condensation domain
Cml	chloramphenicol
Co-A	co-enzyme A
C-terminal	carboxy terminal
Da	Dalton
DH domain	dehyrdatase domain
DIC	differential interference contrast
DMSO	dimethyl sulphoxide
DNA	deoxyribonucleic acid
DNase	deoxyribonuclease
dNTP	deoxynucleoside triphosphate
DTT	dithiothreitol
EDTA	ethylenediamine tetraacetate
ER domain	enoylreductase
FITC	fluorescein isothiocyanate
g	gram
Gfp	green fluorescent protein
HPLC	high performance liquid chromatogrpahy
HRP	horse radish peroxidase

IM	inner membrane
IPTG	isopropyl β-D-1-thiogalactopyranoside
Kan	kanamycin
kb	kilobase pairs (1000 bp)
KS domain	ketosynthase domain
KR domain	ketoreductase domain
l	litre
LB	Luria and Bertani (medium)
LC-MS	liquid chromatography-mass spectrometry
μ	micro
M	molar
m	milli
min	minute
mRNA	messenger RNA
MM	minimal medium
m/z	mass to charge
NMR	nuclear magnetic resonance
NRPS	non-ribsosomal peptide synthetase
N-terminal	amino terminal
OD	optical density
OM	outer membrane
ORF	open reading frame
PAGE	polyacrylamide gel electrophoresis
PCP domain	peptidyl carrier protein domain
PCR	polymerase chain reaction
PBS	phosphate buffered saline
PKS	polyketide synthase
P-pant	4’-phosphopantetheine
PPTase	phosphopantetheinyl transferase
RNA	ribonucleic acid

rpm	rotations per minute
rRNA	ribosomal RNA
RT-PCR	reverse transcriptase PCR
SDS	sodium dodecyl sulphate
Sec	secretory
Strep	streptomycin
TAE	Tris-acetate EDTA
Tat	twin arginine translocase
Tdt	terminal deoxynucleotidyl transferase
Te domain	thioesterase domain
Tet	tetracycline
TEMED	N,N,N′,N′-tetramethylethylenediamine
TRITC	tetramethylrhodamine
TSA	tryptic soya agar
TSB	tryptic soya broth
TRIS	tris(hydroxymethyl) aminomethane
UHPLC	ultra high performance liquid chromatogrpahy
UV	ultra-violet
V	volts
v/v	volume per volume
w/v	weight per volume

Acknowledgments

First and foremost, I want to say a massive thank you to both of my supervisors, Nicola and Sarah, for being so amazing. You have both supported me so much from start to finish and I can't imagine having completed my PhD with anyone else. Your help and guidance throughout my PhD (in science and life in general!) has been so much appreciated.

I want to say a massive thanks to my Mum, Dad and Susan for supporting me, and putting up with me, for the past 4 years. You've done so much for me and I wouldn't be where I am without your help.

I'm sure I've asked almost everyone in the lab a question at some point during the past 4 years, so thank you MMB. Special thanks to past and current members of the SJC and NSW labs, particularly Victoria for help with microscopy. I'd also like to thank Lijiang and Greg at the University of Warwick, who were great collaborators and who taught me a lot during my visit to their lab. I've been so lucky to have met so many lovely people! I think Lynne deserves a special mention for managing to share an office with me for so long. I will miss the giggles (although not so much the occasional singing…)!

Finally, thank you Markus for always managing to be there for me, despite living in a different country. You've been everything I've needed and more.

Declaration

I declare that I am the author of the thesis; that, unless otherwise stated, all references cited have been consulted; that the work of which the thesis is a record has been performed by me, and that it has not been previously accepted for a higher degree: where the thesis is based upon joint research, the nature and extent of my individual contribution is defined.

Amy Gerc

July 2014

Abstract

The Gram-negative bacterium, *Serratia marcescens*, is an important opportunistic human pathogen capable of causing serious infections, particularly in immunocompromised patients. *S. marcescens* Db10 is an insect pathogen that is closely related to *S. marcescens* strains which cause disease in humans. The genome sequence of *S. marcescens* Db10 is available and tools exist which allow the genetic manipulation of this bacterium, making it an ideal model organism. In this work, contact dependent and independent antibacterial strategies employed by *S. marcescens* Db10 are investigated at the molecular level.

Non-ribosomal peptide synthetases (NRPS) and polyketide synthases (PKS) are widespread in bacteria and fungi and are responsible for the biosynthesis of many metabolites with medically relevant properties, including antibiotics. The activity of NRPS and PKS enzymes is dependent on their modification by a phosphopantetheinyl transferase (PPTase) enzyme. In this work we identify the biosynthetic genes, *alb2-6*, which are required for the production of the NRPS-PKS antibiotic, althiomycin, in *S. marcescens* Db10. The role of the Major Facilitator Superfamily protein, Alb1, in the export of and resistance to althiomycin is also defined. Using a combination of bioinformatic, biochemical and genetic approaches we demonstrate that a PPTase enzyme, PswP, is essential for althiomycin production. We further show that PswP is required for the biosynthesis of the surfactant, serrawettin W2, and an enterobactin-like siderophore. These PswP dependent metabolites are all shown to possess antimicrobial activity against the Gram-positive bacterium, *Staphylococcus aureus*.

The Type VI Secretion System (T6SS) is the most recently identified Gram-negative bacterial secretion system and has been demonstrated to play important roles in mediating contact dependent interactions with neighbouring bacterial and eukaryotic cells. *S. marcescens* Db10 is known to encode an anti-bacterial T6SS. In this study, *S. marcescens* Db10 strains are constructed which harbour fusions of T6SS components to fluorescent proteins. The functionality of these fusion proteins and their localisation profiles are analysed by fluorescence microscopy. We demonstrate that different sub-complexes of the T6SS show distinct patterns of localisation. We additionally show that the T6SS assembles within many cells within a population of *S. marcescens* Db10 and that assembly is not dependent on the presence of neighbouring cells. Strains constructed in this study will comprise a toolbox for further investigations into the mechanisms of assembly and dynamics of the T6SS.

Chapter 1

Introduction

1.1 *Serratia marcescens*

The genus *Serratia* belongs to the Enterobacteriaceae family and comprises 14 different species and two subspecies. This Gram-negative bacterium is found ubiquitously in the environment and has been isolated from insects, plants, water, animals, nematodes and soil (Mahlen, 2011). The earliest reports of the existence of *Serratia* date back to 1819, when a pigmented species of *Serratia* was isolated from polenta in Italy. Initially believed to be a fungus, the red micro-organism was named *Serratia marcescens* (Bizio, 1823). Several species of *Serratia* are pigmented due to the production of the red metabolite, prodigiosin (Williams, 1973). This attribute, as well as the belief that *Serratia* species were non-pathogenic, led to the widespread use of *Serratia* as a tracer organism to study the transmission and spread of bacteria in the environment, during the latter half of the 20th century (Mahlen, 2011). However, certain species of *Serratia*, notably *S. marcescens*, are now recognised as important opportunistic human pathogens and many reports exist which implicate this bacterium in disease, especially in neonates and immunocompromised patients (Haddy *et al.*, 1996; Hejazi & Falkiner, 1997; Mahlen, 2011; Manfredi *et al.*, 2000; Voelz *et al.*, 2010). *S. marcescens* infections are not limited to these groups of patients and reports exist which implicate *Serratia* in almost every type of infection, including: urinary tract infections (Su *et al.*, 2003), blood stream infections (Blossom *et al.*, 2009), surgical site infections (Chiang *et al.*, 2013), conjunctivitis (Dias *et al.*, 2013) and endocarditis (Korner *et al.*, 1994). The treatment of *S. marcescens* infections is complicated by the fact that many isolates are resistant to a range of antibiotics. Resistance to antibiotics was first described thoroughly in the early 1980s and, whilst recognised as a potential issue, it was noted that *S. marcescens* remained sensitive to aminoglycosides and cephalosporins (Sleigh, 1983). More recently, reports of resistance to these antibiotics have also been described (Coria-Jimenez & Ortiz-Torres, 1994; Hejazi & Falkiner,

1997). *S. marcescens* is therefore an important nosocomial pathogen and, since this species is by far the most frequent species of *Serratia* isolated from affected patients, it is the most well studied member of the genus.

S. marcescens isolate Db10, used in this work, is an insect pathogen and a non-pigmented strain of *Serratia* which was originally isolated from *Drosophila* flies (Flyg *et al.*, 1980). The genome of *S. marcescens* Db11, which is a streptomycin resistant derivative of the parental Db10 strain, has been sequenced (Sanger Institute, United Kingdom). This isolate of *S. marcescens* is also genetically tractable, with tools and methods to manipulate its genome being available, making it an ideal model organism for molecular investigation.

1.2 Competitive inter-bacterial interactions

Bacteria must constantly sense and respond to their environment in order to survive. In most instances, the environment in which a bacterium lives will harbour many bacteria, often of multiple species. Within a confined environment, different species of bacteria may interact directly, for example, through the use of contact dependent secretion systems (Fronzes *et al.*, 2009), or they may influence neighbouring bacteria indirectly by altering the immediate environment, for example, through the release of antibiotics (Alanis, 2005). Interactions between competing bacteria may be co-operative or competitive. Co-operative interactions include examples such as quorum sensing (where bacteria are able to produce and sense extracellular chemicals in order to monitor population density (Ng & Bassler, 2009)) and biofilm formation (whereby a community of cells adhere to a surface or interface and encase themselves in a self-produced extracellular matrix (Flemming & Wingender, 2010)). In this work, two examples of competitive inter-bacterial interactions mediated by *S. marcescens* Db10

were investigated, namely antibiotic production and Type VI secretion system-dependent bacterial killing.

1.2.1 Antibiotics

1.2.1.1 Biological role of antibiotics

Antibiotics are defined as chemicals that are capable of killing or inhibiting the growth of micro-organisms. Antibiotics are produced by a wide variety of bacteria, particularly soil dwelling micro-organisms. At high concentrations, antibiotics kill or inhibit growth of bacteria by a variety of mechanisms which include inhibition of cell wall synthesis, inhibition of protein synthesis, inhibition of DNA or RNA synthesis and disruption of the cell membrane (Figure 1.1) (Alanis, 2005).

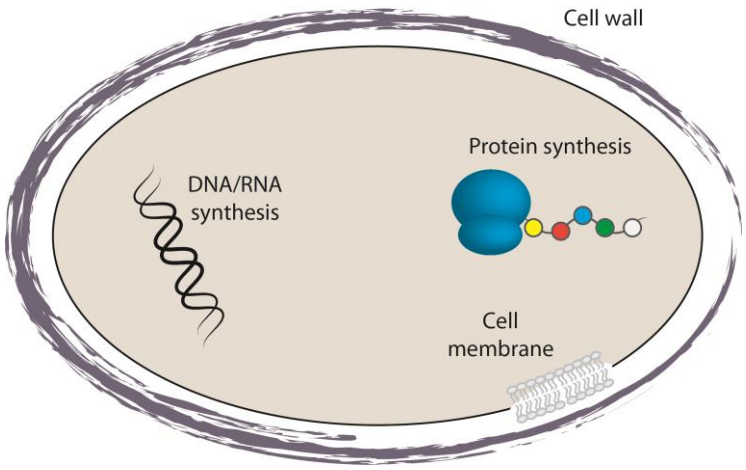

Figure 1.1. Potential targets of antibiotics in the bacterial cell. Antibiotics may target cell wall biosynthesis (e.g. β-lactams), protein synthesis (e.g. tetracyclines), DNA synthesis (e.g. fluoroquinolones), RNA synthesis (e.g. rifampin) or the cell membrane (e.g. polymyxins)

The advantages of such drugs have certainly been exploited in the medical profession, so much so that resistance to antibiotics is now a pressing issue, as discussed further below. In a polymicrobial environment, antibiotic producing organisms have better access to physical space and nutrients by eliminating neighbouring competing bacteria. In this case, the advantages of antibiotic biosynthesis to the producing organism seem

apparent and this type of bacterial interaction would be detrimental to the susceptible bacterium. However, it has also been suggested that, in the natural environment, antibiotics may never reach concentrations high enough to inhibit growth of surrounding bacteria and that antibiotics rather serve as signalling molecules (Davies, 2006; Fajardo & Martinez, 2008; Yap, 2013). Demonstrably, transcriptomic responses to the presence of antibiotics at a low concentration have been shown to be extensive with around 5% of the genome of *Salmonella typhimurium* and *Escherichia coli* responding to the antibiotics rifampicin and erythromycin (Goh *et al.*, 2002). Also in support of this theory, bacteria appear to respond differently to closely related antibiotics that have a similar mode of action (Goh *et al.*, 2002). In this instance, antibiotics mediate a very different type of bacterial interaction.

1.2.1.2 Therapeutic role of antibiotics and the need for discovery of novel agents

As described in section 1.2.1.1, the antibacterial properties of antibiotics have been harnessed by the medical profession for the treatment of bacterial infections, so much so that it is estimated that well over one million tonnes of antibiotics have been produced since their discovery in the 1940s (Andersson & Hughes, 2010). Antibiotics remain essential medicines for the treatment of infectious disease, which remains the second leading cause of death worldwide (WHO, 2011). Not only are antibiotics used for the treatment of disease in humans, they are also used extensively in agriculture and aquaculture to increase growth rates of livestock. It is estimated that 80% of antibiotics consumed in the United States are used in agriculture (Hollis & Ahmed, 2013). These vast quantities of drugs constitute an enormous selection pressure for the evolution of resistant organisms. Infection with antibiotic resistant organisms is becoming more and more prevalent and these infections are becoming increasingly difficult to treat. For

example, seven countries have now reported cases of treatment failure with third generation cephalosporins against *Neisseria gonorrhoeae,* which is the causative agent of gonorrhoea (WHO, 2014). Antibiotic resistance is recognised as a serious threat to human health, and infections caused by antibiotic resistant bacteria have twice the mortality rate of those caused by the same non-resistant bacteria (WHO, 2014). Although there has been an increase in the number of infections caused by multidrug resistant pathogens, the number of new antibiotics coming into use follows an inverse trend and has dramatically declined over the past 20 years, with the most recent distinct class of antimicrobial being discovered in 1987 (Figure 1.2) (Silver, 2011). The decrease in the discovery of novel agents is partly due to the huge cost and the large amount of time associated with development; it has been estimated to cost $800 million and take 8-15 years to develop such a drug (Gwynn *et al.*, 2010). Further, once a drug has been developed, the nature of the treatment course with antimicrobials means that antibiotics should eliminate the need for their own use. Antibiotics are therefore usually used over a short time period, by comparison with drugs which are taken for long term illnesses. These factors do not make antibiotics the most attractive drugs to develop. However, it should not be assumed that the lack of development of novel drugs is entirely due to a lack of research by pharmaceutical companies. The screening of fermentation products to identify novel agents, which proved so fruitful in the early days of antibiotic discovery, is no longer a viable means of discovery due to saturation (Silver, 2011). The difficulties associated with the development of novel antibiotics are recognised, yet the pressing need for the discovery of novel antibiotics remains. Our understanding of antibiotic biosynthesis pathways in bacteria is essential if we are to harness the potential application of these biosynthetic pathways in the synthetic production of novel drugs.

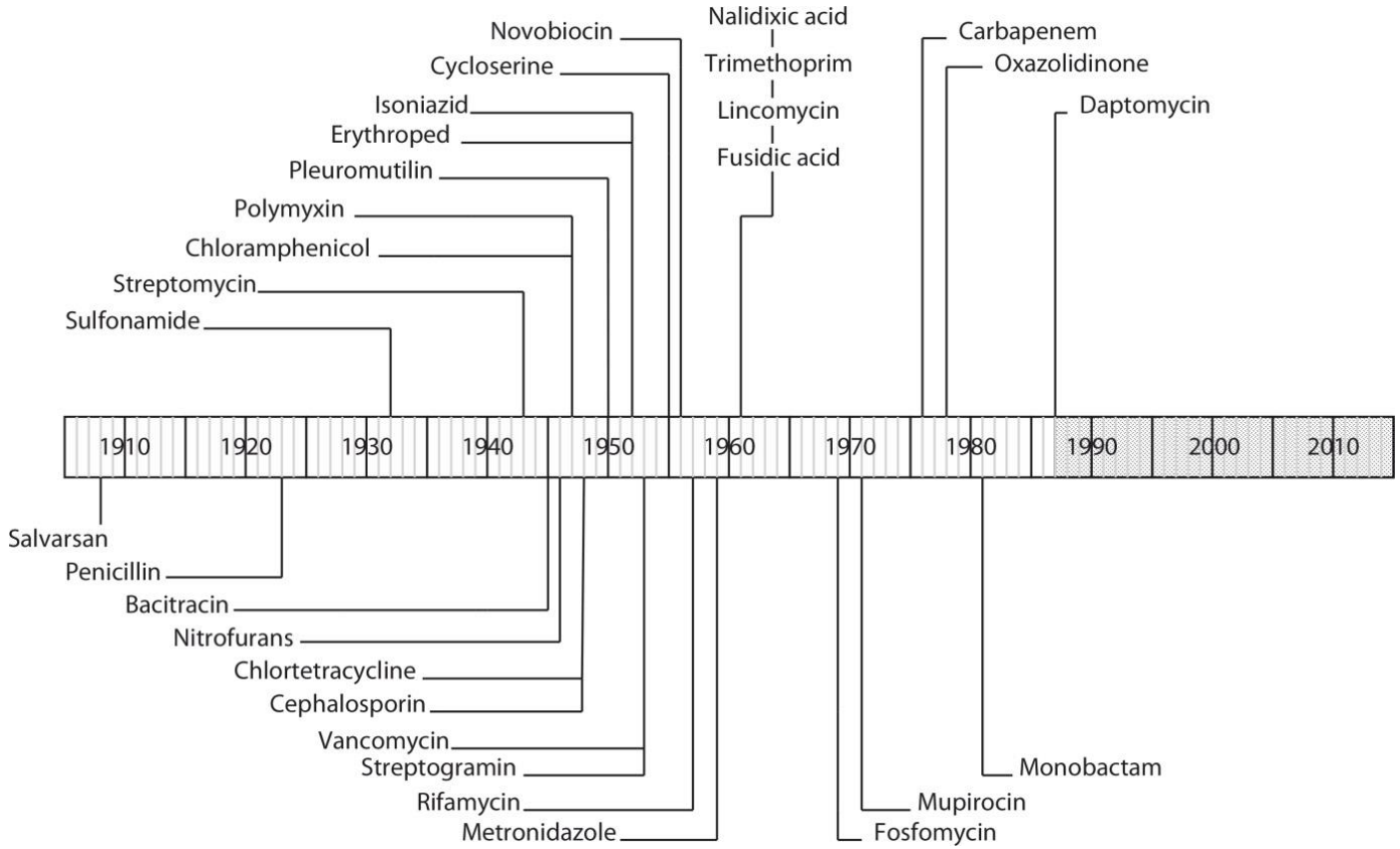

Figure 1.2. Timeline illustrating the discovery of novel classes of antibiotics. The shaded area represents the most recent time period, during which no new classes of anti-bacterials have been discovered. Adapted from (Silver, 2011).

1.2.2 Interactions mediated by bacterial secretion systems

Not only are Gram-negative bacteria capable of interacting with surrounding bacteria by the production of antibiotics, they can also mediate interactions with neighbouring bacteria (as well as eukaryotic cells or their abiotic environment) via the assembly of secretion systems. These protein secretion machines transport proteins from the cytoplasm of the producing cell to the extracellular environment, where the proteins may remain associated with the outside of the bacterial cell, released into the extracellular milieu or be directly transported into a target cell (Chagnot *et al.*, 2013; Fronzes *et al.*, 2009). Protein secretion machines therefore may alter the extracellular environment or they may alter the intracellular environment of a target cell. To date, six different bacterial secretion systems have been described in Gram-negative bacteria, namely the Type I to Type VI Secretion Systems. The Gram-negative cell envelope consists of the inner membrane (IM), the periplasm (which contains a layer of peptidoglycan) and the outer membrane (OM). The nature of the Gram-negative cell envelope therefore allows secretion to occur as a one-step or a two-step event (Figure 1.3).

1.2.2.1 One-step secretion systems

In one-step secretion systems (Type I, III, IV and VI), substrates are transported directly from the bacterial cytoplasm into the extracellular environment and are never free in the periplasm. The Type I Secretion System (T1SS) transports proteins that vary greatly in size and function, although many play an essential role in pathogenesis or in nutrient degradation and acquisition. The machinery itself is relatively simple and consists of three membrane proteins: an ABC transporter to transport substrates across

the inner membrane, a membrane fusion protein which spans the periplasm and an OM factor which shapes a pore in the OM (Figure 1.3) (Kanonenberg *et al.*, 2013).

Type III Secretion Systems (T3SSs) comprise more than 20 different proteins that assemble as three distinct "parts". The basal body spans the IM, periplasm and the OM. Substrates are then thought to be transported through an extracellular needle like structure, which together with the basal body, comprises the "needle complex". The third component of the T3SS is the translocon at the distal end of the needle, which inserts into the membrane of the eukaryotic target cell (Figure 1.3). Many plant and animal pathogens employ the T3SS to inject virulence proteins directly into target cells. Of note, several components of the T3SS show homology at the sequence or structural level to components of the bacterial flagellum (Izore *et al.*, 2011).

Type IV Secretion Systems (T4SSs) are unusual in that they mediate transport of both DNA and proteins. Three subgroups of T4SSs can be distinguished based on function. The first and most widespread sub-group comprises conjugation systems. These systems mediate the transfer of single stranded DNA and one or more proteins from the donor cell directly into a target bacterial or eukaryotic cell through a transenvelope channel (Bhatty *et al.*, 2013). Conjugation represents an important mechanism of horizontal gene transfer and the spread of genes within a population facilitates bacterial adaption to the environment. The second subgroup of T4SSs are the effector translocation systems. These systems deliver proteins into eukaryotic cells and play an important role in virulence in many medically relevant pathogens. Substrate release or uptake systems comprise the third subgroup of T4SSs and in this case the Type IV apparatus functions independently of cell-cell contact. They mediate the export of DNA or the uptake of DNA and proteins (Bhatty *et al.*, 2013). It should be noted that T4SS are not exclusively involved in secretion, and the T4SS can also be involved in

the synthesis of extracellular pili (Trokter *et al.*, 2014). T4SSs are usually composed of 12 proteins that are organised as four "parts", these are: three cytoplasmic ATPases, the inner membrane channel and the periplasmic complex and the extracellular pilus (Figure 1.3) (Fronzes *et al.*, 2009).

The Type VI Secretion System (T6SS) represents the most recently discovered Gram-negative bacterial secretion system. This secretion system comprises a minimum of 13 core components and mediates the transfer of proteins directly into target cells which may be bacterial or eukaryotic (Filloux, 2013). The T6SS is therefore an important mediator of bacterial-bacterial interactions and will be discussed in more detail in section 1.4.

1.2.2.2 Two-step secretion systems

In two-step secretion systems (Type II and V), substrates are firstly targeted to the export systems, Sec or Tat, for transport across the IM. Type II Secretion Systems (T2SSs) are employed by many bacteria for the transport of exoenzymes into the environment, where they are essential for the breakdown of extracellular nutrients. This system is composed of 12-16 proteins which exist in the cytoplasm, inner membrane, periplasm and outer membrane (Figure 1.3) (Nivaskumar & Francetic, 2014).

Type V secretion systems (T5SSs) are relatively simple secretion systems which can be divided into five different sub groups; Va-e. All members of T5SS subgroups traverse the IM via the Sec transport system and are dependent on a β-barrel transporter domain that inserts into the OM for translocation of the passenger domain (Figure 1.3). The passenger domain refers to the domain that is being translocated into the extracellular milieu (Leo *et al.*, 2012). Subgroup Va substrates are termed autotransporters; the information required to traverse the IM and the OM is contained

within a single polypeptide chain and translocation does not require the aid of additional proteins. Subgroup Vb describes two partner secretion whereby a passenger protein interacts with a separate transporter protein via two POTRA (polypeptide transport-associated) domains. Subgroup Vc substrates are trimeric autotransporters, which mediate the export of three passenger domains. Subgroup Vd substrates are also contained within a single polypeptide chain, however, in this case, the passenger domain is fused to a single POTRA domain within the transporter. Finally, subgroup Ve substrates are thought to resemble Va substrates, except that the orientation of the N- and C-terminus of the β-barrel transporter domain is reversed. Substrates of the T5SS function as adhesins, toxins or enzymes (Gawarzewski *et al.*, 2013; Leo *et al.*, 2012). Of particular relevance, Type V secretion systems also include contact dependent growth inhibition (CDI) systems. CDI systems were discovered in *E. coli*, where they were found to include the two partner secretion system, CdiAB (Aoki *et al.*, 2005). CdiB is a β-barrel transporter that mediates the translocation of CdiA across the producing cell envelope and its attachment to the target cell. CdiA then appears to be cleaved, allowing its C-terminal toxin domain to be translocated into the target cell. The C-terminal domain of CdiA likely exerts its toxic effects through perturbation of the proton motive force. These toxic effects are neutralised in cells of the producing organism by the immunity protein, CdiI. Genes encoding Cdi systems have since been discovered in many α-, β- and γ- proteobacteria and the diverse C-termini of different CdiA proteins represent various different toxins, each associated with a specific cognate CdiI protein (Ruhe *et al.*, 2013).

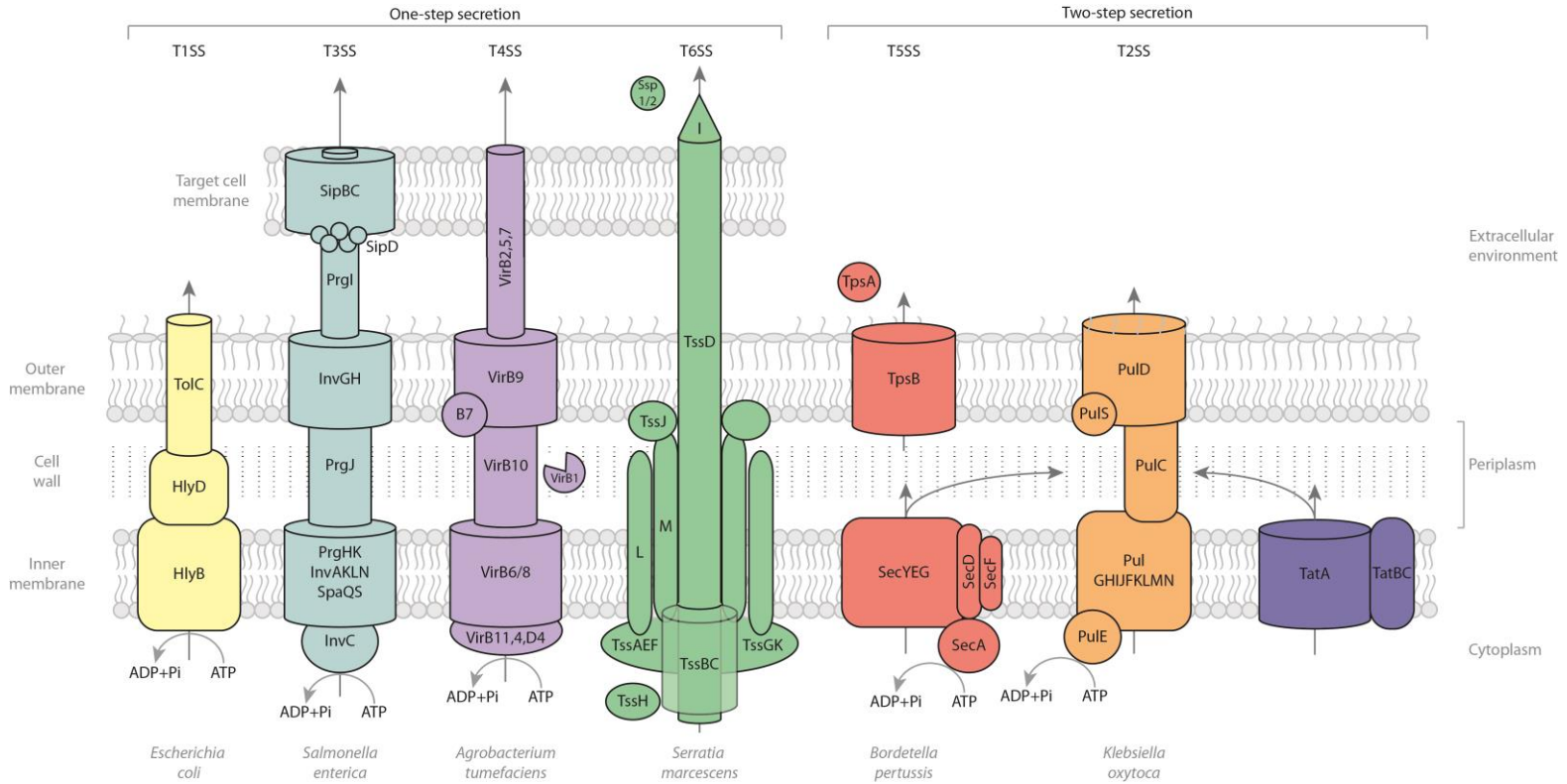

Figure 1.3. Schematic representation of secretion systems in Gram-negative bacteria. Adapted from (Fronzes *et al.*, 2009; Gerlach & Hensel, 2007; Zoued *et al.*, 2014). Secretion systems may be divided into one-step systems or two step systems. In one-step systems, secreted substrates traverse the envelope of the host cell in a single step and intermediates are not released into the periplasm. In T3SS, T4SS and T6SS, substrates are additionally transported across the membrane of a target cell. In two-step systems, substrates are first transported across the inner membrane by the Sec or Tat transport pathways and then subsequently transported across the outer membrane by separate machineries. Components of the secretion systems presented are named as indicated in the organism below the corresponding secretion system. See section 1.2.2 for details of each secretion system.

1.2.3 Other mechanisms of competitive bacterial-bacterial interactions

Antibiotic production and the secretion of substrates via secretion systems represent two mechanisms by which bacteria may affect the behaviour of neighbouring cells. Additional mechanisms of competitive bacterial-bacterial interactions include the synthesis of bacteriocins and cannibalism.

Bacteriocins are ribosomally synthesised peptides of bacterial origin that possess antimicrobial properties. Bacteriocins can be divided into two classes, Class I bacteriocins are post-translationally modified, whereas class II bacteriocins are unmodified (Cotter *et al.*, 2013). Bacteriocins are released into the extracellular environment and interact with specific molecules on the target cell surface that act as receptors (Hammami *et al.*, 2013). Bacteriocins are diverse in terms of their mode of action. Several class I, as well as some class II, bacteriocins target the bacterial cell envelope. This can either be through the formation of pores in the membrane or through binding to lipid II, which is required for the biosynthesis of peptidoglycan. Additional targets of bacteriocins include DNA, RNA and protein synthesis. Bacteriocin producing bacteria must produce immunity proteins in order to protect themselves from the toxic effects of the bacteriocin. These immunity proteins may bind the bacteriocin itself, or they may compete for binding to the target of the bacteriocin (Nishie *et al.*, 2012). It has been suggested that bacteriocin production by invading bacteria may allow these bacteria to become established in a stable microbial community. Alternatively, bacteriocin production may prevent invasion by foreign species of bacteria which are susceptible to the antimicrobial effects of the peptide (Riley & Wertz, 2002).

Cannibalism in bacteria is distinct from the above mechanisms of antibacterial interactions in that bacteria kill genetically identical siblings rather than bacteria of a different strain or species. In *Bacillus subtilis*, cannibalism occurs upon the early stages

of sporulation of a sub-population of cells within a biofilm. In this example, cells sporulate in response to nutrient deprivation. The killing of non-sporulating cells within the population releases nutrients to delay the onset of sporulation, thus ensuring the energetically expensive process of sporulation only proceeds if absolutely necessary (Gonzalez-Pastor *et al.*, 2003). In *Streptococcus pneumoniae*, cannibalism is referred to as fratricide and is induced upon entry into the "competent state". In this instance, competent cells kill non-competent siblings. The reasoning behind the co-incidence of competence and fratricide is not as obvious as in *B. subtilis*, but it has been suggested that the induction of competence is a general stress response and fratricide is therefore also a stress response (Claverys & Havarstein, 2007).

1.3 Non-ribosomal peptide synthetases and polyketide synthase enzymes

Non-ribosomal peptide synthetases (NRPS) and polyketide synthases (PKS) enzymes synthesise a variety of medically important small molecules in bacteria and fungi, including many antibiotics, such as erythromycin (Donadio *et al.*, 1991), tetracycline (Binnie *et al.*, 1989), penicillin, cephalosporin (Aharonowitz *et al.*, 1992) and vancomycin (Bischoff *et al.*, 2005). The potential utilisation of these enzymes for the synthesis of novel products depends on our understanding of their mechanism of function. NRPS and PKS systems are large enzymes (they may be megadaltons in size) which are comprised of multiple units called modules. These modules each incorporate several essential domains and may include auxiliary domains. Linker regions between adjacent domains allow domains to interact whilst keeping them apart (Weissman & Muller, 2008). NRPS and PKS systems function in a very similar manner where each module within a system is responsible for the incorporation of a specific building block, or monomer, into the final product. Essential modules within an NRPS system differ

from those in a PKS system, and these differences result in two different classes of monomer being incorporated (Keating & Walsh, 1999). NRPS systems incorporate amino acids and catalyze peptide bond formation between monomers. PKS systems incorporate carboxylic acids and catalyze C-C bond formation between monomers.

In the majority of systems discovered to date, the number and order of modules in the NRPS or PKS enzyme is equivalent to the number and order of monomers in the final product; these enzymes are therefore described as linear (Fischbach & Walsh, 2006). The correlation between the sequence of modules in the enzyme and the sequential incorporation of monomers has led to these enzymes being termed "assembly lines". However, several examples of NRPS and PKS enzymes which do not act in a linear manner have been described. In these cases, the enzymes are described as iterative or nonlinear (Mootz *et al.*, 2002). In iteratively acting enzymes, a single module or modules act more than once to incorporate the same monomer into the final product. For example, during the biosynthesis of the siderophore enterobactin, the NRPS module, EntF, incorporates three molecules of 2,3-dihydroxybenzoate into the final product (Gehring *et al.*, 1998). In enzymes that act in a non-linear manner, modules may not be comprised of the standard domains. "Essential" domains within modules may appear to be missing but are in fact supplied *in trans* from a separate module. For example, the PKS antibiotic, mupirocin, is synthesised non-linearly whereby essential domains exist separately from other biosynthetic modules (El-Sayed *et al.*, 2003). Alternatively, entire modules may be skipped during biosynthesis (Mootz *et al.*, 2002). It should be noted that many NRPS and PKS enzymes cannot be neatly categorized into one of the three assembly pathways described above and in many cases fusions of different types of assembly pathways exist.

In bacteria, individual modules are normally spread over several proteins, whereas in fungi these enzymes are often formed from a single polypeptide chain (Schwarzer & Marahiel, 2001). Docking domains seem to mediate interactions between modules that act consecutively but are found on separate polypeptides. The specificity of these docking domains for their corresponding NRPS or PKS enzyme has been shown to be important for efficiency of catalysis as these interactions may prevent non-productive module pairing (Wu *et al.*, 2002). Individual modules are an average of 145kDa in size, however, entire NRPS/PKS enzymes can be much larger. For example, the phytotoxin syringopeptin (which itself is composed of only 22 amino acids) is synthesized by an NRPS enzyme that totals 2.7MDa in size (Fischbach & Walsh, 2006; Scholz-Schroeder *et al.*, 2003). Despite the enormous energy cost involved in the synthesis of these enzymes, they do offer an advantage over the ribosomal system; they can incorporate hundreds of different building blocks into the final product and are not limited to the 20 proteinogenic amino acids (Finking & Marahiel, 2004).

Enzymatic domains involved in modification of the NRP or PK product during biosynthesis are described below. Additionally, however, NRP or PK modifying enzymes may also act in *trans* during synthesis, or after release. For example, the synthesis of the PKS antibiotic, erythromycin, is dependent on the action of post assembly line, *trans* acting tailoring enzymes which include hydroxylases, glycosyl transferases and methyltransferases (Staunton & Wilkinson, 1997). Thus, NRPS/PKS systems can incorporate different monomers, and intermediates can be enzymatically modified in *cis* or in *trans* during synthesis or after synthesis. Therefore the structural diversity of NRPS/PKS products is huge.

1.3.1 NRPS enzymes

NRPS systems may incorporate proteinogenic, non-proteinogenic or modified amino acids, as well as other aryl acids, into the final product. To date, more than 500 different NRPS monomers have been described (Walsh & Fischbach, 2010). Essential domains in an NRPS module are the adenylation (A) domain, the peptidyl carrier protein (PCP) domain and the condensation (C) domain. However, the initiation and termination modules frequently deviate from this paradigm; the C domain is often absent from the initiation module and the termination module often includes an additional domain for release or cyclisation of the product, as described below (Figure 1.4) (Conti *et al.*, 1997; Stachelhaus *et al.*, 1996; Stachelhaus *et al.*, 1998). The A domain acts as a gatekeeper and is responsible for monomer selection and activation as an acyl adenylate. This process is ATP dependent (Conti *et al.*, 1997). Numerous mutagenesis studies revealed specificity conferring residues within core motifs of the A domain. This knowledge can be applied to predict A domain specificity and thus the NRPS product from analysis of the protein sequence of the A domain (Challis *et al.*, 2000; Eppelmann *et al.*, 2002; Stachelhaus *et al.*, 1999). The activated monomer is then covalently tethered to a thiol group on a 4'-phosphopantetheine (P-pant) arm belonging to the PCP domain (Stachelhaus *et al.*, 1996). This P-pant arm is post-translationally added to the PCP domain and this process is termed priming. Priming of the PCP domain is catalysed by a phosphopantetheinyl transferase (PPTase) enzyme, which uses acyl coenzyme A as the source of the P-pant group (Lambalot *et al.*, 1996). PPTase enzymes will be discussed in more detail in section 1.3.5. The sequestration of intermediates by covalent attachment to the PCP domain allows microcompartmentalisation of the reaction (which is particularly relevant in bacteria) and prevents reaction of the intermediates with cytoplasmic constituents (Weissman & Muller, 2008). Lastly, the C domain catalyzes peptide bond formation between two

monomers tethered to adjacent PCP domains. Since peptide bond formation cannot occur on the first module of the NRPS enzyme, this domain is often absent from the initiation module. (Stachelhaus *et al.*, 1998). A fourth essential domain, the thioesterase (TE) domain, is found as part of the terminal module and catalyses NRP release from the enzyme via hydrolysis or cyclization (Tseng *et al.*, 2002). In addition to the thioesterase enzyme which catalyses release of the NRP product, many NRPS systems include a type II TE enzyme. The majority of co-enzyme A present within the cell exists as acetyl-CoA and so PCP domains are often mis-primed, resulting in the P-pant arm terminating in an acetyl group rather than an sulfhydryl group. Type II TE enzymes hydrolyze these non-functional acetyl groups, freeing the P-pant arm (Mootz *et al.*, 2002).

Enzymes responsible for modification of the intermediates may also be found along the assembly line in the form of additional domains within the NRPS modules. Examples of these domains include epimerization, oxidase and cyclization domains. These domains allow further modification of the NRP to increase the diversity of the products synthesised (Fischbach & Walsh, 2006).

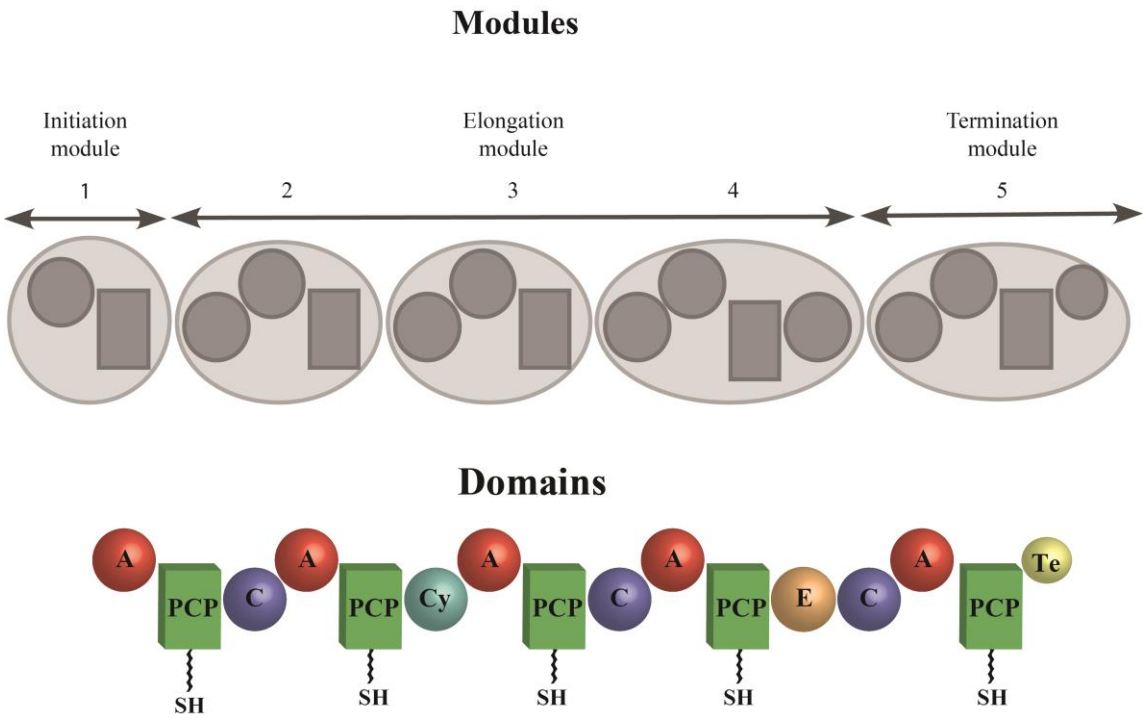

Figure 1.4 . Representation of a typical non-ribosomal peptide synthetase (NRPS) assembly line. Each module is responsible for the incorporation of a specific amino acid into the non-ribosomal peptide. Modules can be further divided into domains. Essential elongation domains are the condensation (C), adenylation (A) and peptidyl carrier protein (PCP). The termination module may also comprise a thioesterase (TE) domain. The C domain (which catalyzes bond formation between peptides) is usually absent in the initiation module. Additional domains, such as the epimerisation (E) domain, or alternative domains, such as the cyclization (Cy) domain, may be found along the assembly line and these function to modify the growing polypeptide chain during synthesis.

1.3.2 PKS enzymes

PKS systems incorporate short carboxylic acids activated as coenzyme A (CoA) linked thioesters. The first monomer to be incorporated into the product is termed the starter unit whereas subsequent monomers are termed extender units. Starter units include a plethora of carboxylic acids. By comparison with NRPS enzymes which incorporate a diverse range of monomers, the majority of extender units for PKS enzymes are either malonyl-CoA or methylmalonyl-CoA (Chan *et al.*, 2006; Chan *et al.*, 2009). Core domains in PKS systems are the acyltransferase (AT) domain, the acyl carrier protein (ACP) domain and the ketosynthase (KS) domain (Figure 1.5) (Bibb *et al.*, 1989). These domains have functions similar to the A, PCP and C domains, respectively, of NRPS systems. Similar to the PCP domain of NRPS enzymes, the ACP domain must be post-translationally modified by the addition of a P-pant group. The AT domain selects the monomer to be incorporated and catalyses transfer of the acyl group of the monomer to the P-pant arm of the ACP domain. This step does not require any energy input as monomers are selected as activated acyl-CoA thioesters (Schwarzer & Marahiel, 2001). The KS domain catalyzes C-C bond formation via a decarboxylative condensation reaction between acyl thioesters attached by adjacent ACP domains (Fischbach & Walsh, 2006). The initiation module of the PKS enzyme may lack the KS domain entirely, in which case acyl CoA starter units are incorporated. Alternatively, the initiation module may contain a KS domain, which does not catalyse a condensation reaction, but rather decarboxylates the ACP bound malonyl or methylmalonyl groups to yield ACP bound acetyl or propionyl groups (Moore & Hertweck, 2002). Similar to NRPS biosynthesis, the termination module of PKS enzymes frequently contains a TE domain, which effects release of the PK product by hydrolysis or cyclization (Fischbach & Walsh, 2006).

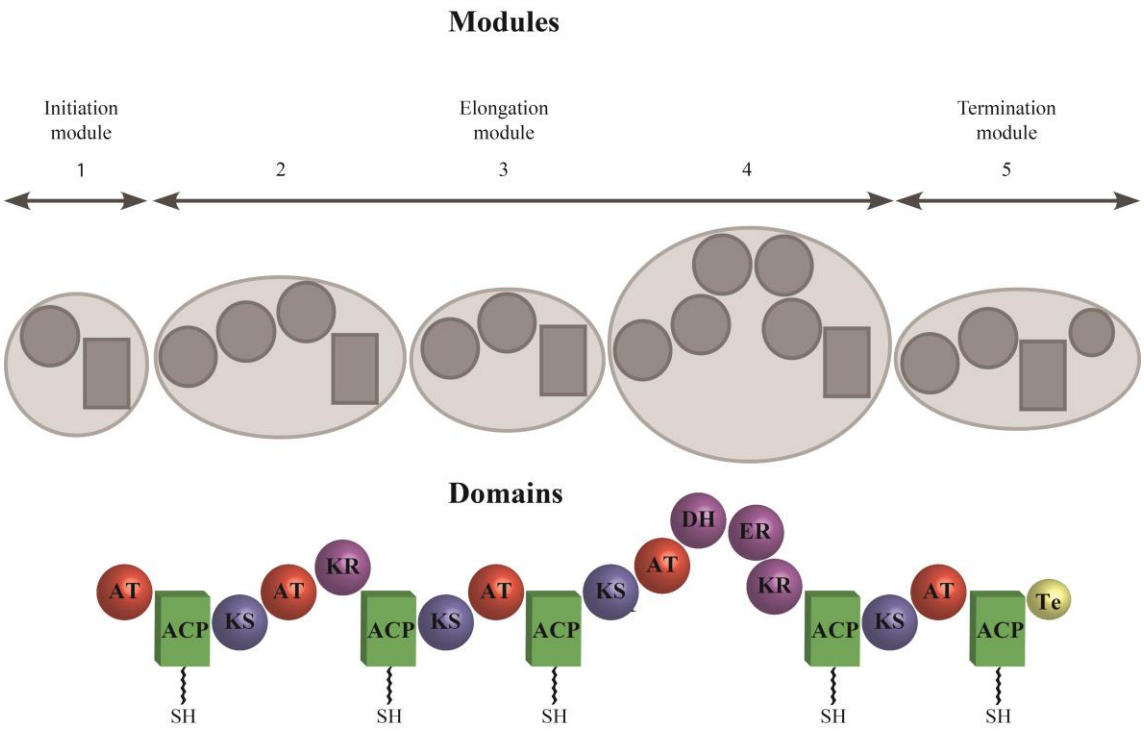

Figure 1.5. Representation of a typical polyketide synthase (PKS) assembly line. Each module is responsible for the incorporation of a specific acyl unit into the polyketide. Similar to non-ribosomal peptide synthetases, modules can be subdivided into domains. Typically essential domains in the PKS elongation module are the acyl transferase (AT), ketosynthase (KS), acyl carrier protein (ACP), although many PKS enzymes deviate from this paradigm (see text for more information). A thioesterase (TE) domain is frequently found on the termination module. Additional ketoreductase (KR), dehydratase (DH) and enoylreductase (ER) domains may also be found along the assembly line. These accessory domains alter the oxidation state of the β-keto moiety on the growing ketide (see figure 1.6). The KS domain (which catalyzes bond formation between ketides) is usually absent in the initiation module.

PKS enzymes can be classed as type I, type II or type III. In type I PKS systems, modules are arranged linearly and catalytic domains are fused *in cis*. Type I enzymes may be modular, whereby each module incorporates a single starter or extender unit, or they may be iterative, where one module functions more than once. Type I modular enzymes are found in bacteria, whereas type I iterative enzymes are mainly found in fungi. In type II PKS systems, domains exist as discrete entities that come together as a complex during PK biosynthesis. Type II systems act iteratively and contain the essential PKS domains, but possess an additional KS domain which controls the length of the PK product. Type II systems have thus far only been described in bacteria (Chan *et al.*, 2009; Hertweck, 2009). Type III PKS systems often lack essential catalytic domains and substrates are incorporated in an ACP domain independent manner. In these systems, a single enzyme is responsible for monomer selection and extension. Type III PKS enzymes are most frequently found in plants, but examples of type III systems have recently been described in bacteria and fungi (Yu *et al.*, 2012).

Up to three additional domains - the ketoreductase (KR), dehydratase (DH) and enoylreductase (ER) domain can be found in each PKS module. They function in this order and they alter the oxidation state of the β-keto moiety on the growing PK. The β-keto group is initially reduced by the KR domain to β-hydroxyacyl. The DH domain catalyzes dehydration of the β-hydroxyacyl to α,β-enoyl. Lastly, the ER domain catalyzes reduction to the methyl group (Figure 1.6) (Katz, 1997).

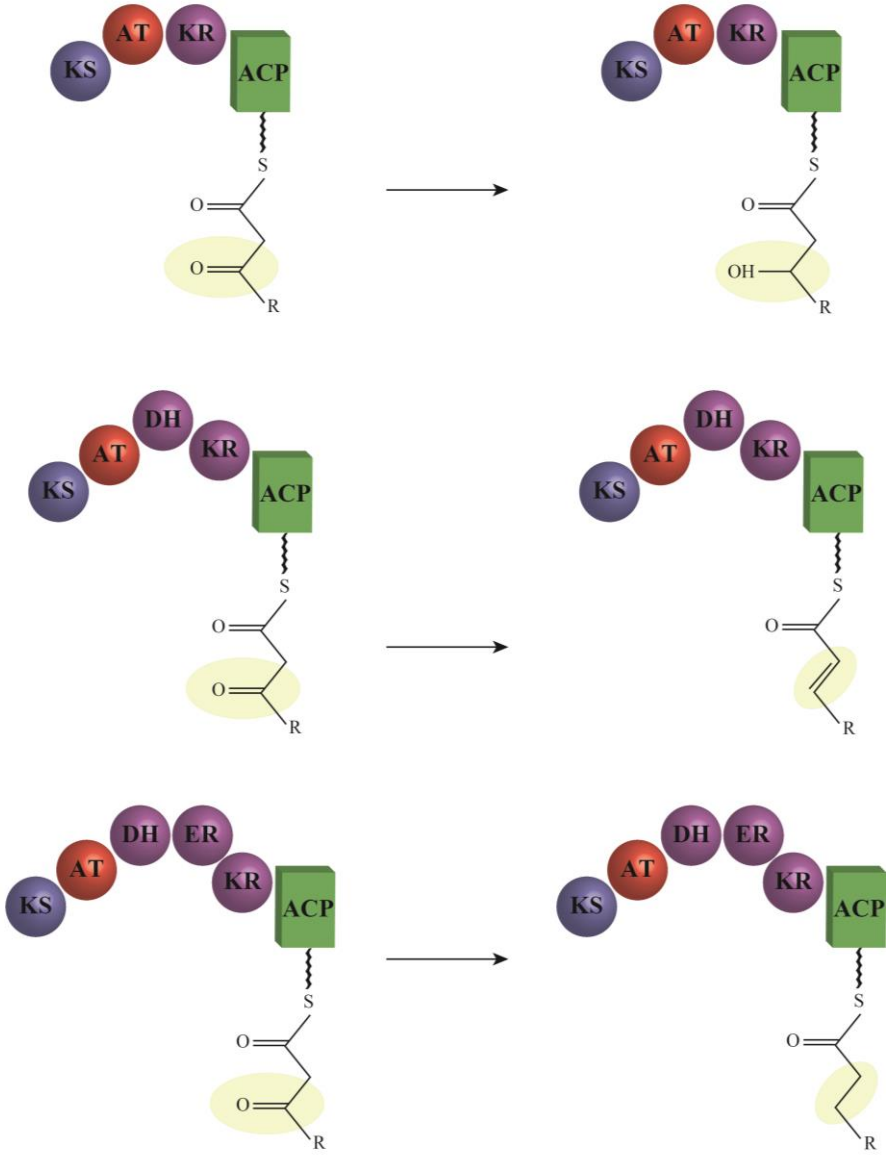

Figure 1.6. Representation of the optional β-carbon reducing steps in polyketide assembly. The ketoreductase (KR), dehydratase (DH) and enoylreductase (ER) domain function to alter the oxidation state of the β-keto moiety of the ketide. The reactions these domains catalyze are illustrated above. The carbonyl group of the β-carbon may be reduced to a hydroxyl group (top panel), an alkene group (middle panel) or a saturated methylene (bottom panel).

1.3.3 NRPS-PKS hybrid enzymes

The modular nature of NRP and PK synthases has allowed nature to form functional fusions of these enzymes, called hybrids. A variety of medically important small molecules are synthesized by hybrid enzymes, including the immunosuppressant,

rapamycin (Schwecke *et al.*, 1995) and the anti-tumour drug, bleomycin (Du *et al.*, 2000). The similarities in the organisation of these enzymes mean that the same underlying principles of NRP and PK biosynthesis can be applied when trying to understand hybrid enzymes. In hybrid NRPS-PKS enzymes, domains are generally thought to be less specific for their usual substrates, since they must accept both peptide and ketide intermediates (Walsh & Fischbach, 2010). By combining NRPS and PKS enzymes, the potential diversity of the resulting products is greatly increased.

1.3.4 Manipulation of NRPS and PKS enzymes

Breakthroughs in our understanding of NRPS and PKS systems led to the realisation that NRPS and PKS enzymes may be utilised in the biosynthesis of "unnatural" natural products. However, technical difficulties associated with modification of these enzymes were perhaps not fully appreciated in the early days of research into this field. Indeed it was proposed that it would be possible to modify the product of these enzymes as precisely as we are able to modify the amino acid sequence by alteration of the encoding gene (Cane *et al.*, 1998). Nevertheless, progress has been made in engineering NRPS and PKS enzymes.

Modification of NRPS and PKS enzymes to alter the resulting product may involve swapping of entire domains or modules or it may involve mutagenesis of specific residues within domains. Several attempts to engineer NRPS and PKS enzymes have been described, specific examples and limitations with this approach are detailed below. The principle of increasing natural product diversity by substitution of domains was proven by engineering of the 6-deoxyerythronolide B synthase (DEBS), which is the PKS responsible for the production of the macrolide antibiotic erythromycin. In this example, AT domains or β-keto processing domains from the rapamycin PKS were

used to substitute the natural DEBS PKS domains. Single, double and triple domain substitutions were incorporated to create a library of more than 50 variants (McDaniel *et al.*, 1999). Modules from different systems can also, like building blocks, be taken apart and recombined to create a novel protein. In an attempt to bioengineer the daptomycin antibiotic NRPS, single and multiple homologous and heterologous modules were introduced. The resulting products were no more potent than daptomycin, but the results demonstrated the possibility of swapping modules to synthesise new proteins (Giessen & Marahiel, 2012). Another mechanism by which the NRP or PK product can be modified is by altering the specificity of the AT domain (PKSs) or A domain (NRPSs). Since these domains control selection of the incorporated monomer, mutagenesis of specific residues involved in this process can result in the incorporation of alternative monomers. This is particularly relevant in engineering NRPS directed biosynthesis, since the diversity of NRPS monomers is much larger than PKS monomers. In the A domain of NRPS enzymes, elucidation of the specificity conferring code has been pivotal in allowing rational design of these domains. This code consists of specific residues within the A domain binding pocket that determine specificity (Stachelhaus *et al.*, 1999). Recently, the A domain within module 10 of the calcium dependent antibiotic, CdaPS3, NRPS was altered by site directed mutagenesis. Mutagenesis of a single residue was sufficient to alter the specificity of the module from glutamic acid and methyl glutamic acid, to glutamine and methyl glutamine (Thirlway *et al.*, 2012). A significant issue when engineering NRPS and PKS enzymes is the reduction in yield of the novel product by comparison with wildtype levels. It is likely that NRPS and PKS domains are specific not only for their incorporated monomer, but also for the product of the upstream modules. More conservative mutations, such as alteration of the A domain specificity rather than module substitution, may make these enzymes more tolerant to manipulation (Williams, 2013).

1.3.5 Phosphopantetheinyl transferase (PPTase) enzymes

As described above, PKSs and NRPSs are dependent upon the catalytic action of PPTase enzymes to function. PPTase enzymes catalyse the transfer of a P-pant prosthetic group from coenzyme A to a conserved serine residue in the carrier protein domain of PKSs and NRPSs (Beld *et al.*, 2014; Lambalot *et al.*, 1996). The P-pant prosthetic group of the carrier protein domain fulfils two main functions: the thiol terminated P-pant arm serves as the point of attachment for the PKS or NRPS intermediate to the biosynthetic machinery and the flexibility of this arm allows the biosynthetic intermediate access to the catalytic reaction centres within the PKS or NRPS module (Figure 1.7) (Beld *et al.*, 2014).

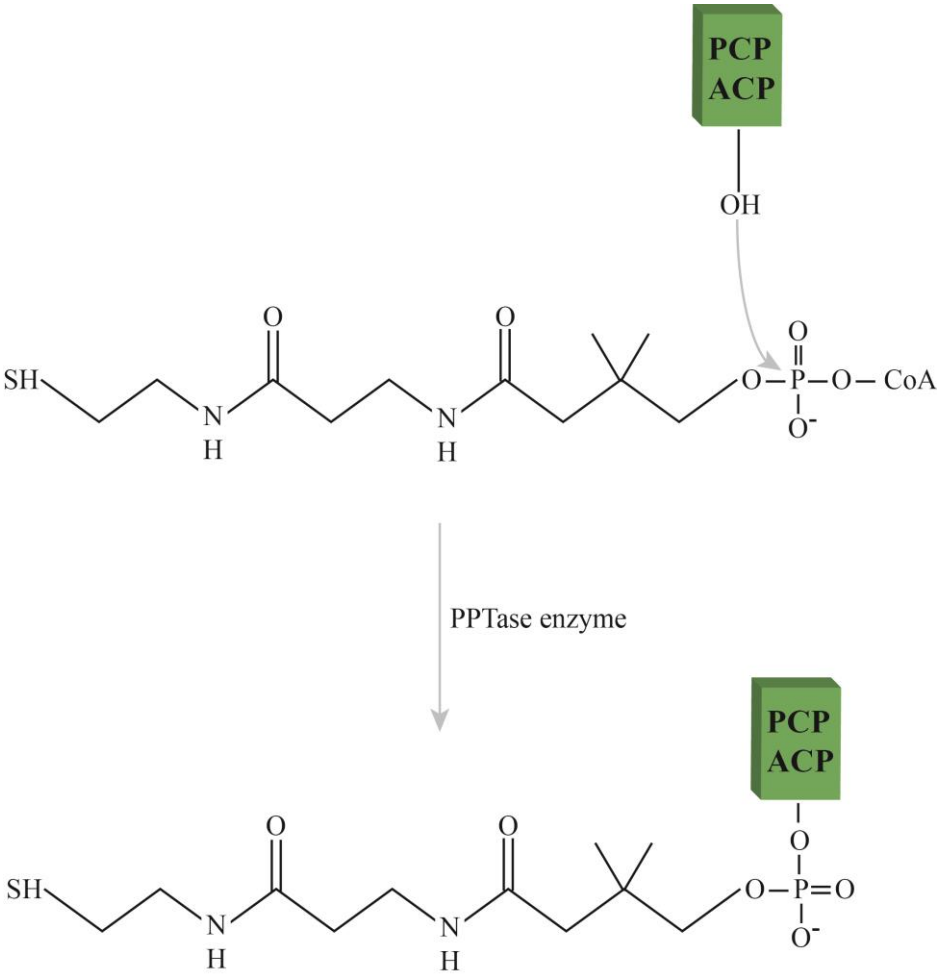

Figure 1.7. Representation of the reaction catalysed by phosphopantetheinyl transferase (PPTase) enzymes. PPTase enzymes are essential for the modification of the peptidyl carrier domain (PCP) or the acyl carrier domain (ACP) of non-ribosomal peptide synthetases or polyketide synthases. They catalyse the transfer of a 4'-phosphopantetheine group from co-enzyme A to the PCP or ACP domain.

PPTase enzymes can be divided into three families: the Sfp family whose prototype is Sfp of *B. subtilis* (Lambalot *et al.*, 1996; Reuter *et al.*, 1999); the AcpS family whose prototype is AcpS of *Escherichia coli* (Elovson & Vagelos, 1968; Lambalot & Walsh, 1995); and a third family whose members are integrated as domains within the FAS or PKS enzyme that they modify (Beld *et al.*, 2014; Copp & Neilan, 2006; Lambalot *et al.*, 1996; Walsh *et al.*, 1997). The Sfp family of PPTases have broad substrate specificity

and are generally required for the activation of PKS and NRPS enzymes of secondary metabolism (Mootz *et al.*, 2001; Quadri *et al.*, 1998); these enzymes are approximately 230 residues in length and exist as monomers (Reuter *et al.*, 1999). Based on sequence comparisons, members of the Sfp family were further divided into the F/KES or W/KEA subfamily (Copp & Neilan, 2006; Lambalot *et al.*, 1996). F/KES family members were shown to largely be associated with NRPS enzymes whereas W/KEA family members are more often associated with PKS enzymes (Copp & Neilan, 2006). Members of the AcpS family of PPTases are generally around 120 residues in length and are thought to exist as trimers (Chirgadze *et al.*, 2000; Parris *et al.*, 2000). AcpS family PPTases show a higher degree of specificity towards the carrier protein domain that they modify and are generally required for the modification of FAS enzymes of primary metabolism (Lambalot *et al.*, 1996; Mootz *et al.*, 2001; Parris *et al.*, 2000). Despite limited overall sequence similarity between AcpS and Sfp family members, these enzymes share homology at the structural level: an AcpS dimer resembles one Sfp monomer (Lambalot *et al.*, 1996; Reuter *et al.*, 1999). As previously described, there exists a third family of PPTases which are translationally fused to the FAS or PKS enzyme that they modify (Copp & Neilan, 2006; Fichtlscherer *et al.*, 2000; Lambalot *et al.*, 1996). Examples of these integrated PPTases are few and, to date, only two bacterial integrated PPTases have been experimentally validated (Murugan & Liang, 2008; Weissman *et al.*, 2004).

1.4 The Type VI Secretion System (T6SS)

1.4.1 Identification of the T6SS

The T6SS is the most recently described secretion system in Gram-negative bacteria. The genetic locus encoding this secretion system was first identified in 1997 in *Rhizobium leguminosarum* bv. *trifolii*. In this bacterium, it was noted that mutation of

this locus extended the spectrum of plants that *R. leguminosarum* bv. *trifolii* was able to nodulate. However, at the time, the genetic locus showed no homology to characterised genes and so the significance of the identified genes was not appreciated (Roest *et al.*, 1997). Hints at the function of this locus came in 2003 when it was shown that mutation of the identified genetic locus impaired secretion of a number of proteins in a temperature dependent manner. The authors also noted that many open reading frames (ORFs) within this gene cluster showed homology to ORFs in *Vibrio cholerae* and *Pseudomonas aeruginosa* (Bladergroen *et al.*, 2003). In the intervening and following years, several studies implicated this secretion system in virulence in *Salmonella* (Folkesson *et al.*, 2002), *Francisella* (Nano *et al.*, 2004) and *Edwardsiella* (Rao *et al.*, 2004). However, it was not until 2006 that seminal work conducted in the Mekalanos laboratory revealed that these genes encoded a novel secretion system, termed the T6SS, in *V. cholerae* and *P. aerunginosa* (Mougous *et al.*, 2006; Pukatzki *et al.*, 2006). In *V. cholerae,* the T6SS was implicated in cell-cell contact dependent virulence towards *Dictostelium* amoebae and towards macrophages (Pukatzki *et al.*, 2006). In *P. aeruginosa*, the T6SS was identified as being required for the secretion of a component of the secretion system, Hcp1 (a TssD family protein). Further, Hcp1 was detected in the lungs of cystic fibrosis patients infected with *P. aeruginosa* (Mougous *et al.*, 2006). Together, these studies demonstrated the potential importance of the T6SS in the survival and virulence of medically relevant pathogens.

1.4.2 Identification of conserved components of the T6SS and predicted function

T6SS-encoding gene clusters are large, variable and have been identified in at least 25% of all sequenced Gram-negative bacterial species. One third of T6SS encoding bacterial genomes contain more than one system and some organisms contain

many systems, for example six T6SSs were identified in the genome of *Burkholderia pseudomallei* (Boyer *et al.*, 2009). Systematic mutation of components of the T6SS combined with bioinformatics analysis revealed the system is comprised of a minimum of 13 conserved core components (Boyer *et al.*, 2009; Zheng & Leung, 2007). These components will be referred to by their Tss (Type Six Secretion) name throughout (TssA-M), although it should be noted that TssD, TssI and TssH are also widely known by their common names, Hcp, VgrG and ClpV, respectively (Shalom *et al.*, 2007). These essential components form a secretion system which extends from the cytoplasm of the producing cell, across its cell envelope and then across the cell membrane of a target cell (Figure 1.3). T6SS components may be cytoplasmic, anchored within the inner or outer membrane, or part of an extracellular puncturing device (Figure 1.8). Effectors are translocated in a single step, either through, or in association with, the extracellular puncturing structure. Additional components are likely to be involved in regulation of the system or tailoring of the system to suit the lifestyle of the particular bacterium (Zoued *et al.*, 2014).

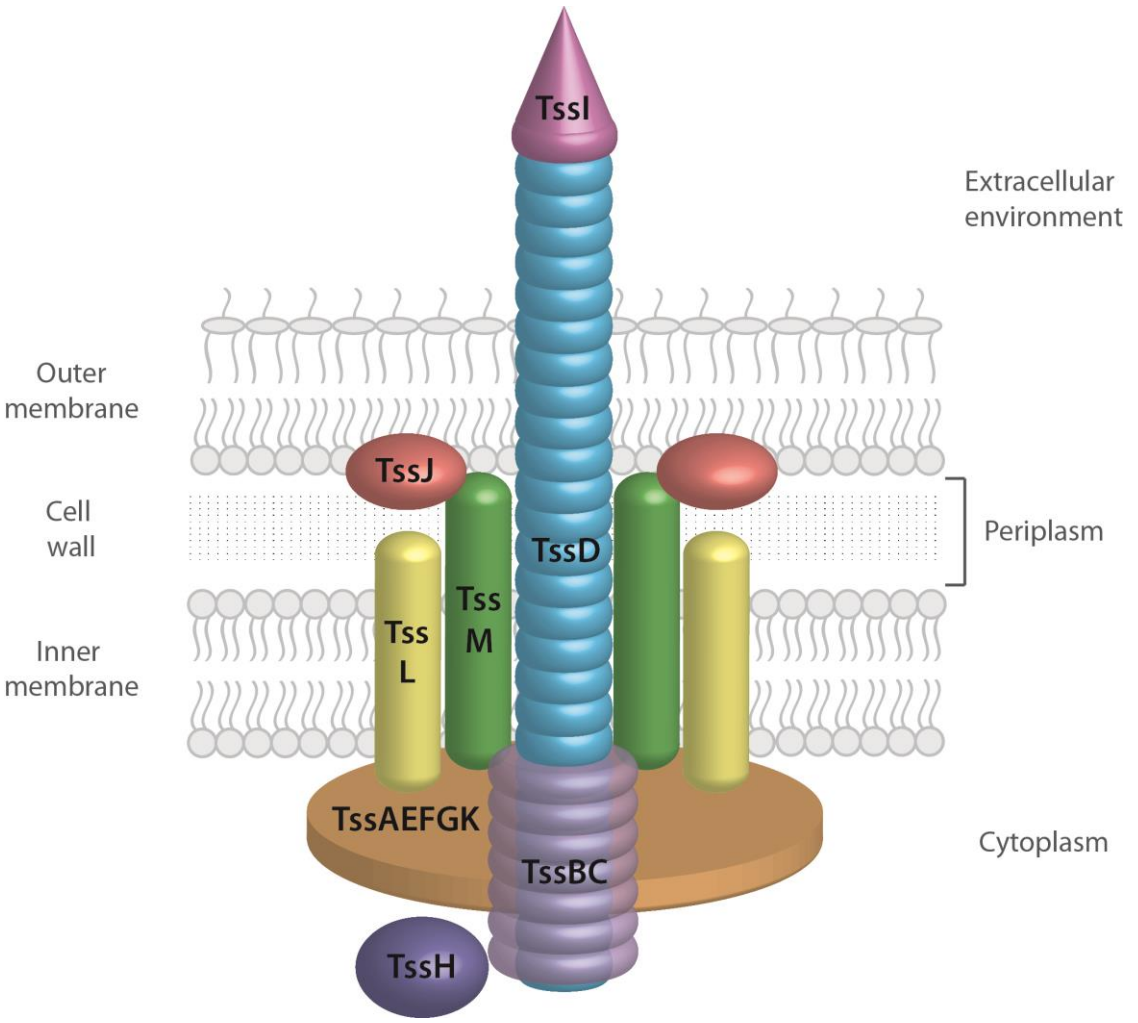

Figure 1.8. Schematic representation of the bacterial Type VI Secretion System (T6SS). The essential, conserved components are indicated by their Tss name. The proposed localisation of each of the components is indicated. Briefly, TssD (Hcp) is thought to form a tube through which certain substrates are transported. The TssD tube is capped by the TssI (VgrG) protein, which is predicted to puncture the membrane of target cells. Contraction of the TssBC sheath, which surrounds the TssD tube, is thought to propel the TssDI needle out of the host cell and into the target cell. TssH (ClpV) is required for disassembly and recycling of the TssBC sheath following contraction. TssLMJ have been hypothesised to anchor the T6SS to the cell envelope. The role of TssAEFGK remains speculative, although these proteins may form part of a baseplate-like structure. See section 1.5.2 for details.

1.4.2.1 Bacteriophage-like components of the T6SS

Several components of the T6SS "needle-like" structure share structural homology with the bacteriophage tail (Figure 1.9). TssD forms hexameric rings that stack together head to tail to form a 40 Å channel through which many T6SS substrates are thought to be transported (Ballister *et al.*, 2008; Brunet *et al.*, 2014; Mougous *et al.*, 2006). TssD is structurally similar to the gpV protein of the non-contractile phage, λ (Pell *et al.*, 2009). Trimers of TssI are thought to sit at the top of this TssD tube. TssI is structurally very similar to the gp5-gp27 cell puncturing device of bacteriophage T4; the C-terminus of TssI shares homology with gp5 whereas the N-terminus shares homology with gp27. These similarities have led to the hypothesis that TssI is involved in piercing the target cell membrane. More recently, a protein of unknown function known to bind to the tip of the central spike protein, gp5, was used as bait to identify so-called PAAR domain containing proteins encoded within T6SS gene clusters. It was proposed that the PAAR domain of these proteins binds to the tip of TssI and therefore 'sharpens' the needle, and that these PAAR domain containing proteins are involved in the assembly of TssI trimers or translocation of TssI across the host cell envelope. Additionally, PAAR domain containing proteins may harbour additional toxin domains that are delivered into target cells in a T6SS dependent manner (Shneider *et al.*, 2013). In bacteriophage T4, a sheath composed of gp18 surrounds the gp19 tail tube and contraction of this sheath propels the gp19 tube forwards and into the bacterial target cell (Figure 1.9) (Filloux, 2013). An analogous mechanism of contraction has been proposed for the T6SS. In the case of the T6SS, two proteins (TssB and TssC) have been shown to form a stable complex and are believed to assemble to form a contractile sheath-like structure. Tubules of TssBC have been visualised by electron microscopy and, further, fluorescent labelling of TssB has allowed visualisation of cycles of extended and contracted conformations (Basler & Mekalanos, 2012; Basler *et al.*, 2012;

Lossi *et al.*, 2013). The internal diameter of the TssBC sheaths has been shown to be ~100 Å, which would be sufficient to accommodate the TssD tube (Lossi *et al.*, 2013). Indirect evidence for the presence of the TssD tube within the TssBC sheath was provided by electron microscopic analysis of extended and contracted versions of the TssBC sheath; the contracted sheath appears hollow whilst the extended sheath contains electron dense material (Kapitein *et al.*, 2013). Again, in support of this theory, the C-termini of TssBC show homology to tail sheath proteins of various bacteriophages (Lossi *et al.*, 2013). Additionally, the cytoplasmic T6SS protein, TssE, shares homology with gp25, one of the components of the bacteriophage T4 baseplate (Figure 1.9) (Lossi *et al.*, 2011). However, to date, the function of TssE remains elusive. All the above data suggest that the contractile bacteriophage tail and the T6SS are evolutionarily related, however, a lack of sequence identity between structurally homologous proteins suggests these systems diverged a long time ago (Lossi *et al.*, 2013). Based on the similarities between these two systems, the T6SS has been proposed to function like an inverted bacteriophage, whereby the T6SS fires from the inside of the bacterial cell (Figure 1.9 and Figure 1.10) (Records, 2011).

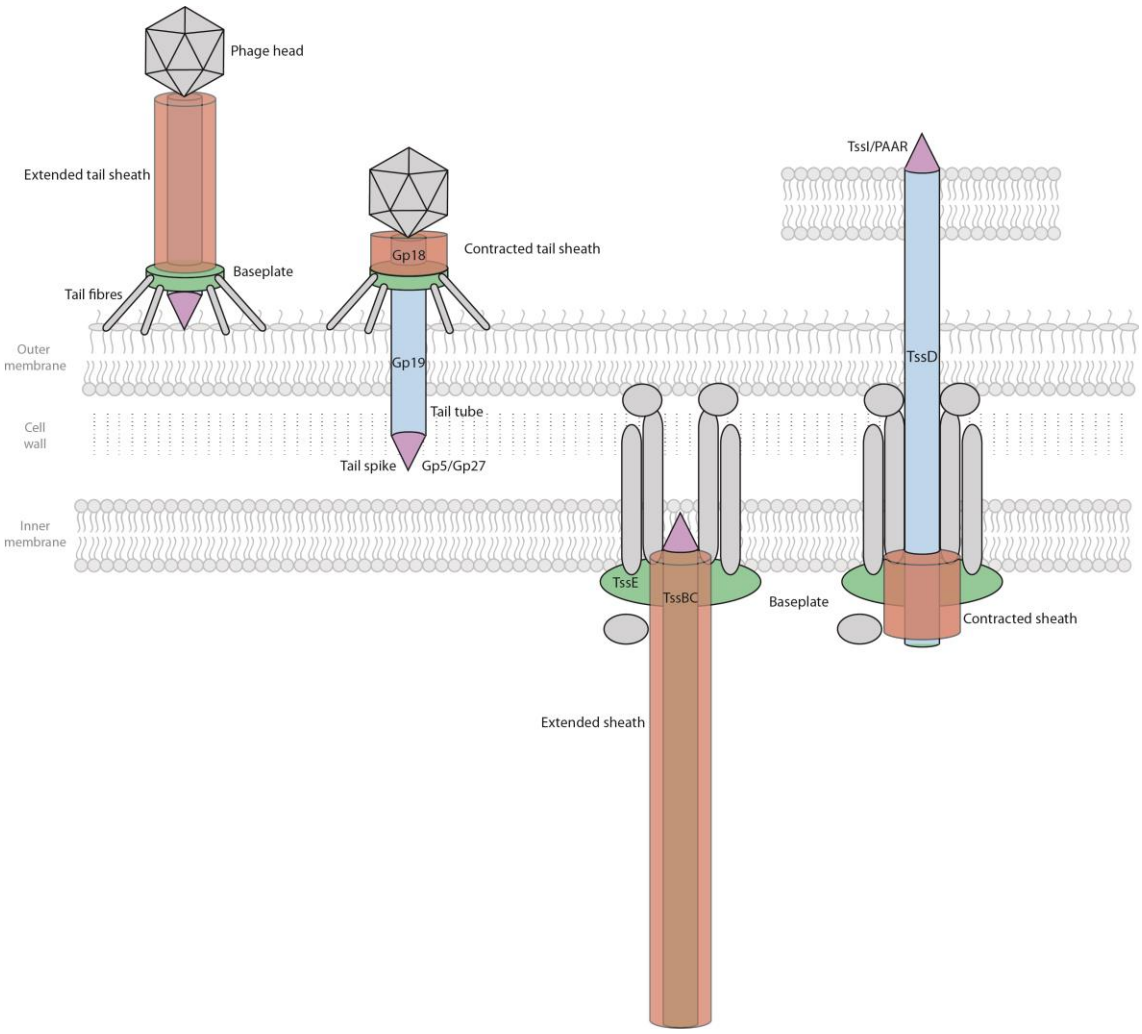

Figure 1.9. Comparison of the bacteriophage T4 cell puncturing machinery with the Type VI Secretion System (T6SS) cell puncturing machinery. Structurally homologous proteins are indicated by the same colour. Adapted from (Ho *et al.*, 2014).

1.4.2.2 The membrane anchored components of the T6SS

Additional components of the T6SS do not share homology with bacteriophage proteins. These include the components comprising the so-called "membrane anchoring" complex. This complex is composed of TssJ, TssL and TssM. TssJ is a lipoprotein that is anchored in the OM and protrudes into the periplasm, where it may self-interact (Aschtgen *et al.*, 2008). TssJ has also been shown to interact with the periplasmic domain of TssM (Felisberto-Rodrigues *et al.*, 2011). TssM is an integral inner membrane protein that possesses three transmembrane domains, a cytoplasmic N-

terminus and a periplasmic facing C-terminus (Ma *et al.*, 2009b). In certain systems, the ATPase activity of TssM has been shown be required for the formation of the membrane anchoring complex and for recruitment of TssD to the membrane (Ma *et al.*, 2009b). Lastly, TssL is anchored in the inner membrane via a single transmembrane spanning domain in its C-terminus, however the majority of the protein is cytoplasmic (Aschtgen *et al.*, 2012). TssL has been shown to interact with, and stabilize, TssM (Ma *et al.*, 2009b). In some systems there exists an additional inner membrane protein called TagL. TagL encodes a peptidoglycan binding domain that has been suggested to anchor the T6SS to the cell wall. In the absence of TagL, a C-terminal extension of TssL fulfils this anchoring role by interacting with peptidoglycan. It is likely that, in some systems, TssL and TagL have fused at some point to form a single protein (Aschtgen *et al.*, 2010).

1.4.2.3 Additional, cytoplasmic components of the T6SS

Additional essential components of the T6SS include TssA, F, G, H and K, however, very little data exists for TssA, F and G. In the absence of secretion signals or domains which would hint at the localisation of these components, they have been predicted to be cytoplasmic. TssK is an intrinsically cytoplasmic protein that has been shown by bacterial two-hybrid (BTH) studies and immunoprecipitation experiments to interact with TssA, D, C and L of entero-aggregative *E. coli* (EAEC) (Zoued *et al.*, 2013). In *S. marcescens* Db10, experiments in the native organism have shown that TssK interacts with TssF and TssG (English *et al.*, 2014). Rather more information is available for TssH. TssH was one of the initial proteins identified as playing an essential role in Type VI dependent secretion (Mougous *et al.*, 2006). TssH belongs to the AAA+ family ATPases and is responsible for disassembly of the TssBC sheath following

contraction (Bonemann *et al.*, 2009). TssH has been shown to specifically co-localise with the contracted form of the T6SS sheath and its deletion prevents recycling of the sheath components (Basler & Mekalanos, 2012; Kapitein *et al.*, 2013). TssH may also play an important role in removal of aberrantly polymerised TssBC which is not associated with the secretion system (Kapitein *et al.*, 2013).

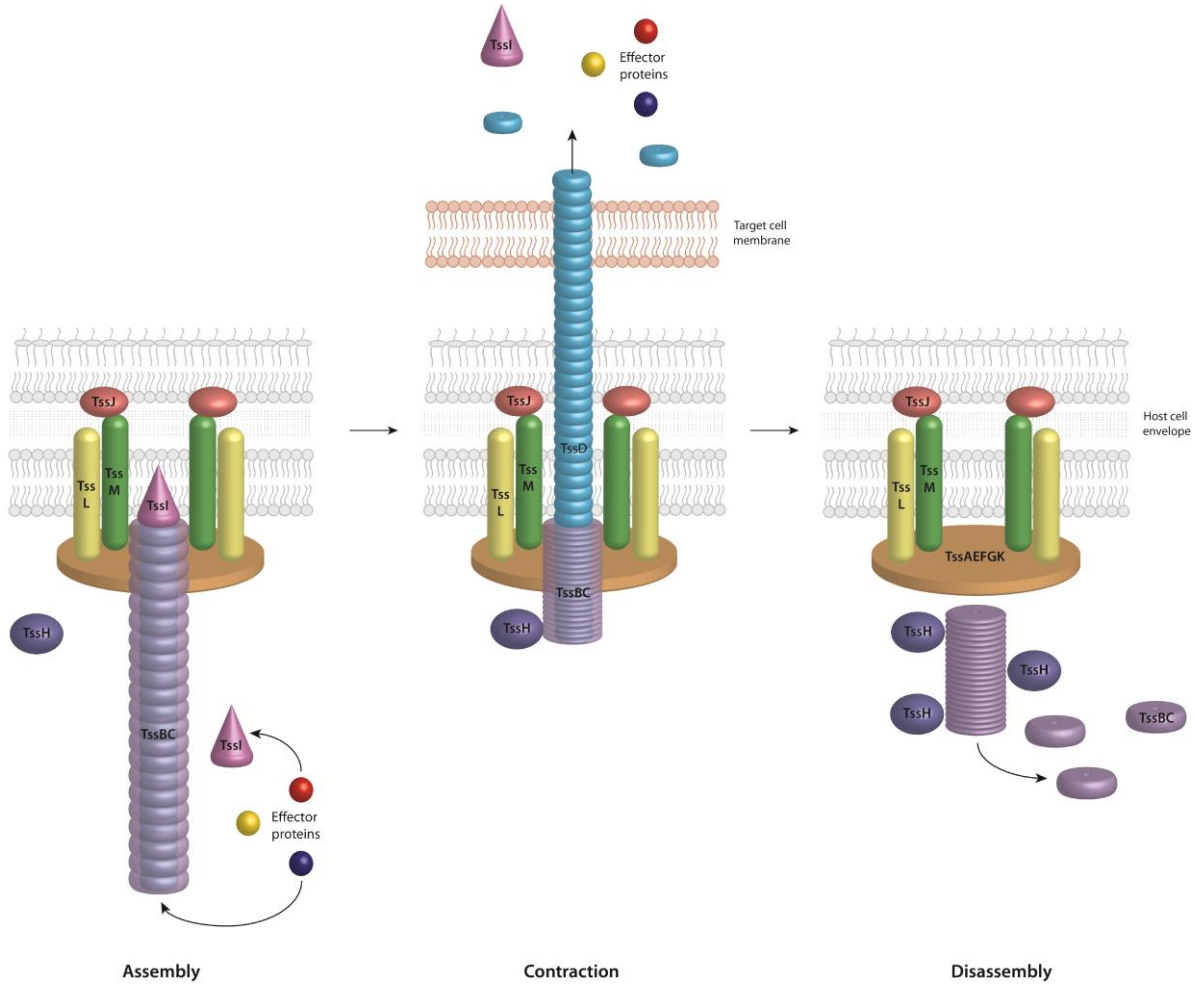

Figure 1.10. Schematic representation of the mechanism of action of the Type VI secretion system (T6SS). The different stages of assembly, contraction and disassembly are depicted. Assembly of the system involves elongation of the TssBC sheath, which surrounds the TssD tube. Effectors of the T6SS may associate with the TssD tube or with the TssI/PAAR protein structure. Contraction of the TssBC sheath is thought to propel the TssD tube forwards, out of the secreting cell and into the target cell. TssD, TssI and effector proteins can therefore be detected in the extracellular environment. Following contraction, the TssBC sheath is disassembled by the action of the ATPase, TssH, presumably allowing recycling of these components. In *Vibrio cholerae*, the T6SS has been shown to fire from the same site, suggesting that the membrane associated complex or the baseplate structure remain intact between T6SS cycles. Conversely, in *P. aeruginosa*, assembly and re-assembly occur at different sites (Basler & Mekalanos, 2012).

1.4.3 Secreted effectors of the T6SS

The T6SS functions as either an anti-bacterial or an anti-eukaryotic system. The distinction between the target cell profile is at least partially dependent upon the type of effector proteins secreted by the system (Figure 1.11). In addition to this distinction, effector proteins of the T6SS may be divided into two different categories. A subset of effector proteins are fused to components of the T6SS, such as the effector domains of evolved VgrG (TssI) proteins and PAAR domain containing proteins. Alternatively, non-fused effectors are thought to be delivered by the T6SS via the interior of the TssB tube or non-covalent interactions with TssI proteins (Ho *et al.*, 2014).

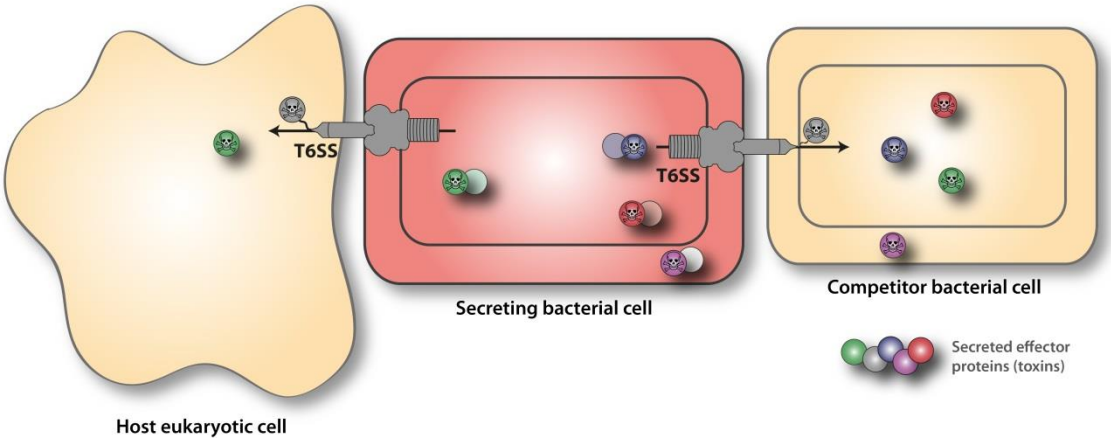

Figure 1.11. Schematic representation of Type VI Secretion System (T6SS) effector protein secretion into eukaryotic or bacterial target cells. The T6SS of the producing bacteria may target effector proteins to eukaryotic or bacterial cells. In order to protect against self-intoxication, the T6SS producing bacteria must also biosynthesise cognate immunity proteins (adapted from S. Coulthurst).

1.4.3.1 Anti-bacterial effector proteins of the T6SS

Many T6SSs, including the T6SS of *S. marcescens* Db10, target bacteria and several anti-bacterial effector proteins have been identified. The first identified and best characterised of these are the non-fused Tse1-3 proteins of *P. aeruginosa* (Hood *et al.*, 2010; Russell *et al.*, 2011). Comparison of the secretome of *P. aeruginosa* between

strains with an activated T6SS versus an inactive T6SS identified proteins that were present in the secretome only in the activated sample. Three of these proteins, Tse1-3, were shown to be dispensable for function of the Type VI system (Hood *et al.*, 2010; Russell *et al.*, 2011). Tse1 and Tse3 were subsequently shown to be peptidoglycan hydrolases that target distinct bonds within peptidoglycan (Russell *et al.*, 2011). Tse2 is known to exert its effects in the cytoplasm, however, the target of Tse2 remains elusive (Hood *et al.*, 2010). In addition to the identification of effector proteins, so called Tsi immunity proteins were also identified. The genes encoding cognate pairs of Tse and Tsi effector and immunity proteins are arranged in bicistronic operons, and are therefore expressed together (Hood *et al.*, 2010; Russell *et al.*, 2011). In *E. coli*, expression of the Tsi1 and Tsi3 immunity proteins negates the toxic effects of the cognate effector proteins Tse1 and Tse3, respectively. These toxic effects are alleviated through direct physical interaction between the cognate immunity and effector proteins (Russell *et al.*, 2011). Resolution of the crystal structure of the Tse1-Tsi1 complex revealed the mechanism of this inhibition; binding of Tsi1 occludes the active site of Tse1 (Benz *et al.*, 2012). Immunity proteins have therefore been proposed to protect against self or sibling cell intoxication.

Despite a lack of primary sequence homology, various T6SS secreted antibacterial effector proteins have been since been discovered in other bacteria. These bacteria include *V. cholerae* (Pukatzki *et al.*, 2009), *Pseudomonas protegens* (Whitney *et al.*, 2013), *Burkholderia thailandensis* (Russell *et al.*, 2012) and *S. marcescens* (English *et al.*, 2012). The repertoire of antibacterial effectors encoded within the bacterial genome is potentially extensive; in *B. thailandensis*, analysis of the secretome unveiled 13 putative effector proteins. On closer inspection, two effector proteins were found to resemble bacteriocins and one was shown to possess peptidoglycan hydrolase activity (Russell *et al.*, 2012). Subsequently, another putative effector protein was

demonstrated to possess phospholipase activity, which would result in perturbation of the bacterial membrane (Russell *et al.*, 2013). In *S. marcescens* Db10, Ssp1 and Ssp2 (secreted small protein 1 and 2), which are encoded within the T6SS gene cluster, were identified as non-fused T6SS dependent effectors that exert their toxic effect in the periplasm through the hydrolysis of peptidoglycan (Figure 1.12) (English *et al.*, 2012; Srikannathasan *et al.*, 2013). The cognate immunity proteins of Ssp1 and Ssp2 are Rap1a and Rap2a (resistance associated protein 1a and 2a). In *S. marcescens* Db10, the Rap resistance proteins appear to be highly specific to their immunity proteins and no cross interactions between non-cognate pairs of proteins are observed (English *et al.*, 2012). In addition to Ssp1 and Ssp2, the Ssp3, Ssp4, Ssp5 and Ssp6 proteins were subsequently identified as non-fused antibacterial effectors of the T6SS in this organism. Ssp3-6 are encoded outwith the T6SS and were identified by comparing the secretome of wildtype *S. marcescens* Db10 with that of a T6SS mutant (Figure 1.12). Ssp4 likely exerts its toxic effects in the periplasm of target cells whereas Ssp3, Ssp5 and Ssp6 are likely cytoplasmic toxins, although the target of these toxins remains to be identified (Fritsch *et al.*, 2013).

1.4.3.2 Anti-eukaryotic effector proteins of the T6SS

Not only can the T6SS target effectors to bacterial cells, but it can also secrete eukaryotic specific effectors. The first of these to be identified was the VgrG-1 protein (a TssI family protein) of *V. cholerae*. In this case, an extra C-terminal extension of the core protein was identified as possessing actin crosslinking activity (Pukatzki *et al.*, 2007). In phagocytes, the actin crosslinking domain is only translocated into the target upon internalization of the bacteria. This results in impairment of phagocytosis and phagocytic cell death (Ma *et al.*, 2009a). Since bacteria must be internalized for

activation of the actin crosslinking activity, it has been suggested that this behaviour is altruistic, and functions to protect remaining external bacteria from phagocytosis (Coulthurst, 2013). In addition to the VgrG-1 protein of *V. cholera*, only two other experimentally verified anti-eukaryotic TssI proteins have been identified. These are VgrG-1 of *Aeromonas hydrophila* and VgrG-5 of *Burkholderia pseudomallei* (Suarez *et al.*, 2010; Toesca *et al.*, 2014). In *A. hydrophila*, VgrG-1 induces ADP ribosylation of target cell actin in a T6SS dependent manner, leading to cell rounding and eventual death. Since *A. hydrophila* causes gastroenteritis, these effects have been proposed to play a role in disruption of the host's intestinal epithelial barrier (Suarez *et al.*, 2010). In *B. pseudomallei*, VgrG-5 is required for the fusion of mammalian cells to generate mononucleated giant cells (MNGCs). These MNGCs aid in the intracellular spread of *Burkholderia* (Toesca *et al.*, 2014). In the above examples, the effector domain is fused to part of the TssI protein, and so these proteins have been named "evolved VgrGs". To date, non-fused anti-eukaryotic effector proteins have only been described in two organisms. In *P. aeruginosa*, the effector proteins PldA and PldB were shown to be phospholipases required for internalization of bacteria into HeLa and epithelial cells (Jiang *et al.*, 2014). In *V. cholerae*, the effector proteins TseL (also a phospholipase) and VasX were shown to be required for killing of *Dictyostelium discoideum (Dong et al., 2013; Miyata et al., 2011).*

1.4.3.3 Selection of secreted effectors of the T6SS

In the case of the evolved VgrG proteins, specific mechanisms for targeting the effector to the secretion apparatus is are unnecessary. However, non-fused effector proteins must be targeted to the secretion apparatus for translocation. T6SS effector proteins do not possess a recognisable secretion signal, partly contributing to the

difficulties associated with identifying novel effectors. The mechanism of effector export is not yet fully understood, however, some progress has been made recently in trying to elucidate this process. The Tse1-3 effector proteins of *P. aeruginosa* have been shown to interact with the inner surface of the TssD1 tube and this interaction was demonstrated to be essential for secretion of the effectors (Silverman *et al.,* 2013). Alternatively, effector proteins may associate with TssI. Many PAAR repeat proteins, which were demonstrated to bind to the tip of the TssI needle, are predicted to possess extra domains with toxic enzymatic activities. Interaction with TssI proteins through the effector protein PAAR repeat domain was proposed to mediate export (Shneider *et al.,* 2013). Additionally, several Rhs family proteins, which are examples of evolved PAAR proteins, are genetically closely associated with TssI genes. These Rhs family proteins were shown to exert toxic effects on bacterial target cells only in the presence of their cognate TssI protein (Hachani *et al.,* 2014). It therefore seems that in certain instances association with TssD mediates export, whilst in other cases binding to TssI facilitates export of effectors.

1.4.4 Regulation of the T6SS

As might be expected, regulation of the T6SS varies in different organisms and likely reflects the different lifestyles inhabited by different bacteria. The T6SS is regulated at the transcriptional, post-transcriptional and post-translational level. At the transcriptional level, the T6SS can be regulated by quorum sensing, temperature, biofilm formation, iron depletion, salinity or in response to general stress conditions (Ho *et al.,* 2014). Several transcriptional regulators have been identified as playing a role in T6SS regulation under variations of the conditions described above (Ho *et al.,* 2014). Notably, organisms that possess more than one T6SS may display differential

regulation of the systems (Salomon *et al.*, 2013). At the post-transcriptional level, the RNA binding protein, Hfq, has been implicated in the regulation of the T6SS in certain organisms, including *S. marcescens* Db10 (S. Murdoch, unpublished).

At the post-translational level, a protein called Fha has been implicated in the regulation of the T6SS via the threonine phosphorylation pathway (TPP). Fha has been identified in around 40% of T6SSs, including that of *S. marcescens* Db10 (Figure 1.12) (Boyer *et al.*, 2009; Fritsch *et al.*, 2013). In *S. marcescens* Db10 and in *P. aeruginosa* Fha dependent activation of the T6SS is reliant on its phosphorylation status, this is controlled by a threonine kinase (PpkA) and a phosphatase (PppA) (Fritsch *et al.*, 2013; Mougous *et al.*, 2007). Post-translational regulation through Fha has been best described in *P. aeruginosa*. In this organism, activation of PpkA results in autophosphorylation of PpkA and subsequent phosphorylation of Fha (Mougous *et al.*, 2007). Since PpkA is required for activation of the system, deletion of the kinase abolishes T6 dependent secretion. Conversely, deletion of PppA results in an up-regulation of T6SS dynamics (Mougous *et al.*, 2007). Additional Tag (Type VI secretion associated gene) proteins (TagQRST) control the activation of PpkA. TagS and TagT are hypothesised to form an inner membrane bound complex in *P. aeruginosa*, although their specific role in regulation of PpkA activation remains unclear. TagQ is an outer membrane lipoprotein that is required for the correct localisation of the periplasmic protein, TagR, to the outer membrane. It is thought that TagQRST may form a trans-membrane signalling complex that functions to transduce the T6SS activating signal through the TPP (Casabona *et al.*, 2013). It has been suggested that the TPP in *P. aeruginosa* is activated upon sensing of membrane pertubations, which may be induced by the T6SS, or some other secretory system, of an adjacent cell. This allows the T6SS to become assembled at the point of an exogenous attack (Basler *et al.*, 2013; Ho *et al.*, 2013). This phenomenon has been termed duelling.

Since the T6SS of *P. aeruginosa* only fires upon sensing of incoming Type VI attacks from neighbouring cells, it has been described as defensive. In other systems, the T6SS is described as offensive, as bacteria do not need to sense an incoming attack to deploy the T6SS. This appears to be the case in *S. marcescens* Db10, where the system is constitutively active even when there is no cell-cell contact (Fritsch *et al.*, 2013; Murdoch *et al.*, 2011). Phosphorylation of Fha by PpkA is also required for activation of the T6SS in *S. marcescens* Db10. PppA also has an important modulatory role, as seen by a reduction in T6-dependent bacterial killing in its absence. For example, PppA may be required to facilitate disassembly and reassembly of the system at new spatial locations, as suggested for *P. aeruginosa* (Basler 2013). However, activation of the TPP in *S. marcescens* Db10 does not depend on cell-cell contact and is seen under all conditions tested. The TagQRST genes are also absent in *S. marcescens* Db10, implying that the signal which activates secretion in this organism is sensed via a different mechanism (Figure 1.12) (Fritsch *et al.*, 2013).

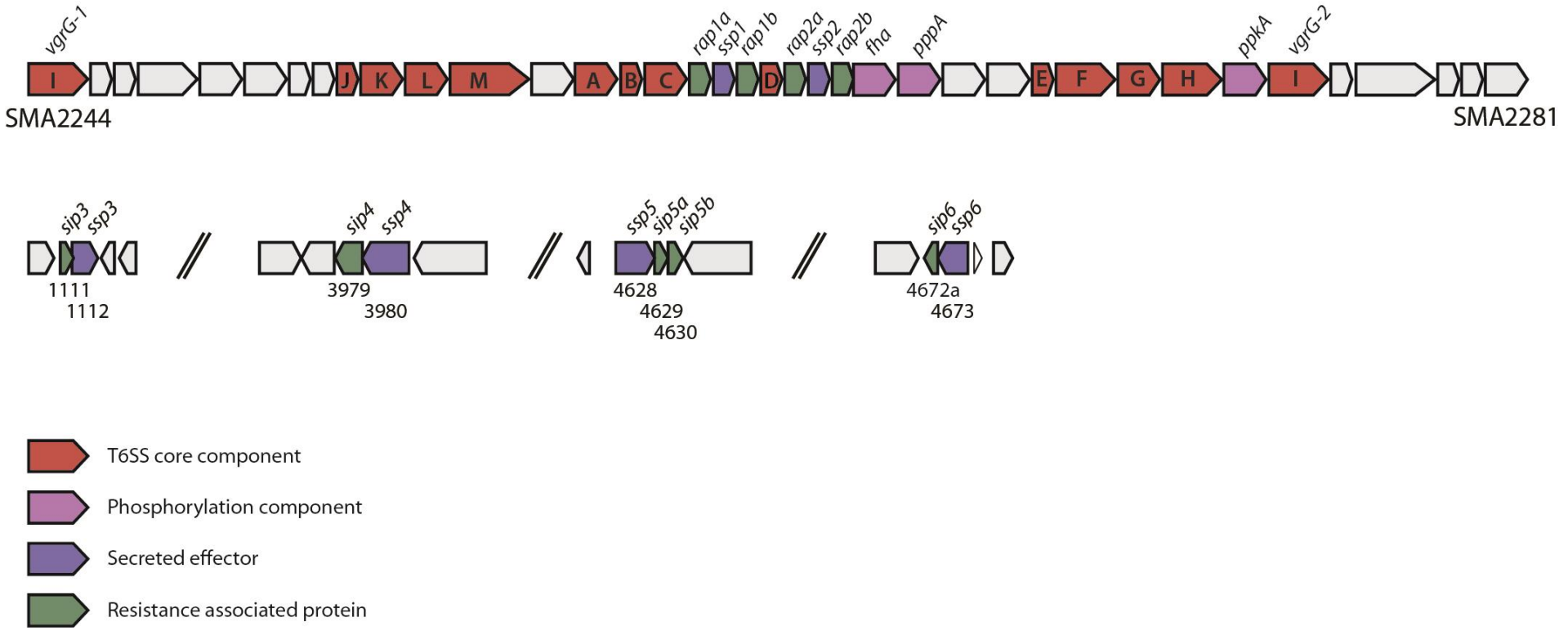

Figure 1.12. Schematic representation of the Type VI Secretion System (T6SS) of *Serratia marcescens* Db10. Core T6SS components, phosphorylation components, effector proteins and resistance associated proteins are indicated. Arrows represent open reading frames and are drawn approximately to scale. The direction of transcription is indicated by the direction of the corresponding arrow. Adapted from (Fritsch *et al.*, 2013).

Chapter 2

Materials and methods

2.1 Bacterial strains and plasmids

Bacterial strains and plasmids used in this study are provided in Table 2.1.

Table 2.1. Bacterial strains and plasmids used in this study

Bacterial Strain / Plasmid	**Description** [a]	**Source or Reference** [b]
Bacillus subtilis		
NCIB3610	Wild type NCIB3610 prototroph	B.G.S.C.
NRS1473	NCIB3610 *sacA-P* hy-spac-*gfp* (Kan)	(Verhamme *et al.*, 2009)
Micrococcus luteus ATCC4698		M. Bibb
Staphylococcus aureus 113	ATCC35556	T. Palmer
Escherichia coli		
MC1061	*F'lacIQ lacZM15* Tn*10* (Tet) Cloning host	(Perego & Hoch, 1988)
CC118λ*pir*	Cloning host and donor strain for pKNG101-derived marker exchange plasmids (λ*pir*)	(Herrero *et al.*, 1990)
HH26 pNJ5000	Mobilizing strain for conjugal transfer (Tet)	(Grinter, 1983)

Bacterial Strain / Plasmid	**Description** [a]	**Source or Reference** [b]
Serratia marcescens		
Db10	Wild type strain	(Flyg *et al.*, 1980)
ATCC274	Wild type	A.T.C.C.
NRS2992	*S. marcescens* Db10 *SMA2290::*Tn*5*	This Study
SJC13	*S. marcescens* Db10 *SMA2290::*Tn*5*	This Study
SAN2	*S. marcescens* Db10 (Δ*alb1*) in-frame	This study
SAN89	*S. marcescens* Db10 (Δ$alb1_{5\text{-}105}$) in-frame	This study
SAN177	*S. marcescens* Db10 (Δ$alb1_{300\text{-}400}$) in-frame	This study
SAN3	*S. marcescens* Db10 (Δ*alb2*) in-frame	This study
SAN4	*S. marcescens* Db10 (Δ*alb3*) in-frame	This study
SAN88	*S. marcescens* Db10 (Δ$alb3_{51\text{-}262}$) in-frame	This study
SAN5	*S. marcescens* Db10 (Δ*alb4-5*) in-frame	This study
SAN60	*S. marcescens* Db10 (Δ*alb6*) in-frame	This study
SAN100	*S. marcescens* Db10 P_{T5}-*alb1-6* (T5 promoter replacing native promoter upstream of *alb1*)	This study
SAN96	*S. marcescens* Db10 (Δ*SMA4147*) in-frame	This study
SAN112	*S. marcescens* Db10 (*SMA2452*::Cml)	This study
JESM267	*S. marcescens* Db10 *swrA::Tn5*	(Pradel *et al.*, 2007)

Bacterial Strain / Plasmid	**Description** [a]	**Source or Reference** [b]
SAN124	*S. marcescens* Db10 *swrA::Tn5* (Δ*alb4-5*) in-frame	This study
SAN176	*S. marcescens* Db10 (Δ*SMA4415/entB*) in-frame	This study
SAN180	*S. marcescens* Db10 (Δ*SMA4415/entB*) in-frame, (Δ*alb4-5*) in-frame	This study
SAN181	*S. marcescens* Db10 (Δ*SMA4415/entB*) in-frame, (Δ*alb4-5*) in-frame, *swrA::Tn5*	This study
SAN157	*S. marcescens* Db10 *tssJ-mCherry* (translational fusion)	This study
SAN158	*S. marcescens* Db10 *tssK-mCherry* (translational fusion)	This study
SAN159	*S. marcescens* Db10 *tssH-mCherry* (translational fusion)	This study
SAN162	*S. marcescens* Db10 *tssL-mCherry* (translational fusion)	This study
SAN163	*S. marcescens* Db10 *tssB-mCherry* (translational fusion)	This study
SAN164	*S. marcescens* Db10 *fha-mCherry* (translational fusion)	This study
SAN166	*S. marcescens* Db10 *tssE-mCherry* (translational fusion)	This study
SAN186	*S. marcescens* Db10 *vgrG2-mCherry* (translational fusion)	This study
SAN195	*S. marcescens* Db10 *lacZ::*P_{T5}*-gfpmut2-kan*	This study
SAN199	*S. marcescens* Db10 *lacZ::*P_{T5}*-gfpmut2-kan*, *tssB-mCherry* (translational fusion)	This study
SAN207	*S. marcescens* Db10 *tssB-gfpmut2*	This study
SAN208	*S. marcescens* Db10 *tssB-gfpmut2 tssJ-mCherry*	This study
SAN209	*S. marcescens* Db10 *tssB-gfpmut2 tssH-mCherry*	This study
SAN210	*S. marcescens* Db10 *tssB-gfpmut2 tssL-mCherry*	This study

Bacterial Strain / Plasmid	**Description** [a]	**Source or Reference** [b]
Plasmids		
pSUPROM	Vector for constitutive expression of cloned genes under the control of the *E. coli tat* promoter (Kan)	(Jack *et al.*, 2004)
pBluescript KS+	High copy cloning vector (Amp)	Stratagene
pKNG101	Suicide vector for marker exchange (Sm, *sacBR, mobRK2*, ori *R6K*)	(Kaniga *et al.*, 1991)
pQE-80L	Protein overexpression vector; source of T5 promoter	Qiagen
pmCherry-N1	Source of *mCherry* for generation of translational fusion strains	C. Rickman
pBL165	Source of *gfpmut2* for generation of translational fusion strains and for generation of constitutively expressing *gfp* strain	(Stanley *et al.*, 2003)
pNW573	pKNG101-derived marker exchange plasmid for the generation of chromosomal Δ*alb1*	This study
pSAN25	pKNG101-derived marker exchange plasmid for the generation of chromosomal Δ$alb1_{5\text{-}105}$	This study
pSAN66	pKNG101-derived marker exchange plasmid for the generation of chromosomal Δ$alb1_{300\text{-}400}$	This study
pNW577	pKNG101-derived marker exchange plasmid for the generation of chromosomal Δ*alb2*	This study
pNW579	pKNG101-derived marker exchange plasmid for the generation of chromosomal Δ*alb3*	This study
pSAN24	pKNG101-derived marker exchange plasmid for the generation of chromosomal Δ$alb3_{51\text{-}262}$	This study
pNW572	pKNG101-derived marker exchange plasmid for the generation of chromosomal Δ*alb4-5*	This study
pSAN8	pKNG101-derived marker exchange plasmid for the generation of chromosomal Δ*alb6*	This study
pSAN31	pKNG101-derived marker exchange plasmid for the generation of chromosomal Δ*SMA4147*	This study

Bacterial Strain / Plasmid	**Description** [a]	**Source or Reference** [b]
pSAN40	pKNG101-derived marker exchange plasmid for the generation of chromosomal *SMA2452*(*pswP*)::Cml	This study
pSAN1	*alb1* coding sequence in pSUPROM	This study
pSAN2	*alb2* coding sequence in pSUPROM	This study
pSAN3	*alb3* coding sequence in pSUPROM	This study
pSAN32	*alb6* coding sequence in pSUPROM	This study
pSAN81	*SMA2452* (*pswP*) coding sequence in pSUPROM	This study
pSAN51	pKNG101-derived marker exchange plasmid for the generation of *tssJ-mCherry* translational fusion	This study
pSAN52	pKNG101-derived marker exchange plasmid for the generation of *tssK-mCherry* translational fusion	This study
pSAN53	pKNG101-derived marker exchange plasmid for the generation of *tssH-mCherry* translational fusion	This study
pSAN57	pKNG101-derived marker exchange plasmid for the generation of *tssE-mCherry* translational fusion	This study
pSAN58	pKNG101-derived marker exchange plasmid for the generation of *fha-mCherry* translational fusion	This study
pSAN60	pKNG101-derived marker exchange plasmid for the generation of *tssL-mCherry* translational fusion	This study
pSAN61	pKNG101-derived marker exchange plasmid for the generation of *tssB-mCherry* translational fusion	This study
pSAN70	pKNG101-derived marker exchange plasmid for the generation of *vgrG2-mCherry* translational fusion	This study
pSAN72	pKNG101-derived marker exchange plasmid for the generation of chromosomal *lacZ::*P_{T5}*-gfpmut2-kan*	This study
pSAN79	pKNG101-derived marker exchange plasmid for the generation of *tssB-gfpmut2* translational fusion	This study

a. The antibiotic resistances are represented as follows: Amp, ampicillin; Cml, chloramphenicol; Kan, kanamycin; Tet, tetracycline; Sm, streptomycin.
b. B.G.S.C. is the *Bacillus* genetic stock centre.

2.2 Primers

Table 2.2. Primers used in this study

Primer Name	Sequence (5'- 3')[a]	Amplified Region
NSW755	GACTAGGAAGTTGAGTCG	3’ end of the Tn5 cassette
NSW756	TAGTGCGTAGAAGGGCTG	3’ end of the Tn5 cassette
NSW686	CGATAAAGACGTAGCTGGCCAT	internal *alb1*
NSW688	CGTGGCGTCATTTTCAATCC	internal *alb1*
NSW681	CATCAGGCGTCACTTCAAAA	internal *alb2*
NSW682	TCGCCAGACATATGATCAATC	internal *alb2*
NSW1105	GCATCCCGCTGGAAAACCC	internal *alb3*
NSW1107	GGTGGCGTGAGGAAACTGA	internal *alb3*
NSW689	GGCGCTACGTAATGCGCTTT	internal *alb4*
NSW674	GGCCAAGGAAGAACAACAGGCGTT	internal *alb4*
NSW695	CCAGAACTTGCTTTGATTTTCAGG	internal *alb5*
NSW697	CATCTTGAGCGAGGCGAATG	internal *alb5*
NSW692	GCACAACGCCTCTGAAAAG	internal *alb6*
NSW693	CGGATAGCGTCATATTCTTGC	internal *alb6*
NSW1101	TAACGGAGAGCGTATACCCTGC	internal *sma2294*
NSW1102	CTTCGTCGAATATCAAAATGCGGAA	internal *sma2294*

Primer Name	**Sequence (5'- 3')[a]**	**Amplified Region**
NSW699	GTCAAAGCTTGAAAAAACGCAC	junction *alb1* to *sma2294*
NSW1100	GCAGGGTATACGCTCTCCGTTA	junction *alb1* to *sma2294*
NSW685	GCGCTGTTCCCATTTATCAG	junction *alb1* to *alb2*
NSW687	ATGGCCAGCTACGTCTTTATCG	junction *alb1* to *alb2*
NSW696	CCTGAAAATCAAAGCAAGTTCTGG	junction *alb5* to *alb6*
NSW694	GCAAGAATATGACGCTATCCG	junction *alb5* to *alb6*
DEN5	TCACGRCACGAGCTGACGAC	internal 16S rRNA
DEN7	ACTCCTACGGGAGGCAGC	internal 16S rRNA
SC2127	TATATCTAGACAAGGCGCAGGACAAAGC	Forward primer for the upstream flanking region of *alb1*; encodes *Xba*I site. For generation of Δ*alb1* strain.
SC2128	TGTGAAGCTTACAGAACATTAATCCGAATGTTAATAACC	Reverse primer for the upstream flanking region of *alb1*; encodes *Hind*III site. For generation of Δ*alb1* strain.
SC2129	TATAAAGCTTCCCGGGAAAGCTGAAGAATAAATAATCGTTTTCGC	Forward primer for the downstream flanking region of *alb1*; encodes *Hind*III site. For generation of Δ*alb1* strain.
SC2130	TATAGGGCCCAGAACTCCACCAGCTCTCTCACC	Reverse primer for the downstream flanking region of *alb1*; encodes *Apa*I site. For generation of Δ*alb1* strain.
AG41	TATATCTAGATGCGCGGGTATTGGGC	Forward primer for the upstream flanking region of the 5' end of *alb1*; encodes *Xba*I site. For generation of Δ$alb1_{5\text{-}105}$ strain.

Primer Name	**Sequence (5'- 3')[a]**	**Amplified Region**
AG42	TATAAAGCTTCCAACAGAACATTAATCCG	Reverse primer for the upstream flanking region of the 5' end of *alb1*; encodes *Hind*III site. For generation of Δ*alb1*$_{5\text{-}105}$ strain.
AG43	TATAAAGCTTACTTCAATCGATCTTTTGATGTTG	Forward primer for the downstream flanking region of the 5' end of *alb1*; encodes *Hind*III site. For generation of Δ*alb1*$_{5\text{-}105}$ strain.
AG44	TATAGGGCCCTAGAGCGAGAATGCTG	Reverse primer for the downstream flanking region of the 5' end of *alb1*; encodes *Apa*I site. For generation of Δ*alb1*$_{5\text{-}105}$ strain.
AG147	TATAAAGCTTAAAGCTGAAGAATAAATAATCGTTTTC	Reverse primer for the downstream flanking region of the 3' end of *alb1*; encodes *Hind*III site. For generation of Δ*alb1*$_{300\text{-}400}$ strain.
AG148	TATATCTAGACAGGTAACCGTTTCATCACC	Forward primer for the downstream flanking region of the 3' end of *alb1*; encodes *Xba*I site. For generation of Δ*alb1*$_{300\text{-}400}$ strain.
AG149	TATAAAGCTTGCTGACGATGGCTAACG	Forward primer for the upstream flanking region of the 3' end of *alb1*; encodes *Hind*III site. For generation of Δ*alb1*$_{300\text{-}400}$ strain.
AG150	TATAGGGCCCGGATGTACCTACGCCACTTC	Reverse primer for the upstream flanking region of the 3' end of *alb1*; encodes *Apa*I site. For generation of Δ*alb1*$_{300\text{-}400}$ strain.
SC2155	TGTGTCTAGAATTCATGCGATTATCGTTGATTCC	Forward primer for the upstream flanking region of *alb2*; encodes *Xba*I site
SC2156	TGTGAAGCTTATTTTCCATAGATATTCTCCAGATGAAGG	Reverse primer for the upstream flanking region of *alb2*; encodes *Hind*III site

Primer Name	**Sequence (5'- 3')[a]**	**Amplified Region**
SC2157	TATAAAGCTTCCCGGGCAGGGATTCGAAAATATTGGTTGG	Forward primer for the downstream flanking region of *alb2*; encodes *Hind*III site
SC2158	TATAGGGCCCGACGATACAAAGCCACC	Reverse primer for the downstream flanking region of *alb2*; encodes *Apa*I site
SC2151	TATATCTAGACAGATTAAATTGAATGCCTATACCGTC	Forward primer for the upstream flanking region of *alb3*; encodes *Xba*I site. For generation of Δ*alb3* strain.
SC2152	TATAAAGCTTGAAACTATCCATACCCATCTCCATGA	Reverse primer for the upstream flanking region of *alb3*; encodes *Hind*III site. For generation of Δ*alb3* strain.
SC2153	TATAAAGCTTCCCGGGGCGGTAAAACCCTGATAACCC	Forward primer for the downstream flanking region of *alb3*; encodes *Hind*III site. For generation of Δ*alb3* strain.
SC2154	TATAGGGCCCTGGAAAGCCAACAGCAAAGC	Reverse primer for the downstream flanking region of *alb3*; encodes *Apa*I site. For generation of Δ*alb3* strain.
AG037	TATATCTAGACATTGCGGTGTGCATTTTC	Forward primer for the upstream flanking region of *alb3*; encodes *Xba*I site. For generation of $\Delta alb3_{51\text{-}262}$.
AG038	TATAAAGCTTCAGTTCAAGATTTCTCTCTAATGG	Reverse primer for the upstream flanking region of *alb3*; encodes *Hind*III site. For generation of $\Delta alb3_{51\text{-}262}$.
AG039	TATAAAGCTTATCTTTGGCGACATTATTC	Forward primer for the downstream flanking region of *alb3*; encodes *Hind*III site. For generation of $\Delta alb3_{51\text{-}262}$.

Primer Name	**Sequence (5'- 3')[a]**	**Amplified Region**
AG040	TATAGGGCCCAATATCCAGATCTTTC	Reverse primer for the downstream flanking region of *alb3*; encodes *Apa*I site. For generation of $\Delta alb3_{51\text{-}262}$.
SC2123	TATATCTAGATACTACCGTTATCAGACCTTGCTGG	Forward primer for the upstream flanking region of *alb4*; encodes *Xba*I site
SC2124	TGTGAAGCTTAATCTTCATGGATATTACTCTTTTGGG	Reverse primer for the upstream flanking region of *alb4*; encodes *Hind*III site
SC2125	TATAAAGCTTCCCGGGTGGACGCTGGCTTGATGG	Forward primer for the downstream flanking region of *alb5*; encodes *Hind*III site
SC2126	TATAGGGCCCGCTTCTGAAATCAACGTCATCC	Reverse primer for the downstream flanking region of *alb5*; encodes *Apa*I site
AG011	TATAAAGCTTCTCAAACCACATACGG CTTCC	Forward primer for the upstream flanking region of *alb6*; encodes *Hind*III site
AG012	TATATCTAGAAGGACAGGGAAATCT GCC	Reverse primer for the upstream flanking region of *alb6*; encodes *Xba*I site
AG013	TATAAAGCTTCAGCAGCTGGCGTAAA GCG	Forward primer for the downstream flanking region of *alb6*; encodes *Hind*III site
AG014	TATAGGGCCCACCTTTCTGGCGGCGG AATAC	Reverse primer for the downstream flanking region of *alb6*; encodes *Apa*I site
AG049	TATAGGGCCCGAATATGAAAATGCG	Forward primer for the upstream flanking region of the *alb* promoter; encodes *Apa*I site
AG050	TATAAAGCTTCCCTCTTCTGTCATGAGC	Reverse primer for the upstream flanking region of the *alb* promoter; encodes *Hind*III site
AG051	TATAAAGCTTAAATCATAAAAAATTTATTTGCTTTG	Forward primer to amplify the T5 promoter from pQE80; encodes *Hind*III site

Primer Name	**Sequence (5'- 3')[a]**	**Amplified Region**
AG052	TATAGGATCCTGTGTGAAATTGTTATCCG	Reverse primer to amplify the T5 promoter from pQE80; encodes *Bam*HI site
AG053	TATAGGATCCTTAACATTCGGATTAATGTTCTG	Forward primer for the downstream flanking region of the *alb* promoter; encodes *Bam*HI site
AG054	TATATCTAGATTTCTTCGTTTCCGGCAG	Reverse primer for the downstream flanking region of the *alb* promoter; encodes *Xba*I site
AG001	GCATGGATCCATGTTCTGTTGGAG	Forward primer for the *alb1* coding region; encodes *Bam*HI site for cloning into pSUPROM
AG002	GCATCTCGAGTTATTCTTCAGCTTTGC	Reverse primer for the *alb1* coding region; encodes *Xho*I site for cloning into pSUPROM
AG003	GCATGGATCCATGGAAAATGAAACC	Forward primer for the *alb2* coding region; encodes *Bam*HI site for cloning into pSUPROM
AG004	GCATCTCGAGTTAAATTATCCAACC	Reverse primer for the *alb2* coding region; encodes *Xho*I site for cloning into pSUPROM
AG007	GCATGGATCCATGGATAGTTTCGCCT CGCAT	Forward primer for the *alb3* coding region; encodes *Bam*HI site for cloning into pSUPROM
AG008	GCATCTCGAGTCAGGGTTTTACCGCC ACGAG	Reverse primer for the *alb3* coding region; encodes *Xho*I site for cloning into pSUPROM
AG035	TATAGGATCCTTGATTACGCCGCTCCCG	Forward primer for the *alb6* coding region; encodes *Bam*HI site for cloning into pSUPROM
AG036	GATACTCGAGTTACGCCAGCTGCTGATTC	Reverse primer for the *alb6* coding region; encodes *Xho*I site for cloning into pSUPROM
AG024	TTCGTCAAATTTGACAGCGAGATCG	Gene specific primer 1 (GSP1) internal to *alb2*; for ' Rapid amplification of cDNA ends (5'RACE)
AG025	ACAACATCAAAAGATCGATTGAAGTGG	GSP1 internal to *alb1*; for 5'RACE
NSW697a	CTTCCTCTCATTGTCCATGCC	GSP2 internal to *alb2*; for 5'RACE

Primer Name	**Sequence (5'- 3')[a]**	**Amplified Region**
NSW698	CAACGCGCCAAACACAAAT	GSP2 internal to *alb1*; for 5'RACE
SM044	GACCACGCGTATCGATGTCGACTTTTTTTTTTTTTTT	Anchor primer complimentary to poly(A) tail of cDNA; for 5'RACE
NSW685	GCGCTGTTCCCATTTATCAG	GSP3 internal to *alb2*; for 5'RACE
NSW699	GGACATCTCCACTTCAATACACCCAG	GSP3 internal to *alb1*; for 5'RACE
SM045	GACCACGCGTATCGATGTCGAC	Second anchor primer; for 5' RACE
AG063	TATATCTAGAGCGAACCTTGTACCGTGAG	Forward primer for the upstream flanking region of *SMA4147*; encodes *Xba*I site
AG064	TATAAAGCTTAAAATGACACGCCATTG	Reverse primer for the upstream flanking region of *SMA4147*; encodes *Hind*III site
AG065	TATAAAGCTTAAGACGCCCGGTTAAC	Forward primer for the downstream flanking region of *SMA4147*; encodes *Hind*III site
AG066	TATAGGGCCCCAGGCTTGTTCATTAC	Reverse primer for the downstream flanking region of *SMA4147* (*pswP*); encodes *Apa*I site
AG067	TATATCTAGACTATCAGGATTCGCTGTTCAC	Forward primer for the upstream flanking region of *SMA2452* (*pswP*); encodes *Xba*I site
AG068	TATAAAGCTTGATAAAAGTGGGCAACG	Reverse primer for the upstream flanking region of *SMA2452* (*pswP*); encodes *Hind*III site
AG071	TATAGGGCCCTTGTTTAAAGCGGCTGAC	Reverse primer for the downstream flanking region of *SMA2452* (*pswP*); encodes *Apa*I site
AG072	TATAAAGCTTGAAGGTGACGATGTCACG	Forward primer for the downstream flanking region of *SMA2452* (*pswP*); encodes *Hind*III site
AG092	TATAGGATCCTTGCCCACTTTTATCCG	Forward primer for the *SMA2452* (*pswP*) coding region; encodes *Bam*HI site for cloning into pSUPROM

Primer Name	**Sequence (5'- 3')[a]**	**Amplified Region**
AG093	TATACTCGAGTTAGCAAAAAATAAAAGTCGTGACAT	Forward primer for the *SMA2452* (*pswP*) coding region; encodes *Xho*I site for cloning into pSUPROM
AG157	TATAAAGCTTTTTTGGAATGGCCATCGA	Reverse primer for the upstream flanking region of *SMA4415* (*entD*); encodes *Hind*III site
AG158	TATAGGGCCCACATCCTGACGACGCAAG	Forward primer for the upstream flanking region of *SMA4415* (*entD*); encodes *Apa*I site
AG159	TATAAAGCTTGAAGAGAAAGCCTGATTTTAATAATG	Forward primer for the downstream flanking region of *SMA4415* (*entD*); encodes *Hind*III site
AG160	TATATCTAGATATTTGCCGGTGTCGGTC	Reverse primer for the downstream flanking region of *SMA4415* (*entD*); encodes *Xba*I site
AG097	CGCAAGGAACCGGAAAGGGAGCAGGAGCACCGGTCGCCACCATGG	Forward primer for amplification of *mCherry* from pmCherry-N1; overlaps with reverse primer for the upstream flanking region of the 3' end of *SMA2254* (*tssL*)
AG098	CCATGGTGGCGACCGGTGCTCCTGCTCCCTTTCCGGTTCCTTGCG	Reverse primer for the upstream flanking region of the 3' end of *SMA2254* (*tssL*); overlaps with forward primer for amplification of *mCherry* from pmCherry-N1
AG099	TATATCTAGACTTCCTGGCTTCGCTGC	Forward primer for the upstream flanking region of the 3' end of *SMA2254* (*tssL*); encodes *Xba*I site
AG100	CCTTGCGGCAAGCCGTTCTTGTACAGCTCGTCCATGCC	Reverse primer for amplification of *mCherry* from pmCherry-N1; overlaps with forward primer for the downstream flanking region of the 3' end of *SMA2254* (*tssL*)

Primer Name	**Sequence (5'- 3')[a]**	**Amplified Region**
AG101	GGCATGGACGAGCTGTACAAGAACGGCTTGCCGCAAGG	Forward primer for the downstream flanking region of the 3' end of *SMA2254* (*tssL*); overlaps with reverse primer for amplification of *mCherry* from pmCherry-N1
AG102	TATAGGGCCCGTGTCGAGCAGCA	Reverse primer for the downstream flanking region of the 3' end of *SMA2254* (*tssL*); encodes *Apa*I site
AG103	GCCCCGTAAAAAAGGTCGACGGAGCAGGAGCACCGGTCGCCACCATGG	Forward primer for amplification of *mCherry* from pmCherry-N1; overlaps with reverse primer for the upstream flanking region of the 3' end of *SMA2252* (*tssJ*)
AG104	CCATGGTGGCGACCGGTGCTCCTGCTCCGTCGACCTTTTTTACGGGGC	Reverse primer for the upstream flanking region of the 3' end of *SMA2252* (*tssJ*); overlaps with forward primer for amplification of *mCherry* from pmCherry-N1
AG105	TATATCTAGAAACAGGACTGCGTCAAAGTC	Forward primer for the upstream flanking region of the 3' end of *SMA2252* (*tssJ*); encodes *Xba*I site
AG106	CAGCGCAGCGGTAGGTCACTTGTACAGCTCGTCCATGCC	Reverse primer for amplification of *mCherry* from pmCherry-N1; overlaps with forward primer for the downstream flanking region of the 3' end of *SMA2252* (*tssJ*)
AG107	GGCATGGACGAGCTGTACAAGTGACCTACCGCTGCGCTG	Forward primer for the downstream flanking region of the 3' end of *SMA2252* (*tssJ*); overlaps with reverse primer for amplification of *mCherry* from pmCherry-N1
AG108	TATAGGGCCCCCTGGCAGTTCAGCATCG	Reverse primer for the downstream flanking region of the 3' end of *SMA2254* (*tssJ*); encodes *Apa*I site

Primer Name	**Sequence (5'- 3')[a]**	**Amplified Region**
AG109	CAGCCATACGGACCGGGGAGCAGGAGCACCGGTCGCCACCATGG	Forward primer for amplification of *mCherry* from pmCherry-N1; overlaps with reverse primer for the upstream flanking region of the 3' end of *SMA2253* (*tssK*)
AG110	CCATGGTGGCGACCGGTGCTCCTGCTCCCCGGTCCGTATGGCTG	Reverse primer for the upstream flanking region of the 3' end of *SMA2253* (*tssK*); overlaps with forward primer for amplification of *mCherry* from pmCherry-N1
AG111	TATATCTAGACCACCTCGATCATCTGCAC	Forward primer for the upstream flanking region of the 3' end of *SMA2253* (*tssK*); encodes *Xba*I site
AG112	GCTATTTTCCTGAGTCATAGGTTACTTGTACAGCTCGTCCATGCC	Reverse primer for amplification of *mCherry* from pmCherry-N1; overlaps with forward primer for the downstream flanking region of the 3' end of *SMA2253* (*tssK*)
AG113	GGCATGGACGAGCTGTACAAGTAACCTATGACTCAGGAAAATAGC	Forward primer for the downstream flanking region of the 3' end of *SMA2253* (*tssK*); overlaps with reverse primer for amplification of *mCherry* from pmCherry-N1
AG114	TATAGGGCCCGGCCGCCACAGCTTCT	Reverse primer for the downstream flanking region of the 3' end of *SMA2253* (*tssK*); encodes *Apa*I site
AG115	ATTCATTTGTCAATTTCAGGCAGGAGCAGGAGCACCGGTCGCCACCATGG	Forward primer for amplification of *mCherry* from pmCherry-N1; overlaps with reverse primer for the upstream flanking region of the 3' end of *SMA2274* (*tssH*)

Primer Name	**Sequence (5'- 3')[a]**	**Amplified Region**
AG116	CCATGGTGGCGACCGGTGCTCCTGCTCCTGCCTGAAATTGACAAATGAAT	Reverse primer for the upstream flanking region of the 3' end of *SMA2274* (*tssH*); overlaps with forward primer for amplification of *mCherry* from pmCherry-N1
AG117	TATATCTAGACTATGTCGGCTACGGCG	Forward primer for the upstream flanking region of the 3' end of *SMA2274* (*tssH*); encodes *Xba*I site
AG118	CTCGGCGGCCGCGGCGTTACTTGTACAGCTCGTCCATGCC	Reverse primer for amplification of *mCherry* from pmCherry-N1; overlaps with forward primer for the downstream flanking region of the 3' end of *SMA2274* (*tssH*)
AG119	GGCATGGACGAGCTGTACAAGTAACGCCGCGGCCGCCGAG	Forward primer for the downstream flanking region of the 3' end of *SMA2274* (*tssH*); overlaps with reverse primer for amplification of *mCherry* from pmCherry-N1
AG120	TATAGGGCCCGCGCCGATCCGAAGTC	Reverse primer for the downstream flanking region of the 3' end of *SMA2254* (*tssH*); encodes *Apa*I site
AG121	CAACAACGAGCGTGAGGATGGAGCAGGAGCACCGGTCGCCACCATGG	Forward primer for amplification of *mCherry* from pmCherry-N1; overlaps with reverse primer for the upstream flanking region of the 3' end of *SMA2258* (*tssB*)
AG122	CCATGGTGGCGACCGGTGCTCCTGCTCCATCCTCACGCTCGTTGTTG	Reverse primer for the upstream flanking region of the 3' end of *SMA2258* (*tssB*); overlaps with forward primer for amplification of *mCherry* from pmCherry-N1
AG123	TATATCTAGATGTTCTCTTGACGCATCCG	Forward primer for the upstream flanking region of the 3' end of *SMA2258* (*tssB*); encodes *Xba*I site

Primer Name	**Sequence (5'- 3')[a]**	**Amplified Region**
AG124	GCTCGTTGTTGTCGTCGTTCTTGTACAGCTCGTCCATGCC	Reverse primer for amplification of *mCherry* from pmCherry-N1; overlaps with forward primer for the downstream flanking region of the 3' end of *SMA2258* (*tssB*)
AG125	GGCATGGACGAGCTGTACAAGAACGACGACAACAACGAGC	Forward primer for the downstream flanking region of the 3' end of *SMA2258* (*tssB*); overlaps with reverse primer for amplification of *mCherry* from pmCherry-N1
AG126	TATAGGGCCCTCCATCTGCATCACGCTC	Reverse primer for the downstream flanking region of the 3' end of *SMA2258* (*tssB*); encodes *Apa*I site
AG127	CTTCGATCTGAAAGACATAGGGGGAGCAGGAGCACCGGTCGCCACCATGG	Forward primer for amplification of *mCherry* from pmCherry-N1; overlaps with reverse primer for the upstream flanking region of the 3' end of *SMA2271* (*tssE*)
AG128	CCATGGTGGCGACCGGTGCTCCTGCTCCCCCTATGTCTTTCAGATCGAAG	Reverse primer for the upstream flanking region of the 3' end of *SMA2271* (*tssE*); overlaps with forward primer for amplification of *mCherry* from pmCherry-N1
AG129	TATATCTAGAGAATTCCCACTGCACAGC	Forward primer for the upstream flanking region of the 3' end of *SMA2271* (*tssE*); encodes *Xba*I site
AG130	CCTATGTCTTTCAGATCGAAGTGCTTGTACAGCTCGTCCATGCC	Reverse primer for amplification of *mCherry* from pmCherry-N1; overlaps with forward primer for the downstream flanking region of the 3' end of *SMA2271* (*tssE*)

Primer Name	**Sequence (5'- 3')[a]**	**Amplified Region**
AG131	GGCATGGACGAGCTGTACAAGCACTTCGATCTGAAAGACATAGG	Forward primer for the downstream flanking region of the 3' end of *SMA2271* (*tssE*); overlaps with reverse primer for amplification of *mCherry* from pmCherry-N1
AG132	TATAGGGCCCGGCCAGGTAAAACATCAATTG	Reverse primer for the downstream flanking region of the 3' end of *SMA2271* (*tssE*); encodes *Apa*I site
AG139	GACCAAACCGGACGCGGGAGCAGGAGCACCGGTCGCCACCATGG	Forward primer for amplification of *mCherry* from pmCherry-N1; overlaps with reverse primer for the upstream flanking region of the 3' end of *SMA2267* (*fha*)
AG140	CCATGGTGGCGACCGGTGCTCCTGCTCCCGCGTCCGGTTTGGTC	Reverse primer for the upstream flanking region of the 3' end of *SMA2267* (*fha*); overlaps with forward primer for amplification of *mCherry* from pmCherry-N1
AG141	TATATCTAGAAAGTGGCGACGCATTGG	Forward primer for the upstream flanking region of the 3' end of *SMA2267* (*fha*); encodes *Xba*I site
AG142	CGGTTTGGTCTGTGAGTCTTTCTTGTACAGCTCGTCCATGCC	Reverse primer for amplification of *mCherry* from pmCherry-N1; overlaps with forward primer for the downstream flanking region of the 3' end of *SMA2267* (*fha*)
AG143	GGCATGGACGAGCTGTACAAGAAAGACTCACAGACCAAACCG	Forward primer for the downstream flanking region of the 3' end of *SMA2267* (*fha*); overlaps with reverse primer for amplification of *mCherry* from pmCherry-N1
AG144	TATAGGGCCCGCAGCGACTGTTCCAGTTC	Reverse primer for the downstream flanking region of the 3' end of *SMA2267* (*fha*); encodes *Apa*I site

[a] Primer engineered DNA restriction sites are underlined.

2.3 Materials

2.3.1 Growth media and growth conditions

Growth media used in this study are provided in Table 2.3 and Table 2.4. *E. coli* and *B. subtilis* were routinely cultured in LB medium overnight at 37 ^{o}C and with shaking at 200 rpm. *S. marcescens* and *Micrococcus luteus* were routinely cultured in low salt LB medium overnight at 30 ^{o}C and with shaking at 200 rpm, unless otherwise stated. S. *aureus* was routinely grown in TSB overnight at 37 ^{o}C and with shaking at 200 rpm, unless otherwise stated. Growth media were solidified through addition of agar to 1.5% (w/v).

When appropriate, antibiotics and supplements were added as described in Table 2.5.

Table 2.3. Growth media used in this study

Media	Components	Final concentration
Luria-Bertani (LB) medium	Tryptone Yeast extract NaCl	1 % (w/v) 0.5 % (w/v) 1 % (w/v)
Low salt LB medium	Tryptone Yeast extract NaCl	1 % (w/v) 0.5 % (w/v) 0.5 % (w/v)
Tryptic Soya Broth (TSB)	Tryptone Soyatone NaCl	1.5 % (w/v) 0.5 % (w/v) 0.5 % (w/v)
Minimal media glucose (MM)	Phosphate buffer $(NH_4)_2SO_4$ $MgSO_4$ Glucose	1 % (w/v) 0.1 % (w/v) 0.41 mM 0.2 % (w/v)
Minimal media high sucrose	Phosphate buffer $(NH_4)_2SO_4$ $MgSO_4$ Sucrose	1 % (w/v) 0.1 % (w/v) 0.41 mM 0.2 % (w/v)

Table 2.4. Composition of Chrome azurol S indicator plates

Media	Final volume	Components	Components
Chrome azurol S indicator (CAS) plates	100 ml	10x MM9 (pH7)	22.04 mM KH_2PO_4
			85.55 mM NaCl
			186.94 mM NH_4Cl
	100 ml	CAS-HDTMA	1 mM CAS
			1mM $FeCl_3$•6 H_20 in 10 mM HCl
			2 mM Hexadecyltrimethylammonium bromide (HDTMA)
	30 ml	Deferrated Casamino Acids	10 % Casamino acids (w/v)
	750 ml	CAS agar (pH 7)	112.5 mM NaOH
			75 mM Piperazine-N,N′-bis (2-ethanesulfonic acid) (PIPES)
	10 ml	20 % glycerol	
	1 ml	1 M $MgCl_2$	
	1 ml	1 M $CaCl_2$	

Table 2.5. Antibiotics or supplements used in this study

Antibiotic or supplement	**Final concentration**
Ampicillin or carbenicillin (Amp) (Cabenicillin was unsuitable for use with *S. marcescens*)	100 μg ml^{-1}
Kanamycin (Kan)	100 μg ml^{-1}
Tetracycline (Tet)	10 μg ml^{-1}
Streptomycin (Strep)	100 μg ml^{-1}
Isopropyl β-D-1-thiogalactopyranoside	50 μM

Table 2.6. Buffers and Solutions

Buffer / Solution	Component	Final concentration
Phosphate buffered saline (PBS)	NaCl	137 mM
	KCl	2.7 mM
	Na_2HPO_4	10 mM
	KH_2PO_4	1.8 mM
PBS Tween	NaCl	137 mM
	KCl	2.7 mM
	Na_2HPO_4	10 mM
	KH_2PO_4	1.8 mM
	Tween 20	0.1 % (v/v)
Phosphate buffer	Na_2HPO_4	57.5 mM
	NaH_2PO_4	42.3 mM
Phage buffer	Tris HCl pH 7.4	10 mM
	$MgSO_4$	10 mM
	Gelatine	0.1 % (w/v)
2x Sample buffer	Tris HCl pH 6.8	62.5 mM
	SDS	2 % (v/v)
	β-mercaptoethanol	15 % (v/v)
	Glycerol	25 % (v/v)
	Bromophenol blue	0.01% (w/v)
SDS-PAGE running buffer	Tris	25 mM
	Glycine	192 mM
	SDS	0.1 % (w/v)
Coomassie stain	Methanol	10 % (v/v)
	Acetic acid	20 % (v/v)
	Coomassie blue	Few grains per litre
Transfer buffer	Tris	25 mM
	Glycine	192 mM
	Methanol	10 % (v/v)

TAE buffer	Tris Acetic acid EDTA	40 mM 1.142 % (v/v) 1 mM

2.3.3 Antibodies

Table 2.7. Antibodies used in this study

Antibody	Dilution	Raised in	Supplier
Polyclonal Hcp antiserum	1 : 6,000	Rabbit	Eurogentec
Polyclonal Ssp2 antiserum	1 : 1,000	Rabbit	Eurogentec
mCherry	1 : 1,000	Rabbit	Eurogentec
Gfp	1 : 1,000	Mouse	Roche
Anti-Rabbit IgG – HRP conjugate	1 : 20,000	Goat	Thermo

2.4 Molecular biology techniques

2.4.1 DNA methods

2.4.1.3 Agarose gel electrophoresis

Separation of DNA fragments ranging from 100 bp – 10 kb in size was achieved by running the sample through 1 – 2 % (w/v) horizontal agarose gels containing 1x GelRed nucleic acid stain (Biotium). Agarose powder was dissolved in 1x TAE buffer by heating (Table 2.6). 1x TAE buffer was also used as a running buffer. DNA samples were mixed with 5x DNA loading dye (Bioline) prior to being loaded into the wells. DNA fragments were separated through application of a constant voltage of 80 – 120 V. DNA fragments were visualised by exposure to UV light and were photographed using a Bio-Rad Gel Doc XR. The approximate size of DNA fragments was estimated according to a DNA standard (100 bp ladder (Bioline) or 1kb ladder (NEB)), which was run alongside the DNA samples.

2.4.1.2 Plasmid purification

To purify plasmids from *E. coli*, the QIAprep Miniprep Kit (Qiagen) was used and manufacturer's instructions were followed. This technique is based on the alkaline lysis method originally described by Birnboim and Doly (Birnboim & Doly, 1979). Briefly, cells from an overnight culture were harvested by centrifugation at 13,000 rpm for 1 min. Cells were then re-suspended 250 µl buffer P1, containing RNase to degrade any RNA present. Cells were lysed by the addition of buffer P2, which contains SDS and NaOH to destroy the cell membrane and denature DNA. The addition of buffer N3 neutralised the cell lysate and allowed re-naturation of plasmid DNA. Cell debris, including chromosomal DNA, was removed by centrifugation at 13,000 rpm for 10 min. Cleared lysate was then loaded onto the binding column, which selectively binds DNA under high salt and low pH conditions. RNA, proteins and other metabolites were washed from the column by the addition of buffer PE. Since MC1061 is *endA*+, when purifying plasmids from this strain, an additional wash step with buffer PB was required to remove this endonuclease from the silica membrane. Plasmid DNA was then eluted from the binding column by the addition of 50 µl H_2O.

2.4.1.3 Genomic DNA (gDNA) purification

To extract gDNA for PCR purposes, the DNeasy Blood and Tissue Kit (Qiagen) was used. Manufacturer's instructions for extraction of gDNA from Gram-negative bacteria were followed. Briefly, cells from a 0.5 ml overnight culture were harvested by centrifugation at 13,000 rpm for 1 min. Cells were re-suspended in 180 µl Buffer ATL and were lysed by the addition of 20 µl proteinase K and then incubation at 56 ^{o}C for 25 min. Samples were vortexed thoroughly following the incubation step. 400 µl of a 1:1 ratio of Buffer AL : ethanol were then added to the sample and the sample mixed well

by vortexing. Cell lysate was then loaded onto the spin column which selectively binds DNA at the appropriate pH. The column was then washed by the addition of 500 µl Buffer AW1 and centrifugation at 13,000 rpm for 1 min. Buffer AL and Buffer AW1 contain guanidine hydrochloride for the denaturation of proteins. A second wash step was then performed by the addition of 500 µl Buffer AW2 and centrifugation at 13,000 rpm for 1 min. DNA was then eluted by the addition of 200 µl elution buffer to the column, incubation for 1 min at room temp and centrifugation at 8,000 rpm for 1 min.

2.4.1.4 Amplification of DNA by polymerase chain reaction

DNA fragments were amplified by the polymerase chain reaction (PCR) using the oligonucleotide primers described in Table 2.2. Qiagen Taq DNA polymerase was predominantly used for screening of potential clones whereas PCR fragments required for construction of new stains and plasmids were amplified using Phusion (NEB). Reaction mixes and cycling conditions for standard PCR reactions are detailed in Table 2.8, Table 2.9, Table 2.10 and Table 2.11

Table 2.8. Reaction mix for Taq polymerase (Qiagen) PCR reaction

Component	**Volume**
DNA template	1 µl
10x PCR buffer	5 µl
25 mM $MgCl_2$	5 µl
Q buffer	10 µl
10 mM dNTPs	1 µl
25 mM Forward primer	1 µl
25 mM Reverse primer	1 µl
Taq DNA polymerase	1 µl
H_2O	25 µl
Final volume	50 µl

Table 2.9 Reaction mix for Phusion (NEB) polymerase PCR reaction

Component	**Volume**
DNA template	1 μl
5x Phusion buffer	10 μl
10 mM dNTPs	1 μl
25 ml Forward primer	1 μl
25 ml Reverse primer	1 μl
Phusion DNA polymerase	0.5 μl
H_2O	35.5 μl
Final volume	50 μl

Table 2.10. Cycling conditions for Taq (Qiagen) polymerase

Step	**Temperature**	**Time (Min:Sec)**	**Cycles**
Denaturation	94 ^{o}C	2:00	1
Denaturation Annealing Elongation	94 ^{o}C 5 ^{o}C below primer Tm 72 ^{o}C	0:30 0:30 1:00 per kb	30
Final elongation	72 ^{o}C	10:00	1

Table 2.11. Cycling conditions for Phusion (NEB) DNA polymerase

Step	**Temperature**	**Time (Min:Sec)**	**Cycles**
Denaturation	98 ^{o}C	0:30	1
Denaturation Annealing Elongation	98 ^{o}C 3 ^{o}C above primer Tm 72 ^{o}C	0:10 0:30 0:30 per kb	35
Final elongation	72 ^{o}C	5:00	1

2.4.1.5 Restriction endonuclease digests

Purified DNA was digested by restriction endonuclease enzymes (NEB). Digests were performed using the supplied endonuclease buffer and were incubated at the recommended temperature for a minimum of 3 hours. Digests typically contained 1.5 μl of enzyme and 1 μg DNA in a 50 μl reaction.

2.4.1.6 Phosphatase treatment of digested plasmids

As required, digested vector DNA was dephosphorylated with 200 U of Calf Intestinal Phosphatase (CIP) (NEB) in the recommended buffer and in a total volume of 60 µl. The reaction was incubated at 37 ^{o}C for 30 min followed by a 5 min incubation at 65 ^{o}C to inactivate the enzyme.

2.4.1.7 Extraction of DNA from agarose gels

DNA fragments were excised from agarose gels and purified using QIAquick Gel Extraction kit (Qiagen) following the manufacturer's instructions.

2.4.1.8 DNA ligation

DNA fragments were inserted into linearised vectors using T4 DNA ligase (NEB). Reactions totalling 20 µl contained 1x T4 DNA ligase buffer, 400 U of T4 ligase, 2 µl purified vector DNA and 2, 4 or 6 µl insert DNA. Reactions were incubated at room temperature for a minimum of 1 hour. Following the ligation reaction, 10 µl ligation reaction was to transform 100 µl competent *E. coli* MC1061 cells.

2.4.1.9 DNA sequencing

Sequencing of DNA was performed by the DNA Sequencing Service at the College of Life Sciences, University of Dundee. Resulting sequences were analysed using the BLAST tool (Altschul *et al.*, 1997).

2.4.2 Generation of chemically competent *Escherichia coli* and transformation with plasmid DNA

Chemically competent *E. coli* cells were generated using the $CaCl_2$ method. An overnight culture of *E. coli* cells was diluted 10-fold into LB media. This culture was grown at 37^{o} C with shaking at 200 rpm until the OD_{600} was approximately 0.3. The cells were then chilled on ice for 30 min prior to centrifugation at 4,200 rpm for 10 min. Recovered cells were then re-suspended in 0.1 volume ice cold 0.1 M $CaCl_2$ and then pelleted as before. Cell pellets were again re-suspended in 0.04 volumes ice cold 0.1 M $CaCl_2$. The cells were then incubated overnight on ice. Glycerol was added to a final concentration of 10% and cells were stored at -80 ^{o}C.

Prior to transformation, *E. coli* cells were thawed on ice. Following the addition of plasmid DNA to the cells, cells were incubated on ice for 30 min. The cells were then heat shocked at 42 ^{o}C for 90 sec. The cells were then chilled on ice for 3 min prior to the addition of 1 ml LB. Finally, cells were allowed to recover at 37 ^{o}C for 1 hour prior to plating on selective media.

2.4.3 Generation of electro-competent *Serratia* and transformation with plasmid DNA

For preparation of electro competent cells, an overnight culture of *S. marcescens* was diluted 10-fold into low salt LB.media. The culture was grown at 30 ^{o}C with shaking at 200 rpm until the OD_{600} reached 0.4 – 0.6. The culture was then chilled on ice for a minimum for 1 hour prior to centrifugation at 4,200 rpm for 10 min. The cell pellets were re-suspended in 10 ml ice cold sterile H_2O and pelleted as before. The above wash step was repeated and cell pellets were then re-suspended in 10 ml ice cold

sterile 10 % (v/v) glycerol and pelleted as before. Finally, cell pellets were re-suspended in 1ml ice cold sterile 10 % (v/v) glycerol.

To transform electro competent cells, 100 µl cells were incubated 1 µl of DNA on ice for 10 min. Cells were transferred to an electro cuvette, then pulsed using Bio-Rad GenePulser with following settings: *E. coli*, 2 mm cuvette, 2.5 kV. 1 ml of LB medium was immediately added to the transformed cells and the cultures were incubated at 30 ^{o}C for 1 hour with shaking at 200 rpm. Cells were pelleted by centrifugation at 13,000 rpm for 1 min and then re-suspended in 100 µl of LB medium. Finally, cells were plated onto selective media.

2.4.4 Allelic marker exchange

S. marcescens Db10 chromosomal mutants with in-frame deletions in selected genes were constructed by allelic marker exchange using the suicide vector pKNG101. Upstream and downstream flanking regions (600-700 bp in length) of the target gene were cloned into pBluescript to generate a nonpolar, in-frame deletion of the gene (Table 2.1). This deletion allele was then cloned into pKNG101, and the resulting marker exchange plasmid was used to transform *E. coli* CC118λpir to generate a donor strain for introduction of the plasmid into *S. marcescens* Db10 by conjugation. A tri-parental mating was performed by mixing equal volumes of overnight cultures of the donor strain, recipient *S. marcescens* Db10 strain and a helper strain HH26 (pNJ5000) and then spotting 30 µl onto an LB plate which was incubated overnight at 30ºC.

Co-integrants were selected by streaking cells from the mating onto Minimal Medium glucose (MM) agar supplemented with streptomycin (100 µg ml^{-1}) and incubating overnight, at 30 ºC. Three single colonies were then purified on MM glucose agar supplemented with streptomycin (100 µg ml^{-1}) three times. To isolate resolvants,

overnight cultures of co-integrants were grown in LB medium with no selection, diluted to 10^{-6} in phosphate buffer and 100 µl plated on to MM high sucrose agar. A second round of growth on MM high sucrose was then performed.

Colonies on the MM high sucrose agar were replica patched onto LB agar and LB agar supplemented with streptomycin. Streptomycin sensitive candidates were chosen for further analysis. Candidates could be wild-type or mutant depending on the direction of the resolution event; therefore PCR was performed on gDNA using suitable primers to identify candidates with the correct allele. Candidates with the correct allele were struck through single colonies twice on LB agar. gDNA of final candidates was prepared and the mutation confirmed by PCR of the region surrounding mutation followed by sequencing of PCR products.

To construct the *mCherry* and *gfpmut2* translational reporter fusions, *mCherry* or *gfpmut2* coding regions were amplified from the relevant plasmid (Table 2.1) and cloned into pBluescriptKS+ containing the appropriate upstream and downstream flanking regions of the target gene. To construct the $T5_{alb1\text{-}6}$ strain (SAN100) expressing elevated levels of althiomycin, the T5 promoter was amplified from the relevant plasmid (Table 2.1) and cloned into pBluescriptKS+ containing the appropriate upstream and downstream flanking regions of the 5' start of *alb1*. The relevant fusions were then cloned into pKNG101 for introduction into the chromosome as described above.

2.4.5 Phage preparation and transduction

To prepare phage lysate, the required *S. marcescens* Db10 strain was grown overnight. Pre-existing ϕIF3 lysate was diluted 10^{-1} to 10^{-5} in phage buffer (Table 2.6) and each dilution then mixed with 200 µl *S. marcescens* Db10 overnight culture. Phage were incubated with the culture for 5 min prior to the addition of 4 ml molten low salt

LB 0.35 % agar. The mixture was then poured onto an LB plate and the plate incubated overnight at 30 ^{o}C. The following day, phage were harvested from the plate by collection of the top agar and addition of 3 ml phage buffer. 0.5 ml chloroform saturated with $NaHCO_3$ was added and the phage mixture then vortexed for 3 min. Agar was separated from the phage lysate by centrifugation of the phage mixture at 4,000 rpm at 4 ^{o}C for 20 min. The phage lysate was collected and stored with 20 μl chloroform and at 4 ^{o}C.

To transduce the allele of interest into the required strain, an overnight culture of the recipient strain was grown. 10 μl and 100 μl phage lysate were mixed with 2 ml of the overnight culture and the samples then incubated for 30 min statically at 22 ^{o}C. 10 ml low salt LB was then added and the samples mixed well. Cells were harvested by centrifugation at 4,000 rpm for 10 min at 22 ^{o}C. Cells were then re-suspended in 10 ml LB and harvested by centrifugation as before. Cells were re-suspended in 5 ml LB and incubated at 30 ^{o}C for 20 min. Finally, cells were again harvested by centrifugation as above and re-suspended in 30 μl LB. These cells were then plated onto LB containing the appropriate antibiotic to select for the required allele. At the same time, a cell only and phage only control were plated onto selective media to monitor background resistance. Plates were incubated overnight at 30 ^{o}C and candidate transductants were re-streaked twice on selective media to restrict phage carryover. The presence of the required allele was confirmed by PCR.

2.5 Transposon mutagenesis

2.5.1 Generation of transposon mutants

Random transposon mutagenesis was performed by a bi-parental conjugation with the donor strain (*E. coli* S17-1λPir harbouring plasmid pUT-mini-Tn5lacZ1 –

LacZ Kn^R transposon) and *S. marcescens* Db10 as the recipient strain. Donor and recipient strains were grown overnight at the required temperature and in the appropriate media; LB Amp for the donor strain and low salt LB for the recipient strain. The following day, the OD_{600} of the overnight cultures was adjusted to 1 and the donor and recipient strains were mixed at a ratio of 2:1 donor : recipient in a total volume of 40 μl. The cells were then recovered by centrifugation at 13,000 rpm for 1 min and re-suspended in 40 μl LB. 40 μl of the mixed culture, along with 40 μl of the donor and 40 μl of the recipient were then spotted onto an LB agar plate and incubated for 16 hours at 30 ^oC. The following day, the bacterial spots were harvested and re-suspended in 1ml LB. These cultures were then diluted 10 fold and 100 fold in LB. 100 μl of each of the diluted cultures were plated onto LB agar supplemented with 10 μg ml^{-1} Tet (to kill the donor strain) and 100 μg ml^{-1} Kan (to kill the recipient strain), 100 μl of the undiluted donor and recipient strains were also plated on the same medium to check for any background growth. Plates were then incubated at 30 ^oC for 24 hours.

To select for *S. marcescens* Db10 mutants affected positively or negatively in their ability to kill *B. subtilis*, individual *S. marcescens* Db10 Tn5 mutant colonies were streaked onto an LB agar plate and an LB agar plate + *B subtilis* lawn. 2,800 *S. marcescens* Db10 Tn5 mutants were screened. Mutants that showed an increased or decreased ability to kill *B. subtilis* were isolated from the LB agar plate and re-streaked to single colonies. From these single colonies, the mutant isolates were stocked.

2.5.2 Mapping of transposon insertion

Candidate mutants identified in the transposon mutagenesis screen were analysed to map the location of the transposon insertion. gDNA was isolated from each mutant, as described above, and diluted 1 in 2. This gDNA was digested with the

restriction enzyme αTaq1, as previously described. The restriction digest reaction was cleaned and 1 μl of the digested products were self-ligated in a total volume of 50 μl, as described above. The ligated DNA products were then amplified by PCR using outwardly directed primers (Table 2.2) that were designed to be specific for the terminal 3' fragment of Tn5. PCR products were visualised by gel electrophoresis and purified from the agarose gel as detailed above. Purified PCR products were then sequenced.

2.6 RNA techniques

2.6.1 Preparation of RNA

To isolate RNA from *S. marcescens* Db10, strains were grown in low salt LB for 6 hours and 10 μl of culture was then spotted onto an LB agar plate. For each strain, 3 culture spots were grown. These plates were then incubated for 16 hours at 30 ^{o}C. The following day, culture spots were harvested and 3 spots re-suspended in a total of 750 μl RNAwiz (Ambion). RNA was harvested using the RiboPure Bacteria RNA extraction kit (Ambion) according to the manufacturer's instructions. RNA was checked for quality and quantified using a Nanodrop.

2.6.2 Preparation of cDNA

RNA samples were reverse transcribed to cDNA for use in PCR. 1 μg of RNA was incubated with 2.1 μM random hexamers, 0.83 mM dNTPs and H_2O to a total of 12 μl. Samples were heated at 65 ^{o}C for 5 min then chilled to 4 ^{o}C before the addition of the following components: 4 mM dithiothreitol (DTT), 40 U RNaseOUT (Invitrogen), 1x First strand buffer (Invitrogen) and either 200 U Superscript III reverse transcriptase or RNase free H_2O as a negative control. Samples were then incubated at 25 ^{o}C for 5

min, 50 ^{o}C for 1 hour and 70 ^{o}C for 15 min. Samples were made to a final volume of 100 µl with RNase free H_2O for use in further applications.

2.6.3 5' Rapid amplification of cDNA ends (5'RACE)

The transcriptional start site for the *alb* operon was determined using 5'RACE conducted using DNase treated RNA harvested from *S. marcescens* Db10, as described above. To identify potential transcriptional start sites upstream of *alb1* or *alb2* we attempted to synthesise cDNA corresponding to the potential promoter regions for both genes. 5'RACE involves the generation of cDNA using a Gene Specific antisense Primer (GSP) which permits cDNA conversion of the mRNA of interest to the 5' end of the message. cDNA was synthesised using 250 ng RNA and the Gene Specific Primers (GSPs) AG024 and AG025, which were internal to *alb2* and *alb1*, respectively. RNA was mixed with 1 mM dNTPs, 5 µmol of either primer and H_2O to a total of 10µl. The reaction was then incubated at 65 ^{o}C for 10 minutes. The reaction mixture was then made up to a total volume of 20 µl with the addition of 1x first strand buffer, 5 mM $MgCl_2$, 10 mM DDT, 40 U RNase OUT (Invitrogen) and either 200 U Superscript III reverse transcriptase or RNase free H_2O as a control. The mixture was then incubated at 25 ^{o}C for 10 min, 50 ^{o}C for 50 min and 85 ^{o}C for 5 min (to inactivate the reverse transcriptase). The reaction was then cooled on ice. To remove any remaining RNA template, 5 U RNase H (NEB) was added to the reaction and the reaction incubated for a further 20 min at 37 ^{o}C. Finally the cDNA was purified using the Gel Extraction Kit (Qiagen) according to manufacturer's instructions.

Following cDNA synthesis, it is necessary to polyA tail the cDNA product. This allows amplification of the cDNA from GSP1 to the unknown 5' end of the cDNA. A polyT- anchor primer complementary to the polyA tail of the cDNA and a GSP2, which anneals upstream of GSP1, are required to amplify this product. To polyA tail the

cDNA, 12.5 µl cDNA was added to 1x *Terminal Deoxynucleotidyl Transferase (TDT) buffer, 0.5 mM $CoCl_2$, 0.5 mM dATP and 25 U Terminal Transferase (NEB). The reaction was incubated at 37 ^oC for 15 min and then 70 ^oC for 10 min to inactivate the terminal transferase. To amplify the resulting product, the anchor primer SM044 and the GSP2 primers NSW 697a (alb2*) and NSW698 (*alb1*) were used. 5 µl polyA tailed cDNA was added to 0.63 µM SM044, 0.63 µM GSP2, 0.1 mM dNTPs, 1x PCR buffer (Roche), 1.18 U Taq polymerase (Roche) and H_2O to a total of 50 µl. Reactions were then incubated as described in Table 2.12.

Table 2.12 Cycling conditions for PCR amplification of polyA tailed cDNA for 5'RACE

Step	Temperature	Time (Min:Sec)	Cycles
Denaturation	95 ^{o}C	2:00	1
Denaturation Annealing Elongation	95 ^{o}C 51 ^{o}C 72 ^{o}C	0:15 0:30 0:40	10
Denaturation Annealing Elongation	95 ^{o}C 51 ^{o}C 72 ^{o}C	0:15 0:30 2:00	25
Final elongation	72 ^{o}C	7:00	1

The presence of a PCR product was confirmed by agarose gel electrophoresis. It was determined that a second round of PCR was necessary to increase the quantity of product. This PCR was performed using the anchor primer SM045 and the GSP3 primers NSW685 (*alb2*) and NSW699 (*alb1*). 1 µl of PCR product from the previous reaction was added to 0.63 µM SM045, 0.63 µM GSP3, 0.1 mM dNTPs, 1x PCR buffer (Roche), 1.18 U Taq polymerase (Roche) and H_2O to a total of 50 µl. Reactions were then incubated as described in Table 2.13.

.

Table 2.13. Cycling conditions for second PCR amplification of polyA tailed cDNA for 5'RACE

Step	Temperature	Time (Min:Sec)	Cycles
Denaturation	95 ^{o}C	2:00	1
Denaturation 	95 ^{o}C 50 ^{o}C 72 ^{o}C	0:15 0:30 2:00	 35
	72 ^{o}C	5:00	1

The final PCR products were run on an agarose gel and the major bands purified by gel extraction (2.4.1.7). It should be noted that 3 major bands could be observed from the *alb2* PCR. All three bands were excised. The purified products were then cloned into pGEM-T Easy Vector (Promega) according to manufacturer's instructions. 10 plasmids from two independent rounds of 5'RACE were sequenced and the transcriptional start site was defined as the point at which the sequence of interest was no longer homologous to the upstream region of the relevant gene and instead became the polyA tail.

2.7 Protein methods

2.7.1 SDS polyacrylamide gel electrophoresis

The Bio-Rad mini-PROTEAN II System was used to separate proteins under denaturing conditions by SDS-polyacrylamide gel electrophoresis (SDS-PAGE) (Laemmli, 1970). The 15 % resolving gel for SDS-PAGE contained the following: 15 % (v/v) Acrylamide; 375 mM Tris-HCl pH 8.8; 0.1 % (v/v) SDS; 0.1 % (v/v) ammonium persulfate (APS); 0.04 % (v/v) Tetramethylethylenediamine (TEMED) and H_2O to a total volume of 10 ml. The resolving gel was poured to approximately 2 cm from the top between the two glass plates. Ethanol was applied to the top of the resolving gel to ensure a level gel. The ethanol was removed following polymerisation of the gel. The

stacking gel for SDS-PAGE contained the following: 5 % (v/v) acrylamide, 125 mM Tris-HCl pH6.8, 0.1 % (v/v) SDS, 0.1 % (v/v) APS, 0.1 % TEMED and H_2O to a total volume of 6 ml. Prior to loading, protein samples were mixed with the appropriate volume of Laemmli sample buffer (Table 2.6. Buffers and Solutions) and boiled for 5 min. Protein samples were run against 6 μl of Precision Plus Protein All Blue standards marker (Biorad). The gels were run in 1x SDS-PAGE running buffer (Table 2.6) for 15 min at 100 V, then for approximately 1 hour at 180 V.

2.7.2 Coomassie staining of polyacrylamide gels

Visualisation of proteins separated by electrophoresis through SDS-PAGE gels was achieved by staining with coomassie (Table 2.6. Buffers and Solutions.). Gels were incubated for 12 min with boiling coomassie and gentle shaking. To remove non-specifically bound stain, the gels were washed twice briefly with boiling H_2O and then washed overnight in H_2O.

2.7.3 Immunoblotting

Immunoblotting was conducted in order to detect TssD in cellular and secreted supernatant fractions and to detect Ssp2 in secreted supernatant samples. TssD cellular and supernatant samples were prepared as follows: an overnight low salt LB culture of the strain of interest was grown at 30 ^oC with shaking at 200 rpm and the following morning was diluted 1 in 200 in 25 ml low salt LB. This culture was grown for 7 hours in low salt LB medium with shaking at 200 rpm at 30^oC. The OD_{600} of the culture was then measured. Cellular samples were prepared by harvesting cells in 100 μl culture by centrifugation at 13,500 rpm for 1 min. The resulting cell pellet was then re-suspended in 200 μl Laemmli sample buffer and boiled for 10 min. Supernatant samples were prepared by centrifugation of a 1 ml sample of culture. 100 μl cell free supernatant was

then mixed with 100 µl Laemmli sample buffer and boiled for 10 min. To ensure equal volumes of protein were loaded, 6 µl of sample were loaded per OD_{600} 5.

To prepare Ssp2 protein samples, an overnight low salt LB culture of the strain of interest was grown at 30 ^{o}C with shaking at 200 rpm and the following morning was diluted 1 in 200 in 25 ml low salt LB. This culture was grown for 7 hours in low salt LB medium with shaking at 200 rpm at 30 ^{o}C. 20 ml culture was centrifuged at 16,000 rpm for 20 min to harvest the cells. 15 ml of the resulting supernatant was then mixed with 15 ml 1:1 (v/v) chloroform : methanol. This mix was centrifuged at 4,000 rpm for 5 min resulting in the secreted protein forming an interface between the aqueous layer at the top and the chloroform layer at the bottom. The liquid was removed from the precipitated protein and the protein pellet then washed in 1 ml methanol. The protein precipitate was again harvested by centrifugation at 13,500 rpm for 2 min and then re-suspended in 200 µl Laemmli sample buffer.

Following SDS-PAGE, proteins were transferred onto polyvinylidene difluoride (PVDF) membrane (Millipore). Electroblotting was performed using the Mini Trans-Blot Electrophoresis Transfer (Biorad) and transfer buffer (Table 2.6). The PVDF membrane was activated in 100 % methanol and rinsed in transfer buffer. The transfer cassette was then assembled as follows: transfer sponge-paper-gel-PVDF-paper-transfer sponge (cathode side up). Proteins were transferred at 4^{o}C for 90 min at 250 mA. Following transfer of the proteins, the PVDF membrane was washed briefly in PBST (Table 2.6) and then incubated for 1 hour at room temperature in 5 % (w/v) milk powder in TBST. To detect Hcp or Ssp2, the PVDF membrane was then incubated with the primary antibiody (Table 2.7) in 5 % (w/v) milk powder in PBST for 1 hour at room temperature. The membrane was then washed briefly 3 times and then 4 times for 5 min in PBST. The PVDF membrane was then incubated with the secondary antibody (Table

2.7) in PBST for 1 hour at room temperature. The membrane was washed again, as before, in PBST prior to the detection of proteins using a chemiluminescent detection kit (Millipore) according to manufacturer's instructions. The PVDF membrane was then exposed to X-ray film and developed using a Medical Film Processor SRX-101A (Konica Minolta).

2.7.5 Mass spectrometry

To identify protein bands in Coomassie gels, bands were excised from SDS-PAGE gels and subjected to in-gel trypsin digestion followed by one-dimensional nLC-ESI-MS/MS using a 4000 QTrap (Applied Biosystems) tandem mass spectrometry system by the FingerPrints Proteomics Facility at the College of Life Sciences, University of Dundee. The raw data was analysed using MASCOT software for protein identification. Proteins were identified using a combination of the highest MASCOT score and maximum peptide coverage.

2.8 UHPLC-ESI-TOF-MS analysis to identify althiomycin

5 ml of low salt LB was inoculated with 10 µl of overnight culture and the resulting culture was grown for 48 hours under the same conditions. Supernatant and methanol extracts of biomass were analysed by LC-MS on a Dionex 3000RS UHPLC coupled to a Bruker MaXis Q-TOF mass spectrometer. A Sigma Ascentis Express column (C18, 150 x 2.1 mm, 2.7 µm) was used. Mobile phases consisted of A (water containing 0.1% formic acid) and B (methanol containing 0.1% formic acid). A gradient of 20% B to 100% B in 15 minutes was employed with a flow rate of 0.2 ml/min. Absorbance at 270 nm was monitored. The mass spectrometer was operated in electrospray positive ion mode with a scan range of 50-2,000 m/z. Source conditions were: end plate offset at -500V; capillary at -4500V; nebulizer gas (N_2) at 1.6 bar; dry

gas (N_2) at 8 L/min; dry Temperature at 180 °C. Ion tranfer conditions: ion funnel RF at 200 Vpp; multiple RF at 200 Vpp; quadruple low mass at 55 m/z; collision energy at 5.0 ev; collision RF at 600 Vpp; ion cooler RF at 50-350 Vpp; transfer time at 121 µs; pre-Pulse storage time at 1 µs. Calibration was performed with sodium formate (10 mM) through a loop injection of 20 µL of standard solution at the beginning of each run.

2.9 Purification of althiomycin by HPLC for NMR

Althiomycin was purified from the supernatant of a spent LB culture by semi-preparative HPLC (Agilent Zorbax, RP-C18, 100 x 21 mm, 5 µm) on an Agilent 1100 instrument. Mobile phases consisted of A: water containing 0.1% formic acid and B: methanol containing 0.1% formic acid. The flow rate was 5 ml/min and absorbance at 270 nm was monitored. A gradient of 20% B (see above) to 100% B in 25 minutes was employed for the first purification. Fractions containing althiomycin were identified by MS and pooled. The pooled fractions were freeze-dried after solvent removal at reduced pressure; the dried material was then dissolved in a small volume of methanol and re-purified on the same column with a gradient of 60% B to 100% B over 25 minutes. Fractions containing althiomycin were freeze-dried and dissolved in 200 µl of d6-DMSO for NMR analysis

2.10 Phenotypic assays

2.10.1 Growth curves

Growth curves were performed to determine whether novel strains carried a growth defect. An overnight low salt LB culture of the strain of interest was grown overnight and the following morning was diluted 1 in 200 in 180 µl low salt LB in a 96 well plate. A Synergy 2 plate reader (Biotek) was used to incubate the plate at 30 ^{o}C

with continuous shaking. OD_{600} readings were taken every 20 min for 16 hours and results were then plotted on a logarithmic scale.

2.10.2 Antibacterial bioassay

Antibacterial bioassays were performed to determine whether the *S. marcescens* strain of interest was capable of producing of antibacterial metabolites. Both the *S. marcescens* strain and the bacterial strain used as the indicator lawn (*B. subtilis, M. luteus* or *S. aureus*) were grown in the appropriate media for 7 hours at the appropriate temperature. 100 µl of the indicator lawn was then spread onto an LB plate (*B. subtilis* and *M. luteus*) or a TSA plate (*S. aureus*), supplemented with antibiotics as required, and the plate allowed to dry. 10 µl of the *S. marcescens* culture was then spotted on top of the indicator lawn and the spots allowed to dry. Plates were then incubated at 30 ^{o}C for 16 hours (*B. subtilis* and *S. aureus*) or 30 hours (*M. luteus*). Photographs of plates were acquired with a Nikon D600 camera.

2.10.3 Competition assays

S. marcescens Db10 attacker and *S. marcescens* Db10, *P. fluorescens* and *S. marcescens* 274 target strains were grown overnight (*S. marcescens*) or for 48 hours (*P. fluorescens*) on an LB plate at 30 ^{o}C. Cells on the plate were harvested and re-suspended in LB, normalized to an OD_{600} of 0.5 and mixed at a ratio of 5:1 attacker : target. 25 µl of the mixture was then spotted onto an LB plate and incubated for 4 hours at 30 ^{o}C (*P. fluorescens* and *S. marcescens* 274) or for 16 hours at 30 ^{o}C (*S. marcescens*). A control containing LB rather than the attacker strain was also included. Cells were recovered from the spot and re-suspended in 1 ml low salt LB. Dilutions

were made and cells were plated onto the LB Strep plates to enumerate surviving target bacteria. The recovery of surviving cells is reported as the total number of bacterial target cells recovered per co-culture spot.

2.10.4 Chrome azurol S (CAS) assay

S. marcescens strains being tested for siderophore biosynthesis were grown to stationary phase at 30^{o}C and 10 µl of culture was spotted on to the CAS agar plate. The plates were incubated (15 h) at 30^{o}C prior to photography. For the complementation analysis, plasmids were maintained by the addition of Kan to culture media and to the CAS agar plates.

2.11 Microscopy

Cells were prepared for microscopy in one of two ways. For initial imaging of the mCherry protein fusion strains (SAN157, SAN158, SAN159, SAN162, SAN163, SAN164, SAN166 and SAN186), cells were plated onto LB and incubated for 16 hours at 30 ^{o}C. The following morning, cells were harvested from the plate and re-suspended in 1 ml 1x PBS. These cells were then diluted 1 in 10 in 1x PBS. 2 ml of this diluted cell suspension was spotted onto a 1.5 % agarose pad prior to microscopy. To optimize microscopy conditions, the relevant bacterial strains were grown overnight in low salt LB. The following morning the cultures were diluted to an OD_{600} of 0.15 in 25ml minimal media glucose (Table 2.3). Cells were grown for approximately 4 hours at 30^{o}C with shaking at 200 rpm and 1.5 µl of the cell suspension then was spotted onto a minimal media glucose pad solidified through the addition of 1.5 % agarose. SAN157, SAN159, SAN162, SAN163, SAN199, SAN207, SAN208, SAN209 and SAN210 were imaged under optimized microscopy conditions. Cells were grown for timelapse

fluorescence microscopy as for static imaging. Prior to imaging, the cell culture was diluted to an OD_{600} of 0.007. 1.5 µl of the cell suspension then was spotted onto a minimal media glucose pad solidified through the addition of 1.5 % agarose. Cells were allowed to equilibriate on the slide for 1 hour prior to imaging. Images were acquired using a DeltaVision Core widefield microscope (Applied Precision) mounted on an Olympus IX71 inverted stand with an Olympus 100X 1.4 NA lens and Cascade2_512 EMCCD camera (Photometrics), with Differential interference contrast (DIC) and fluorescence optics. Datasets (512 × 512 pixels with 13 Z sections spaced by 0.2 µm were acquired. GFP and mCherry were detected using a 100 W mercury lamp and an FITC (fluorescein isothiocyanate) filter set (excitation 490/20; emission 528/38) and a TRITC (Tetramethylrhodamine) filter set (excitation 555/28; emission 617/73), respectively. DIC images were acquired with an LED Transmitted light source (Applied precision) at 32 % intensity and exposure times between 25 and 100 ms. Post-acquisition data sets were rendered and analysed using OMERO software (http://openmicroscopy.org) (Allan *et al.*, 2012).

Chapter 3

The mechanism of biosynthesis of the antibiotic althiomycin in *Serratia marcescens* Db10

3.1 Introduction

Althiomycin is a broad-spectrum antibiotic that was first identified as a product of *Streptomyces althioticus* in 1957. The X-ray crystal structure of the molecule was solved in 1974 (Sakakibara *et al.*, 1974) and the total chemical synthesis of althiomycin and analogues has been achieved (albeit with low efficiency) (Inami & Shiba, 1985; Zarantonello *et al.*, 2002). However, despite being identified more than 50 years ago, prior to the initiation of this project, the mechanism of althiomcyin biosynthesis was unknown. Difficulties encountered during the chemical synthesis of althiomycin and the lack of availability of a genetically tractable producing organism likely hampered further studies into the medical potential of this antibiotic. The work presented in this chapter delineates the biological pathway for althiomycin synthesis in *S. marcescens* Db10 and was performed in collaboration with Gregory Challis and Lijiang Song (University of Warwick). Additionally, we investigate the role of *alb1* in althiomycin resistance and export. Whilst this project was underway, work was published describing the mechanism of althiomycin biosynthesis in the Gram-negative δ-proteobacteria, *Myxococcus xanthus*, and so a comparison of the proposed mechanism of althiomycin biosynthesis in both bacteria is discussed. Finally, the biotechnological potential for exploitation of the althiomycin NRPS/PKS biosynthetic proteins is considered.

3.2 Identification of the althiomycin biosynthetic gene cluster

3.2.1 *S. marcescens* Db10 is able to inhibit growth of Gram-positive bacteria

It was serendipitously discovered that *S. marcescens* Db10 produced a diffusible molecule capable of inhibiting the growth of the Gram-positive soil bacterium *Bacillus subtilis* (Figure 3.13.A). To establish whether or not this effect was restricted to *B. subtilis*, the analysis was extended to include the Gram-positive human pathogen

Staphylococcus aureus and Gram-positive human commensal *Micrococcus luteus*, revealing that these organisms are indeed also susceptible (Figure 3.13.A). To establish the point in growth at which *S. marcescens* Db10 produced the molecule capable of inhibiting the growth of *B. subtilis*, the presence of this activity in the cell-free culture supernatant was assayed over 8 hours of growth. From this it was established that the activity was detectable in the stationary phase of growth, consistent with the diffusible compound being a secondary metabolite (Figure 3.13.B). On the basis of these experiments it was concluded that *S. marcescens* Db10 was capable of inhibiting the growth of Gram-positive bacteria by biosynthesis of a diffusible compound with antimicrobial activity.

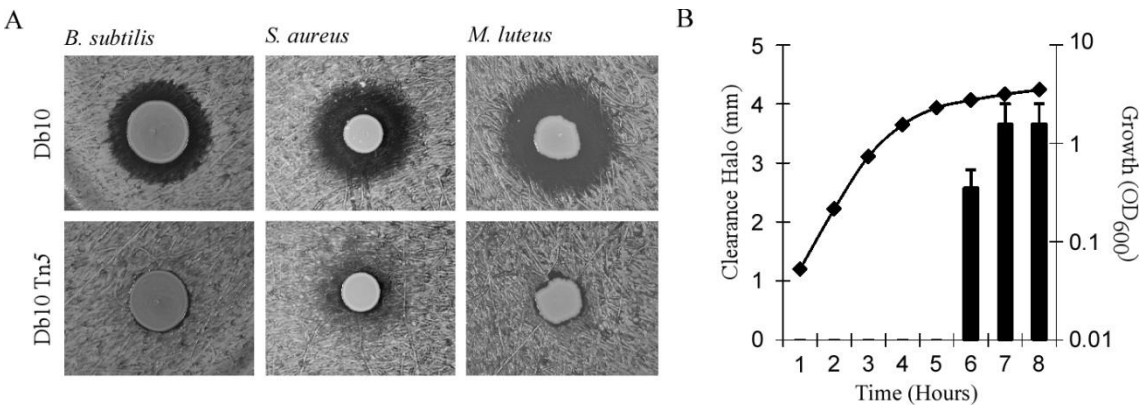

Figure 3.13 *Serratia marcescens* Db10 is able to inhibit growth of Gram-positive bacteria. **A.** Activity assays using *Bacillus subtilis* NCIB3610, *Staphylococcus aureus* 113 and *Micrococcus luteus* ATCC4698 as indicator strains, with *S. marcescens* Db10 or *S. marcescens* Db10 *SMA2290::*Tn*5* (NRS2992) as the producer strains. **B.** Culture supernatant assays (described in experimental procedures) indicate the diffusible molecule is produced by *S. marcescens* Db10 in stationary phase. Clearance halo sizes (radius of cleared area) are averages of three replicates; error bars represent standard error of the mean. A representative growth curve is shown for reference.

3.2.2 Isolation of a mutant of *S. marcescens* Db10 unable to produce antimicrobial activity

Based on the hypothesis that *S. marcescens* Db10 synthesized and secreted an antimicrobial compound, random transposon mutagenesis was used to screen for mutant isolates of *S. marcescens* Db10 that could no longer inhibit the growth of *B. subtilis* and *S. aureus*. Six mutants were isolated exhibiting reduced killing activity towards both *B. subtilis* NCIB3610 and *S. aureus* 113 (e.g. Figure 3.13.A). To ensure that disruption of the killing activity was associated with the transposon insertion, bacteriophage-mediated transduction was used to introduce one of the Tn5 insertions back into wild type *S. marcescens* Db10. The resulting strain (SJC13) displayed an identical phenotype to the original Tn5 isolate (data not shown). Therefore we concluded that the lack of bioactivity was directly associated with the transposon insertion. The location of the transposon insertion in all six of the isolated transposon mutant strains was mapped, by interrogation of the publicly-available complete genome sequence of *S. marcescens* Db11 (Sanger Institute, UK). All of the insertions were located within the coding region of *SMA2290* (Figure 3.14). In each case the site of insertion was identical, indicating that the strains were most likely clonal isolates.

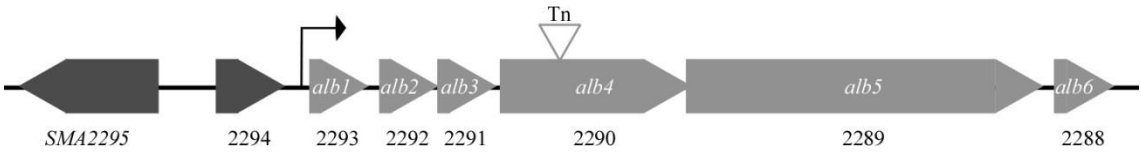

Figure 3.14. Map of the *alb* operon. Genes belonging to the *alb* operon are indicated as light grey arrows, genes that do not belong to the *alb* operon are indicated as dark grey arrows. Each gene is shown to scale. The transcription start site is shown as a black arrow. The site of the transposon (Tn) insertion (at nucleotide 2745) in *alb4* is indicated with a grey triangle.

3.3 Characterisation of the althiomycin biosynthetic operon

3.3.1 *alb1-alb6* (*SMA2293-2288*) constitute an operon

Examination of the genetic context of *SMA2290* revealed it was the fifth of seven genes on the same strand (Figure 3.14), and thus likely part of a biosynthetic operon. To define the 5' boundary of the operon responsible for the biosynthesis of the potential antimicrobial compound, RT-PCR analysis was used. This was performed using cDNA synthesized from mRNA isolated from *S. marcescens* Db10 and *S. marcescens* Db10 *SMA2292*::Tn*5* (NRS2922). Primers designed to span the intergenic regions between 1) *SMA2294* and *SMA2293*; and 2) *SMA2293* and *SMA2292* were used to assess co-transcription. In addition, primers designed to amplify internal coding regions of *SMA2294*, *SMA2293*, *SMA2292*, *SMA2290*, *SMA2289* and *SMA2288* were used to confirm that the gene in question was expressed. The evidence suggests that *SMA2293-SMA2288* form a single operon since *SMA2293-SMA2292* are co-transcribed (Figure 3.15), there is less than 5 bp between *SMA2292-SMA2291* and *SMA2290-SMA2289*, and translational coupling is observed between *SMA2291-SMA2290* (see below). Furthermore while there is a 146 bp intergenic gap between *SMA2289-SMA2288*, SMA2288 is clearly needed for maximal althiomycin biosynthesis (see below) and insertion of the transposon in *SMA2290* disrupted transcription of both the downstream genes *SMA2289* and *SMA2288* (Figure 3.15). We renamed genes *SMA2293-SMA2288* as *alb1-alb6* for **al**thiomycin **b**iosynthetic cluster. Interestingly, the GC content of the althiomycin biosynthetic gene cluster was determined to be 55.1%, compared with the average GC content of the genome which is 59.5%. These data perhaps suggest that the *alb1-6* genes have been horizontally acquired.

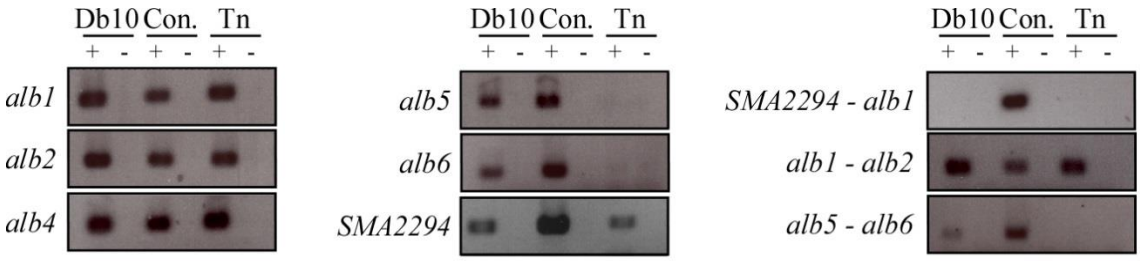

Figure 3.15 RT-PCR analysis of the biosynthetic gene cluster. The template used in the PCR reaction is indicated above the gels as Db10 (wild type *Serratia marcescens* Db10 cDNA) or transposon (Tn*5* mutant cDNA). Reactions were performed in the presence (+) and absence (-) of reverse transcriptase. Con. represents *S. marcescens* Db10 genomic DNA as a positive control (+) and water as a negative control (-). The region of the chromosome amplified is indicated to the left of each gel. Primers were designed to amplify a product internal to a single gene, or spanning the intergenic region between two genes. Twenty five cycles of PCR amplification were used with the exception of *SMA2294* and *SMA2294-alb1* where 30 cycles were used.

3.3.2 A transcriptional start site is present upstream of *alb1*

The above findings indicated that *SMA2294* was not co-transcribed with *alb1* and that a promoter element should be present in the 305 bp gap between the stop codon of *SMA2294* and start codon of *alb1* to drive expression of *alb1-alb6*. To determine the location of the transcription start site, rapid amplification of cDNA 5' ends (5' RACE) was performed. The transcription start site was localised to -40 bp upstream and either -41 bp or -42 bp upstream of the *alb1* translation initiation codon (Figure 3.16). It is not possible to distinguish between the -41 bp or -42 bp sites because the anchor primer that is needed for the 5' RACE contains a series of thymine residues, which cannot be distinguished from the thymine residue at position -42 bp in the promoter region by sequencing (Figure 3.16). Putative -10 and -35 binding sites for RNA polymerase were identified (Figure 3.16). The -10 region (TAGTTT) shows a three out of six base pair

match to the consensus sequence of TATAAT, whilst the -35 region (TTTACA) shows a five out of six base pair match to the consensus sequence of TTGACA. There is a 98 bp gap between the stop codon of *alb1* and the start codon of *alb2* but when 5' RACE was applied to the region upstream from the *alb2* translation start site, no transcription initiation site could be identified (not shown). Taken together the data strongly indicate that *alb1-alb6* are co-transcribed, with *alb6* forming the final gene in the operon.

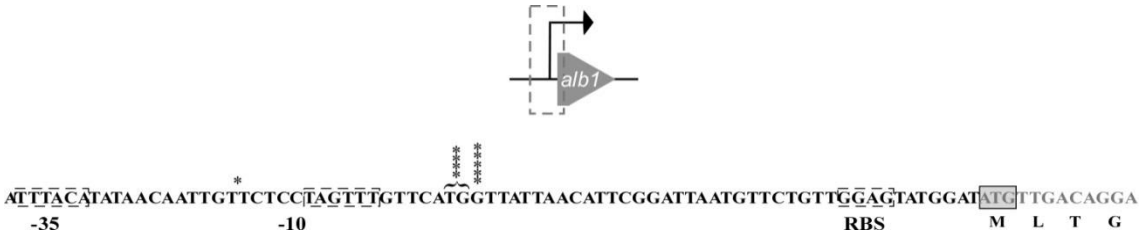

Figure 3.16 5' RACE analysis to identify the transcriptional start site of the *alb* operon. The region upstream of the *alb1* gene highlighted with a broken box, the corresponding sequence is shown the methionine start codon is boxed. Asterisks indicate the number of times a particular base was identified as the transcriptional start site. Putative -10 and -35 regions are highlighted by a broken box. The -41 bp and -42 bp start sites are highlighted together as it is not possible to distinguish between these sites more specifically (see text).

3.4 Predictive sequence analysis of *alb* gene products

The likely functions for each of the gene products in the *alb1-alb6* operon were deduced by sequence comparisons with proteins of known function. This analysis predicted that the operon encodes a three protein hybrid NRPS-PKS assembly line (*alb4, alb5* and *alb6*), associated tailoring enzymes (*alb2* and *alb3*) and an export and/or resistance protein (*alb1*). One of the genes encoding the hybrid NRPS-PKS multienzyme (*alb4*) was disrupted by the transposon insertion. The Alb4-5 NRPS-PKS multi-enzyme comprises six modules, the first two in Alb4 and the remainder in Alb5 (Figure 3.17). The first five modules are typical NRPS modules predicted to

sequentially incorporate Gly, Cys, Ser, Cys and Gly residues (Challis *et al.*, 2000; Stachelhaus *et al.*, 1999), with heterocyclisation of the two cysteine residues and oxidation to the thiazole of the thiazoline resulting from the first. The final module is a PKS module and is predicted to incorporate a malonyl unit (Haydock *et al.*, 1995). The thioesterase domain at the end of Alb5 is hypothesized to catalyse release of the fully assembled chain (see below). The products of the *alb2* and *alb3* genes are predicted to act as 'tailoring' enzymes which further modify the NRPS-PKS-generated intermediate. Alb3 is predicted to be a SAM-dependent methyltransferase, whereas Alb2 is predicted to be an *N*-oxygenase, exhibiting 41% sequence similarity to the aureothin biosynthetic enzyme AurF of *Streptomyces althioluteus* (Krebs *et al.*, 2007). AurF is a diiron-dependent oxygenase that catalyses the 6-electron oxidation of 4-aminobenzoic acid to 4-nitrobenzoic acid. The product of *alb6* is predicted to function as a Type II thioesterase which likely represents an external 'editing' thioesterase. The *alb1* gene is predicted to encode a member of the major facilitator superfamily of membrane proteins, suggesting a possible role in self-resistance or efflux, as discussed further below.

Database searches for known compounds with structural similarity to the intermediates predicted to be assembled on the module 6 ACP domain suggested althiomycin (or a closely related molecule) as the likely metabolic product of the *alb* gene cluster. The conversion of the intermediate attached to the ACP domain of module 6 to althiomycin can be hypothesised to occur via Alb2-catalysed oxidation of the amino group in the intermediate to the corresponding oxime, followed by Alb3-mediated O-methylation. Subsequent TE-catalysed cyclisation of the resulting intermediate would afford althiomycin (Figure 3.17).

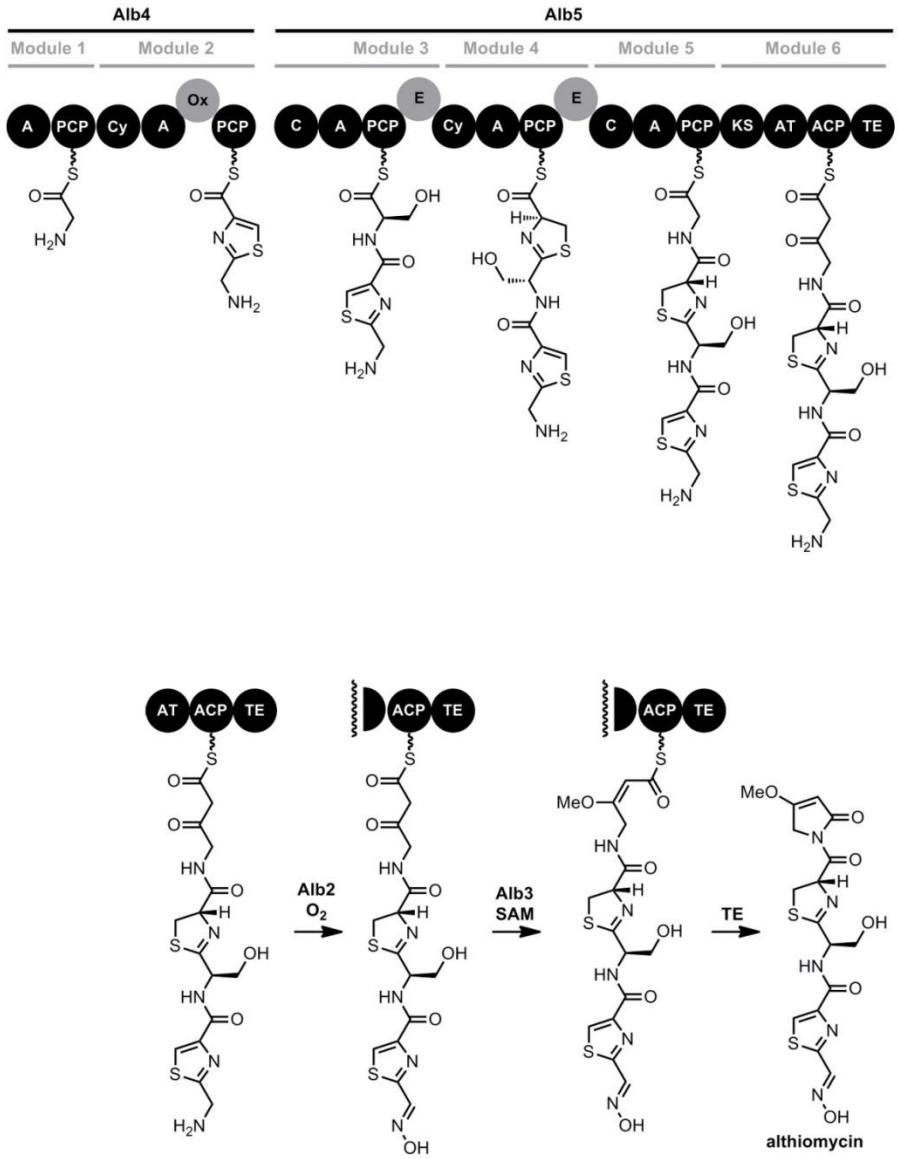

Figure 3.17. Proposed pathway for althiomycin biosynthesis in *Serratia marcescens* Db10. Alb4 and Alb5 form a hybrid NRPS-PKS assembly line, which consists of six modules as indicated. Domains within the NRPS-PKS are as follows. A: adenylation; PCP: peptidyl carrier protein; C: condensation; Cy: condensation/heterocyclisation; Ox: flavin-dependent oxidase; E: epimerisation; KS: ketosynthase; AT: acyl transferase; ACP: acyl carrier protein; TE: thioesterase. Alb6 (not shown) likely functions as an external 'editing' thioesterase. Alb3 is similar to known S-adenosylmethionine (SAM)-dependent methyltransferases and Alb2 is similar to known oxidases. The fact that no althiomycin-related compounds accumulate in *alb2*/*alb3* mutants suggests that N-oxidation and O-methylation take place in *trans* during chain assembly on the hybrid NRPS-PKS. However, the precise timing of the N-oxidation reaction is currently unclear. Analysis performed in collaboration with Greg Challis and Lijiang Song, University of Warwick.

3.5 Identification of the antimicrobial metabolite as althiomycin

To determine whether the metabolic product of the *alb* gene cluster is althiomycin, ultra high resolution UHPLC-ESI-TOF-MS analysis of the culture supernatant from the wild-type strain and the *alb4* transposon mutant of *S. marcescens* Db10 was performed. This identified a compound present in the wild type, but lacking in the *alb4* transposon mutant, that yields an ion with the same molecular formula as protonated althiomycin (calculated *m/z* for $C_{16}H_{18}N_5O_6S_2^+$: 440.0688, observed: 440.0693 and Figure 3.18).

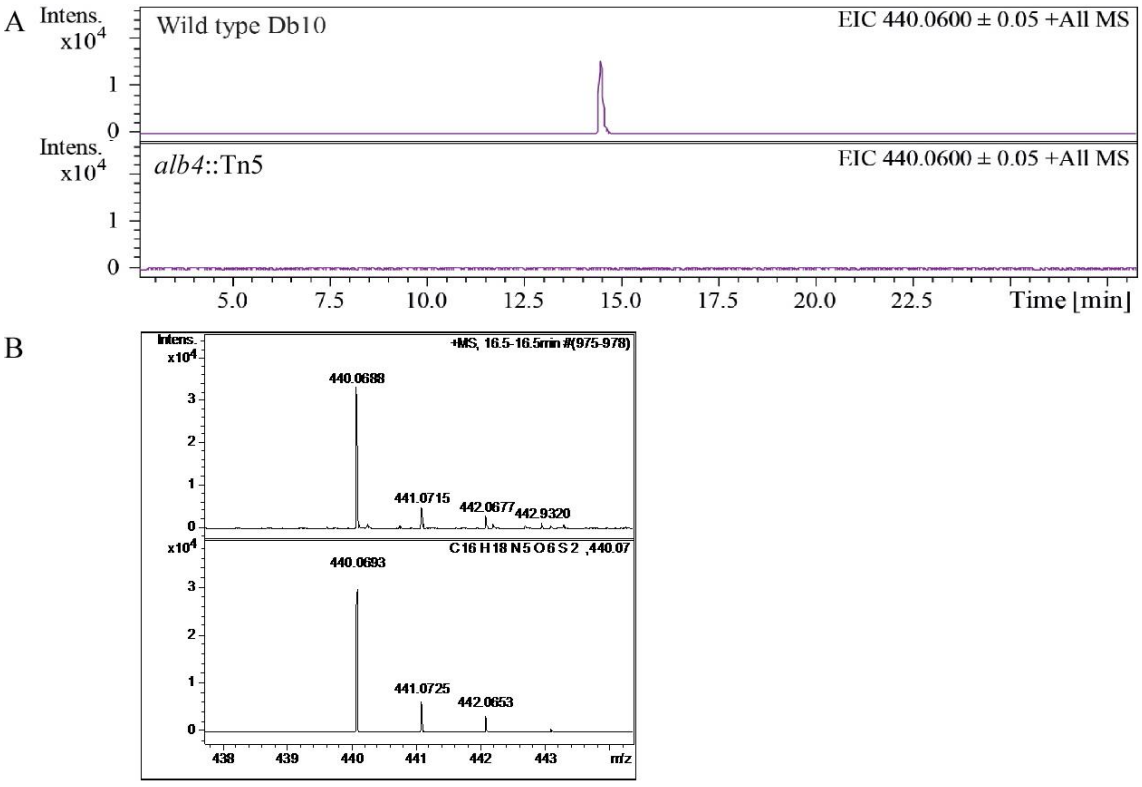

Figure 3.18 Spectroscopic analysis of althiomycin produced by *Serratia marcescens* Db10. A. Extracted ion chromatograms at m/z=440.0600 for wild type and the *alb4* transposon mutant strain (NRS2992) of *S. marcescens* Db10 **B.** Top panel: high resolution mass spectrum of althiomycin detected in culture supernatant of *S. marcescens* Db10. Bottom panel: simulated mass spectrum for the $C_{16}H_{18}N_5O_6S_2^+$ ion. Analysis performed in collaboration with Greg Challis and Lijiang Song, University of Warwick.

In order to unambiguously identify the metabolite as althiomycin, NMR spectroscopic analysis was performed on HPLC purified material (Figure 3.19). Due to the rich medium used for production, some impurities were present. Nevertheless, careful inspection of ^{1}H, COSY, HBMC and HSQC spectra confirmed that the compound is althiomycin (Figure 3.19).

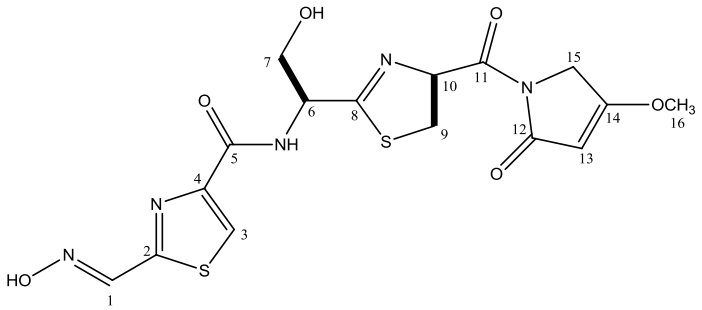

Carbon	δ_H(ppm)	δ_C (ppm)*	HMBC	Literature (Cortina *et al.*, 2011)	
				δ_H(ppm)	δ_C (ppm)
1	8.37(s)	143.0	C2	**8.37(s)**	**143.2**
2		162.6			**162.6**
3	8.29 (s)	124.8	C2, C5	**8.35(s)**	**125.3**
4		149.6			**149.7**
5		160.4			**159.8**
C5-NH-C6	8.39(br)		C5, C6	**8.41(m)**	
6	4.84(m)	53.5	C5, C7, C8	**4.88(m)**	**53.9**
7	3.79(m)	61.8	C6, C8	**3.80(m)**	**62.2**
8		173.5			**173.4**
9	3.40/3.58(m)	34.9	C8, C10, C11	**3.40/3.58(m)**	**34.6**
10	6.14(t, 8.6)	77.8	C8, C9, C11	**6.16(m)**	**78.0**
11		168.1			**168.3**
12		169.5			**169.6**
13	5.39(s)	94.3	C12, C15, C16	**5.43(m)**	**94.4**
14		177.2			**177.2**
15	4.29(s)	47.9	C11, C12, C13, C14	**4.33(m)**	**48.0**
16	3.88(s)	58.9	C14	**3.88(s)**	**59.2**

Figure 3.19 NMR assignment for althiomycin (DMSO-d6, 700MHz, 25°C). * Carbon shift obtained from HSQC and HMBC. Analysis performed in collaboration with Greg Challis and Lijiang Song, University of Warwick.

To further confirm that the lack of althiomycin production in the *alb4* Tn*5* mutant was due solely to disruption of the althiomycin biosynthetic gene cluster, an in-frame Δ*alb4-5* deletion strain (SAN5) was constructed. First, the ability of the Δ*alb4-5* deletion strain to inhibit the growth of *B. subtilis* was assessed. It was observed that the Δ*alb4-5* strain was unable to inhibit the growth of *B. subtilis* either when directly spotted onto an indicator lawn (Figure 3.20.A) or when the culture supernatant was harvested and tested in the bioassay (data not shown). Second, ultra high resolution UHPLC-ESI-TOF-MS analysis showed that althiomycin was lacking from the culture supernatant of the Δ*alb4-5* mutant (Figure 3.20.A). These findings unequivocally demonstrate that production of althiomycin is dependent on the *alb* gene cluster.

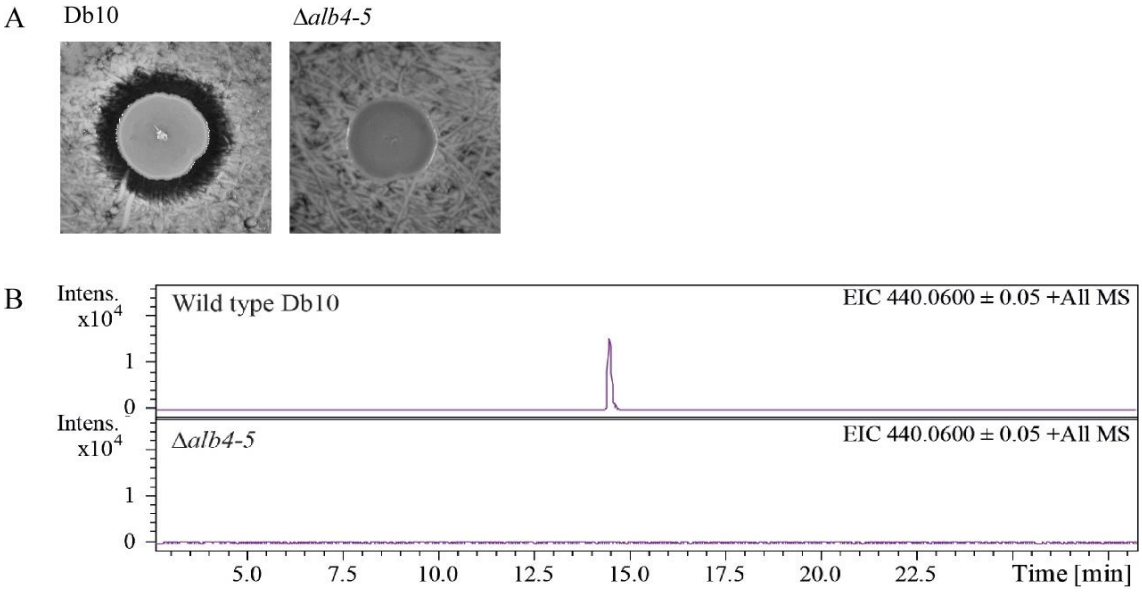

Figure 3.20. Alb4-5 are required for the biosynthesis of althiomycin. A. Assay to assess antimicrobial activity of *Serratia marcescens* Db10 and the *alb4-5* mutant strain (SAN5) against *Baccilus subtilis* 3610. **B.** Extracted ion chromatograms at m/z=440.0600 for wild type and the *alb4-5* mutant strain (SAN5) of *S. marcescens* Db10. Analysis performed in collaboration with Greg Challis and Lijiang Song, University of Warwick.

3.6 The tailoring enzymes Alb2, Alb3 and Alb6 are required for althiomycin biosynthesis

Alb4 and Alb5, comprising the core NRPS-PKS machinery, are clearly required for althiomycin biosynthesis. To determine whether Alb2, Alb3 and Alb6 are also needed to produce althiomycin, in-frame deletions of *alb2*, *alb3* and *alb6* were constructed by allelic exchange. Similar to the Δ*alb4-5* mutant strain, the Δ*alb2* andΔ*alb3* strains no longer exhibited antimicrobial activity towards *B. subtilis* (Figure 3.21.A). The lack of althiomycin production was confirmed using ultra high resolution UHPLC-ESI-TOF-MS analyses (data not shown). Interestingly, no potential intermediates in althiomycin biosynthesis could be detected in the culture supernatant of either mutant, suggesting that the modification reactions may occur on intermediates that are covalently attached to the assembly line. It is also possible that non-oxidised or non-methylated intermediates are not detected in the culture supernatant because they are unstable. However, it is unlikely that retention within the cell is responsible for our inability to detect potential intermediates because they were not detectable in cellular extracts either (data not shown). In contrast with the *S. marcescens* Db10 Δ*alb2* and Δ*alb3* mutant analysis, bioassays indicated that in the Δ*alb6* mutant strain a small amount of antimicrobial activity was retained (Figure 3.21.A). Ultra high resolution UHPLC-ESI-TOF-MS analyses confirmed that althiomycin production in the Δ*alb6* mutant strain was roughly 10% that of the wild type Db10 strain (Figure 3.21.B). These results indicate that *alb2* and *alb3* are essential for althiomycin production whereas Alb6 increases the efficiency of the process.

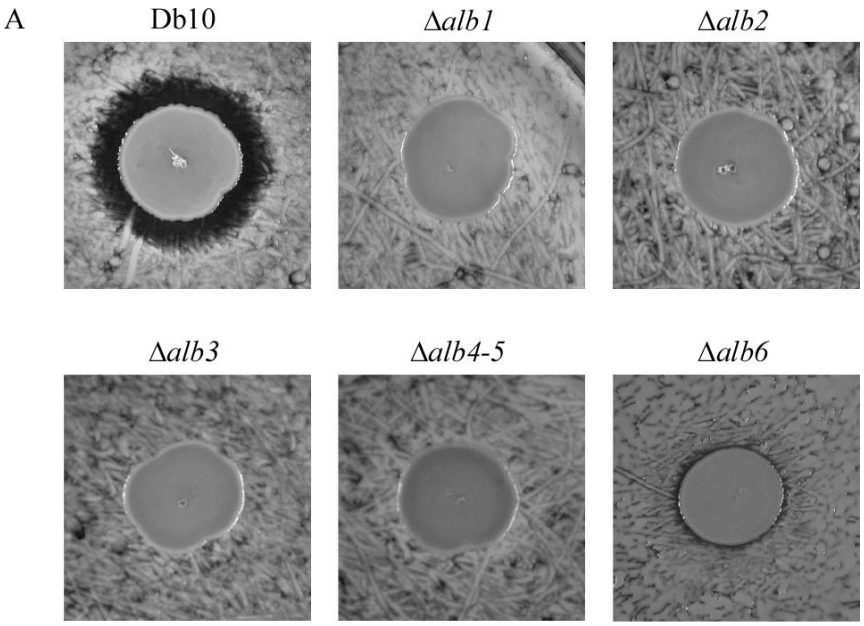

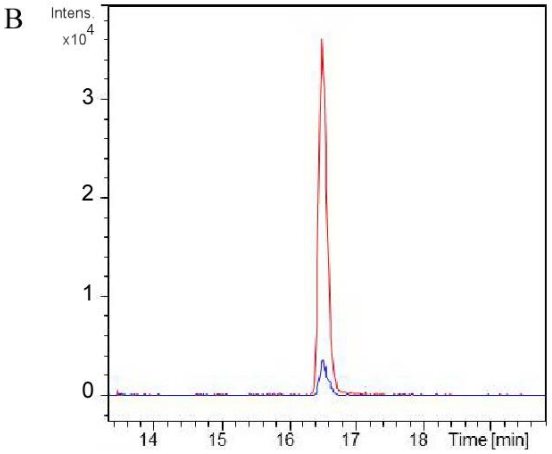

Figure 3.21. Analysis of *alb* mutant strains of *Serratia marcescens* Db10. A. Assay to assess antimicrobial activity of *S. marcescens* Db10 and the *alb1* (SAN2), *alb2* (SAN3), *alb3* (SAN4), *alb4-5* (SAN5) and *alb6* (SAN60) mutant strains against *Bacillus subtilis* 3610. B. Comparison of the extracted ion chromatogram at *m/z* 440.0600 for wild type *S. marcescens* Db10 (red line) and Db10 Δ*alb6* (SAN60) (blue line). Analysis performed in collaboration with Greg Challis and Lijiang Song, University of Warwick.

To confirm that the loss of althiomycin production in each of the mutant strains directly resulted from the in-frame deletion constructed, genetic complementation

analysis was performed. To this end, medium-copy number plasmids carrying the complete *alb2*, *alb3* and *alb6* coding region*s* were introduced into the Δ*alb2*, Δ*alb3* and Δ*alb6* strains, respectively, and the bioassay was performed. The growth inhibition activity in all cases was restored (Figure 3.22.B). Interestingly, in the case of *alb3*, on construction of an almost-complete in-frame deletion, Δ*alb3* (SAN4), in which only a fusion of the first three and final ten amino acids remained, the althiomycin defect could not be complemented by expression of *alb3 in trans* (not shown). Given that there is only a 21 bp gap between *alb3* and *alb4*, we wondered if there might be translational coupling between these two genes. Supporting this idea, in the Δ*alb3* mutant, transcription of *alb4* and *alb5* was retained but SDS-PAGE analysis indicated that protein bands consistent with Alb4 (266.68 kDa) and Alb5 (597.17 kDa) were no longer easily detectable, compared with the wild type (Figure 3.22.A; the identity of Alb4 as the primary constituent of the ~250 kDa band in the wild type was confirmed by mass spectrometry; not shown). Generation of the $\Delta alb3_{51\text{-}262}$ mutant (SAN88), missing 211 amino acids from the middle of the protein and thus preserving in-frame translation of the 3' end of the gene, again abrogated althiomycin production, but this time the defect could be complemented be expressing *alb3 in trans* (Figure 3.22.B). Furthermore, consistent with translational coupling between *alb3* and *alb4*, protein bands consistent with Alb4 and Alb5 were readily detected in the $\Delta alb3_{51\text{-}262}$ mutant (SAN88) strain (data not shown). This implies tight co-ordination between the production of Alb3 and Alb4-5, perhaps to ensure a 1:1:1 stoichiometry of Alb3:Alb4:Alb5 which would be consistent with O-methylation of a PKS-bound intermediate.

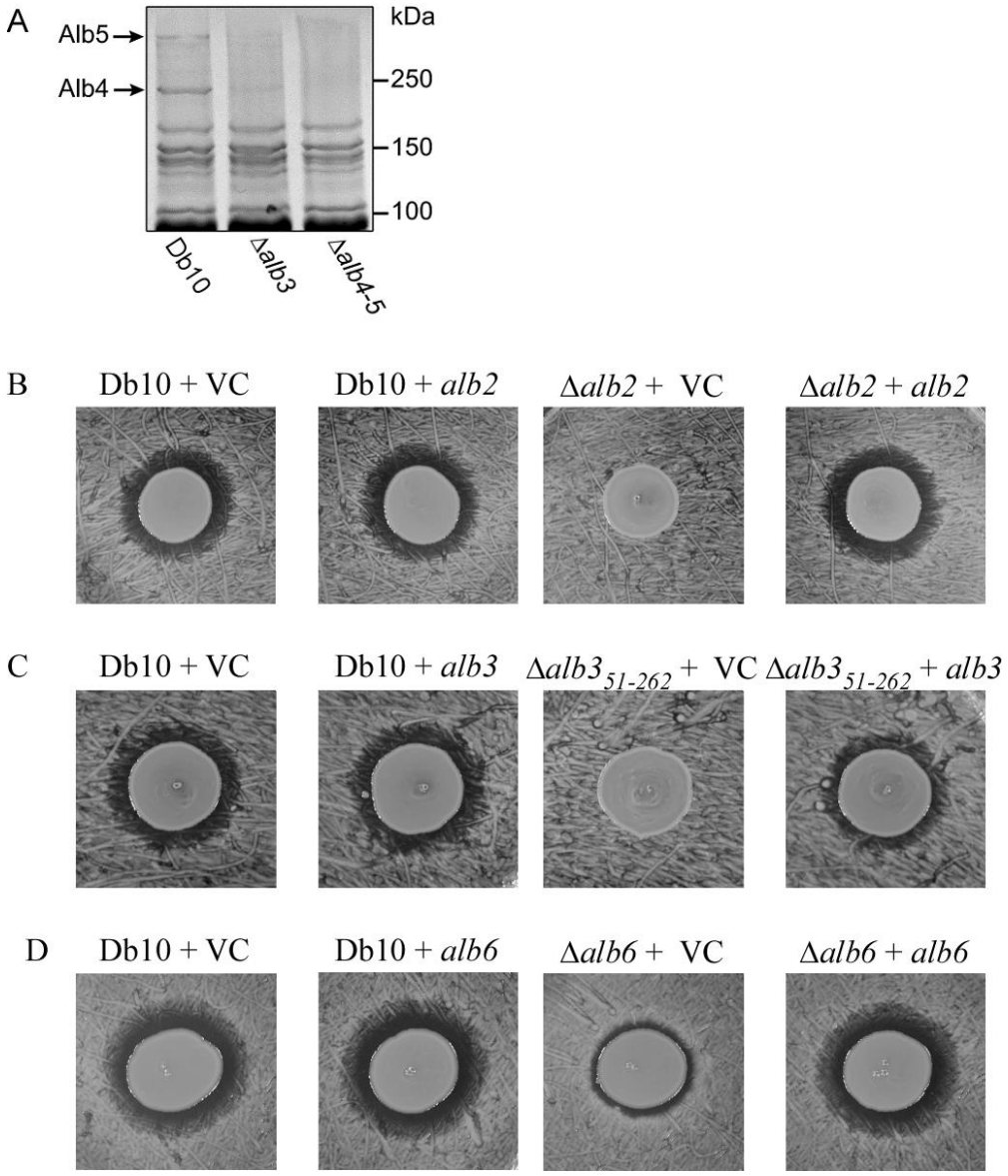

Figure 3.22 The tailoring enzymes are required for althiomycin production. A. Visualisation of proteins corresponding to the predicted size of Alb4 and Alb5. Total cellular protein from Db10 (wild type *Serratia marcescens* Db10), Δ*alb3* (SAN4) or Δ*alb4-5* (SAN5) mutants was isolated from cultures grown to stationary phase and separated by SDS-PAGE, followed by staining with Coomassie blue. **B.** Activity assays were performed using *Bacillus subtilis* NRS1473 as the indicator lawn. The producer strains used are indicated above as: Db10 + VC (*S. marcescens* Db10 pSUPROM); Db10 + *alb2* (*S. marcescens* Db10 pSAN2); Δ*alb2* + VC (SAN3 pSUPROM); Δ*alb2* + *alb2* (SAN3 pSAN2); Db10 + *alb3* (*S. marcescens* Db10 pSAN3);Δ$alb3_{51\text{-}262}$+ VC (SAN88 pSUPROM); Δ$alb3_{51\text{-}262}$+ *alb3* (SAN88 pSAN3); Db10 + *alb6* (*S. marcescens* Db10 pSAN38); Δ*alb6* + VC (SAN60 pSUPROM); Δ*alb6* + *alb6* (SAN60 pSAN38). 'VC' represents the empty vector control.

3.7 The role of Alb1 in althiomycin biosynthesis

3.7.1 Alb1 is not essential in *S. marcescens* Db10 and the *alb1* deletion mutant is not sensitive to the effects of althiomycin

Alb1 is predicted to be a member of the major facilitator superfamily (MFS) of membrane proteins. In many cases these proteins act as export or efflux pumps (Fluman & Bibi, 2009). In antibiotic producing organisms, resistance genes are commonly located within the antibiotic biosynthetic gene cluster (Hopwood, 2007). We therefore hypothesised that Alb1 was required for self-resistance to althiomycin and/or export of althiomycin from the cell into the surrounding environment. We predicted that if *alb1* was essential for self-resistance, it might not be possible to make an althiomycin-producing *alb1* mutant due to lethality. Of note, it was not possible to construct a Δ*alb1* (*almE*) mutant in *M. xanthus*, the authors therefore propose a role for this protein in host self-resistance (Cortina *et al.*, 2011). Surprisingly, an *alb1* mutant was successfully constructed in *S. marcescens* Db10 and this mutant did not exhibit a growth defect (data not shown). To confirm whether *alb1* was required for resistance to althiomycin in *S. marcescens* Db10, competition assays and plate bioassays were performed. Competition assays involve mixing wild type *S. marcescens* Db10 and a streptomycin resistant target bacterium, coculturing them on the surface of an agar plate and then recovering and enumerating the number of surviving target cells (Figure 3.23.A-C) .

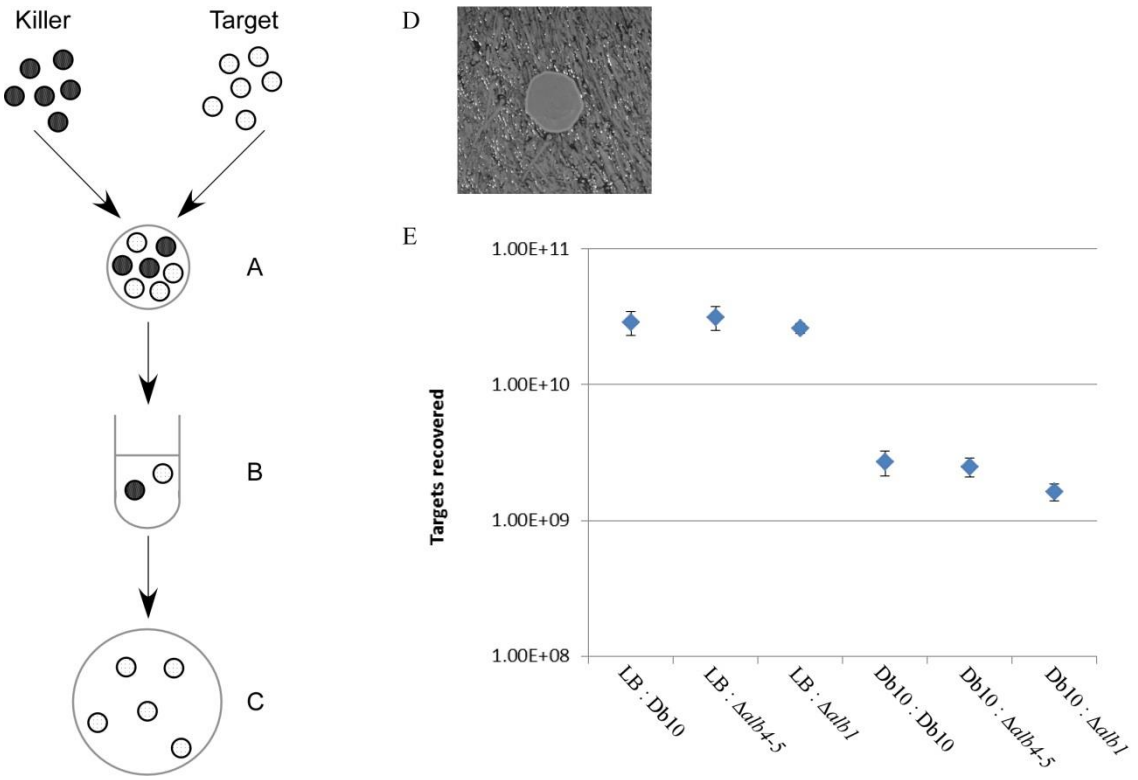

Figure 3.23. The *alb1* mutant strain of *Serratia marcescens* Db10 (SAN2) is not sensitive to althiomycin produced by wild type *S. marcescens* Db10. A-C. Diagram of competition assay set up. **A**. Cultures of the killer strain (*S. marcescens* Db10) and target strains (*S. marcescens* Db10 Strep^R, Δ*alb4-5* Strep^R and Δ*alb1* Strep^R) are mixed and spotted onto an LB agar plate. **B**. After a period of incubation to allow time for the killer strain to have an effect on the target strain, cells from the culture spot are recovered. **C**. Recovered cells are plated onto selective media which allows for the enumeration of the surviving target cells. **D.** Activity assays were performed using Δ*alb1* as an indicator lawn and Db10 as the producer strain. **E.** Recovery of viable streptomycin resistant Db10, Δ*alb4-5* (SAN5) or Δ*alb1* (SAN2) cells after 16 h incubation with wild type *S. marcescens* Db10. Points show means ± standard error of the mean (n=3).

In contrast to the *B. subtilis* plate bioassays, when wild type *S. marcescens* Db10 was spotted on top of a lawn of the *alb1* mutant, no antibiosis halo could be observed (Figure 3.23.D). Furthermore, when a competition assay was performed with *S. marcescens* Db10 and streptomycin resistance derivatives of *S. marcescens* Db10, the *alb4-5* mutant strain or the *alb1* mutant strain, no significant difference in the number of cells recovered between the three target strains could be observed (Figure 3.23.E).

Together, these data show that *alb1* is not essential to confer resistance to althiomycin in *S. marcescens* Db10.

3.7.2 Transcriptional analysis of *alb2-6* in *alb1* deletion mutants

Plate bioassays revealed that upon the deletion of *alb1*, *S. marcescens* Db10 was no longer able to produce extracellular althiomycin (Figure 3.24.A). These results suggested that the *alb1* mutant was either unable to biosynthesise althiomycin, or that althiomycin was not efficiently exported from the cell. To distinguish between these possibilities, we attempted to complement the Δ*alb1* mutant phenotype. The *alb1* coding region was expressed *in trans* using exactly the same vector system as was used to successfully complement the *alb2*, Δ$alb3_{51\text{-}262}$ and *alb6* mutant phenotypes. However, no complementation could be observed, suggesting that althiomycin was not biosynthesised in this mutant strain (Figure 3.24.A).

To investigate why genetic complementation of the *alb1* mutant was unsuccessful, the impact of deleting each of the *alb* genes on transcription within the *alb* operon was assessed by RT-PCR using the wild type *S. marcescens* Db10 and the Δ*alb1* (SAN2), Δ*alb2* (SAN3), Δ*alb3* (SAN4), Δ*alb4-5* (SAN5) and Δ*alb6* (SAN60) deletion strains. We observed that deletion of *alb2-6* had no effect on transcription of other genes in the *alb* gene cluster (Figure 3.24.B). However, in the Δ*alb1* strain, we could only detect a very low level of transcription from each of the remaining *alb* genes (Figure 3.24.B). Expression of *alb1 in trans* in the Δ*alb1* mutant was not sufficient to restore transcription of *alb2-6* to wild type levels, thus explaining why it was not possible to genetically complement the *alb1* mutant strain (Figure 3.24.C).

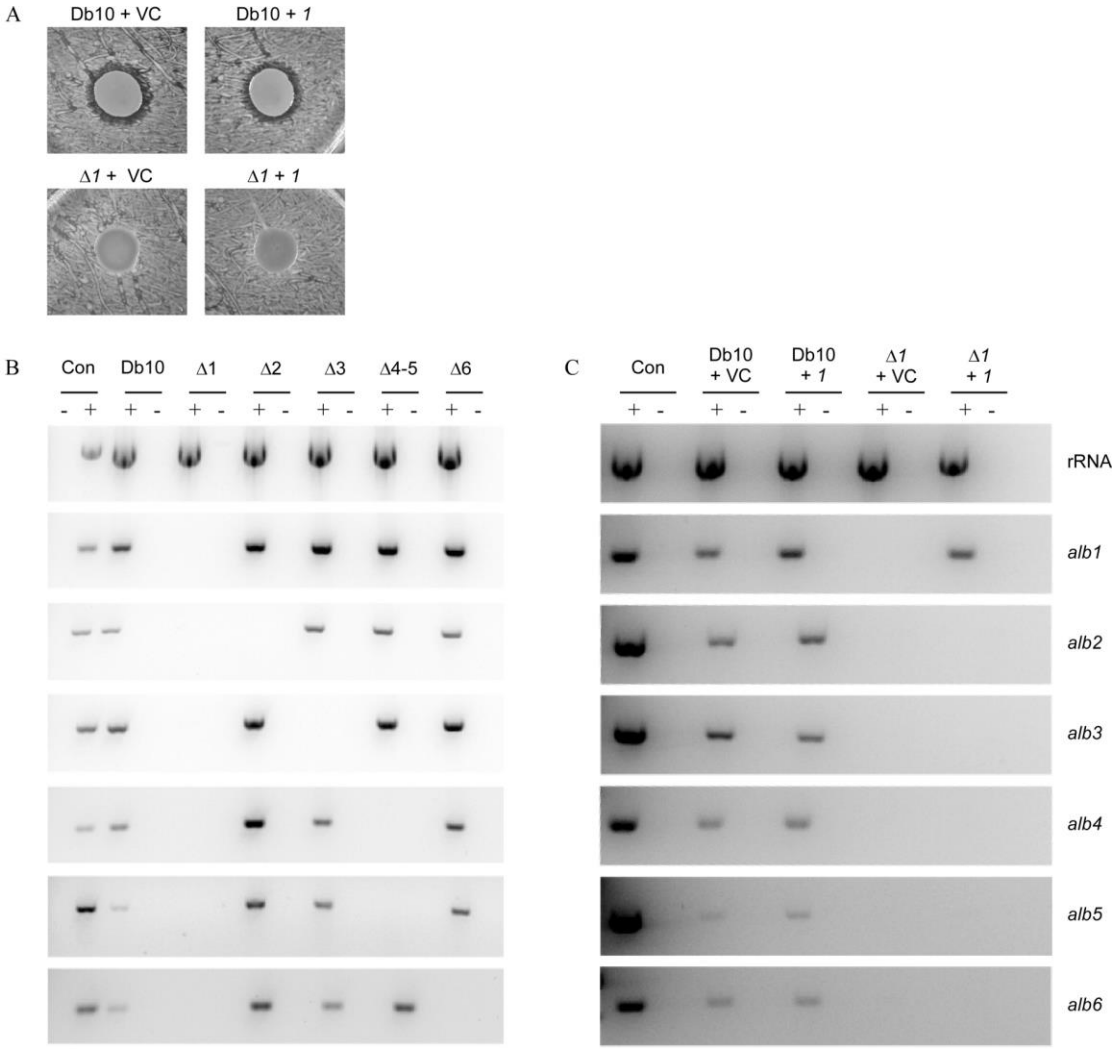

Figure 3.24. The deletion of *alb1* reduces transcript levels of *alb2-6* and this phenotype cannot be complemented by expression of *alb1* in trans. A. Activity assays using *Bacillus subtilis* NRS1473 as the indicator lawn for the producer strains: Db10 + VC (*Serratia marcescens* Db10 pSUPROM); Db10 + *1* (*S. marcescens* Db10 pSAN1*)*; Δ*1* +VC (SAN2 pSUPROM); Δ*1* + *1* (SAN2 pSAN1) **B.** RT-PCR analysis of *alb1-alb6* transcript levels in each of the *alb* mutant strains. The template used in the PCR reaction is indicated above the gels as: Db10 (wild type *S. marcescens* Db10 cDNA); Δ1 (SAN2(Δ*alb1*) cDNA); Δ2 (SAN2 (Δ*alb2*) cDNA); Δ3 (SAN4 (Δ*alb3*) cDNA); Δ4-5 (SAN5 (Δ*alb4-5*) cDNA); Δ6 (SAN60 (Δ*alb6*) cDNA). **C.** RT-PCR analysis of *alb1-6* transcript levels in Db10 + VC (*S. marcescens* Db10 pSUPROM), Db10 + *1* (*S. marcescens* Db10 pSAN1*)*, Δ*1* +VC (SAN2 pSUPROM) and Δ*1* +*1* (SAN2 pSAN1). RT-PCR reactions were performed in the presence (+) or absence (-) of reverse transcriptase. Con. represents *S. marcescens* Db10 genomic DNA as a positive control (+) and water as a negative control (-). The primer pairs used to amplify a product internal to a particular gene are indicated to the right of each gel. Twenty five cycles of PCR amplification were used.

3.7.3 Construction and characterisation of an *alb1* mutant which can be complemented by expression of *alb1 in trans*

The above data indicated that *alb1* is not required for self-resistance to althiomycin in *S. marcescens* Db10. However, a region within the coding sequence of *alb1* is required *in cis* for the transcription of downstream genes. Since it was not possible to conserve transcription of *alb2-6* in the complete *alb1* deletion mutant, we postulated that there may be a regulatory region at either the 5' or 3' end of the *alb1* coding region. Accordingly, we constructed two new *alb1* mutant strains in which either the first (Δ$alb1_{5\text{-}105}$ SAN89) or the final 100 amino acids were deleted (Δ$alb1_{295\text{-}395}$ SAN177) thus retaining the majority of the *alb1* coding sequence (Figure 3.25). Analysis of the Δ$alb1_{5\text{-}105}$ mutant strain revealed it phenocopied the complete Δ*alb1* mutant; extracellular althiomycin could not be detected by the *B. subtilis* bioassay, transcript levels of *alb2-6* were reduced (Figure 3.24.A and B) and expression of *alb1* in trans did not restore althiomycin biosynthesis (data not shown). However, as described below, the Δ$alb1_{295\text{-}395}$ mutant exhibited different phenotypic behaviours to the Δ*alb1* and the Δ$alb1_{5\text{-}105}$ mutant strains. Alb1 is 400 amino acids in length and thus in the Δ$alb1_{295\text{-}395}$ mutant 25% of the full length protein was deleted. This deletion included three of 11 predicted transmembrane domains (data not shown). It therefore seemed highly likely that deletion of this region of the protein would abolish the function of Alb1. To assess the impact of deletion of a functional Alb1 protein, plate bioassays were performed and transcript levels of *alb2-6* were assessed by RT-PCR. When plate bioassays were performed, by comparison with the Δ*alb1* and Δ$alb1_{5\text{-}105}$ strains, a small antibiosis halo could be observed to surround the Δ$alb1_{295\text{-}395}$ mutant. These findings indicate that either a small amount of althiomycin was biosynthesised or that export of althiomycin was impaired in the Δ$alb1_{295\text{-}395}$ mutant (Figure 3.26.A). Consistent with

this finding, RT-PCR analysis of the Δ*alb1*$_{295\text{-}395}$ mutant revealed that transcription of *alb2-6* could be detected (Figure 3.26.B). Taking these results together with those indicating that *S. marcescens* Db10 is not sensitive to althiomycin in the absence of *alb1* (Figure 3.23), we predicted that it would be possible to complement the mutant phenotype by expression of *alb1 in trans*. Upon re-introduction of the *alb1* coding region, extracellular althiomycin could be detected by the *B. subtilis* bioassay, indicating that the presence of Alb1 was sufficient to restore export of althiomycin (Figure 3.26.C). Together, these data demonstrate that a region within the 5' end of *alb1* is required *in cis* for the transcription of *alb2-6* and that Alb1 increases the efficiency of althiomycin export from the cell.

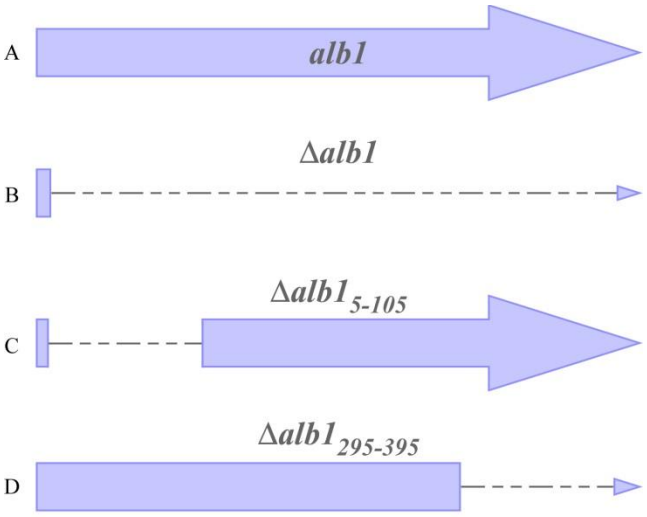

Figure 3.25. Schematic representation of Δ*alb1* mutant strains constructed. A. Wild type *alb1*, which is 400 amino acids in length. **B.** The complete *alb1* deletion mutant, in which only the first three, and the final five amino acids of *alb1* are conserved. **C.** The Δ*alb1*$_{5\text{-}105}$ mutant in which 300 nucleotides at the 5' end of *alb1* have been deleted. **D.** The Δ*alb1*$_{295\text{-}395}$ mutant in which 300 nucleotides at the 3' end of *alb1* have been deleted.

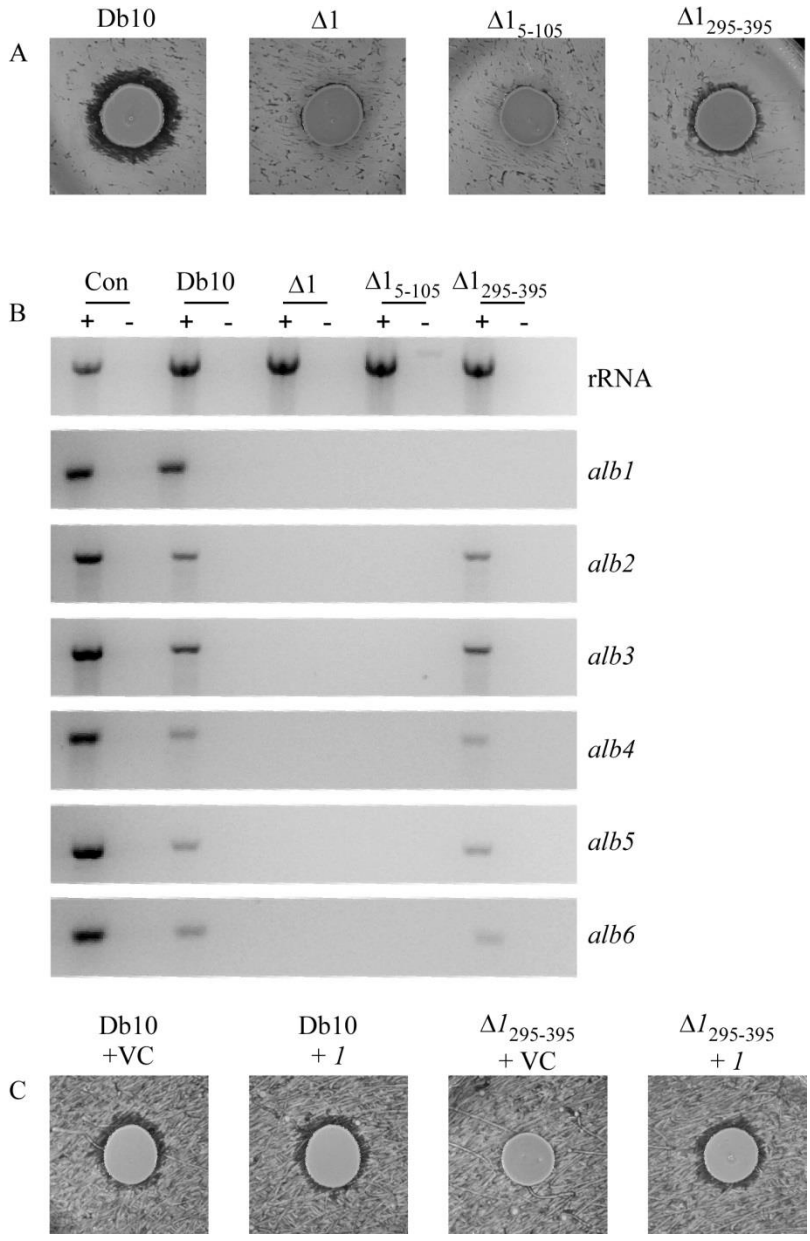

Figure 3.26. Characterisation of the *alb1* mutant strains. A. Activity assays using *Bacillus subtilis* 3610 as the indicator lawn for the producer strains: Db10 (*Serratia marcescens* Db10), Δ1 (Δ*alb1* SAN2), $\Delta 1_{5\text{-}105}$ (Δ$alb1_{5\text{-}105}$ SAN89) and $\Delta 1_{295\text{-}395}$ (Δ$alb1_{295\text{-}395}$ SAN177). **B.** RT-PCR analysis of *alb1-alb6* transcript levels in each of the *alb1* mutant strains. The template used in the PCR reaction is indicated above the gels as: Db10 (*S. marcescens* Db10), Δ1 (Δ*alb1* SAN2), $\Delta 1_{5\text{-}105}$ (Δ$alb1_{5\text{-}105}$ SAN89) and $\Delta 1_{295\text{-}395}$ (Δ$alb1_{295\text{-}395}$ SAN177). RT-PCR reactions were performed in the presence (+) or absence (-) of reverse transcriptase. Con. represents *S. marcescens* Db10 genomic DNA as a positive control (+) and water as a negative control (-). The primer pairs used to amplify a product internal to a particular gene are indicated to the right of each gel. Twenty five cycles of PCR amplification were used. **C.** Activity assays using *B. subtilis* NRS1473 as the indicator lawn for the producer strains: Db10 + VC (*S. marcescens*

Db10 pSUPROM); Db10 + *1* (*S. marcescens* Db10 pSAN1*)*; $\Delta 1_{295\text{-}395}$ +VC (SAN177 pSUPROM); $\Delta 1_{295\text{-}395}$ + *1* (SAN177 pSAN1)

3.7.4 Alb1 is sufficient to confer resistance to extracellularly produced althiomycin

The above data suggest that Alb1 greatly improves the efficiency of export of althiomycin in *S. marcescens* Db10. We predicted that if Alb1 was sufficient to export althiomycin then introduction of the *alb1* coding region into a bacterial strain that was sensitive to althiomycin should improve resistance. Accordingly, we first tested whether *S. marcescens* ATCC274, a prodigiosin-producing environmental isolate of *S. marcescens,* produced althiomycin. This was assessed using two methods: firstly *S. marcescens* ATCC274 was found to be unable to produce a zone of inhibition in the *B. subtilis* bioassay (Figure 3.27.A). Secondly, PCR using primers specific to the *S. marcescens* Db10 *alb* gene cluster indicated the *alb* operon was most likely absent from *S. marcescens* ATCC274 (Figure 3.27.B). Consistent with *S. marcescens* ATCC274 not producing althiomycin, we also showed that it was sensitive to althiomycin produced by *S. marcescens* Db10 (Figure 3.27.C), providing an ideal heterologous background to test the role of Alb1. The coding region for Alb1 was expressed in *S. marcescens* ATCC274 and resistance of the transformed strain to althiomycin was observed. Introduction of Alb1 into *S. marcescens* ATCC274 was indeed able to eliminate the antimicrobial effect of althiomycin, demonstrating that *alb1* is sufficient to confer resistance to althiomycin in ATCC274 (Figure 3.27.C). Since the zone of growth inhibition surrounding the *S. marcescens* Db10 spot on the *S. marcescens* ATCC274 lawn was relatively small, we generated a strain of Db10 producing higher levels of althiomycin to further confirm these results. The native althiomycin promoter was replaced with the constitutive T5 promoter on the chromosome of *S. marcescens* Db10. This strain was found to produce increased levels of althiomycin (data not shown). Using this strain as the althiomycin

producer, we were able to clearly demonstrate that resistance to althiomycin was observed in the *S. marcescens* ATCC274 strain expressing Alb1 (Figure 3.27.C), most likely due to a decrease in the intracellular levels of althiomycin. To summarise, Alb1 is not essential to confer resistance to althiomycin in *S. marcescens* Db10 but increases the abundance of extracellular althiomycin. By comparison, *S. marcescens* ATCC274 is sensitive to the effects of althiomycin and the expression of Alb1 is sufficient to confer resistance to the presence of extracellularly produced althiomycin. Thus, secondary resistance mechanisms to althiomycin that are not present in ATCC274 must exist in *S. marcescens* Db10.

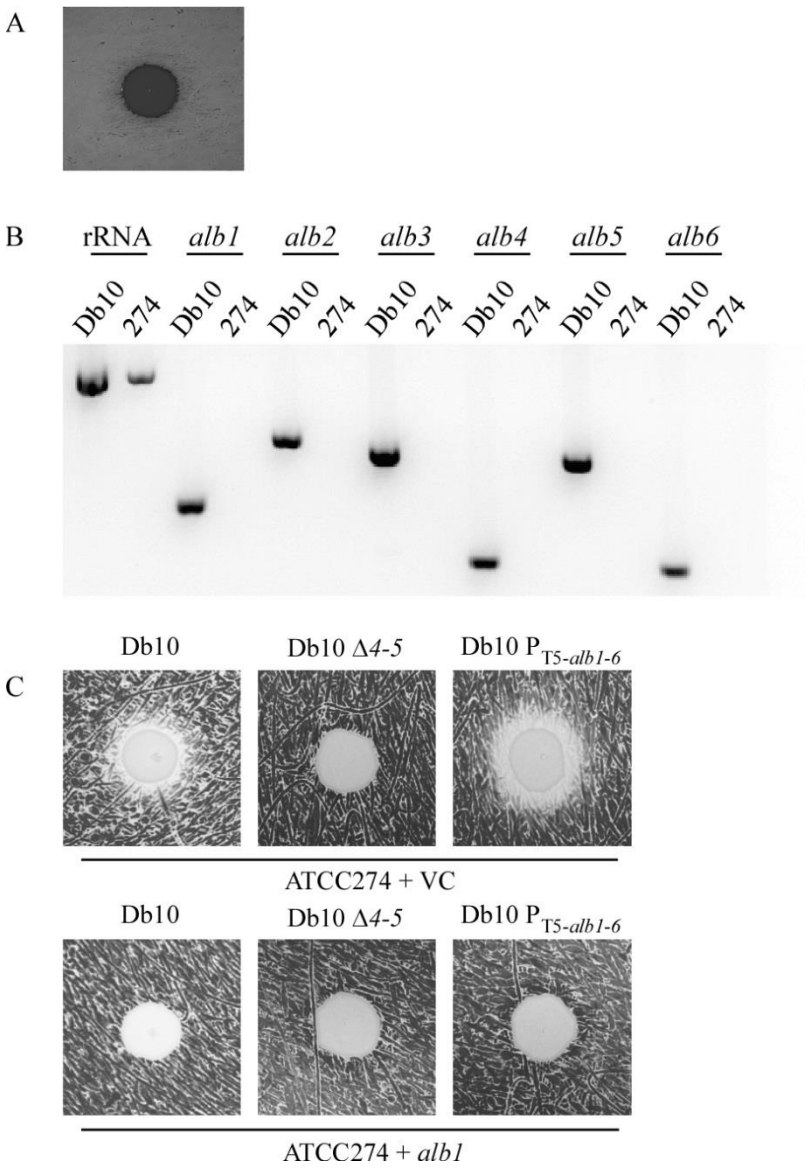

Figure 3.27. Alb1 is sufficient to confer resistance to althiomycin in *Serratia marcescens* ATCC274. **A**. Activity assays in which *S. marcescens* ATCC274 has been grown on top of an indicator lawn of *Bacillus subtilis* 3610. **B.** PCR on gDNA extracted from *S. marcescens* Db10 and ATCC274 using primers specific to the *alb* gene cluster. The template used in the PCR reaction is indicated above the gels as Db10 (*S. marcescens* Db10) or 274 (*S. marcescens* ATCC274). The primer pairs used to amplify a product internal to a particular gene are also indicated above the gel. Twenty five cycles of PCR amplification were used. **C.** Activity assays using Db10 (*S. marcescens* Db10 pSUPROM), Db10 Δ*4-5* (SAN5 pSUPROM) and Db10 P_{T5}-*alb1-6* (SAN100 pSUPROM) as the producer strain and using ATCC274 + VC (*S. marcescens* 274 pSUPROM) and ATCC274 + *alb1* (*S. marcescens* 274 pSAN1) as the indicator lawn. 'VC' represents the empty vector control.

3.8 Discussion

We have identified and characterised an NRPS-PKS biosynthetic gene cluster (*alb1-6*) which we demonstrate is required for the production and export of the antibiotic, althiomycin, in *S. marcescens* Db10. The production of althiomycin was initially detected as this antibiotic possesses antimicrobial activity against several species of Gram-positive bacteria. Although the antimicrobial activity of althiomycin was also tested against Gram-negative bacteria, including several strains of *E. coli*, *Klebsiella aerogenes* and *Pseudomonas fluorescens*, killing of these strains could not be detected (data not shown). These results may indicate that the outer membrane (OM) of Gram-negative bacteria, which is intrinsically resistant to many antibiotics, is also impermeable to althiomycin. Alternatively or additionally, Gram-negative bacteria are known to possess numerous multi-drug resistance (MDR) efflux pumps which may play a role in the export of althiomycin (Nikaido, 1994). The latter hypothesis seems plausible given that the MFS efflux pump, Alb1, is sufficient to confer resistance to althiomycin in *S. marcescens* 274 (Figure 3.27).

In addition to delineating the biosynthetic pathway for althiomycin production, the role of MFS efflux pump, Alb1, was also defined. Initially, we hypothesised that Alb1 was essential for resistance to althiomycin in *S. marcescens* Db10, since resistance determinants are frequently encoded in the same gene cluster as the biosynthetic genes and since Alb1 was predicted to encode a member of the MFS family of efflux pumps. However, plate bioassays and competition assays revealed that the *alb1* deletion mutant was not sensitive to extracellularly produced althiomycin (Figure 3.23). These results indicate that *S. marcescens* Db10 possesses alternative resistance mechanisms to althiomycin. Since althiomycin is thought to target the bacterial ribosome (Fujimoto *et al.*, 1970), *S. marcescens* Db10 may modify its ribosomes to confer resistance to althiomycin, for example by methylation (Vester and Long, 2009). Our finding that the

deletion of *alb1* dramatically reduced transcript levels of *alb2-6* seemed to contradict the above results; we would otherwise have hypothesised that this phenotype was due to a "self-protection mechanism" against the toxic effects of althiomycin in the absence of the resistance protein. The function of Alb1 in althiomycin production, resistance and export was therefore unclear and further experiments were designed to characterise the mechanism behind the *alb1* mutant phenotype and the role of Alb1 in althiomycin biosynthesis.

Additional experiments revealed that it was not possible to complement the phenotype of the complete *alb1* deletion mutant since the transcription of *alb2-6* could not be restored upon expression of Alb1 *in trans*. These results indicated that the presence of the Alb1 protein alone was not sufficient for transcription of *alb2-6* and that a region of the *alb1* coding region was required *in cis* for the transcription of downstream genes. In light of these results, we attempted to construct an *alb1* mutant that would no longer synthesise a functional Alb1 protein, but that was competent for the transcription of *alb2-6*. This was achieved by the construction of a strain lacking 100 amino acids at the C-terminal end of Alb1 (Δ$alb1_{295\text{-}395}$ SAN177). We observed that the Δ $alb1_{295\text{-}395}$ strain produced lower amounts of extracellular althiomycin but that this phenotype could be complemented by the expression of *alb1 in trans* (Figure 3.26). We note the difference in the size of the antibiosis halos between the *alb1* mutant strains (Figure 3.26.A) and the complemented Δ$alb1_{295\text{-}395}$ mutant strain (Figure 3.26.C). To maintain the *alb1* plasmid in the complementation activity assays, kanamycin was added to the media and the *B. subtilis* indicator strain used was therefore kanamycin resistant. In *B. subtilis*, kanamycin resistance is conferred by the expression of an aminoglycoside 3'-phosphotransferase which catalyses phosphorylation of a hydroxyl group of kanamycin (Middleton & Hofmeister, 2004; Mingeot-Leclercq *et al.*, 1999). The kanamycin resistance cassette is therefore unlikely to additionally confer resistance

to althiomycin. However, under conditions of stress, e.g. in the presence of antibiotics, bacteria are known to become generally more resilient to the effects of antibiotics (Poole, 2012). This may explain why the althiomycin antibiosis halo appears reduced when *B. subtilis* is grown in the presence of kanamycin. Further experiments into the role of *alb1* revealed that expression in *S. marcescens* 274 was sufficient to confer resistance to extracellularly produced althiomycin, again implicating Alb1 in the export of althiomycin. *S. marcescens* Db10 therefore does not produce althiomycin in the absence of the region encoding the protein required for export; this is not due to self-protection mechanisms but perhaps to avoid the energetically expensive biosynthesis of antibiotic that cannot be exported to fulfil its function.

Our results indicated that a region within the first 300 nucleotides of *alb1* were required for transcription of *alb2-6* (Figure 3.26). Interestingly, experiments conducted simultaneously by S. Murdoch (SJC lab, unpublished) suggested a role for the RNA binding protein, Hfq, in the regulation of althiomycin production; it was observed that the Hfq mutant was unable to kill *B. subtilis* in the antimicrobial bioassay (data not shown). Further analysis of the Hfq mutant revealed that the transcript levels of *alb1-6* were dramatically reduced, similar to the complete *alb1* deletion mutant (data not shown). Hfq is a global post-transcriptional regulator that facilitates the interaction between small regulatory RNA (sRNA) and messenger RNA (mRNA) (Vogel & Luisi, 2011). It is possible that Hfq is a positive regulator of althiomycin biosynthesis; the 5' region of *alb1* may serve as a binding site for Hfq and the deletion of either Hfq or the binding site encoded by *alb1* might abolish transcription of *alb2-6*. Our understanding of the role of Hfq and the potential overlap with the requirement for the 5' end of *alb1* is incomplete and further experiments would be required to confirm this hypothesis. However, to date, experiments to identify direct interactions between Hfq and the *alb* mRNA have been unsuccessful (SJC lab, unpublished).

Concurrent with our independent, *de novo* identification, analysis and characterisation of the althiomycin biosynthetic gene cluster of *S. marcescens* Db10, a similar cluster directing althiomycin production was identified in the Gram-negative, soil dwelling bacterium, *Myxococcus xanthus* strain DK897 (Cortina *et al.*, 2011), following earlier reports of althiomycin production by this organism (Kunze *et al.*, 1982). *S. marcescens* Db10 and *M. xanthus* are only distantly related, being members of the Gamma and Delta Proteobacteria, respectively. Therefore to determine the level of similarity between the two althiomycin biosynthetic gene clusters, a comparative bioinformatic analysis was performed (Table 3.14 Comparative analysis of the althiomycin biosynthetic proteins). The althiomycin biosynthetic gene clusters of *M. xanthus* and *S. marcescens* Db10 both contain six genes: *almA-F* and *alb1-6*, respectively. Five of the six gene products are clearly equivalent and the gene order is conserved, suggesting that the clusters are related. The Alb1-5 proteins share reasonable identity with the corresponding proteins in *M. xanthus* at the primary amino acid sequence level (Table 3.14). Our predictions for the role played by each of these proteins in althiomycin biosynthesis by *S. marcescens* Db10 are similar to those made for the corresponding proteins in *M. xanthus* (Cortina *et al.*, 2011). Although similar at the protein level, Alb1 and AlmE likely fulfil different functions in *S. marcescens* Db10 and *M. xanthus*, respectively. As discussed in detail above, we propose that Alb1 is not essential in *S. marcescens* to confer resistance to althiomycin but is rather required for export of the antibiotic. Contrastingly, in *M. xanthus*, it was not possible to make an *almE* deletion mutant and this led the authors to speculate that AlmE was required for self-resistance in this strain in addition to being required for export of the antibiotic. Surprisingly, Alb6 and AlmF show no detectable identity with each other at the primary amino acid sequence level. Alb6 is predicted to be a type II thioesterase, with an 'editing' or 'proofreading' function, required for the removal of incorrect intermediates from the

NRPS/PKS machinery or acetyl moieties from incorrectly primed ACP or PCP domains (Fischbach & Walsh, 2006). This finding is corroborated by the finding that althiomycin production is reduced to ~ 10% of wild type levels in the *alb6* mutant. By contrast, AlmF of *M. xanthus* is predicted to be a proline iminopeptidase (TIGR01250) and Cortina *et al.* (2011) prefer a model where AlmF catalyses the formation of the methyoxypyrrolinone ring of althiomycin following release from the NRPS-PKS enzyme. These authors do note, however, that this step could also be performed by the integrated (Type I) thioesterase domain at the end of AlmB (equivalent to that of Alb5). Alb6 and AlmF are both members of the α/β hydrolase superfamily of proteins (Pfam 12697) and consistent with this, similarities in the predicted protein secondary structures of these proteins can be seen (data not shown). Additionally, minor differences exist in the organisation of the biosynthetic operons between the two organisms. In *M. xanthus*, *almB* and *almF* (equivalent to *alb5* and *alb6*) are predicted to be translationally coupled. In the *S. marcescens* Db10 *alb* gene cluster, *alb5* and *alb6* are separated by a 146 bp gap suggesting that translational coupling is unlikely.

Table 3.14 Comparative analysis of the althiomycin biosynthetic proteins from *Serratia marcescens* Db10 and *Myxococcus xanthus*

S. marcescens	**Length [a]**	***M. xanthus***	**Length [a]**	**% identity / similarity [b]**	**Proposed Function**
Alb1	393	AlmE	446	56 / 72	Resistance/export
Alb2	318	AlmD	317	55 / 70	Fe/Mn-dependent N-oxygenase
Alb3	303	AlmC	302	55 / 69	O-Methyltransferase
Alb4	2376	AlmA	2396	44 / 59	NRPS
Alb5	5347	AlmB	5428	46 / 61	NRPS/PKS
Alb6	244	AlmF	322	None	Thioesterase

[a] The length of the protein is given as the number of amino acids.

[b] The percentage similarity and identity was obtained using pairwise protein-protein BLAST analysis across the entire length of the protein (Altschul *et al.*, 1997).

Althiomycin has attracted pharmaceutical interest as a potentially useful antibiotic, but progress has been curtailed by the lack of efficient chemical syntheses and availability of the biosynthetic genes/enzymes. Furthermore, of broader interest is the 4-methoxy-3-pyrrolin-2-one moiety of althiomycin (Figure 3.28). This is a key structural feature of numerous other bioactive natural products that are mostly of marine origin, including sintokamide A, malyngamide A, mirabimide E and the extremely potent anticancer agent dolastatin 15 (Figure 3.28). Nothing is known about the biosynthesis of these remarkable natural products (Bai *et al.*, 1992; Cardellina, 1979; Paik, 1994; Sadar *et al.*, 2008). We hypothesise that they, like althiomycin, are the products of hybrid NRPS-PKS assembly lines and that the 4-methoxy-3-pyrrolin-2-one unit in these molecules is assembled by analogous enzymatic logic to that employed in the assembly of althiomycin (Figure 3.17). Thus, NRPS-mediated chain extension with glycine (in the case of malyngamide) or L-phenyalanine (in the case of dolastatin-15) followed by PKS-mediated chain extension with malonyl-CoA, O-methylation of the

resulting beta-ketothioester and thioesterase-mediated cyclisation, equivalent to the action of Alb3 and the final two modules of Alb5, would yield the corresponding 4-methoxy-3-pyrrolin-2-ones.

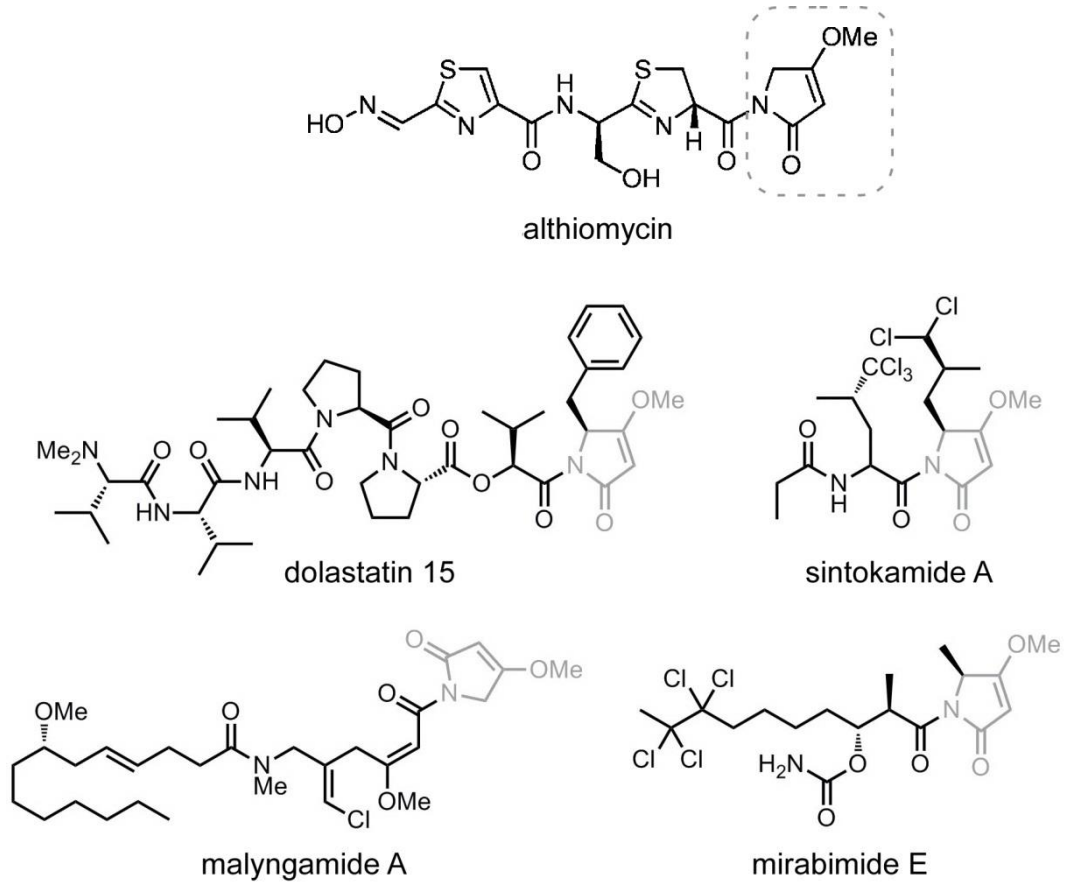

Figure 3.28. The 4-methoxy-3-pyrrolin-2-one moiety of althiomycin is shared by other bioactive natural products. The position of the 4-methoxy-3-pyrrolin-2-one moiety in althiomycin is highlighted by a broken box and this moiety is depicted in grey within the other molecules. Analysis performed in collaboration with Greg Challis and Lijiang Song, University of Warwick.

3.9 Conclusions

We identify *alb1-6* as being required for the biosynthesis and export of the broad spectrum antibiotic, althiomycin, in *S. marcescens* Db10 and we propose a function for each of the identified biosynthetic proteins. Reassuringly, our predictions for the function of *alb2-5* overlap with those presented by Cortina *et al*. 2011. We demonstrate that Alb1 is required for efficient export of althiomycin but that it is not required for

resistance in *S. marcescens* Db10. Additionally, the identification and characterisation of the althiomycin biosynthetic gene cluster in *S. marcescens*, which is a fast-growing and highly genetically tractable organism, offers an exciting "tool box" for the potential future exploitation of Alb proteins as a starting point for the generation and synthesis of useful and modified natural products, such as the 4-methoxy-3-pyrrolin-2-one pharmacophore.

Chapter 4

The role of the phosphopantetheinyl transferase enzyme, PswP, in the biosynthesis of antimicrobial secondary metabolites in *Serratia marcescens* Db10

4.1 Introduction

Phosphopantetheinyl transferase (PPTase) enzymes catalyse the transfer of a phosphopantetheinyl (PPT) group from coenzyme A to a conserved serine residue within the carrier protein domains of fatty acid synthases, non-ribosomal peptide synthases (NRPSs) and polyketide synthetases (PKSs) and this modification is essential for the activity of the enzymes (Figure 1.7) (Beld *et al.*, 2014). Given that PPTase enzymes are essential for NRPS and PKS dependent biosynthesis, we reasoned that *S. marcescens* Db10 must encode at least one PPTase enzyme required for althiomycin biosynthesis. We describe the identification of a PPTase enzyme, PswP, that is required for althiomycin biosynthesis. Upon further characterisation of PswP, it was determined that this enzyme is additionally required for the biosynthesis at least two other NRPS products in *S. marcescens* Db10, namely serrawettin W2 and an enterobactin-like molecule. All three metabolites identified as being dependent on PswP for biosynthesis possess antimicrobial activity, illustrating the essential nature of this PPTase enzyme in secondary metabolite production in *S. marcescens* Db10.

4.2 Identification of the phosphopantetheinyl transferase enzyme, SMA2452 (PswP)

Prior results indicated that the genome of *S. marcescens* Db10 encoded at least one functional NRPS-PKS enzyme; Alb4-5, which is required for the biosynthesis of the antibiotic, althiomycin. It known that functional NRPS and PKS enzymes must be activated by PPTase enzymes, which catalyse the addition of a PPT group (Figure 1.7) (Lambalot *et al.*, 1996). We therefore hypothesised that the genome of *S. marcescens* Db10 encoded a PPTase enzyme and we sought to identify the encoding gene. The gene encoding the PPTase required for activation of an NRPS or PKS enzyme may or may

not be encoded in the same region of the genome as the NRPS or PKS biosynthetic gene cluster (Beld *et al.*, 2014). The *alb1-alb6* gene cluster does not encode a PPTase enzyme; therefore we extended our search for the PPTase needed for althiomycin biosynthesis to the entire genome of *S. marcescens* Db10.

As described above, the Sfp family of PPTases are generally required for the activation of PKS and NRPS enzymes of secondary metabolism. We therefore hypothesised that the PPTase required for althiomycin biosynthesis would belong to this family. Two well characterised PPTases belonging to the Sfp family were thus used to identify Sfp type PPTases in *S. marcescens* Db10 by searching for homologous proteins; Sfp of *B. subtilis* (which is required for surfactin biosynthesis) and EntD of *E. coli* (which is required for the biosynthesis of a siderophore called enterobactin). Two PPTases were identified based on their similarity to Sfp and EntD; SMA4147 and SMA2452, respectively (Figure 4.29).

Figure 4.29. Sequence alignments of *S. marcescens* PPTase enzymes with the characterised PPTases used to identify them. Sequence alignments performed using Clustal 2.1 **A.** SMA2452 and EntD of *Escherichia coli* H730. Percentage identity and similarity between the corresponding proteins was calculated as 37% and 54%, respectively. **B.** SMA4147 and Sfp of *Bacillus subtilis* subsp. *subtilis* RO-NN-1. Percentage identity and similarity between the corresponding proteins was calculated as 26% and 43%, respectively. Asterisk indicates positions which have a single, fully conserved residue. Colon indicates conservation between groups of strongly similar properties. Full stop indicates conservation between groups of weakly similar properties.

As the *SMA2452* and *SMA4147* genes represented likely candidates for the PPTase needed for althiomycin biosynthesis, deletion strains were constructed. Althiomycin production was assessed using the *B. subtilis* bioassay and by UHPLC-ESI-TOF-MS analysis. Deletion of *SMA4147* did not affect althiomycin production; in contrast, mutation of *SMA2452* abolished althiomycin production (Figure 4.30.A and

B). To confirm that the loss of althiomycin production in the *SMA2452* mutant strain was specific to this gene, complementation analysis was performed. To this end, a plasmid carrying the complete *SMA2452* coding region was introduced into the *SMA2452* mutant strain, and the bioassay was performed. The growth inhibition activity was restored (Figure 4.30.C). It is therefore reasonable to conclude that *SMA2452* functions to phosphopantetheinylate the Alb4-5 multi-enzyme during althiomycin biosynthesis.

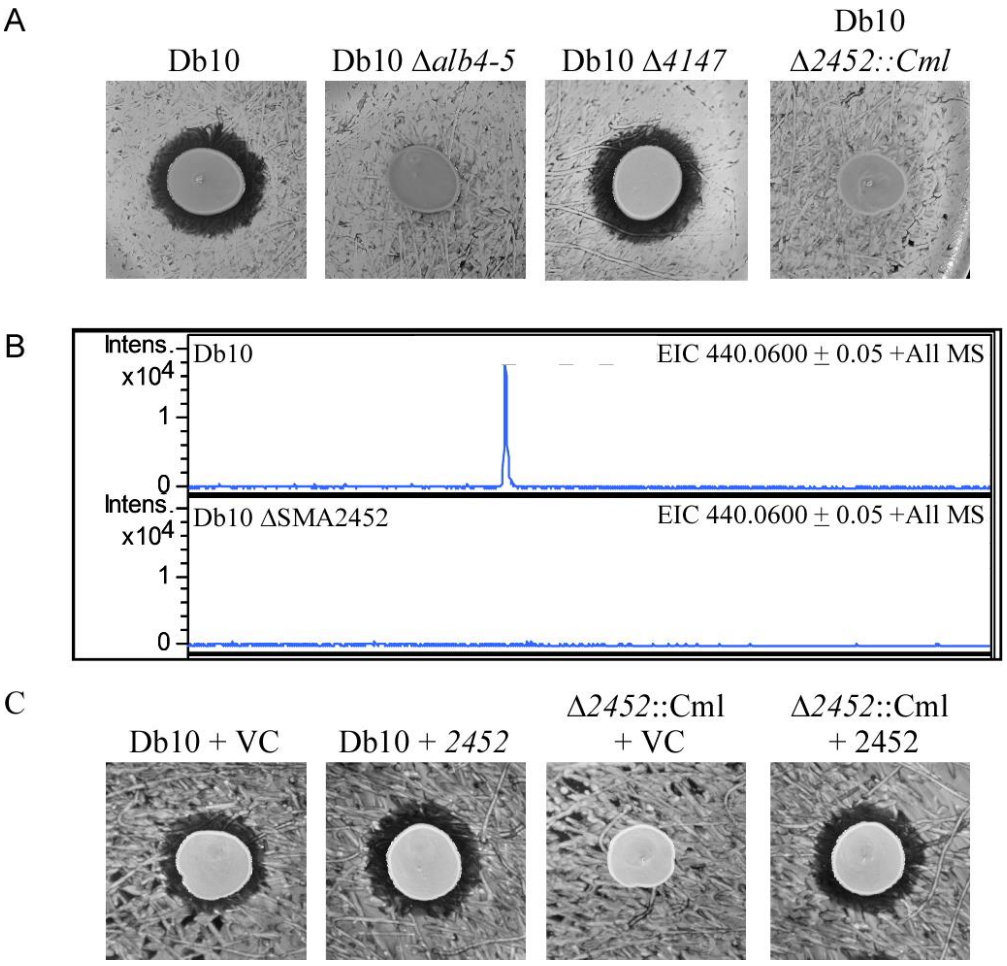

Figure 4.30. The PPTase encoded by *SMA2452* is required for althiomycin biosynthesis. A. Assay to assess the antimicrobial activity of *S. marcescens* Db10, the *alb4-5* mutant strain (SAN5), the Δ*4147* mutant strain (SAN96) and the Δ*2452*::Cml mutant strain (SAN112) against *B. subtilis* 3610. **B.** Extracted ion chromatograms at m/z=440.0600 for *S. marcescens* Db10 and Δ*SMA2452* (SAN112). **C.** Activity assays were performed using *Bacillus subtilis* NRS1473 as the indicator lawn. The producer strains are indicated above as: Db10 + VC (*S. marcescens* Db10 pSUPROM); Db10 + 2452 (*S. marcescens* Db10 pSAN46); Δ*2452*::Cml +VC (SAN112

pSUPROM); Δ*2452*::Cml + *2452* (SAN112 pSAN46). 'VC' represents the empty vector control. Analysis performed in collaboration with Greg Challis and Lijiang Song, University of Warwick.

4.3 Bioinformatic analysis of SMA2452

Having identified *SMA2452* as the PPTase enzyme required for althiomycin biosynthesis, the protein sequence was compared with the sequences of proteins of known function. Further inspection of SMA2452 revealed that it is 96% identical to PswP of *S. marcescens* 274. In *S. marcescens* 274, PswP is the PPTase required for prodigiosin and serrawettin W1 production (Sunaga *et al.*, 2004). Since SMA2452 and PswP are highly similar, SMA2452 will henceforth be referred to as PswP.

As described above, PswP is one of two Sfp type PPTases encoded by *S. marcescens* Db11. Based on the presence of the conserved residues within motifs 1A, 1, 2 and 3, we assigned PswP to the F/KES subfamily of Sfp type PPTases (Figure 4.31).

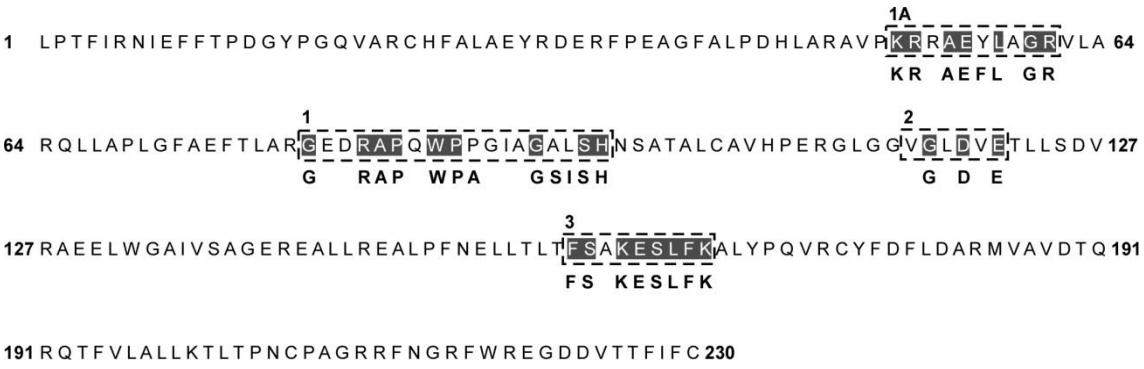

Figure 4.31. Identification of conserved motifs of the F/KES subfamily of Sfp type PPTases within PswP of *Serratia marcescens* Db10. Conserved PPT motifs 1A, 1, 2 and 3 are boxed. Residues previously identified as being highly conserved across the F/KES subfamily are indicated below the sequence; those residues of PswP matching this consensus are shaded black. Analysis based on motif alignment analysis perfomed by Copp and Neilan (Copp & Neilan, 2006).

4.4 The PswP PPTase is required for the biosynthesis of more than one metabolite with antimicrobial activity in *S. marcescens* Db10

The above data demonstrate that when *B. subtilis* is used as an indicator lawn, the deletion of *alb4-5* is sufficient to negate the antimicrobial effect of *S. marcescens* Db10. However, we noted that while *S. aureus* was sensitive to althiomycin, disruption of althiomycin biosynthesis did not completely abolish the antimicrobial effect of *S. marcescens* Db10 against *S. aureus* (Figure 4.32).

Figure 4.32. The althiomycin mutant strain of *Serratia marcescens* Db10 possesses antimicrobial activity against *Staphylococcus aureus*. Antimicrobial activity assays using *S. aureus* as the indicator lawn for the producer strains: Db10 (*S. marcescens* Db10), Δ*alb4-5* (SAN5) and Δ*pswP* (SAN112).

We proceeded to demonstrate that deletion of the PswP PPTase enzyme required for althiomycin biosynthesis is sufficient to negate the antimicrobial activity of *S. marcescens* Db10 against *S. aureus* (Figure 4.32). PPTase enzymes are known to modify the carrier protein domain of FAS, PKS and NRPS enzymes (Lambalot *et al.*, 1996). We thus hypothesised that, in addition to being required for althiomycin biosynthesis, PswP was required for the biosynthesis of one or more FAS, PKS or NRPS product(s) with antimicrobial activity against *S. aureus*. Following this initial observation, we aimed to determine the identity of this metabolite(s).

4.5 Identification of candidate targets of PswP

In *S. marcescens* Db10, the *pswP* coding region is not embedded within or adjacent to an NRPS or PKS biosynthetic gene cluster. We were therefore unable to predict additional PKS or NRPS biosynthetic pathways that might require that activity of PswP based on its genomic context. The bioinformatics tool, antiSMASH, allows identification and preliminary analysis of secondary metabolite gene clusters in bacterial and fungal genomes in an unbiased manner (Blin *et al.*, 2013). Therefore, antiSMASH was employed to identify all genomic regions containing putative PKS, NRPS and NRPS-PKS gene clusters in the *S. marcescens* Db10 genome, on the basis that one or more of these might direct the biosynthesis of the secondary metabolite(s) active against *S. aureus*. The results of this search are summarised in Table 4.15. Five genomic regions containing NRPS or NRPS-PKS gene clusters, whose products could potentially be modified by the action of PswP, were identified. Upon closer inspection of the NRPS and NRPS-PKS gene clusters, the althiomycin biosynthetic machinery and the machinery required for the biosynthesis of the surfactant, serrawettin W2, were identified in clusters three and four (Gerc *et al.* 2012, Pradel *et al.*, 2007). Published data for the three remaining gene clusters was not available and so a bioinformatic approach was adopted. In an attempt to deduce the likely product of the three remaining NRPS biosynthetic gene clusters, the protein sequences encoded by the NRPS genes(s) identified by antiSMASH, together with the products of the flanking genes, were subjected to database searching using BlastP (Altschul *et al.*, 1997). Analysis of the NRPSs in gene cluster one revealed that this locus likely encodes proteins involved in the biosynthesis of a microcin (Table 4.15). SMA1574A shows 41% identity with microcin N of *E. coli* 2424 (Corsini *et al.*, 2010) and the NRPS proteins, SMA1572 and SMA1571, are likely involved in biosynthesis of a modifying group added to the

microcin peptide encoded by this gene cluster (Rebuffat, 2012). In contrast, gene clusters two and five appear to direct the synthesis of multiple siderophores (Table 4.15). The NRPS encoded within gene cluster two shares homology with chrysobactin synthetase component F (Persmark *et al.*, 1989) and within gene cluster five is a locus containing an NRPS and associated genes conserved with the enterobactin biosynthesis and utilisation genes from *E. coli* (see below) (Raymond *et al.*, 2003).

Table 4.15. Characterisation of non-ribosomal peptide synthase (NRPS) or polyketide synthetase (PKS) encoding genes identified by antiSMASH (Blin *et al.*, 2013)

Gene cluster	Genomic region predicted by antiSMASH	Enzyme predicted by antiSMASH	Gene(s) encoding NRPS (or NRPS-PKS)	Previously reported product	Putative product	Comments
1	*SMA1552-1589*	NRPS	*SMA1571-1572*	-	Unknown	Predicted NRPS encoded within a cluster of genes (*SMA1575-1568*) showing similarity with genes involved in biosynthesis and secretion of microcins; may synthesize a modifying group added to the microcin.
2	*SMA1705-1744*	NRPS	*SMA1729*	-	Siderophore	Predicted NRPS similar to chrysobactin synthetase (64% identity over the whole length) and flanked by genes encoding proteins with similarity to proteins mediating siderophore export, uptake and iron release.
3	*SMA2274-1309*	NRPS-PKS	*SMA2289-2290*	Althiomycin	n/a	Althiomycin is a broad-spectrum antibiotic. NRPS-PKS is encoded within the six-gene *alb* operon (*SMA2288-2293*) which also encodes tailoring and export functions.
4	*SMA3659-3702*	NRPS	*SMA3680*	Serrawettin W2	n/a	Serrawettin W2 is a biosurfactant (Pradel *et al.*, 2007).
5	*SMA4386-4438*	NRPS	*SMA4411*	-	Siderophore	Predicted NRPS is similar to enterobactin synthetase EntF and within cluster of genes (*SMA4408-4415*) similar to the enterobactin biosynthesis, export and uptake cluster of *E. coli* (Figure 4.35).
			SMA4402-4404, SMA4406	-	Unknown	Encoded NRPS proteins share similarity with siderophore synthetase enzymes from other organisms but number and nature of product(s) unclear.

4.6 The PswP-dependent surfactant serrawettin W2 has antimicrobial activity against *S. aureus*

Biosurfactants are amphipathic molecules whose primary function is to reduce surface tension to allow bacterial spreading across surfaces (Matsuyama, 2011). Biosurfactants have been shown to possess several properties, including antimicrobial activity (Singh & Cameotra, 2004). Of particular note, Serrawettin W1 produced by *S. marcescens* ATCC274 has been shown to have antimicrobial properties against methicillin resistant *Staphylococcus aureus* (MRSA) (Kadouri & Shanks, 2013). In *S. marcescens* Db10, PswP had previously been shown to be required for the biosynthesis of serrawettin W2 (Pradel *et al.*, 2007). Therefore, to determine whether serrawettin W2 also possessed antimicrobial activity against *S. aureus*, a serrawettin W2 single mutant was obtained (Pradel *et al.*, 2007) and used to construct a double mutant (Δ*swrA::Tn5* Δ*alb4-5*) unable to produce althiomycin or serrawettin W2. Both mutant strains were tested for antimicrobial activity against *S. aureus* (Figure 4.33). Compared with *S. marcescens* Db10, the Δ*swrA::Tn5* mutant showed a slight reduction in antimicrobial activity against *S. aureus*. The reduction in antibiosis halo observed with the double Δ*swrA::Tn5* Δ*alb4-5* mutant was much more pronounced than with either single mutant, however, a small antibiosis halo could still be observed (Figure 4.33). We therefore concluded that serrawettin W2 does indeed possess antimicrobial activity against *S. aureus*, but that *S. marcescens* Db10 must produce another antimicrobial, in addition to serrawettin W2 and althiomycin, which is dependent on the presence of PswP for biosynthesis.

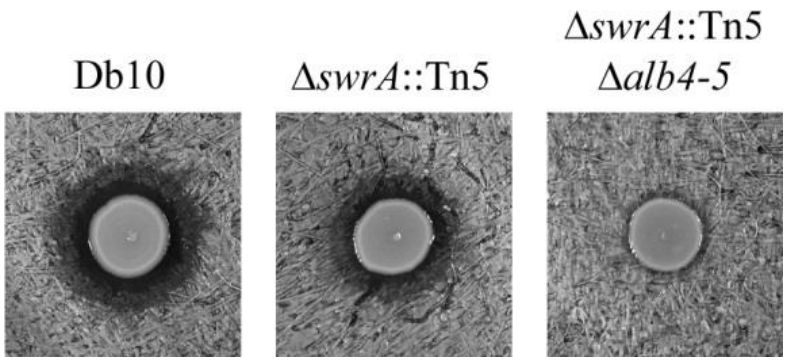

Figure 4.33. The PPTase PswP is required for the biosynthesis of at least three secondary metabolites with antimicrobial activity against *Staphylococcus aureus*. Antimicrobial activity assays using *S. aureus* as the indicator lawn for the producer strains: Db10 (*S. marcescens* Db10), Δ*swrA*::Tn5 (JESM267) and Δ*swrA*::Tn5 Δ*alb4-5* (SAN124).

The *SMA4408-4415* gene cluster encodes a siderophore which is dependent on PswP for biosynthesis and has antimicrobial activity against *S. aureus*

In light of the results presented above, we reasoned that one or more of the three remaining NRPS gene clusters identified by antiSMASH should be responsible for the antimicrobial effect against *S. aureus* in the absence of althiomycin and serrawettin W2. Two of the three remaining NRPS gene clusters identified by antiSMASH encoded proteins with similarity to siderophore biosynthetic proteins (Table 4.15 and Figure 4.35). We therefore hypothesised that either a siderophore produced by *S. marcescens* Db10 was directly toxic toward *S. aureus*, or that siderophore dependent removal of iron from the environment prevented growth of *S. aureus*. In order to distinguish between these possibilities, $FeCl_3$ was added to the growth media and the antimicrobial bioassay repeated. The small antibiosis halo which could be observed with the double Δ*swrA::Tn5* Δ*alb4-5* mutant in the absence of additional iron disappeared upon the addition of $FeCl_3$ (Figure 4.34).

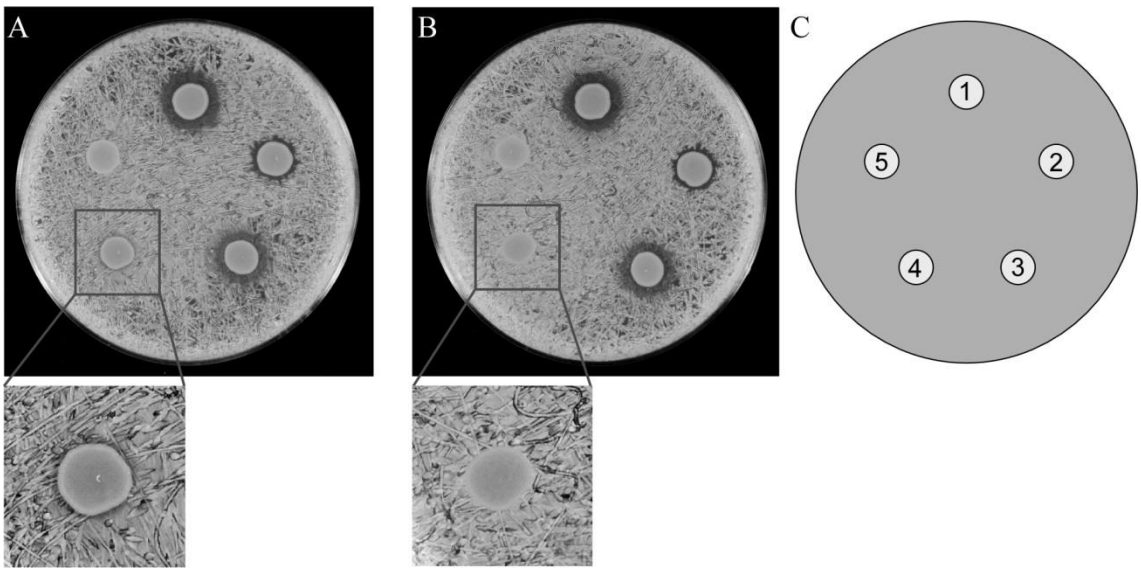

Figure 4.34. An althiomycin and serrawettin W2 mutant of *Serratia marcescens* Db10 is unable to kill *Staphylococcus aureus* in the presence of additional iron. Antimicrobial activity assays in the absence (a) or presence (b) of 50 mM $FeCl_3$, using *S. aureus* as the indicator lawn, with a schematic of the location of each producer strain shown (c). The producing strains were: **1.** *S. marcescens* Db10 (wild type) **2.** SAN5 (Δ*alb4-5*) **3.** JESM267 (Δ*swrA::Tn5*) **4.** SAN112 (Δ*pswP*) **5.** SAN124 (Δ*alb4-5*, D*swrA*::Tn5).

From these results two scenarios are possible: 1) Addition of excess iron negates the iron depletion effect of a siderophore(s) or 2) The addition of iron negatively affects the production of siderophores by *S. marcescens* Db10, as observed in *E. coli* and many other Gram-negative bacteria (Crosa & Walsh, 2002). In either case, these findings indicated that siderophore production by *S. marcescens* Db10 was likely to inhibit *S. aureus* growth.

As mentioned above, a set of genes (*SMA4408-4415*) within cluster five show homology and synteny with the enterobactin gene cluster of *E. coli* (Figure 4.35). It therefore seemed likely that these genes are involved in the synthesis of enterobactin or a closely related molecule. It should be noted, however, that the only close homologue of *entA*, which is located immediately upstream of *entB* in *E. coli*, was identified as *SMA2450* in *S. marcescens* Db11. In contrast with *E. coli*, the *SMA2450* gene is located

at a distant locus from the other enterobactin genes, however it is closely genetically linked with *pswP* (*SMA2452*) in *S. marcescens*. Given both the linkage between *entA* and *pswP* in *S. marcescens* and that the *SMA4408-4415* genomic region showed the most convincing similarity with a well-characterised cluster of genes involved in siderophore biosynthesis and utilisation, we tested whether the product of these genes was responsible for the PswP- and iron-dependent growth inhibition observed in the Δ*swrA::Tn5* Δ*alb4-5* double mutant. The product of *SMA4415* shares significant homology with *entB* of the enterobactin biosynthetic gene cluster (Figure 4.35).

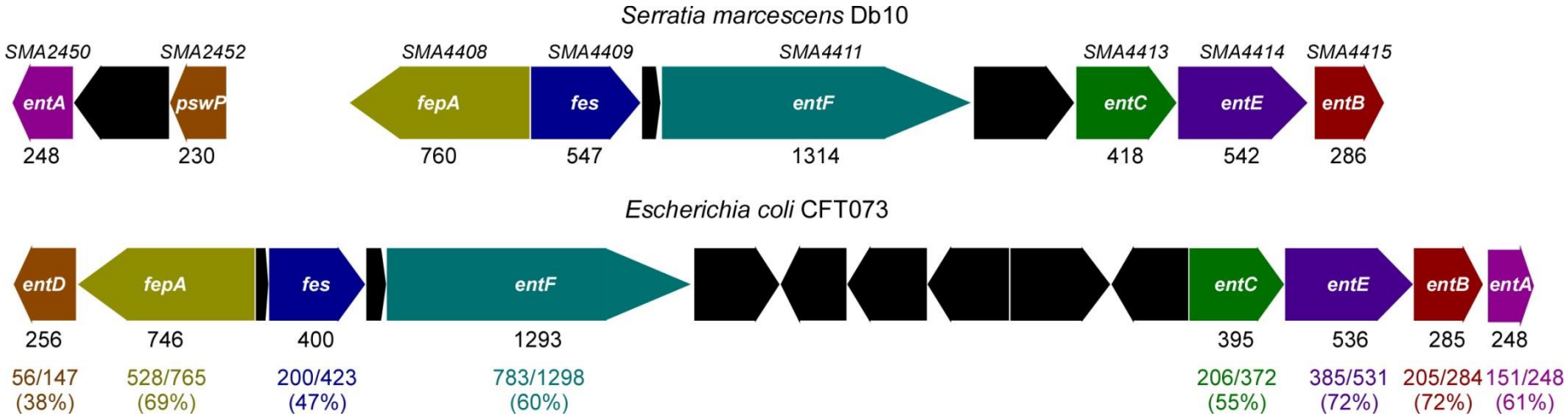

Figure 4.35 Comparison of the *SMA2450-2452* and *SMA4408-4415* gene clusters of *Serratia marcescens* Db10 with the enterobactin biosynthetic gene cluster of *Escherichia coli* CFT073 (*c0668-c0683*). Genes are drawn approximately to scale and protein length is indicated below the encoding gene (as the number of amino acids). Homologous genes are indicated by the same colour and the level of identity between homologous proteins is shown below the corresponding gene. The extent to which two (nucleotide or amino acid) sequences have the same residues at the same positions is indicated as an absolute value or as a percentage.

Since EntB is essential for enterobactin biosynthesis in *Escherichia coli* (Crosa & Walsh, 2002), we reasoned that SMA4415 would be essential for biosynthesis of this siderophore in *S. marcescens* Db10. An in-frame deletion in *entB* was therefore constructed in the althiomycin and serrawettin W2 deficient strain to give a triple althiomycin, serrawettin W2 and enterobactin mutant (Δ*swrA*::Tn5, Δ*alb4-5*, Δ*entB*). and also in the althiomycin and serrawettin W2 mutant background to give a triple althiomycin, serrawettin W2 and Δ*entB* mutant (*swrA*::Tn5 Δ*alb4-5* Δ*entB*). To compare siderophore production by wild type *S. marcescens* Db10 with that of the single Δ*entB* mutant, the triple *swrA*::Tn5 Δ*alb4-5* Δ*entB* mutant and the Δ*pswP* mutant, the relevant strains were grown on chrome azurol S (CAS) indicator plates. The CAS/hexadecyltrimethylammonium bromide/ferric iron complexes present in these plates serve as an indicator of siderophore biosynthesis; in the presence of an iron chelator this indicator turns from a blue to an orange colour (Schwyn & Neilands, 1987). In wild type *S. marcescens* Db10, production of a diffusible siderophore was clearly observed (Figure 4.36). In contrast, no siderophore production was observed in the Δ*entB* single mutant, in the althiomycin, serrawettin W2 and Δ*entB* triple mutant (*swrA*::Tn5 Δ*alb4-5* Δ*entB*), or in the PswP PPTase mutant (Δ*pswP*) (Figure 4.36). The loss of siderophore production was specific to the deletion of *entB* or *pswP*, with siderophore production being unaffected in strains unable to produce althiomycin and/or serrawettin (Figure 4.36). These results clearly show that both *entB* and *pswP* are essential for the biosynthesis of a siderophore in *S. marcescens* Db10.

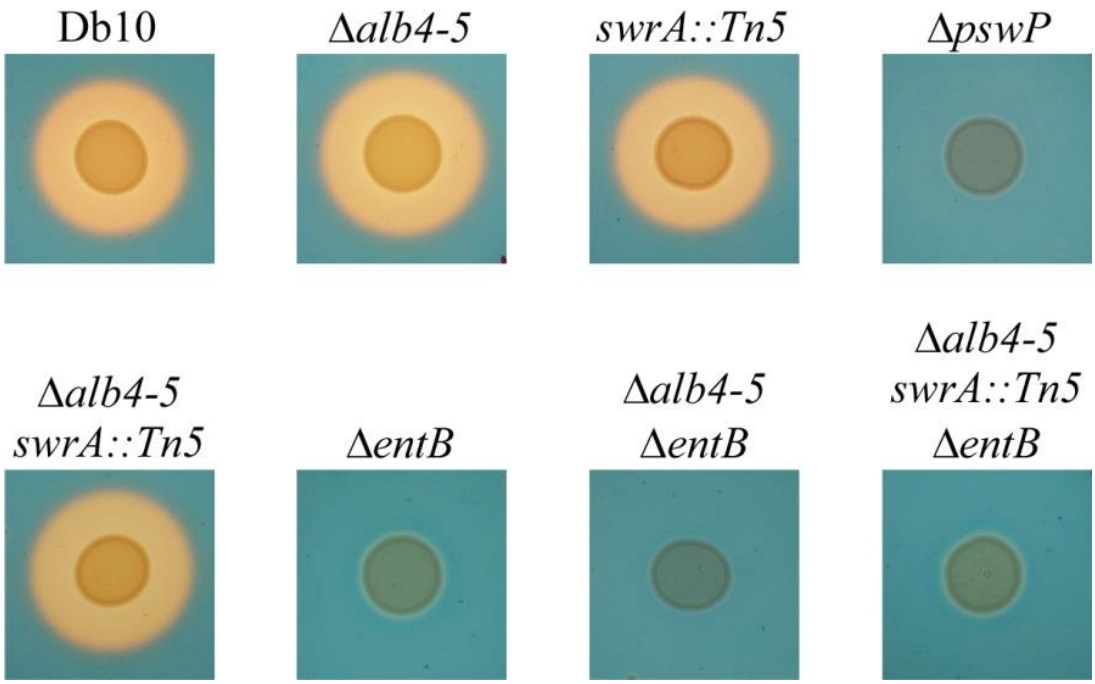

Figure 4.36. The PPTase PswP and SMA4415 (EntB) are required for the biosynthesis of a siderophore in *S. marcescens* Db10. Chrome azurol S (CAS) assay for the detection of siderophore biosynthesis, as indicated by the presence of an orange halo. (a) The producer strains are indicated above as: Db10 (wild type *S. marcescens* Db10), Δ*alb4-5* (SAN5), *swrA*::Tn5 (JESM267), Δ*alb4-5 swrA*::Tn5 (SAN124), Δ*entB* (SAN176), Δ*pswP* (SAN112) and Δ*alb4-5 swrA*::Tn5 Δ*entB* (SAN181).

Additionally, the CAS assay allowed us to confirm that construction of the *pswP* (*SMA2452*) PPTase mutant did not affect siderophore biosynthesis through downstream polar effects on the expression of *SMA2450*, predicted to encode an EntA homologue (Figure 4.35), since the loss of siderophore biosynthesis observed with the *pswP* mutant could be complemented by the expression of *pswP in trans* (Figure 4.37).

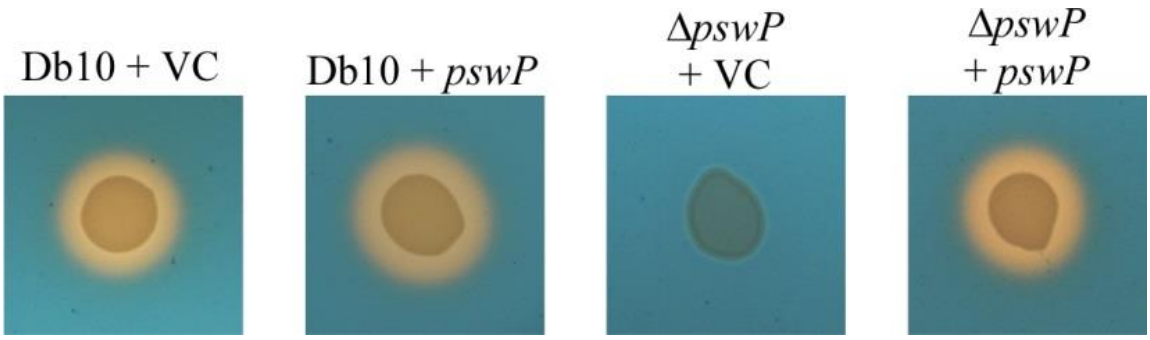

Figure 4.37. The expression of *sma2450* (*entA*) is unaffected in the Δ*pswP* mutant. Complementation of the *pswP* deletion by expression of *pswP in trans*. The producer strains are indicated above as: Db10 + VC (*S. marcescens* Db10 pSUPROM, vector control), Db10 + *pswP* (*S. marcescens* Db10 pSAN46), Δ*pswP* + VC (SAN112 pSUPROM) and), Δ*pswP* + *pswP* (SAN112 pSAN46).

Having shown that *entB* was required for biosynthesis of a siderophore in *S. marcescens* Db10, the triple althiomycin, serrawettin W2 and siderophore mutant was tested for antimicrobial activity against *S. aureus*. No antibiosis halo was observed with the *swrA*::Tn5 Δ*alb4-5* Δ*entB* triple mutant (Figure 4.38), thus providing a phenocopy of the PswP PPTase mutant and indicating that the *entB*-dependent siderophore is the third PswP-dependent antimicrobial secondary metabolite produced by *S. marcescens* Db10.

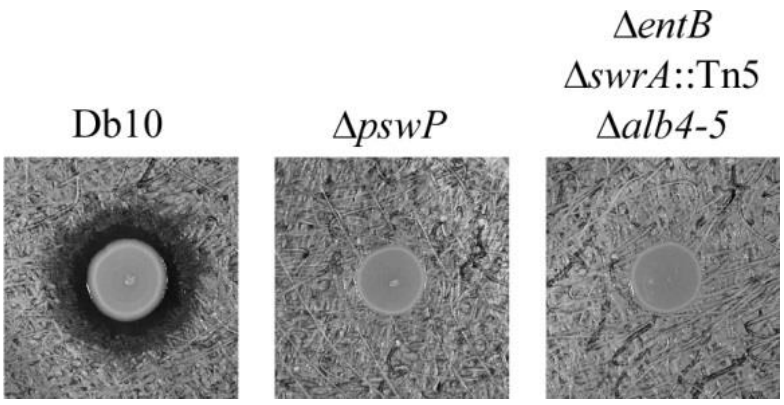

Figure 4.38. The PPTase PswP is required for the biosynthesis of three secondary metabolites with antimicrobial activity against *Staphylococcus aureus*. Antimicrobial activity assays using *S. aureus* as the indicator lawn for the producer strains: Db10 (*S. marcescens* Db10), Δ*pswP* (SAN112) and Δ*entB*, Δ*swrA*::Tn5, Δ*alb4-5* **(**SAN181)

4.7 Discussion

Our data highlights how an individual bacterial PPTase enzyme can play an essential role in the biosynthesis of multiple secondary metabolites with disparate physiological roles and additionally demonstrates how several distinct secondary metabolites can contribute to the inhibition of growth of competitor bacteria. PPTase enzymes may therefore be essential for survival in multispecies environments.

PswP was one of three PPTases identified in *S. marcescens* Db10. *SMA3052* was identified based on homology to AcpS of *E. coli* and likely the sole PPTase involved in primary metabolism (data not shown). Both PswP and *SMA4147* belong to the Sfp family of PPTases and, as mentioned above, were identified based on homology to EntD of *E. coli* and Sfp of *B. subtilis*, respectively (Figure 4.29). In contrast to *pswP*, deletion of *SMA4147* did not influence the antimicrobial effect of *S. marcescens* Db10 on *S. aureus* growth (data not shown). Since no phenotypic effects could be observed upon the deletion of *SMA4147*, the role of this enzyme in secondary metabolite biosynthesis in *S. marcescens* Db10 could not be defined. It appears that the targets of PswP and SMA4147 do not overlap, however, since deletion of PswP alone was

sufficient to abolish althiomycin, serrawettin W2 and enterobactin(-like) biosynthesis. It is possible that SMA4147 is required for the biosynthesis of the additional NRPS products whose encoding genes were identified by antiSMASH.

Given that a single PPTase enzyme may be essential for several metabolic pathways, the potential for PPTase enzymes to serve as targets for the development of antimicrobials seems an obvious step forwards, however, this may not be feasible. In humans, there exists a single PPTase (AASDHPPT) which, surprisingly, was identified through homology to Sfp of *B. subtilis* (Joshi et al., 2003); as described above, Sfp family PPTases are generally associated with NRPS and PKS enzymes of secondary metabolism in micro-organisms (Mootz *et al.*, 2001; Quadri *et al.*, 1998). To date, three metabolic pathways requiring AASDHPPT have been described (Joshi *et al.*, 2003; Strickland *et al.*, 2010), perhaps explaining why a typically promiscuous Sfp family PPTase exists in humans. The overlap in sequence and structural homology between bacterial PPTases and the human AASDHPPT may render the development of bacterial specific PPTase antimicrobials impossible. Further, AASDHPPT has been suggested to be essential, since AASDHPPT silencing by small interfering RNA induces a strong G_1 cell cycle arrest (Joshi *et al.*, 2003).

Work presented in this study is the first to implicate the *SMA4408-4415* gene cluster in the biosynthesis of an enterobactin-like siderophore in *S. marcescens* Db10. In the *Serratia* strain *sp.* V4, a siderophore called serratiochelin was identified as a product of an operon which appeared to share characteristics with the enterobactin gene cluster of *E. coli* and the vibriobactin gene cluster of *Vibrio cholera*. Unfortunately, the genome sequence of the serratiochelin gene cluster has not been published and so it was not possible to directly compare this gene cluster with the enterobactin-like gene cluster that we identified in *S. marcescens* Db10. Within the vibriobactin-like gene cluster of

Serratia sp. V4, *schH* shows a similar level of identity to the corresponding vibriobactin protein as *SMA4402*. The organisation of the *SMA4402-2206* gene cluster also appears to be similar to that of the serratiochelin gene cluster, although not identical; in the *S. marcescens* Db10 gene cluster *entA* is associated with *pswP*, whereas in *Serratia sp.* V4, the equivalent gene is located within the enterobactin-like gene cluster (Seyedsayamdost *et al.*, 2012).

The presence of more than one iron uptake system is common in bacteria, for example, some strains of *E. coli* possess up to eight of these systems (Adler *et al.*, 2012). The *SMA4408-4415* gene cluster was one of two siderophore biosynthetic gene clusters identified in *S. marcescens* Db10. The NRPS SMA1729 was also identified and predicted to encode a chrysobactin-like molecule. Noteably, the chrysobactin like siderophore was either not produced or not active under CAS assay conditions, since deletion of *entB* was sufficient to negate siderophore production.

The antimicrobial effects of siderophores have previously been investigated (Adler *et al.*, 2012; Braun *et al.*, 2009; Wang *et al.*, 2009). For example, pyochelin produced by *Pseudomonas aeruginosa* displays antimicrobial activity against several *Xanthomonas* strains and *S. aureus*. Perhaps surprisingly, the antimicrobial effects were attributed to the generation of reactive oxygen species rather than iron depletion (Adler *et al.*, 2012). In the case of *S. marcescens* Db10, the antimicrobial effects of the enterobactin like siderophore were not defined. The addition of iron to the antimicrobial assay plates abolished the antimicrobial effects of *S. marcescens* Db10 against *S. aureus*. However, the addition of iron may have either turned off expression of the enterobactin like siderophore encoding genes, or it may have negated the iron limiting antimicrobial effects of the siderophore. A distinction between these possibilities was

not made. It is entirely possible that the inhibition of *S. aureus* growth by the enterobactin like siderophore occurs independently of the available iron.

4.8 Conclusions

We demonstrate that the function of the PswP PPTase is essential in several secondary metabolite biosynthesis pathways in *S. marcescens* Db10. We were able to identify althiomycin, serrawettin W2 and an enterobactin (-like) molecule as being dependent on PswP for biosynthesis, since all three metabolites possess anti-microbial activity against *S. aureus*. Our data suggests that a single PPTase can play important roles in a variety of metabolic pathways in bacteria.

Chapter 5

Insights into the assembly and function of the Type VI Secretion System of *Serratia marcescens* Db10

5.1 Introduction

The Type VI secretion system (T6SS) is the most recently discovered of the Gram-negative bacterial secretion systems. This system comprises a minimum of 13 core components and functions to target proteins directly from the producing cell into a bacterial or eukaryotic cell (Boyer et al., 2009). *S. marcescens* Db10 possesses a single T6SS gene cluster (*sma2244-2281*) which encodes the essential core components TssA-TssM. This 38 gene operon additionally encodes effector proteins that are secreted by the system and proteins that are involved in post-translational regulation (Figure 5.39) (English et al., 2012; Fritsch et al., 2013; Murdoch et al., 2011). However, the roles of several proteins encoded by the gene cluster have yet to be defined. In the case of *S. marcescens* Db10, the T6SS is a potent anti-bacterial system (Murdoch et al., 2011). The aim of this work was to gain new insight into the mechanism of the T6SS using *S. marcescens* Db10, specifically by constructing strains encoding translational fusions of components of the T6SS with fluorescent proteins. Analysis of these strains, using several fluorescence microscopy based approaches, should permit aspects of T6SS assembly and function to be investigated. Here, we describe the construction and functional characterisation of eight such fusion strains and the visualisation of the corresponding T6SS components using fluorescence microscopy. Additionally, we further characterise the frequency with which the T6SS assembles by using the strain expressing the TssB-mCherry fusion protein to indicate the site of assembly of an active T6SS.

5.2 Construction and characterisation of strains expressing *tss-mCherry* fusion proteins

As described above, the T6SS is composed of 13 essential conserved components. Seven of these universally conserved components, together with one widely conserved component, were chosen for construction of chromosomally encoded, C-terminal, translational fusions with the fluorescent protein, mCherry. The T6SS components selected were; TssJ, TssK, TssH, TssL, TssB, TssE, VgrG-2 (a TssI family protein) and Fha. As described in detail in the Introduction, these components are believed to occupy distinct locations within the machinery, including the basal cytoplasmic complex (TssK, TssE, Fha), the contractile cytoplasmic sheath (TssB, TssH), the membrane subcomplex (TssL, TssJ) and the expelled puncturing structure (VgrG-2) (Figure 5.39).

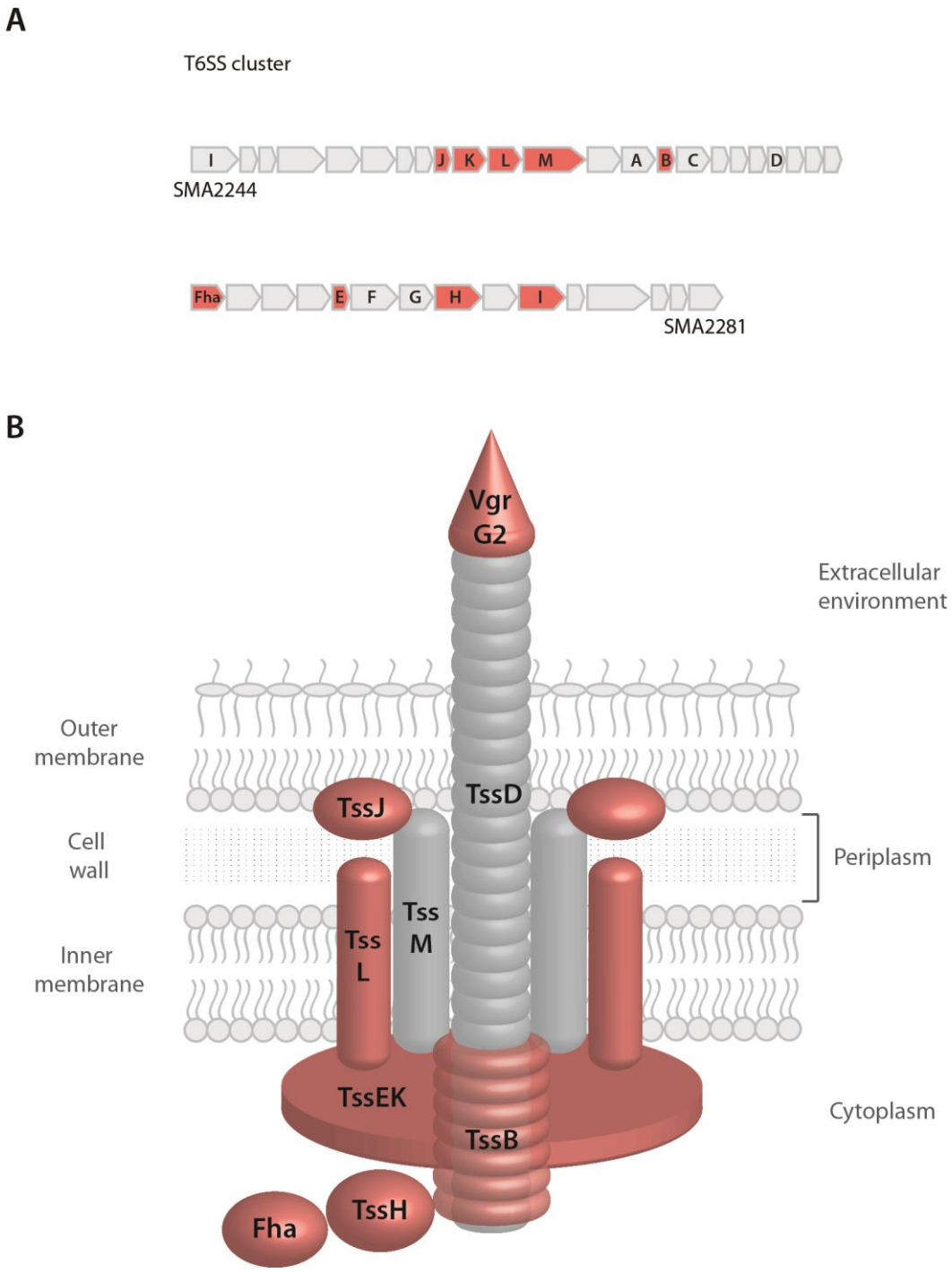

Figure 5.39. Schematic representation of the genomic context and predicted cellular localisation of selected components of the Type VI Secretion System. Components in *Serratia marcescens* Db10 selected to construct chromosomal translational fusions with mCherry are indicated in red. **A.** Schematic representation of the T6SS gene cluster. Genes encoding conserved T6SS components are shown by letter, indicating their Tss name. Of note, two TssI family proteins are encoded by the T6SS in *S. marcescens* Db10, VgrG-1 and VgrG-2 **B.** Schematic representation of the structure of the T6SS. VgrG2 forms a spike-like structure that is thought to puncture the membrane of target cells and may also associate with a subset of effector proteins to mediate translocation. TssJ is a lipoprotein found in the outer membrane.

TssL is anchored in the inner membrane, and possesses a periplasmic peptidoglycan binding domain and a cytoplasmic domain. TssB forms part of the sheath which surrounds the TssD tube in the cytoplasm. Contraction of this sheath is thought to propel the TssD tube forwards and out of the host cell. TssE and TssK are likely components of the cytoplasmic baseplate structure, however, their precise role remains unclear. TssH is a cytoplasmic ATPase that is required for disassembly of the TssBC sheath following contraction. Finally, Fha, when present, is an essential component of the system; it can be a target of post-translational regulation and may be involved in promoting an active conformation of the machinery.

Having constructed strains encoding translational fusions of each of the above T6SS components with mCherry, at the normal chromosomal location, we determined the functionality of the T6SS in each case. To achieve this, three different assays were employed. These were the TssD secretion assay, the Ssp2 secretion assay and bacterial competition assays, schematically depicted in Figure 5.40. Since TssD is an essential component of the T6SS and is secreted when the system fires, detection of this component in the extracellular milieu is used as an indicator of the assembly of an active T6SS (Pukatzki et al., 2009). Ssp2 has been identified as a T6SS dependent bacterial effector, however, it is not an essential component of the system. Detection of Ssp2 in the extracellular milieu indicates that the T6SS is competent for the secretion of "true" effector proteins (English et al., 2012). Finally, the efficiency with which the T6SS kills neighbouring target cells can be assessed by conducting competition assays between the *S. marcescens* strain of interest and a T6-susceptible target bacterium.

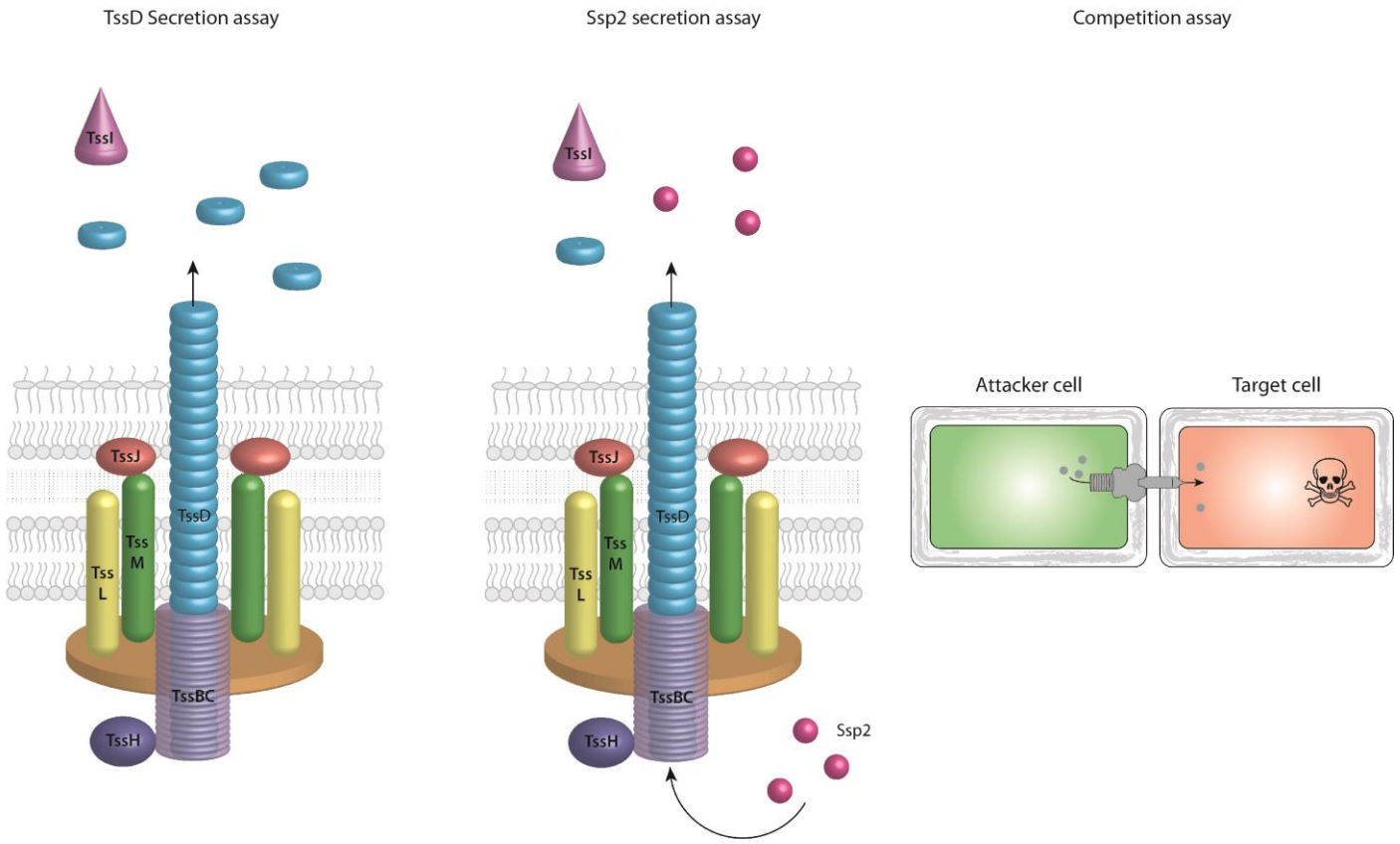

Figure 5.40. Schematic representation of assays used to determine the functionality of the T6SS in each strain expressing a *tss-mCherry* fusion protein. TssD and Ssp2 secretion assays involved the immunoblot detection of these proteins in the culture supernatant of the relevant strain. To assess T6SS functionality by competition assay, the number of viable target cells is determined following a co-incubation period with attacker cells.

5.2.1 Functionality of the T6SS in strains expressing *tss-mCherry* fusion proteins as determined by a TssD secretion assay

TssD secretion was compared between the following strains: wild type *S. marcescens* Db10, *S. marcescens* Db10 Δ*tssH*, *S. marcescens* Db10 *tssJ-mCherry*, *S. marcescens* Db10 *tssK-mCherry*, *S. marcescens* Db10 *tssH-mCherry*, *S. marcescens* Db10 *tssL-mCherry*, *S. marcescens* Db10 *tssB-mCherry*, *S. marcescens* Db10 *tssE-mCherry* (SAN164) and *S. marcescens* Db10 *fha-mCherry*. Since TssH is an essential, conserved component of the T6SS, a strain lacking this gene was used as a negative control. Secretion of TssD in the *S. marcescens* Db10 *vgrG-2-mCherry* strain was assessed separately, since VgrG-2 is not essential in the presence of VgrG-1 in *S. marcescens* Db10 (SJC lab, unpublished). Results revealed that all the fusion strains constructed were competent for the secretion of TssD, with the exception of the strain encoding TssK-mCherry (Figure 5.41). In the case of the strain encoding VgrG-2-mCherry, we observed that VgrG-2-mCherry was able to support secretion of TssD in the absence of VgrG-1, indicating its functionality in this assay (Figure 5.41).

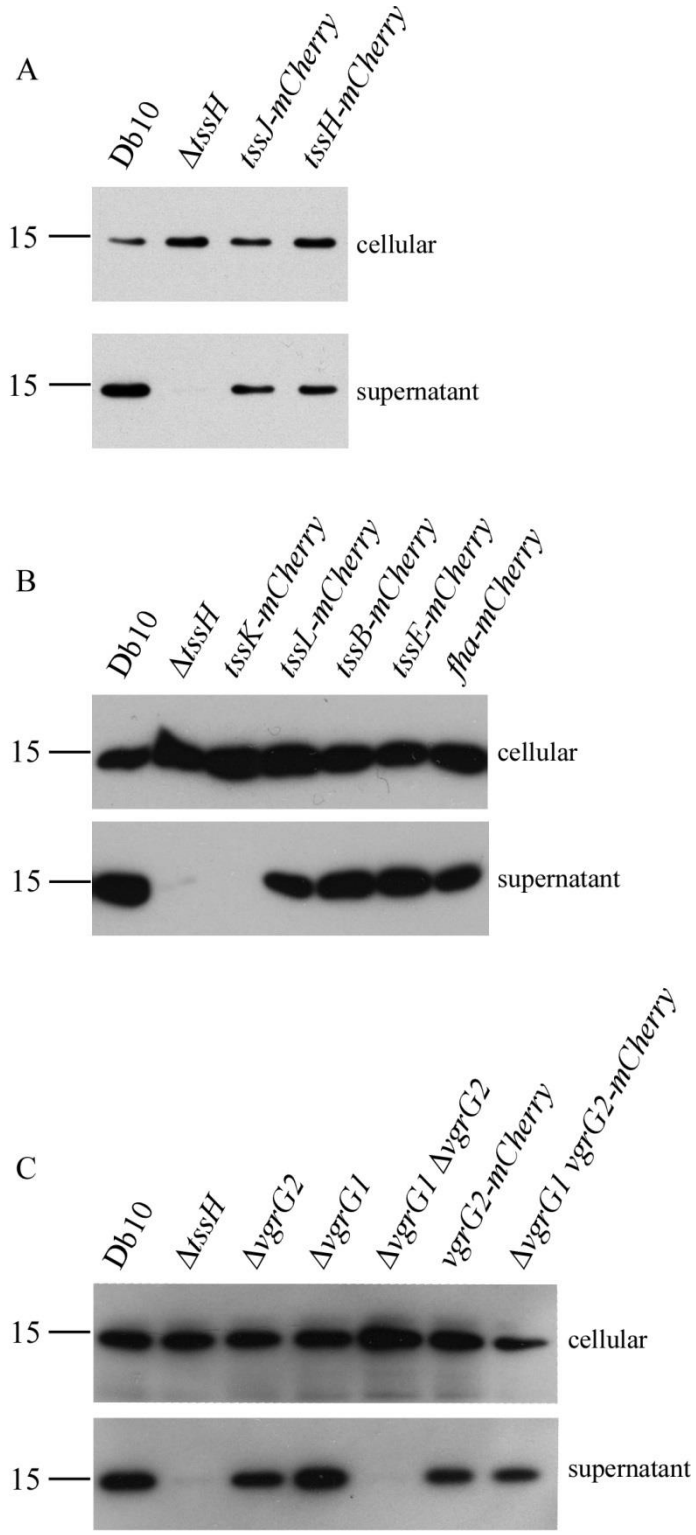

Figure 5.41. TssD secretion assay to assess functionality of the T6SS-mCherry fusion proteins. Immunoblot detection of TssD in the cellular and secreted fractions from: **A.** *Serratia marcescens* Db10, SJC3 (*S. marcescens* Db10 ΔtssH), SAN157 (*S. marcescens* Db10 *tssJ-mCherry*), SAN159 (*S. marcescens* Db10 *tssH-mCherry*) **B.** *S. marcescens* Db10, SJC3 (*S. marcescens* Db10 Δ*tssH*), SAN158 (*S. marcescens* Db10 *tssK-mCherry*), SAN162 (*S.*

marcescens Db10 *tssL-mCherry*), SAN163 (*S. marcescens* Db10 *tssB-mCherry*), SAN166 (*S. marcescens* Db10 *tssE-mCherry*) and SAN164 (*S. marcescens* Db10 *fha-mCherry*) **C.** *S. marcescens* Db10, SJC3 (*S. marcescens* Db10 Δ*tssH*), FRA01 (*S. marcescens* Db10 Δ*vgrG-2*), FRA02 (*S. marcescens* Db10 Δ*vgrG-1*), FRA03 (*S. marcescens* Db10 Δ*vgrG-1* Δ*vgrG-2*), SAN186 (*S. marcescens* Db10 *vgrG-2-mCherry*) and SAN202 (*S. marcescens* Db10 Δ*vgrG-1 vgrG-2-mCherry*)

5.2.2 Functionality of the T6SS in strains expressing *tss-mCherry* fusion proteins as determined by an Ssp2 secretion assay

Ssp2 secretion assays were then performed on the strains, described above, encoding Tss-mCherry fusion proteins. TssE and TssH are essential conserved components of the T6SS and so strains lacking these components were used as negative controls for Ssp2 secretion. Similar to results obtained from the TssD secretion assay, the strain encoding the TssK-mCherry fusion protein was the only strain which harboured a non-functional T6SS (Figure 5.42). Again, in agreement with results obtained from the TssD secretion assay, VgrG-2-mCherry was sufficient for export of TssD in the absence of VgrG-1 (Figure 5.42).

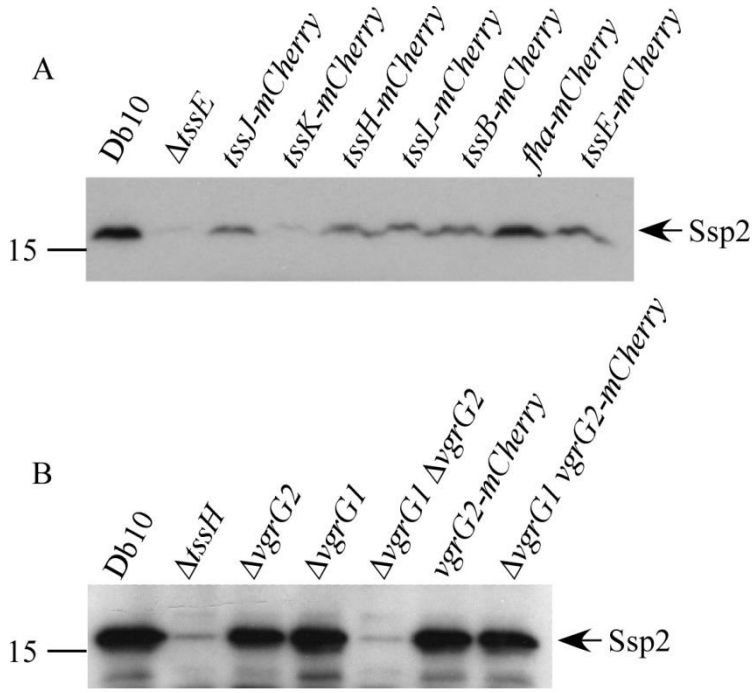

Figure 5.42. Ssp2 secretion assay to assess functionality of the T6SS-mCherry fusion proteins. Immunoblot detection of Ssp2 in secreted fractions from: **A.** *Serratia marcescens* Db10, SJC1 (*S. marcescens* Db10 Δ*tssE*), SAN157 (*S. marcescens* Db10 *tssJ-mCherry*), SAN158 (*S. marcescens* Db10 *tssK-mCherry*), SAN159 (*S. marcescens* Db10 *tssH-mCherry*), SAN162 (*S. marcescens* Db10 *tssL-mCherry*), SAN163 (*S. marcescens* Db10 *tssB-mCherry*), SAN164 (*S. marcescens* Db10 *fha-mCherry*) and SAN166 (*S. marcescens* Db10 *tssE-mCherry*) **B.** *S. marcescens* Db10, SJC3 (*S. marcescens* Db10 Δ*tssH*), FRA01 (*S. marcescens* Db10 Δ*vgrG-2*), FRA02 (*S. marcescens* Db10 Δ*vgrG-1*), FRA03 (*S. marcescens* Db10 Δ*vgrG-1* Δ*vgrG-2*), SAN186 (*S. marcescens* Db10 *vgrG-2-mCherry*) and SAN202 (*S. marcescens* Db10 Δ*vgrG-1 vgrG-2-mCherry*)

5.2.3 Functionality of the T6SS in strains expressing *tss-mCherry* fusion proteins as determined by a competition assay

Finally, competition assays were performed using strains encoding Tss-mCherry fusion proteins in order to monitor their T6SS-mediated bacterial killing ability. Competition assays were performed as described in Figure 3.23, using *Pseudomonas fluorescens* as the target organism. Results from these assays revealed that, consistent with results from the TssD and Ssp2 secretion assays, the TssK-mCherry strain was the

only strain in which the T6SS was completely inactive, with target cell recovery indistinguishable from that observed with the Δ*tssH* mutant (Figure 5.5). The TssJ-mCherry strain showed some reduction in ability to kill *P. fluorescens* when compared with wild type *S. marcescens* Db10, however, it retained significant killing ability, causing a drop of >100x in the number of viable *P. fluorescens* cells recovered when compared with a T6SS-inactive mutant (Figure 5.5).

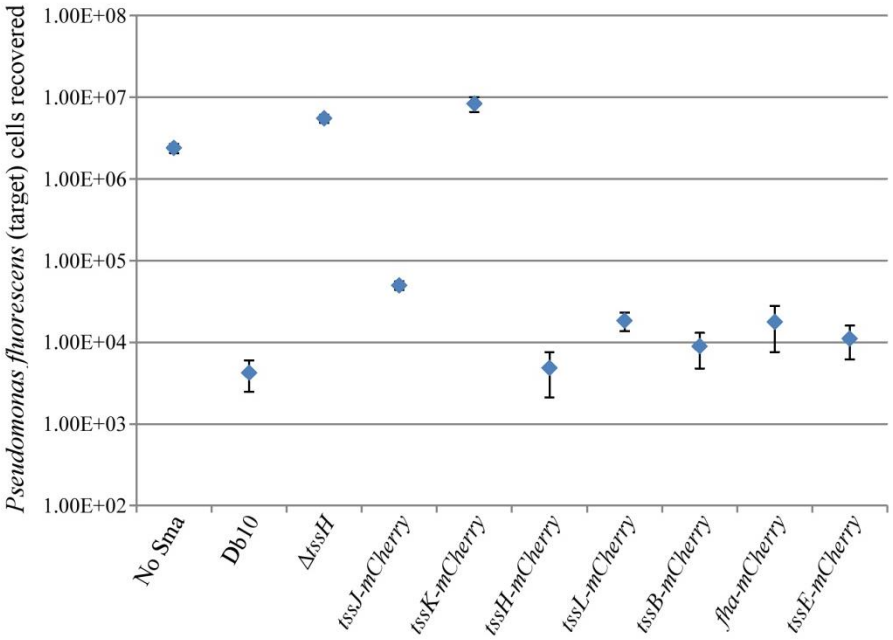

Figure 5.43. Competition assay to determine the number of viable *Pseudomonas fluorescens* cells recovered following co-culture with the *Serratia marcescens* strains indicated. Recovery of viable *P. fluorescens* cells after 4 h co-culture with the *S. marcescens* strain indicated, at 30°C, with an initial ratio of 5:1 *S. marcescens* : *P. fluorescens* (see Materials and Methods for full details). Points and bars show mean +/- standard error of the mean (n=3).

To further investigate the reason behind the reduced killing phenotype of the TssJ-mCherry protein fusion strain, an α-TssJ western blot was performed on samples prepared from wild type *S. marcescens* Db10, a Δ*tssJ* mutant and the *tssJ-mCherry* fusion strain (Figure 5.44). The total amount of protein loaded was normalised

according to the OD_{600} of the culture, however, less TssJ was detected in the strain expressing *tssJ-mCherry* when compared with wild type TssJ in *S. marcescens* Db10 (Figure 5.44). A decrease in the amount of TssJ present in the cell might limit the number of T6SSs that could be assembled, explaining why killing of competitor bacteria is not as efficient as *S. marcescens* Db10 in this strain.

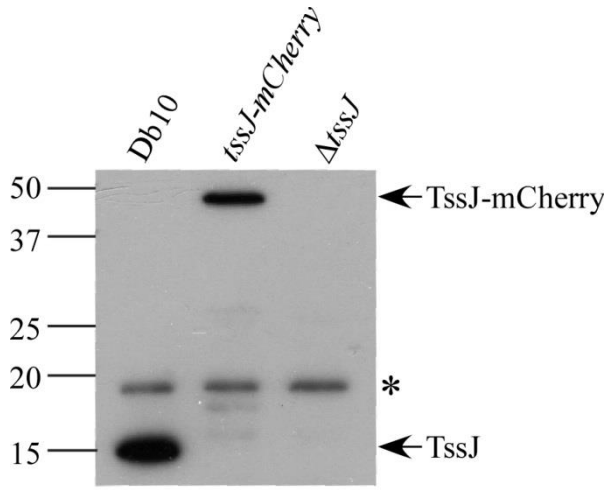

Figure 5.44. Immunoblot detection of TssJ in total cellular fractions of *Serratia marcescens* Db10, SAN157 (*S. marcescens* Db10 *tssJ-mCherry*) and SJC10 (*S. marcescens* Db10 Δ*tssJ*). Asterisk indicates non-specific band.

In the case of the strain encoding the VgrG-2-mCherry fusion protein, *S. marcescens* 274 was used as the target strain since with this strain, unlike many other target strains, a strong phenotype can be observed when the Δ*vgrG-2* mutant is used as the killer (SJC lab, unpublished). The VgrG-2-mCherry strain showed some killing activity when compared with the Δ*vgrG-2* mutant strain, however, the fusion strain was clearly much less efficient than wildtype *S. marcescens* Db10 at killing *S. marcescens* 274 (Figure 5.45).

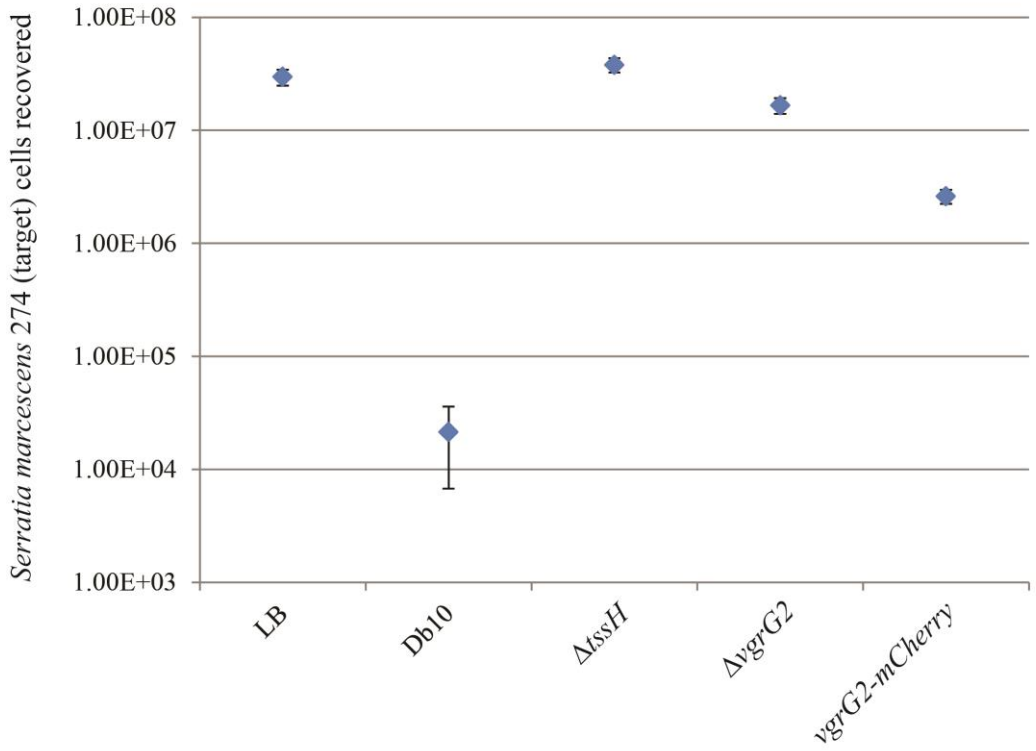

Figure 5.45. Competition assay to determine the number of viable *Serratia marcescens* 274 cells recovered following co-culture with the *S. marcescens* Db10 strains indicated. Recovery of viable *S. marcescens* 274 cells after 4 h co-culture with the *S. marcescens* Db10 strain indicated, at 30°C, with an initial ratio of 5:1 *S. marcescens* Db10 : *S. marcescens* 274 cell (see Materials and Methods for full details). Points show mean +/- standard error of the mean (n=3). For a diagram of the competition assay set up, see Figure 3.11.

From the above results we concluded that all of the strains encoding the mCherry fusion proteins harboured a T6SS that was functional on some level, with the exception of the TssK-mCherry strain. Immunoblot analysis of TssK expression in the TssK-mCherry strain revealed that the TssK-mCherry protein was present at a similar level to wild type *S. marcescens* Db10 (data not shown). In *S. marcescens* Db10, TssK has been shown to interact with the conserved T6SS components, TssF and TssG. Additionally, TssK has been shown to exist in several oligomeric states (English et al., 2014). It is likely that addition of mCherry to the C terminus of this protein interferes with self-self interactions or with its interaction with TssFG.

5.2.4 Analysis of the integrity of the mCherry fusion proteins

To confirm whether the each mCherry fusion protein was full length (in other words that the mCherry was not being cleaved off), an α-mCherry immunoblot was performed on total cellular protein from each strain. For the VgrG-2-mCherry strain, secreted fractions were also probed for mCherry, since VgrG proteins are expelled from the cell when the T6SS fires, similar to TssD.

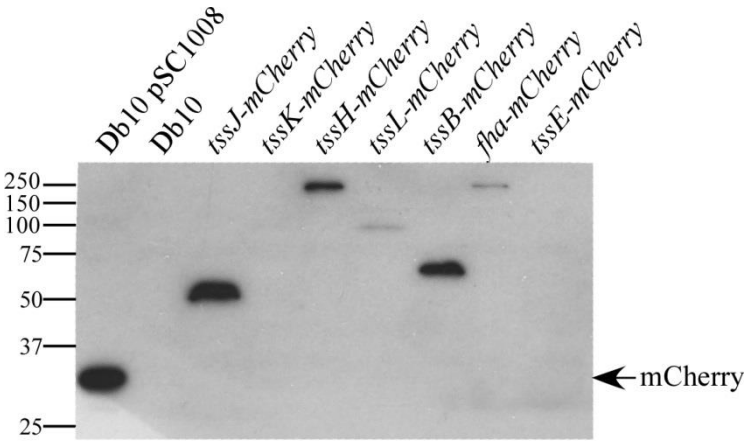

Figure 5.46. α-mCherry immunoblot analysis of cellular fractions isolated from strains encoding the mCherry fusion protein indicated. Immunoblot detection of mCherry in cellular fractions from: *Serratia marcescens* Db10 pSC1008 (in which mCherry is under the control of an inducible promoter), *S. marcescens* Db10, SAN157 (*S. marcescens* Db10 *tssJ-mCherry*), SAN158 (*S. marcescens* Db10 *tssK-mCherry*), SAN159 (*S. marcescens* Db10 *tssH-mCherry*), SAN162 (*S. marcescens* Db10 *tssL-mCherry*), SAN163 (*S. marcescens* Db10 *tssB-mCherry*), SAN164 (*S. marcescens* Db10 *fha-mCherry*) and SAN166 (*S. marcescens* Db10 *tssE-mCherry*)

Full length mCherry fusion proteins were detected for TssJ-, TssH-, TssL-, TssB- and Fha-mCherry (Figure 5.46). In contrast, mCherry could not be detected for the strains expressing TssK, TssE (Figure 5.46) or VgrG-2-mCherry (data not shown). It is likely that these proteins are simply not expressed to a level high enough for detection with the α-mCherry antibody, particularly since full length TssK-mCherry had previously been detected by αTssK immunoblot analysis (data not shown).

5.2.5 Visualisation of the strains expressing Tss-mCherry fusion proteins by fluorescence microscopy

To further characterise the fluorescent fusion strains, the fusion proteins were visualised by fluorescence microscopy (Figure 5.47). Initial observations revealed no fluorescence could be observed for the TssE- and VgrG-2-mCherry fusion strains. These data agree with the data obtained from the α-mCherry immunoblot experiments, whereby TssE- and VgrG-2-mCherry could not be detected, presumably due to low expression levels (Figure 5.47.A). For the remaining strains expressing Tss-mCherry fusion proteins, fluorescence could be detected by microscopy. Initial observations suggested that the localisation of TssJ-mCherry and TssL-mCherry was distinct from the localisation of TssK-mCherry, TssH-mCherry, TssB-mCherry and Fha-mCherry (Figure 5.47.A).

We selected for further analysis the TssJ-, TssH-, TssL- and TssB-mCherry fusions, since these were functional, readily detectable and their localisation was of particular interest (see below). Upon optimisation of microscopy conditions, the localisation of the fluorescent proteins could be seen more clearly (Figure 5.47.B). For TssJ-mCherry and TssL-mCherry, the fluorescent proteins could be visualised around the cell periphery in the majority of cells. Additionally, for TssL-mCherry, foci could be observed in a sub-population of these cells. For the TssH-, and TssB-mCherry fusions, either diffuse cytoplasmic fluorescence or fluorescent foci could be observed. In line with previously published data, we assume that focus formation by TssB represents the assembly of an active T6SS (Basler & Mekalanos, 2012).

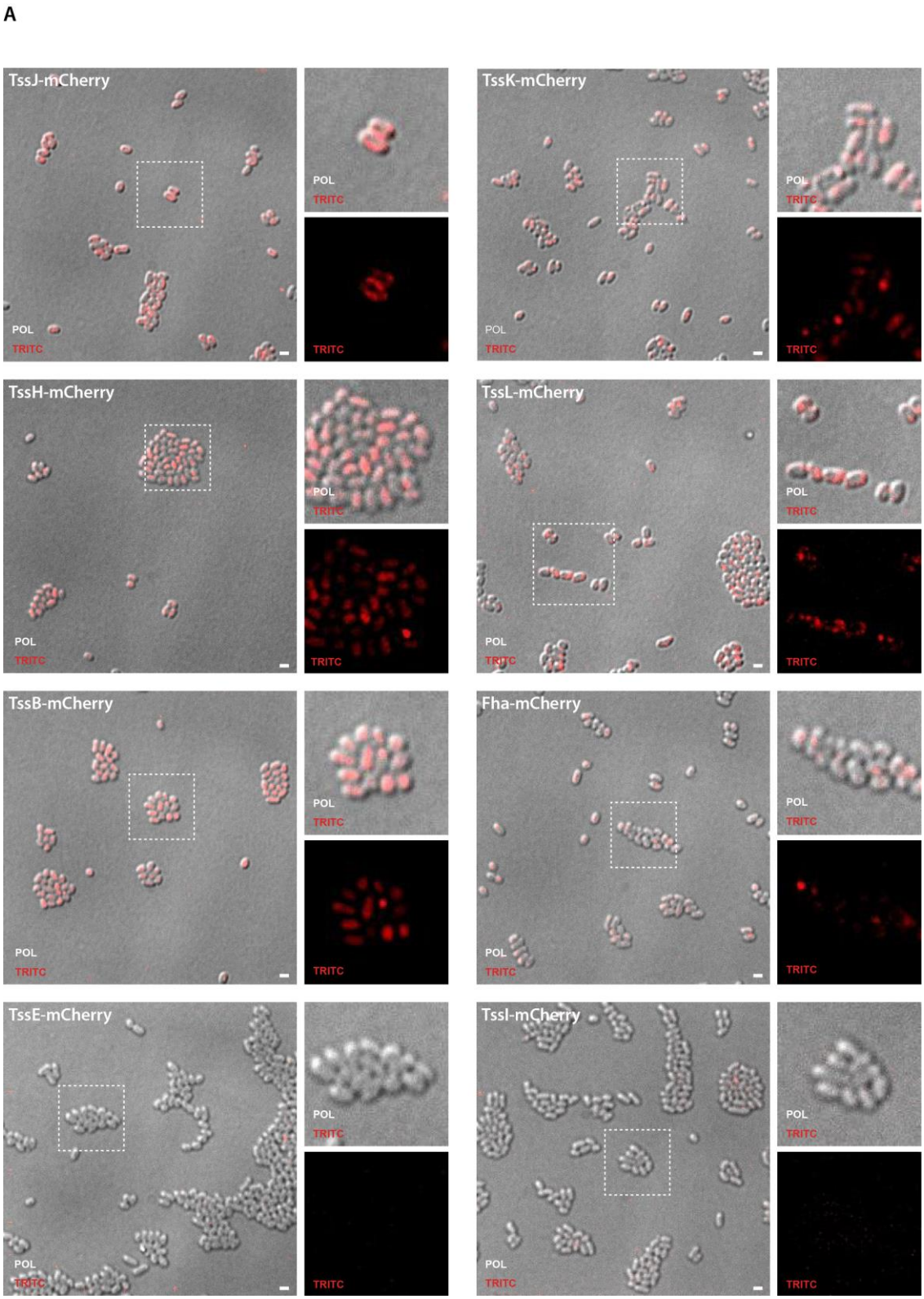
A
TssJ-mCherry
TssK-mCherry
TssH-mCherry
TssL-mCherry
TssB-mCherry
Fha-mCherry
TssE-mCherry
TssI-mCherry
POL
TRITC

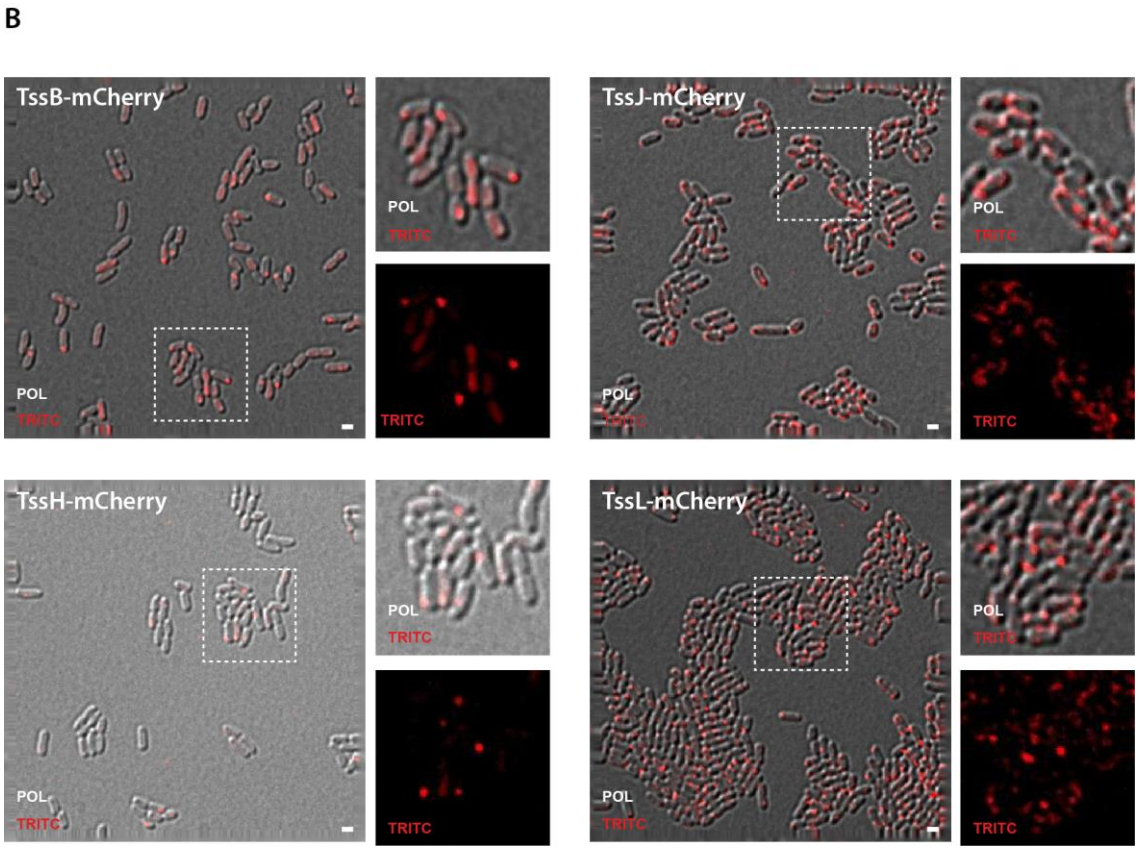

Figure 5.47. Representative examples of fluorescence microscopy images acquired from strains encoding Tss-mCherry fusion proteins. The strains imaged were SAN157 (*S. marcescens* Db10 *tssJ-mCherry*), SAN158 (*S. marcescens* Db10 *tssK-mCherry*), SAN159 (*S. marcescens* Db10 *tssH-mCherry*), SAN162 (*S. marcescens* Db10 *tssL-mCherry*), SAN163 (*S. marcescens* Db10 *tssB-mCherry*), SAN164 (*S. marcescens* Db10 *fha-mCherry*), SAN166 (*S. marcescens* Db10 *tssE-mCherry*) and SAN186 (*S. marcescens* Db10 *vgrG-2-mCherry*); the fusion protein imaged is indicated at the top left of each main panel. In each case, the broken box indicates the area of the main image that has been magnified in the two right hand panels. The channels in which images were acquired are labelled: POL (differential interference contrast) and TRITC (detection of mCherry). The scale bar is 1 μM. **A.** Initial fluorescence microscopy observations with all mCherry fusion strains. To prepare cells for microscopy, the relevant strains were grown overnight on plates. The following day, cells were collected and re-suspended in phosphate buffered saline. The cell suspension was diluted 10-fold and cells were immobilised on an agarose slide prior to imaging. **B.** Observations with selected mCherry fusion strains following optimisation of microscopy conditions. To prepare cells for microscopy, the relevant strains were grown overnight in liquid LB. The following day, these cultures were used to inoculate minimal media glucose to an OD_{600} of 0.15. Cells were grown for four hours and then were immobilised on minimal media glucose solidified through the addition of agarose prior to imaging.

5.2.6 Co-localisation analysis of TssB with TssH, TssJ and TssL

It was of great interest to determine how the foci observed for the individual TssH, TssL and TssJ fusion proteins spatially corresponded with those observed for TssB, since this might provide insight into the spatial and dynamic assembly of different subcomplexes within the machinery. TssH has been shown previously to interact with the contracted TssBC sheath to catalyse disassembly of the structure and, in *Vibrio cholerae*, to co-localise with TssB by microscopy (Basler & Mekalanos, 2012; Kapitein et al., 2013). It might be expected that components of the T6SS should come together either before or upon firing of the system, however, the localisation of TssB in relation to the outer membrane (OM) lipoprotein, TssJ, and the inner membrane (IM) protein, TssL has not been reported. We therefore aimed to visualise the co-localisation of TssB with the cytoplasmic protein, TssH, the IM protein, TssL and the OM lipoprotein, TssJ. In order to achieve this, strains were constructed in which TssB was translationally fused to Gfpmut2 and, simultaneously, TssH, TssL or TssJ were translationally fused to mCherry. To demonstrate that these strains harboured a functional T6SS, TssD secretion assays were performed as described above. Additionally, an α-Gfp immunoblot of total cellular fractions was performed to confirm that the TssB-Gfpmut2 fusion was full length. These data confirmed that the T6SS was functional for the secretion of TssD and that the TssB-Gfpmut2 protein fusion was full length in each case (Figure 5.48).

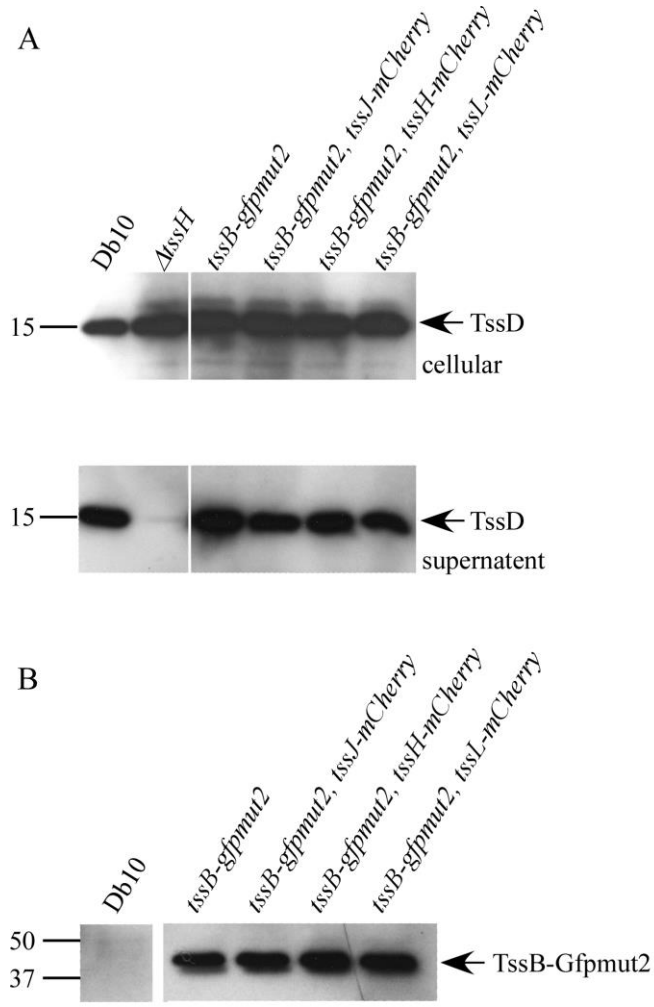

Figure 5.48. α-Gfp and α-TssD immunoblot analysis of cellular fractions or cellular and secreted fractions isolated from strains encoding the TssB-Gfpmut2 protein simultaneously with TssH-, TssL- or TssJ-mCherry. Immunoblot detection of TssD and TssB-Gfpmut2 from: SAN207 (*S. marcescens* Db10 *tssB-gfpmut2*), SAN208 (*S. marcescens* Db10 *tssB-gfpmut2*, *tssJ-mCherry*), SAN209 (*S. marcescens* Db10 *tssB-gfpmut2*, *tssH-mCherry*) and SAN210 (*S. marcescens* Db10 *tssB-gfpmut2*, *tssL-mCherry*). **A.** Detection of TssD in the cellular and secreted fractions of the strains indicated. **B.** Immunoblot detection of TssB-Gfpmut2, which would be expected to be 49 kDa in size.

Each dual fusion strain was imaged by fluorescence microscopy in an attempt to visualise co-localisation of the fluorescently labelled proteins (Figure 5.49). The TssB-Gfpmut2, TssH-mCherry strain served as a reference, as it has already been demonstrated that TssH co-localises with the contracted TssBC sheath in *V. cholerae* (Kapitein et al., 2013).

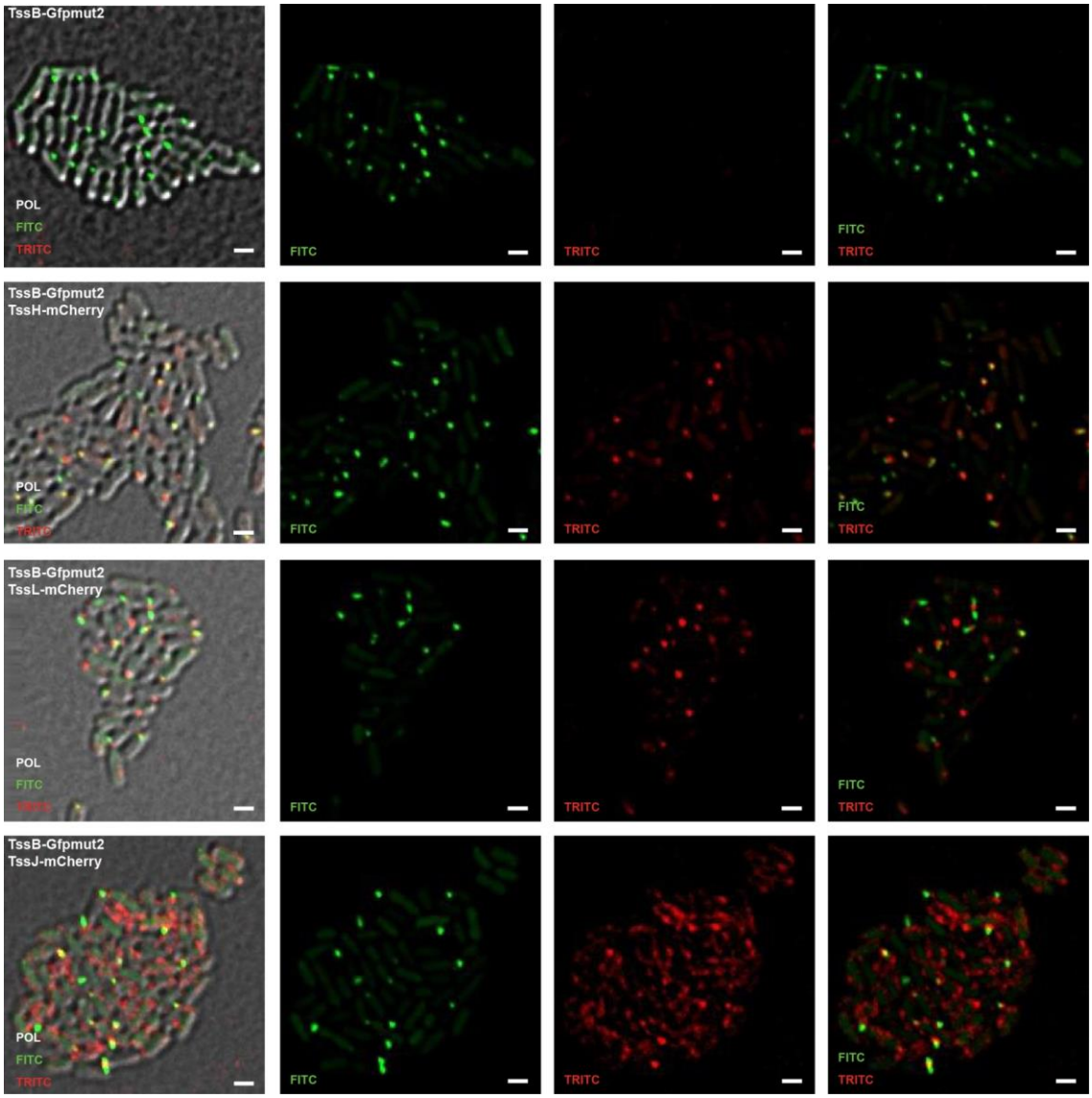

Figure 5.49. Representative examples of co-localisation images from strains encoding TssB-Gfpmut2 alone or with TssH-, TssL- or TssJ-mCherry. Fluorescence microscope images acquired with SAN207 (*S. marcescens* Db10 *tssB-gfpmut2*), SAN209 (*S. marcescens* Db10 *tssB-gfpmut2*, *tssH-mCherry*), SAN210 (*S. marcescens* Db10 *tssB-gfpmut2*, *tssL-mCherry*) and SAN208 (*S. marcescens* Db10 *tssB-gfpmut2*, *tssJ-mCherry*). The channels in which images were acquired are labelled: POL (differential interference contrast), FITC (detection of Gfp) and TRITC (detection of mCherry). The scale bar is 1 μM. To prepare cells for microscopy, the relevant strains were grown overnight in liquid LB. The following day, these cultures were used to inoculate minimal media glucose to an OD_{600} of 0.15. Cells were grown for four hours and then were immobilised on minimal media glucose solidified through the addition of agarose prior to imaging.

Visual inspection of our images revealed that, in agreement with previously published data, TssH-mCherry foci always co-occur with TssB-gfpmut2 foci (Basler & Mekalanos, 2012; Kapitein et al., 2013). However, TssB-gfpmut2 foci do not always co-localise with TssH-mCherry foci. Given that TssH is required for the disassembly of the contracted TssBC sheath but is not required for its assembly, these data agree with the biological function of TssH. In the case of TssL-mCherry and TssB-gfpmut2, there appeared to be more TssL-mCherry foci than TssB-gfpmut2 foci. Only a subset of TssB-Gfpmut2 and TssL-mCherry foci appeared to co-localise. In these instances TssB-Gfpmut2 did not always completely overlay TssL-mCherry, rather the fusion proteins appeared adjacent to one another. With the TssJ-mCherry and TssB-gfpmut2 fusion strain, co-localisation of the fluorescent proteins was not as apparent given that TssJ-mCherry tended not to form foci as distinct as TssH- or TssL-mCherry. Nevertheless, some cells did appear to harbour foci and in some instances we could observe an overlap of TssJ-mCherry and TssB-Gfpmut2. However, given that TssJ-mCherry was distributed abundantly around the periphery of many cells, this might be expected.

5.2.7 Further analysis of the TssB-mCherry fusion strain

The strain expressing the TssB-mCherry fusion protein was chosen for some further analysis as foci appeared brightest in this strain. Visualisation of a TssB-mCherry focus was used as a read out for the assembly of an active T6SS, as has been described in previous studies (Basler & Mekalanos, 2012; Basler *et al.*, 2012). Timelapse fluorescence microscopy using this strain allowed us to follow the dynamics of the T6SS in *S. marcescens* Db10 over a period of hours. Timelapse fluorescence microscopy with the TssB-mCherry fusion strain showed that the T6SS was active throughout growth under the conditions that we tested. Assembly of an active T6SS was

not a rare event, with many cells within the growing microcolony assembling a T6SS (Figure 5.50). Dynamic T6SS assembly and disassembly was readily observed, with foci frequently appearing and disappearing between images taken every 10 min (Figure 5.50 and data not shown).

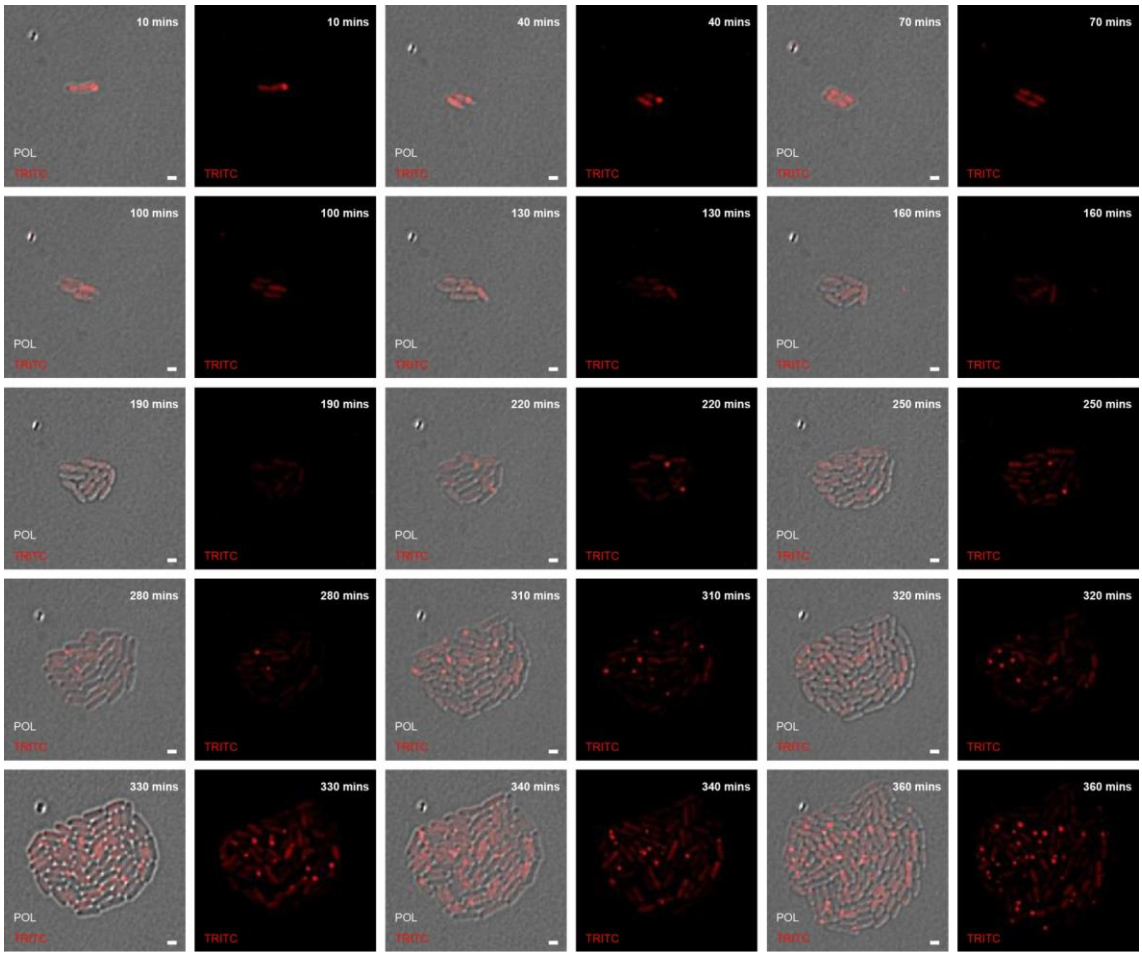

Figure 5.50. Timelapse fluorescence microscopic analysis of the TssB-mCherry fusion strain (SAN163). The channels in which images were acquired are labelled: POL (differential interference contrast) or TRITC (to detect mCherry). The scale bar is 1 μM. To prepare cells for microscopy, the relevant strains were grown overnight in liquid LB. The following day, 25μl was used to inoculate 5ml minimal media glucose (MM glucose). Cells were grown in MM glucose for 18 hours. This culture was then diluted to an OD_{600} of 0.02 and cells were immobilised on MM glucose solidified through the addition of agarose prior to imaging. Cells were imaged over a period of 360 mins. The time of image acquisition is indicated at the top right of each image.

In the longer term, we hope to apply automated spot detection and tracking software to quantify spatial and temporal distribution and dynamics of T6SS foci. To facilitate this, it is desirable to have strains in which the cell boundary is clearly distinguishable. Therefore we constructed a strain in which *gfp* was expressed constitutively from the chromosome using an inducible bacteriophage T5 promoter and Gfp protein was evenly distributed throughout the cytoplasm (SAN195), data not shown. We then introduced this cytoplasmic GFP cassette into the TssB-mCherry background (generating strain SAN199). This strain was then imaged by fluorescence microscopy and preliminary analysis performed by visual inspection of the resulting images. The following conclusions were derived from analysis of a single field of view (Figure 5.51).

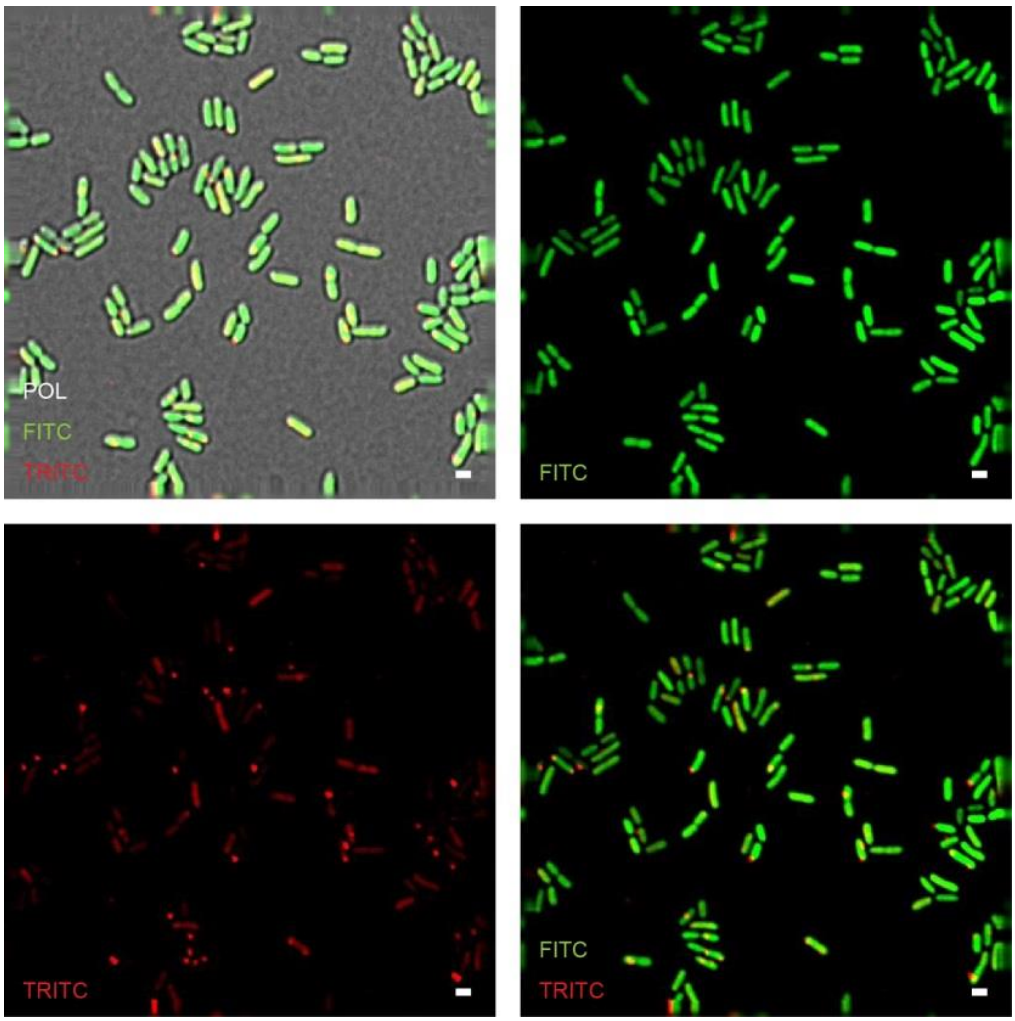

Figure 5.51. Representative example of a fluorescence image acquired from *S. marcescens* Db10 *tssB-mCherry, lacZ::PT5-gfpmut2-kan* (SAN199). The channels in which images were acquired are labelled: POL (differential interference contrast), FITC (to detect GFP) and TRITC (to detect mCherry). The scale bar is 1 μM. To prepare cells for microscopy, SAN199 was grown overnight in liquid LB. The following day, these cultures were used to inoculate minimal media glucose to an OD_{600} of 0.15. Cells were grown for four hours and then were immobilised on minimal media glucose solidified through the addition of agarose prior to imaging.

In this field of view, 123 cells were present. Of these, 32 cells harboured at least one TssB-mCherry focus, meaning that approximately 26% of the population assembles an active T6SS at a single point in time under the conditions that we tested. Several cells within the field of view harboured two TssB-mCherry fluorescent foci, indicating that a cell can assemble more than one T6SS at one time. Interestingly, foci were also

observed in single cells which were not surrounded by neighbouring cells. These results indicate that in *S. marcescens* Db10, the presence of neighbours is not required to stimulate assembly of the T6SS.

5.3 Discussion

Analysis of strains expressing Tss-mCherry or -Gfpmut2 fusion proteins by fluorescence microscopy has allowed visualisation of the localisation of several components of the T6SS in *S. marcescens* Db10 (Figure 5.47 and Figure 5.49). The visualisation of cytoplasmic fluorescence or fluorescent foci for the TssH-, TssB- and Fha-mCherry fusion strains agrees with previous microscopic analysis of these proteins in other organisms (Basler & Mekalanos, 2012; Brunet *et al.*, 2013; Hsu *et al.*, 2009; Kapitein *et al.*, 2013). Foci comprised of fluorescent TssB have previously been proposed to represent the contracted form of the TssBC sheath and the site of assembly of the focus is thought to mark the location for T6SS assembly (Basler *et al.*, 2012). TssB could not be visualised in the extended form under the conditions that we tested. This may be due to the fact that the extended form of the TssBC sheath is thought to exist only transiently prior to contraction, which occurs in approximately 5 ms. Contrastingly, the contracted sheath takes tens of seconds to be disassembled (Basler *et al.*, 2012). Visualisation of the extended TssBC sheath may also be beyond the resolving power of the microscope used in these studes. TssH is known to be required for the disassembly of the contracted TssBC sheath and so its co-localisation with TssBC would be expected and has been demonstrated in *V. cholera* (Basler & Mekalanos, 2012; Basler *et al.*, 2012; Bonemann *et al.*, 2009). Whilst the precise role of Fha remains unclear, evidence is consistent with Fha localising to a partially or completely assembled T6SS (Hsu *et al.*, 2009). To our knowledge, this is the first time that TssJ, TssL and TssK have been visualised by fluorescence microscopy. The

localisation patterns observed with the TssJ-mCherry fusion protein and the TssL-mCherry fusion protein are consistent with biochemical data showing that that TssJ is an lipoprotein anchored in the OM (Aschtgen *et al.*, 2008) and that TssL is an integral IM protein (Aschtgen *et al.*, 2012), however their precise localisation within the cell envelope cannot be accurately determined within the limits of resolution of light microscopy. Whilst TssK also appeared to form foci similar to other cytoplasmic components of the T6SS, we cannot make confident conclusions based on this data since the addition of mCherry to the protein rendered the T6SS non-functional.

Parallel studies performed by a collaborating group have attempted to shed light on the dynamics of components of the T6SS by following fluorescent fusion proteins over different time ranges by fluorescence microscopy. These studies were performed on the same *S. marcescens* Db10 strains expressing the TssJ-, TssH-, TssL- and TssB-mCherry fusion proteins that were constructed in this study. The fusion proteins were imaged over milliseconds, seconds or tens of seconds (A. Diepold, University of Oxford). Of the proteins analysed, TssJ appeared the most motile and some motility could be observed over milliseconds. These data agree with our observation that little TssJ specifically localises upon T6SS assembly. Foci representative of TssH and TssL were more stable than TssJ, suggesting these proteins come together to form a sub-complex upon firing of the system. Foci representative of TssB were most stable and could be observed to disappear and re-appear at different locations in the cell when imaged over tens of seconds (A. Diepold, University of Oxford). It has previously been reported that the TssBC sheath is assembled and disassembled over tens of seconds and that TssH only associates with the contracted version of the sheath (Basler & Mekalanos, 2012; Basler *et al.*, 2012). These data offer an explanation as to why foci representative of TssH appear and disappear more quickly than foci representative of TssB. In our studies, timelapse fluorescence microscopy was performed with the strain

expressing the TssB-mCherry fusion protein. When imaged every 10 mins, foci representative of TssB were observed to appear and disappear at different locations in the cell for the duration of the timelapse (Figure 5.50). These data agree with the microscopic analysis performed by A. Diepold (University of Oxford).

We then proceeded to consider the extent to which TssJ, TssL and TssH were co-localised with TssB. TssH served as a reference as it has previously been shown that TssH co-localises with a subset of TssB foci (Basler & Mekalanos, 2012). Indeed, we also observed the co-occurrence of TssH-mCherry foci with a subset of TssB-Gfpmut2 foci (Figure 5.49). Since TssH only localises with the contracted TssBC sheath, the extended form of the sheath would not be expected to co-localise with TssH (Kapitein *et al.*, 2013). Co-visualisation of TssJ or TssL with TssB has not yet been reported. In *S. marcescens* Db10, little specific co-localisation of TssJ with TssB was observed. Conversely, a subset of TssL foci appeared to co-localise with TssB, however in many instances the fluorescent foci appeared adjacent or overlapping with one another rather than completely co-localised (Figure 5.49). Given that TssL is anchored in the IM whereas TssB is entirely cytoplasmic, these data may reflect the difference in the cellular localisation of TssB versus TssL. Our data suggest that TssJ is distributed throughout the cell envelope and that only a small proportion is specifically recruited upon assembly of the T6SS. In comparison, TssL does appear to aggregate upon assembly of the T6SS. A future quantitative analysis of the co-localisation of the fluorescent proteins will permit more solid conclusions about the extent of co-localisation of TssB with each of the other components, TssJ, TssL or TssH, to be made.

Further analysis of TssB-mCherry allowed us to make some initial, tentative conclusions and comparisons with the T6SS in other organisms. In *V. cholerae*, upon labelling of VipA (TssB) with sfGfp, between zero and five foci per cell were observed

in the wild-type background (Basler *et al.*, 2012). In *S. marcescens* Db10 we observed a maximum of two foci within each cell, implying that the T6SS is not assembled as frequently as in *V. cholerae* under the conditions that we tested (Figure 5.51). In *P. aeruginosa*, it has been reported that T6SS foci are present in 15% of cells at any given time (LeRoux *et al.*, 2012). However it should be noted that in this organism, a fusion of ClpV1 (TssH) with Gfp, rather than TssB, was used to determine the frequency with which an active T6SS assembles and our data have indicated that, at a given instant, there are more detectable TssB than TssH foci. Additionally, in the above study a *P. aeruginosa retS* regulatory mutant, in which the transcription of the T6SS is upregulated, is frequently used in studies concerning the T6SS. These factors mean that the frequency with which the T6SS assembles in *P. aeruginosa* cannot currently be directly compared with *S. marcescens* Db10, although non-quantitative observation suggests that frequency of focus formation is more similar between *P. aeruginosa* and *S. marcescens* Db10 than between *P. aeruginosa* and *V. cholerae*. Future development of an automated analysis tool capable of recognising cells based on cytoplasmic Gfp and recognising fluorescent TssB foci would allow the analysis of many more fields of view and quantification of various parameters including number of foci per cell, distribution of foci along the length of the cell and dependence of focus formation on the presence of a neighbouring cell (see below).

In *P. aeruginosa*, efficient targeting of recipient cells requires that the recipient cells possess a functional T6SS. This phenomenon has been termed "duelling" and can be visualised by microscopy since foci in neighbouring cells appeared to be paired (Basler *et al.*, 2013; LeRoux *et al.*, 2012). Perturbation of the membrane of the recipient cell has recently been reported as the trigger which activates the T6SS in *P. aeruginosa* (Ho *et al.*, 2013). Our analysis of microscopy data obtained with the TssB-mCherry protein fusion in *S. marcescens* Db10 suggests that this system does not require

activation by sensing of an incoming T6SS attack (Figure 5.51). We could readily observe TssB-mCherry foci within single *S. marcescens* Db10 cells that were not in contact with neighbouring cells and we did not see evidence for the 'paired' foci characteristic of duelling. Additionally, it has been demonstrated that *S. marcescens* Db10 can kill a strain of *Serratia marcescens* 274 in which the T6SS has been inactivated as efficiently as it can kill the T6-active wild type strain (SJC lab, unpublished). This is in contrast with *P. aeruginosa*, which cannot efficiently kill *E. coli* cells which are devoid of a functional T6SS (Basler *et al.*, 2013).

In *P. aeruginosa*, the threonine phosphorylation pathway (TPP) has been implicated in response to an incoming T6SS attack (Basler *et al.*, 2013). The TPP includes the cell envelope associated TagQRST system, the threonine kinase PpkA and the cognate phosphatase PppA. TagQRST somehow sense the incoming attack, probably via detecting a membrane breach, and activate PpkA, which then phosphorylates Fha. Phosphorylation of Fha is essential for T6SS activity (for more detail, see section 1.4.4) and appears to trigger assembly of a T6SS at the site of the exogenous attack, allowing the *Pseudomonas* cell to to counter-attack The genes encoding PpkA, PppA and Fha also exist in *S. marcescens* Db10, and phosphorylation of Fha by PpkA is also essential for T6SS activity in this organism (Fritsch *et al.*, 2013). However, in *S. marcescens* Db10, the TagQRST system is not present, meaning that PpkA must be regulated by some other mechanism. These data fit with our microscopy data which suggests that the T6SS of *S. marcescens* Db10 is not activated by the T6SS of a neighbouring cell (Figure 5.51). Additionally, the deletion of PppA in *P. aeruginosa* results in a de-repression of T6 dependent secretion in liquid culture (normally no T6 secretion occurs in liquid culture in this organism since productive cell-cell interactions require close contact on a solid surface), whereas in *S. marcescens* Db10 deletion of PppA does not have any observable effect in liquid culture since the

system is already active in liquid in this organism (Fritsch *et al.*, 2013). Together, the existing data and the single cell microscopy analysis reported here, strongly indicate that signal required to activate the T6SS in *S. marcescens* Db10 is distinct from that in *P. aeruginosa*.

In *P. aeruginosa*, the T6SS has been described as "defensive", since it fires in response to attack from neighbouring cells (Basler *et al.*, 2013). Conversely, in *V. cholera* the T6SS is not activated upon sensing of a T6SS attack from a neighbouring cell (Basler *et al.*, 2012). The T6SS of Enteroaggregative *E. coli* (EAEC) bears some similarities to that of both *P. aeruginosa* and *V. cholera.* In EAEC, *E. coli* target cells devoid of a T6SS are efficiently killed, however, T6SS dynamics are also increased if neighbouring cells possess an active T6SS (Brunet *et al.*, 2013). These data highlight the diversity in T6SS regulation. Our data suggest that the T6SS of *S. marcescens* Db10 is more similar to that of *V. cholera*, which fires constantly and does not exhibit "duelling" behaviour (Basler *et al.*, 2012). The T6SS of *S. marcescens* Db10 therefore appears to be "offensive" rather than "defensive".

5.4 Conclusions

Work conducted in this study has set the stage for further investigation into the mechanism and structure of the T6SS in *S. marcescens* Db10 via fluorescence microscopy. We have shown that strains of *S. marcescens* Db10 carrying fusions of key components of the T6SS with fluorescent proteins may be used as a tool for visualisation of components of the system. In the future, high resolution fluorescence microscopy, for example Fluorescence Activated Photobleaching (FRAP), could be employed to elucidate the dynamics and rate of turnover of T6SS components. Additionally, the strain expressing the TssB-mCherry fusion protein may be used to visualise the subcellular localisation of T6SS assembly and firing and the subsequent

killing of target bacteria. Initial analysis conducted in this study allowed tentative conclusions to be drawn about the frequency with which the T6SS assembles and about the co-localisation of certain components. We have demonstrated that approximately one third of cells harbour an active T6SS. We observed co-localisation of TssB with TssH and TssL and, to a lesser extent, with TssJ. In the future, quantitative and perhaps also automated analysis of larger data sets would strengthen these conclusions. Finally, in contrast with the well-studied T6SS of *P. aeruginosa*, analysis of TssB-mCherry by fluorescence microscopy has provided further evidence that the activating signal for the T6SS machinery of *S. marcescens* Db10 is not incoming attack from another cell.

Chapter 6

Conclusions and outlook

Work conducted in this study has provided important insights into the mechanisms by which *Serratia marcescens* Db10 kills or inhibits the growth of competing bacteria. In this work, two very different strategies of antibacterial activity were investigated, namely the biosynthesis of NRPS/PKS products and the assembly of the Type VI Secretion System (T6SS). NRPS/PKS products biosynthesised by *S. marcescens* Db10 were shown to possess antibacterial activity against several species of Gram-positive bacteria. Conversely, the T6SS has, to date, only been demonstrated to possess antibacterial activity against Gram-negative bacteria (Schwarz *et al.*, 2010). *S. marcescens* Db10 therefore has the capacity to kill a diverse range of bacteria. This is highly likely to give it a competitive advantage in a polymicrobial community.

6.1 Identification and characterisation of althiomycin and its encoding gene cluster

Work on the biosynthesis of althiomycin was initiated upon the serendipitous discovery that *S. marcescens* Db10 was capable of killing or inhibiting the growth of several Gram-positive bacteria through the production of a diffusible substance. This was observable through the production of an antibiosis halo when *S. marcescens* Db10 was grown on a lawn of the susceptible bacterium. The convenient nature of this antibacterial bioassay allowed us to conduct a high throughput transposon mutagenesis screen for the identification of *S. marcescens* Db10 mutants no longer able to kill the target bacterium. A 27 kb antibacterial gene cluster was subsequently identified. Analysis of the operon structure revealed that the antibacterial gene cluster comprised six genes, *alb1-6*, transcribed from a single promoter at the start of the operon. Bioinformatics analysis predicted that the gene cluster encoded NRPS/PKS biosynthetic enzymes, tailoring enzymes associated with modification of the NRPS/PKS product (Figure 3.17) and a protein involved in export of, or resistance to, the antibacterial

product. Experimental data identified the antibacterial product as the ribosome inhibiting antibiotic, althiomycin, and confirmed the essential role of *alb2-6* in its biosynthesis (Figure 3.19 and Figure 3.21). Other strains of *Serratia* have been demonstrated to synthesise the β-lactam antibiotic, carbapenem, and the pigmented antimicrobial, prodigiosin (Thomson *et al.*, 2000). However, this is the first report of althiomycin biosynthesis by the genus *Serratia*, or indeed by any organism outside of *Streptomyces* or *Myxococcus*.

Alb1 was demonstrated to have a role in the export of althiomycin, but, whilst capable of conferring resistance to a heterologous organism, was shown not to play an essential role in conferring resistance in *S. marcescens* Db10 (Figure 3.23 and Figure 3.27). It is not uncommon for bacteria to encode more than one resistance determinant to the antibiotic they produce (Mak *et al.*, 2014). Therefore, whilst not being the sole resistance determinant, Alb1 appears to provide one layer of self-protection against althiomycin (Mak *et al.*, 2014). One or more althiomycin resistance determinants in *S. marcescens* Db10 therefore remain unidentified. Bacteria mediate self-resistance to antibiotics by an array of mechanisms. For example, they may encode export proteins, modify antibiotic intermediates or the final product, synthesise resistant versions of the target or modify the target of the antibiotic (Mak *et al.*, 2014). Given that such a resistance determinant is not encoded within the *alb1-6* gene cluster, identification of the main althiomycin resistance determinant may not be straightforward. However, as *S. marcescens* strain 274 was shown to be sensitive to the effects of althiomycin, comparison of the genomes of these bacteria may give some clues as to how *S. marcescens* Db10 avoids the toxic effects of althiomycin. For example, since althiomycin targets the bacterial ribosome (Fujimoto *et al.*, 1970), *S. marcescens* Db10 may encode alternative ribosomal RNA or proteins. Alternatively, since antibiotic resistance determinants must be expressed prior to or concomitantly with biosynthesis,

if specific regulators of althiomycin biosynthesis can be identified then these may in turn offer clues to the identities of the outstanding resistance determinant(s).

S. marcescens Db10 is a fast growing and genetically tractable organism and so identification of the althiomycin biosynthetic gene cluster in this bacterium paves the way for future studies on the pharmaceutical potential of althiomycin, and also towards engineering compounds containing the bioactive 4-methoxy-3-pyrrolin-2-one moiety.

6.2 Characterisation of the phosphopantetheinyl transferase enzyme, PswP

Phosphopantetheinyl transferase enzymes are known to be essential for the function of NRPS/PKS enzymes (Figure 1.7). Since such an enzyme was not encoded within the althiomycin NRPS/PKS gene cluster, a bioinformatics approach was taken to identify candidate althiomycin PPTase enzymes elsewhere in the genome. Two candidate PPTase enzymes were identified. The deletion of PswP was demonstrated to be sufficient to abolish althiomycin biosynthesis whilst the deletion of the second PPTase enzyme had no observable effect (Figure 4.30). Upon testing of the PswP mutant for antimicrobial activity, it was realised that *Staphylococcus aureus* remained sensitive to diffusible products produced by *S. marcescens* Db10 in an althiomycin mutant but not in the PswP PPTase mutant. These data indicated that PswP was required for the biosynthesis of more than one NRPS/PKS metabolite in *S. marcescens* Db10 and that these metabolites possessed antimicrobial activity against *S. aureus*. Candidate NRPS gene clusters were identified by bioinformatics. Experimental evidence confirmed that two of these NRPS gene clusters, namely the serrawettin W2 gene cluster and a siderophore encoding gene cluster, were responsible for production of these metabolites. Several genes within the siderophore biosynthetic gene cluster were shown to be homologous to genes encoded within the enterobactin biosynthetic gene

cluster. The gene cluster also showed similarities to the serratiochelin gene cluster of *Serratia sp.* V4. Purification and determination of the structure of the enterobactin-like siderophore produced by *S. marcescens* Db10 will be required to unambiguously identify this product. This would require isolation by HPLC and analysis by NMR

Two additional NRPS containing gene clusters were identified by bioinformatics. The *SMA1571-1572* NRPS containing gene cluster was predicted to biosynthesise a microcin, whilst the *SMA1729* containing gene cluster was predicted to be required for the biosynthesis of second siderophore. Since production of these metabolites could not be detected, the necessity for PswP in their biosynthesis could not be assessed. For *Bacillus subtilis, Micrococcus luteus* and *S. aureus*, deletion of althiomycin or PswP was sufficient to negate the antimicrobial activity of *S. marcescens* Db10. These data suggest that either the putative bacteriocin is not synthesised under these conditions or that the bacteria we tested are not sensitive to the effects of the bacteriocin. Isolation and inducible expression of the bacteriocin encoding gene cluster in a heterologous host would determine whether the relevant genes synthesise a toxic molecule. Under the conditions that we tested, the enterobactin-like siderophore was the only detectable siderophore produced by *S. marcescens* Db10 (Figure 4.36). Analysis of different growth conditions may lead to the identification of conditions conducive to the production of the putative siderophore encoded by *SMA1729*, perhaps allowing characterisation of the molecule. If biosynthesis of the microcin or the putative siderophore could be detected under different conditions then the role of PswP in their biosynthesis could also be determined.

Overall, work conducted here has highlighted the importance of a single PPTase enzyme in the production of multiple important secondary metabolites with varying biological functions, namely killing competitors, iron acquisition and motility.

6.3 Insights into the assembly and function of the T6SS of *S. marcescens* Db10

Work conducted in this study involved the construction of *S. marcescens* Db10 strains carrying translational fusions of components of the T6SS to fluorescent proteins. Analysis of these strains revealed that the majority harboured a functional T6SS and the fluorescent proteins could be visualised by fluorescence microscopy. Localisation patterns were distinct between particular T6SS components (Figure 5.47). Differences in the localisation of the T6SS components were further assessed in strains which harboured fusions of TssB to Gfp and TssJ, TssH or TssL to mCherry. The co-localisation of these fluorescent proteins was assessed visually, allowing us tentatively conclude that components of different subcomplexes of the T6SS localise differently during T6SS assembly. Automated analysis of multiple fields of view will strengthen these tentative conclusions. Timelapse fluorescence microscopy over a period of hours with the strain expressing the TssB-mCherry fusion protein confirmed that cells grew well under the conditions that we used and that the T6SS was active in many cells throughout the experiment. Analysis of a strain expressing cytoplasmic Gfpmut2 and the TssB-mCherry fusion protein revealed that approximately a quarter of the population had an active T6SS under the conditions of our study. Development of an analysis tool capable of recognising cells based on the presence of cytoplasmic Gfp and fluorescent foci representative of the T6SS would enable the analysis of many more fields of view. Assembly of the T6SS was shown not to be dependent on the presence of neighbouring cells, indicating that the trigger which activates the T6SS in *S. marcescens* Db10 is distinct from that in Enteroaggregative *E. coli* (EAEC) and *Pseudomonas aeruginosa*. These data agree with previous data demonstrating that the T6SS is constitutively active in *S. marcescens* Db10 (Fritsch *et al.*, 2013; Murdoch *et al.*, 2011).

The strains constructed in this study will comprise a toolbox for further investigations into the mechanisms of assembly and the dynamics of the T6SS. Indeed, further analysis by microscopy may offer several insights into the T6SS of *S. marcescens* Db10. The dynamics and turnover of individual T6SS components could potentially be assessed by Fluorescence Activated Photobleaching (FRAP). This would allow us to determine whether individual T6SS components within the entire machinery or within particular subcomplexes are exchanged or whether they are fixed. The number of molecules of a particular T6SS component within one system may be assessed by stochastic optical reconstruction microscopy (STORM). Analysis of the images obtained with a widefield microscope gave first insight into the co-localisation of TssB with TssJ, TssH or TssL. Fluorescence Resonance Energy Transfer (FRET) microscopy may allow us to further probe the physical proximity of fluorescent proteins. The above analyses have been performed on components or homologues of other bacterial secretion systems, for example, the Type III Secretion System (T3SS) (Delalez *et al.*, 2010; Dickenson & Picking, 2012).

Previous studies have made use of fusions of TssB to fluorescent proteins to mark the site of T6SS assembly (Basler *et al.*, 2012). Further analysis of such fusion proteins in different mutant backgrounds may help in trying to decipher the role of particular T6SS proteins. For example, analysis of T6SS assembly in the PpkA or PppA mutant background may give some clues as to how this kinase and phosphatase spatially or temporally regulate the T6SS. Using the TssB-mCherry fusion protein as a marker for T6SS assembly, it may also be possible to directly visualise the secretion and subsequent toxic effects of T6SS effectors on target cells in *S. marcescens* Db10, as has previously been performed with EAEC (Brunet *et al.*, 2013).

Finally, it will be important to analyse the strains expressing fusions of single T6SS components with fluorescent proteins in different mutant backgrounds. If the localisation of these components changes upon the deletion of certain T6SS proteins then it may be possible to determine when the recruitment of particular T6SS components is dependent on the presence of other components. Additionally the order of assembly of the T6SS may be deduced from this type of analysis, as has previously been performed for the T3SS (Diepold *et al.*, 2010).

6.4 Additional remarks

Interestingly, recent experimental evidence has suggested a link between the althiomycin biosynthetic operon and the T6SS operon. Both gene clusters have been shown to be regulated by the small RNA binding protein, Hfq (SJC lab, unpublished), perhaps indicating that antibacterial strategies in *S. marcescens* Db10 are co-ordinately regulated. The althiomycin and T6SS gene clusters are also located relatively closely on the *S. marcescens* Db10 genome, with only 6 genes separating the two gene clusters.

6.5 Conclusion

Work conducted in this study has significantly contributed to our understanding of the mechanisms by which *S. marcescens* Db10 kills competing bacteria (Figure 6.52).

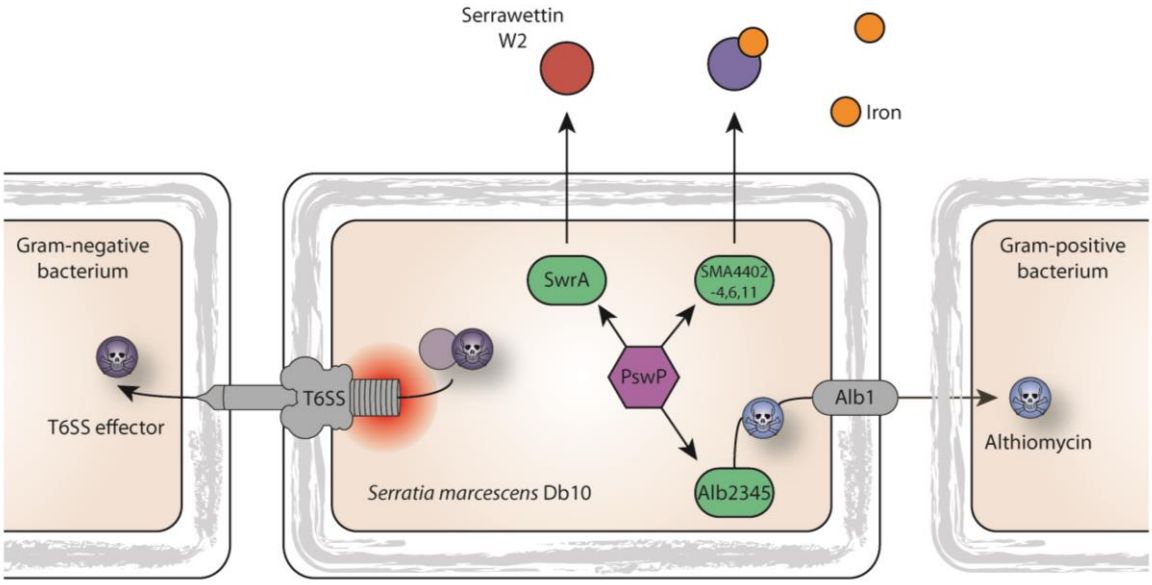

Figure 6.52. Schematic representation of work conducted in this study to elucidate the antibacterial strategies employed by *Serratia marcescens* Db10. The mechanism of biosynthesis and the mode of export of the antibiotic, althiomycin, was elucidated. The phosphopantetheinyl transferase enzyme, PswP, was shown to play an essential role in the biosynthesis of althiomycin, serrawettin W2 and an enterobactin-like siderophore, all of which were shown to possess antibacterial activity against *Staphylococcus aureus*. Lastly, the Type VI Secretion System (T6SS) was visualised through the construction of strains carrying translational fusions of T6SS components to fluorescent proteins.

The mechanism of althiomycin biosynthesis and export was de-lineated and the role of the PPTase enzyme, PswP, in the biosynthesis of secondary metabolites was defined. Strains were constructed which harboured translational fusions of components of the T6SS to fluorescent proteins and these proteins were visualised by fluorescence microscopy. Further analysis of these strains by fluorescence microscopy will contribute to our understanding of the T6SS in this organism

Chapter 7

References

Adler, C., Corbalan, N. S., Seyedsayamdost, M. R., Pomares, M. F., de Cristobal, R. E., Clardy, J., Kolter, R. & Vincent, P. A. (2012). Catecholate siderophores protect bacteria from pyochelin toxicity. *PloS one* 7, e46754.

Aharonowitz, Y., Cohen, G. & Martin, J. F. (1992). Penicillin and cephalosporin biosynthetic genes: structure, organization, regulation, and evolution. *Annual review of microbiology* 46, 461-495.

Alanis, A. J. (2005). Resistance to antibiotics: are we in the post-antibiotic era? *Archives of medical research* 36, 697-705.

Altschul, S. F., Madden, T. L., Schaffer, A. A., Zhang, J., Zhang, Z., Miller, W. & Lipman, D. J. (1997). Gapped BLAST and PSI-BLAST: a new generation of protein database search programs. *Nucleic acids research* 25, 3389-3402.

Andersson, D. I. & Hughes, D. (2010). Antibiotic resistance and its cost: is it possible to reverse resistance? *Nature reviews Microbiology* 8, 260-271.

Aoki, S. K., Pamma, R., Hernday, A. D., Bickham, J. E., Braaten, B. A. & Low, D. A. (2005). Contact-dependent inhibition of growth in *Escherichia coli*. *Science* 309, 1245-1248.

Aschtgen, M. S., Bernard, C. S., De Bentzmann, S., Lloubes, R. & Cascales, E. (2008). SciN is an outer membrane lipoprotein required for type VI secretion in enteroaggregative *Escherichia coli*. *Journal of bacteriology* 190, 7523-7531.

Aschtgen, M. S., Thomas, M. S. & Cascales, E. (2010). Anchoring the type VI secretion system to the peptidoglycan: TssL, TagL, TagP... what else? *Virulence* 1, 535-540.

Aschtgen, M. S., Zoued, A., Lloubes, R., Journet, L. & Cascales, E. (2012). The C-tail anchored TssL subunit, an essential protein of the enteroaggregative *Escherichia coli* Sci-1 Type VI secretion system, is inserted by YidC. *MicrobiologyOpen* 1, 71-82.

Bai, R., Friedman, S. J., Pettit, G. R. & Hamel, E. (1992). Dolastatin 15, a potent antimitotic depsipeptide derived from *Dolabella auricularia*. Interaction with tubulin and effects of cellular microtubules. *Biochemical pharmacology* 43, 2637-2645.

Ballister, E. R., Lai, A. H., Zuckermann, R. N., Cheng, Y. & Mougous, J. D. (2008). In vitro self-assembly of tailorable nanotubes from a simple protein building block. *Proceedings of the National Academy of Sciences of the United States of America* 105, 3733-3738.

Basler, M. & Mekalanos, J. J. (2012). Type 6 secretion dynamics within and between bacterial cells. *Science* 337, 815.

Basler, M., Pilhofer, M., Henderson, G. P., Jensen, G. J. & Mekalanos, J. J. (2012). Type VI secretion requires a dynamic contractile phage tail-like structure. *Nature* 483, 182-186.

Basler, M., Ho, B. T. & Mekalanos, J. J. (2013). Tit-for-tat: type VI secretion system counterattack during bacterial cell-cell interactions. *Cell* 152, 884-894.

Beld, J., Sonnenschein, E. C., Vickery, C. R., Noel, J. P. & Burkart, M. D. (2014). The phosphopantetheinyl transferases: catalysis of a post-translational modification crucial for life. *Natural product reports* 31, 61-108.

Benz, J., Sendlmeier, C., Barends, T. R. & Meinhart, A. (2012). Structural insights into the effector-immunity system Tse1/Tsi1 from *Pseudomonas aeruginosa*. *PloS one* 7, e40453.

Bhatty, M., Laverde Gomez, J. A. & Christie, P. J. (2013). The expanding bacterial type IV secretion lexicon. *Research in microbiology* 164, 620-639.

Bibb, M. J., Biro, S., Motamedi, H., Collins, J. F. & Hutchinson, C. R. (1989). Analysis of the nucleotide sequence of the *Streptomyces glaucescens* tcmI genes provides key information about the enzymology of polyketide antibiotic biosynthesis. *The EMBO journal* 8, 2727-2736.

Binnie, C., Warren, M. & Butler, M. J. (1989). Cloning and heterologous expression in *Streptomyces lividans* of *Streptomyces rimosus* genes involved in oxytetracycline biosynthesis. *Journal of bacteriology* 171, 887-895.

Bischoff, D., Bister, B., Bertazzo, M. & other authors (2005). The biosynthesis of vancomycin-type glycopeptide antibiotics--a model for oxidative side-chain cross-linking by oxygenases coupled to the action of peptide synthetases. *Chembiochem : a European journal of chemical biology* 6, 267-272.

Bizio, B. (1823). Lettera di Bartolomeo Bizio al chiarissimo canonico Angelo Bellani sopra il fenomeno della polenta porporina. Bibl. Ital. G. Lett. Sci. Art. *Anno VIII* 30, 275-295.

Bladergroen, M. R., Badelt, K. & Spaink, H. P. (2003). Infection-blocking genes of a symbiotic *Rhizobium leguminosarum* strain that are involved in temperature-dependent protein secretion. *Molecular plant-microbe interactions : MPMI* 16, 53-64.

Blin, K., Medema, M. H., Kazempour, D., Fischbach, M. A., Breitling, R., Takano, E. & Weber, T. (2013). antiSMASH 2.0--a versatile platform for genome mining of secondary metabolite producers. *Nucleic acids research* 41, W204-212.

Blossom, D., Noble-Wang, J., Su, J. & other authors (2009). Multistate outbreak of *Serratia marcescens* bloodstream infections caused by contamination of prefilled heparin and isotonic sodium chloride solution syringes. *Archives of internal medicine* 169, 1705-1711.

Bonemann, G., Pietrosiuk, A., Diemand, A., Zentgraf, H. & Mogk, A. (2009). Remodelling of VipA/VipB tubules by ClpV-mediated threading is crucial for type VI protein secretion. *The EMBO journal* 28, 315-325.

Boyer, F., Fichant, G., Berthod, J., Vandenbrouck, Y. & Attree, I. (2009). Dissecting the bacterial type VI secretion system by a genome wide in silico analysis: what can be learned from available microbial genomic resources? *BMC genomics* 10, 104.

Braun, V., Pramanik, A., Gwinner, T., Koberle, M. & Bohn, E. (2009). Sideromycins: tools and antibiotics. *Biometals : an international journal on the role of metal ions in biology, biochemistry, and medicine* 22, 3-13.

Brunet, Y. R., Espinosa, L., Harchouni, S., Mignot, T. & Cascales, E. (2013). Imaging type VI secretion-mediated bacterial killing. *Cell reports* 3, 36-41.

Brunet, Y. R., Henin, J., Celia, H. & Cascales, E. (2014). Type VI secretion and bacteriophage tail tubes share a common assembly pathway. *EMBO reports* 15, 315-321.

Cane, D. E., Walsh, C. T. & Khosla, C. (1998). Harnessing the biosynthetic code: combinations, permutations, and mutations. *Science* 282, 63-68.

Cardellina, J. H., Marner, F.J., Moore, R.E. (1979). Malyngamide A, a Novel Chlorinated Metabolite of the Marine Cyanophyte Lyngbya-Majuscula. *Journal of the American Chemical Society* 101, 240-242.

Casabona, M. G., Silverman, J. M., Sall, K. M. & other authors (2013). An ABC transporter and an outer membrane lipoprotein participate in posttranslational activation of type VI secretion in *Pseudomonas aeruginosa*. *Environmental microbiology* 15, 471-486.

Chagnot, C., Zorgani, M. A., Astruc, T. & Desvaux, M. (2013). Proteinaceous determinants of surface colonization in bacteria: bacterial adhesion and biofilm formation from a protein secretion perspective. *Frontiers in microbiology* 4, 303.

Challis, G. L., Ravel, J. & Townsend, C. A. (2000). Predictive, structure-based model of amino acid recognition by nonribosomal peptide synthetase adenylation domains. *Chemistry & biology* 7, 211-224.

Chan, Y. A., Boyne, M. T., 2nd, Podevels, A. M., Klimowicz, A. K., Handelsman, J., Kelleher, N. L. & Thomas, M. G. (2006). Hydroxymalonyl-acyl carrier protein (ACP) and aminomalonyl-ACP are two additional type I polyketide synthase extender units. *Proceedings of the National Academy of Sciences of the United States of America* 103, 14349-14354.

Chan, Y. A., Podevels, A. M., Kevany, B. M. & Thomas, M. G. (2009). Biosynthesis of polyketide synthase extender units. *Natural product reports* 26, 90-114.

Chiang, P. C., Wu, T. L., Kuo, A. J., Huang, Y. C., Chung, T. Y., Lin, C. S., Leu, H. S. & Su, L. H. (2013). Outbreak of Serratia marcescens postsurgical bloodstream infection due to contaminated intravenous pain control fluids. *International journal of infectious diseases : IJID : official publication of the International Society for Infectious Diseases* 17, e718-722.

Chirgadze, N. Y., Briggs, S. L., McAllister, K. A., Fischl, A. S. & Zhao, G. (2000). Crystal structure of Streptococcus pneumoniae acyl carrier protein synthase: an essential enzyme in bacterial fatty acid biosynthesis. *The EMBO journal* 19, 5281-5287.

Claverys, J. P. & Havarstein, L. S. (2007). Cannibalism and fratricide: mechanisms and raisons d'etre. *Nature reviews Microbiology* 5, 219-229.

Conti, E., Stachelhaus, T., Marahiel, M. A. & Brick, P. (1997). Structural basis for the activation of phenylalanine in the non-ribosomal biosynthesis of gramicidin S. *The EMBO journal* 16, 4174-4183.

Copp, J. N. & Neilan, B. A. (2006). The phosphopantetheinyl transferase superfamily: phylogenetic analysis and functional implications in cyanobacteria. *Applied and environmental microbiology* 72, 2298-2305.

Coria-Jimenez, R. & Ortiz-Torres, C. (1994). Aminoglycoside resistance patterns of *Serratia marcescens* strains of clinical origin. *Epidemiology and infection* 112, 125-131.

Corsini, G., Karahanian, E., Tello, M., Fernandez, K., Rivero, D., Saavedra, J. M. & Ferrer, A. (2010). Purification and characterization of the antimicrobial peptide microcin N. *FEMS microbiology letters* 312, 119-125.

Cortina, N. S., Revermann, O., Krug, D. & Muller, R. (2011). Identification and characterization of the althiomycin biosynthetic gene cluster in *Myxococcus xanthus* DK897. *Chembiochem : a European journal of chemical biology* 12, 1411-1416.

Cotter, P. D., Ross, R. P. & Hill, C. (2013). Bacteriocins - a viable alternative to antibiotics? *Nature reviews Microbiology* 11, 95-105.

Coulthurst, S. J. (2013). The Type VI secretion system - a widespread and versatile cell targeting system. *Research in microbiology* 164, 640-654.

Crosa, J. H. & Walsh, C. T. (2002). Genetics and assembly line enzymology of siderophore biosynthesis in bacteria. *Microbiology and molecular biology reviews : MMBR* 66, 223-249.

Davies, J. (2006). Are antibiotics naturally antibiotics? *Journal of industrial microbiology & biotechnology* 33, 496-499.

Delalez, N. J., Wadhams, G. H., Rosser, G., Xue, Q., Brown, M. T., Dobbie, I. M., Berry, R. M., Leake, M. C. & Armitage, J. P. (2010). Signal-dependent turnover of the bacterial flagellar switch protein FliM. *Proceedings of the National Academy of Sciences of the United States of America* 107, 11347-11351.

Dias, C., Goncalves, M. & Joao, A. (2013). Epidemiological study of hospital-acquired bacterial conjunctivitis in a level III neonatal unit. *TheScientificWorldJournal* 2013, 163582.

Dickenson, N. E. & Picking, W. D. (2012). Forster resonance energy transfer (FRET) as a tool for dissecting the molecular mechanisms for maturation of the *Shigella* type III secretion needle tip complex. *International journal of molecular sciences* 13, 15137-15161.

Diepold, A., Amstutz, M., Abel, S., Sorg, I., Jenal, U. & Cornelis, G. R. (2010). Deciphering the assembly of the *Yersinia* type III secretion injectisome. *The EMBO journal* 29, 1928-1940.

Donadio, S., Staver, M. J., McAlpine, J. B., Swanson, S. J. & Katz, L. (1991). Modular organization of genes required for complex polyketide biosynthesis. *Science* 252, 675-679.

Dong, T. G., Ho, B. T., Yoder-Himes, D. R. & Mekalanos, J. J. (2013). Identification of T6SS-dependent effector and immunity proteins by Tn-seq in *Vibrio cholerae*. *Proceedings of the National Academy of Sciences of the United States of America* 110, 2623-2628.

Du, L., Sanchez, C., Chen, M., Edwards, D. J. & Shen, B. (2000). The biosynthetic gene cluster for the antitumor drug bleomycin from *Streptomyces verticillus* ATCC15003 supporting functional interactions between nonribosomal peptide synthetases and a polyketide synthase. *Chemistry & biology* 7, 623-642.

El-Sayed, A. K., Hothersall, J., Cooper, S. M., Stephens, E., Simpson, T. J. & Thomas, C. M. (2003). Characterization of the mupirocin biosynthesis gene cluster from *Pseudomonas fluorescens* NCIMB 10586. *Chemistry & biology* 10, 419-430.

Elovson, J. & Vagelos, P. R. (1968). Acyl carrier protein. X. Acyl carrier protein synthetase. *The Journal of biological chemistry* 243, 3603-3611.

English, G., Trunk, K., Rao, V. A., Srikannathasan, V., Hunter, W. N. & Coulthurst, S. J. (2012). New secreted toxins and immunity proteins encoded within the Type VI secretion system gene cluster of *Serratia marcescens*. *Molecular microbiology* 86, 921-936.

English, G., Byron, O., Cianfanelli, F. R., Prescott, A. R. & Coulthurst, S. J. (2014). Biochemical analysis of TssK, a core component of the bacterial Type VI secretion system, reveals distinct oligomeric states of TssK and identifies a TssK-TssFG sub-complex. *The Biochemical journal*.

Eppelmann, K., Stachelhaus, T. & Marahiel, M. A. (2002). Exploitation of the selectivity-conferring code of nonribosomal peptide synthetases for the rational design of novel peptide antibiotics. *Biochemistry* 41, 9718-9726.

Fajardo, A. & Martinez, J. L. (2008). Antibiotics as signals that trigger specific bacterial responses. *Current opinion in microbiology* 11, 161-167.

Felisberto-Rodrigues, C., Durand, E., Aschtgen, M. S., Blangy, S., Ortiz-Lombardia, M., Douzi, B., Cambillau, C. & Cascales, E. (2011). Towards a structural comprehension of bacterial type VI secretion systems: characterization of the TssJ-TssM complex of an *Escherichia coli* pathovar. *PLoS pathogens* 7, e1002386.

Fichtlscherer, F., Wellein, C., Mittag, M. & Schweizer, E. (2000). A novel function of yeast fatty acid synthase. Subunit alpha is capable of self-pantetheinylation. *European journal of biochemistry / FEBS* 267, 2666-2671.

Filloux, A. (2013). The rise of the Type VI secretion system. *F1000prime reports* 5, 52.

Finking, R. & Marahiel, M. A. (2004). Biosynthesis of nonribosomal peptides. *Annual review of microbiology* 58, 453-488.

Fischbach, M. A. & Walsh, C. T. (2006). Assembly-line enzymology for polyketide and nonribosomal Peptide antibiotics: logic, machinery, and mechanisms. *Chemical reviews* 106, 3468-3496.

Flemming, H. C. & Wingender, J. (2010). The biofilm matrix. *Nature reviews Microbiology* 8, 623-633.

Fluman, N. & Bibi, E. (2009). Bacterial multidrug transport through the lens of the major facilitator superfamily. *Biochimica et biophysica acta* 1794, 738-747.

Flyg, C., Kenne, K. & Boman, H. G. (1980). Insect pathogenic properties of *Serratia marcescens*: phage-resistant mutants with a decreased resistance to Cecropia immunity and a decreased virulence to Drosophila. *Journal of general microbiology* 120, 173-181.

Folkesson, A., Lofdahl, S. & Normark, S. (2002). The *Salmonella enterica* subspecies I specific centisome 7 genomic island encodes novel protein families present in bacteria living in close contact with eukaryotic cells. *Research in microbiology* 153, 537-545.

Fritsch, M. J., Trunk, K., Diniz, J. A., Guo, M., Trost, M. & Coulthurst, S. J. (2013). Proteomic identification of novel secreted antibacterial toxins of the *Serratia marcescens* type VI secretion system. *Molecular & cellular proteomics : MCP* 12, 2735-2749.

Fronzes, R., Christie, P. J. & Waksman, G. (2009). The structural biology of type IV secretion systems. *Nature reviews Microbiology* 7, 703-714.

Fujimoto, H., Kinoshita, T., Suzuki, H. & Umezawa, H. (1970). Studies on the mode of action of althiomycin. *The Journal of antibiotics* 23, 271-275.

Gawarzewski, I., Smits, S. H., Schmitt, L. & Jose, J. (2013). Structural comparison of the transport units of type V secretion systems. *Biological chemistry* 394, 1385-1398.

Gehring, A. M., Mori, I. & Walsh, C. T. (1998). Reconstitution and characterization of the *Escherichia coli* enterobactin synthetase from EntB, EntE, and EntF. *Biochemistry* 37, 2648-2659.

Gerc, A. J., Song, L., Challis, G. L., Stanley-Wall, N. R. & Coulthurst, S. J. (2012). The insect pathogen Serratia marcescens Db10 uses a hybrid non-ribosomal peptide synthetase-polyketide synthase to produce the antibiotic althiomycin. PloS one 7, e44673.

Gerlach, R. G. & Hensel, M. (2007). Protein secretion systems and adhesins: the molecular armory of Gram-negative pathogens. *International journal of medical microbiology : IJMM* 297, 401-415.

Giessen, T. W. & Marahiel, M. A. (2012). Ribosome-independent biosynthesis of biologically active peptides: Application of synthetic biology to generate structural diversity. *FEBS letters* 586, 2065-2075.

Goh, E. B., Yim, G., Tsui, W., McClure, J., Surette, M. G. & Davies, J. (2002). Transcriptional modulation of bacterial gene expression by subinhibitory concentrations of antibiotics.

Proceedings of the National Academy of Sciences of the United States of America 99, 17025-17030.

Gonzalez-Pastor, J. E., Hobbs, E. C. & Losick, R. (2003). Cannibalism by sporulating bacteria. *Science* 301, 510-513.

Gwynn, M. N., Portnoy, A., Rittenhouse, S. F. & Payne, D. J. (2010). Challenges of antibacterial discovery revisited. *Annals of the New York Academy of Sciences* 1213, 5-19.

Hachani, A., Allsopp, L. P., Oduko, Y. & Filloux, A. (2014). The VgrG proteins are "A la carte" delivery systems for bacterial type VI effectors. *The Journal of biological chemistry*.

Haddy, R. I., Mann, B. L., Nadkarni, D. D., Cruz, R. F., Elshoff, D. J., Buendia, F. C., Domers, T. A. & Oberheu, A. M. (1996). Nosocomial infection in the community hospital: severe infection due to *Serratia* species. *The Journal of family practice* 42, 273-277.

Hammami, R., Fernandez, B., Lacroix, C. & Fliss, I. (2013). Anti-infective properties of bacteriocins: an update. *Cellular and molecular life sciences : CMLS* 70, 2947-2967.

Haydock, S. F., Aparicio, J. F., Molnar, I. & other authors (1995). Divergent sequence motifs correlated with the substrate specificity of (methyl)malonyl-CoA:acyl carrier protein transacylase domains in modular polyketide synthases. *FEBS letters* 374, 246-248.

Hejazi, A. & Falkiner, F. R. (1997). *Serratia marcescens*. *Journal of medical microbiology* 46, 903-912.

Hertweck, C. (2009). The biosynthetic logic of polyketide diversity. *Angewandte Chemie* 48, 4688-4716.

Ho, B. T., Basler, M. & Mekalanos, J. J. (2013). Type 6 secretion system-mediated immunity to type 4 secretion system-mediated gene transfer. *Science* 342, 250-253.

Ho, B. T., Dong, T. G. & Mekalanos, J. J. (2014). A view to a kill: the bacterial type VI secretion system. *Cell host & microbe* 15, 9-21.

Hollis, A. & Ahmed, Z. (2013). Preserving antibiotics, rationally. *The New England journal of medicine* 369, 2474-2476.

Hood, R. D., Singh, P., Hsu, F. & other authors (2010). A type VI secretion system of *Pseudomonas aeruginosa* targets a toxin to bacteria. *Cell host & microbe* 7, 25-37.

Hopwood, D. A. (2007). How do antibiotic-producing bacteria ensure their self-resistance before antibiotic biosynthesis incapacitates them? *Molecular microbiology* 63, 937-940.

Hsu, F., Schwarz, S. & Mougous, J. D. (2009). TagR promotes PpkA-catalysed type VI secretion activation in *Pseudomonas aeruginosa*. *Molecular microbiology* 72, 1111-1125.

Inami, K. & Shiba, T. (1985). Total Synthesis of Antibiotic Althiomycin. *B Chem Soc Jpn* 58, 352-360.

Izore, T., Job, V. & Dessen, A. (2011). Biogenesis, regulation, and targeting of the type III secretion system. *Structure* 19, 603-612.

Jiang, F., Waterfield, N. R., Yang, J., Yang, G. & Jin, Q. (2014). A *Pseudomonas aeruginosa* Type VI Secretion Phospholipase D Effector Targets Both Prokaryotic and Eukaryotic Cells. *Cell host & microbe* 15, 600-610.

Joshi, A. K., Zhang, L., Rangan, V. S. & Smith, S. (2003). Cloning, expression, and characterization of a human 4'-phosphopantetheinyl transferase with broad substrate specificity. *The Journal of biological chemistry* 278, 33142-33149.

Kadouri, D. E. & Shanks, R. M. (2013). Identification of a methicillin-resistant *Staphylococcus aureus* inhibitory compound isolated from Serratia marcescens. *Research in microbiology* 164, 821-826.

Kanonenberg, K., Schwarz, C. K. & Schmitt, L. (2013). Type I secretion systems - a story of appendices. *Research in microbiology* 164, 596-604.

Kapitein, N., Bonemann, G., Pietrosiuk, A., Seyffer, F., Hausser, I., Locker, J. K. & Mogk, A. (2013). ClpV recycles VipA/VipB tubules and prevents non-productive tubule formation to ensure efficient type VI protein secretion. *Molecular microbiology* 87, 1013-1028.

Katz, L. (1997). Manipulation of Modular Polyketide Synthases. *Chemical reviews* 97, 2557-2576.

Keating, T. A. & Walsh, C. T. (1999). Initiation, elongation, and termination strategies in polyketide and polypeptide antibiotic biosynthesis. *Current opinion in chemical biology* 3, 598-606.

Korner, R. J., Nicol, A., Reeves, D. S., MacGowan, A. P. & Hows, J. (1994). Ciprofloxacin resistant *Serratia marcescens* endocarditis as a complication of non-Hodgkin's lymphoma. *The Journal of infection* 29, 73-76.

Krebs, C., Matthews, M. L., Jiang, W. & Bollinger, J. M., Jr. (2007). AurF from *Streptomyces thioluteus* and a possible new family of manganese/iron oxygenases. *Biochemistry* 46, 10413-10418.

Kunze, B., Reichenbach, H., Augustiniak, H. & Hofle, G. (1982). Isolation and identification of althiomycin from *Cystobacter fuscus* (myxobacterales). *The Journal of antibiotics* 35, 635-636.

Lambalot, R. H. & Walsh, C. T. (1995). Cloning, overproduction, and characterization of the *Escherichia coli* holo-acyl carrier protein synthase. *The Journal of biological chemistry* 270, 24658-24661.

Lambalot, R. H., Gehring, A. M., Flugel, R. S., Zuber, P., LaCelle, M., Marahiel, M. A., Reid, R., Khosla, C. & Walsh, C. T. (1996). A new enzyme superfamily - the phosphopantetheinyl transferases. *Chemistry & biology* 3, 923-936.

Leo, J. C., Grin, I. & Linke, D. (2012). Type V secretion: mechanism(s) of autotransport through the bacterial outer membrane. *Philosophical transactions of the Royal Society of London Series B, Biological sciences* 367, 1088-1101.

LeRoux, M., De Leon, J. A., Kuwada, N. J. & other authors (2012). Quantitative single-cell characterization of bacterial interactions reveals type VI secretion is a double-edged sword.

Proceedings of the National Academy of Sciences of the United States of America 109, 19804-19809.

Lossi, N. S., Dajani, R., Freemont, P. & Filloux, A. (2011). Structure-function analysis of HsiF, a gp25-like component of the type VI secretion system, in *Pseudomonas aeruginosa*. *Microbiology* 157, 3292-3305.

Lossi, N. S., Manoli, E., Forster, A., Dajani, R., Pape, T., Freemont, P. & Filloux, A. (2013). The HsiB1C1 (TssB-TssC) complex of the *Pseudomonas aeruginosa* type VI secretion system forms a bacteriophage tail sheathlike structure. *The Journal of biological chemistry* 288, 7536-7548.

Ma, A. T., McAuley, S., Pukatzki, S. & Mekalanos, J. J. (2009a). Translocation of a *Vibrio cholerae* type VI secretion effector requires bacterial endocytosis by host cells. *Cell host & microbe* 5, 234-243.

Ma, L. S., Lin, J. S. & Lai, E. M. (2009b). An IcmF family protein, ImpLM, is an integral inner membrane protein interacting with ImpKL, and its walker a motif is required for type VI secretion system-mediated Hcp secretion in *Agrobacterium tumefaciens*. *Journal of bacteriology* 191, 4316-4329.

Mahlen, S. D. (2011). Serratia infections: from military experiments to current practice. *Clinical microbiology reviews* 24, 755-791.

Mak, S., Xu, Y. & Nodwell, J. R. (2014). The expression of antibiotic resistance genes in antibiotic-producing bacteria. *Molecular microbiology*.

Manfredi, R., Nanetti, A., Ferri, M. & Chiodo, F. (2000). Clinical and microbiological survey of *Serratia marcescens* infection during HIV disease. *European journal of clinical microbiology & infectious diseases : official publication of the European Society of Clinical Microbiology* 19, 248-253.

Matsuyama, T. T., T. Nakagawa, Y. (2011). Serrawettins and Other Surfactants Produced by Serratia. *Microbiology Monographs* 20, 93-120.

McDaniel, R., Thamchaipenet, A., Gustafsson, C., Fu, H., Betlach, M. & Ashley, G. (1999). Multiple genetic modifications of the erythromycin polyketide synthase to produce a library of

novel "unnatural" natural products. *Proceedings of the National Academy of Sciences of the United States of America* 96, 1846-1851.

Middleton, R. & Hofmeister, A. (2004). New shuttle vectors for ectopic insertion of genes into Bacillus subtilis. *Plasmid* 51, 238-245.

Mingeot-Leclercq, M. P., Glupczynski, Y. & Tulkens, P. M. (1999). Aminoglycosides: activity and resistance. *Antimicrobial agents and chemotherapy* 43, 727-737.

Miyata, S. T., Kitaoka, M., Brooks, T. M., McAuley, S. B. & Pukatzki, S. (2011). *Vibrio cholerae* requires the type VI secretion system virulence factor VasX to kill Dictyostelium discoideum. *Infection and immunity* 79, 2941-2949.

Moore, B. S. & Hertweck, C. (2002). Biosynthesis and attachment of novel bacterial polyketide synthase starter units. *Natural product reports* 19, 70-99.

Mootz, H. D., Finking, R. & Marahiel, M. A. (2001). 4'-phosphopantetheine transfer in primary and secondary metabolism of *Bacillus subtilis*. *The Journal of biological chemistry* 276, 37289-37298.

Mootz, H. D., Schwarzer, D. & Marahiel, M. A. (2002). Ways of assembling complex natural products on modular nonribosomal peptide synthetases. *Chembiochem : a European journal of chemical biology* 3, 490-504.

Mougous, J. D., Cuff, M. E., Raunser, S. & other authors (2006). A virulence locus of *Pseudomonas aeruginosa* encodes a protein secretion apparatus. *Science* 312, 1526-1530.

Mougous, J. D., Gifford, C. A., Ramsdell, T. L. & Mekalanos, J. J. (2007). Threonine phosphorylation post-translationally regulates protein secretion in *Pseudomonas aeruginosa*. *Nature cell biology* 9, 797-803.

Murdoch, S. L., Trunk, K., English, G., Fritsch, M. J., Pourkarimi, E. & Coulthurst, S. J. (2011). The opportunistic pathogen *Serratia marcescens* utilizes type VI secretion to target bacterial competitors. *Journal of bacteriology* 193, 6057-6069.

Murugan, E. & Liang, Z. X. (2008). Evidence for a novel phosphopantetheinyl transferase domain in the polyketide synthase for enediyne biosynthesis. *FEBS letters* 582, 1097-1103.

Nano, F. E., Zhang, N., Cowley, S. C. & other authors (2004). A *Francisella tularensis* pathogenicity island required for intramacrophage growth. *Journal of bacteriology* 186, 6430-6436.

Ng, W. L. & Bassler, B. L. (2009). Bacterial quorum-sensing network architectures. *Annual review of genetics* 43, 197-222.

Nikaido, H. (1994). Prevention of drug access to bacterial targets: permeability barriers and active efflux. *Science* 264, 382-388.

Nishie, M., Nagao, J. & Sonomoto, K. (2012). Antibacterial peptides "bacteriocins": an overview of their diverse characteristics and applications. *Biocontrol science* 17, 1-16.

Nivaskumar, M. & Francetic, O. (2014). Type II secretion system: A magic beanstalk or a protein escalator. *Biochimica et biophysica acta*.

Paik, S. G., Carmeli, S., Cullingham, J., Moore, R.E., Patterson, G.M.L., Tius, M. A. (1994). Mirabimide-E, an Unusual N-Acylpyrrolinone from the Blue-Green-Alga Scytonema Mirabile - Structure Determination and Synthesis. *Journal of the American Chemical Society* 116, 8116-8125.

Parris, K. D., Lin, L., Tam, A., Mathew, R., Hixon, J., Stahl, M., Fritz, C. C., Seehra, J. & Somers, W. S. (2000). Crystal structures of substrate binding to *Bacillus subtilis* holo-(acyl carrier protein) synthase reveal a novel trimeric arrangement of molecules resulting in three active sites. *Structure* 8, 883-895.

Pell, L. G., Kanelis, V., Donaldson, L. W., Howell, P. L. & Davidson, A. R. (2009). The phage lambda major tail protein structure reveals a common evolution for long-tailed phages and the type VI bacterial secretion system. *Proceedings of the National Academy of Sciences of the United States of America* 106, 4160-4165.

Persmark, M., Expert, D. & Neilands, J. B. (1989). Isolation, characterization, and synthesis of chrysobactin, a compound with siderophore activity from *Erwinia chrysanthemi*. *The Journal of biological chemistry* 264, 3187-3193.

Poole, K. (2012). Bacterial stress responses as determinants of antimicrobial resistance. *The Journal of antimicrobial chemotherapy* 67, 2069-2089.

Pradel, E., Zhang, Y., Pujol, N., Matsuyama, T., Bargmann, C. I. & Ewbank, J. J. (2007). Detection and avoidance of a natural product from the pathogenic bacterium *Serratia marcescens* by *Caenorhabditis elegans*. *Proceedings of the National Academy of Sciences of the United States of America* 104, 2295-2300.

Pukatzki, S., Ma, A. T., Sturtevant, D., Krastins, B., Sarracino, D., Nelson, W. C., Heidelberg, J. F. & Mekalanos, J. J. (2006). Identification of a conserved bacterial protein secretion system in *Vibrio cholerae* using the *Dictyostelium* host model system. *Proceedings of the National Academy of Sciences of the United States of America* 103, 1528-1533.

Pukatzki, S., Ma, A. T., Revel, A. T., Sturtevant, D. & Mekalanos, J. J. (2007). Type VI secretion system translocates a phage tail spike-like protein into target cells where it cross-links actin. *Proceedings of the National Academy of Sciences of the United States of America* 104, 15508-15513.

Pukatzki, S., McAuley, S. B. & Miyata, S. T. (2009). The type VI secretion system: translocation of effectors and effector-domains. *Current opinion in microbiology* 12, 11-17.

Quadri, L. E., Weinreb, P. H., Lei, M., Nakano, M. M., Zuber, P. & Walsh, C. T. (1998). Characterization of Sfp, a Bacillus subtilis phosphopantetheinyl transferase for peptidyl carrier protein domains in peptide synthetases. *Biochemistry* 37, 1585-1595.

Rao, P. S., Yamada, Y., Tan, Y. P. & Leung, K. Y. (2004). Use of proteomics to identify novel virulence determinants that are required for Edwardsiella tarda pathogenesis. *Molecular microbiology* 53, 573-586.

Raymond, K. N., Dertz, E. A. & Kim, S. S. (2003). Enterobactin: an archetype for microbial iron transport. *Proceedings of the National Academy of Sciences of the United States of America* 100, 3584-3588.

Rebuffat, S. (2012). Microcins in action: amazing defence strategies of Enterobacteria. *Biochemical Society transactions* 40, 1456-1462.

Records, A. R. (2011). The type VI secretion system: a multipurpose delivery system with a phage-like machinery. *Molecular plant-microbe interactions : MPMI* 24, 751-757.

Reuter, K., Mofid, M. R., Marahiel, M. A. & Ficner, R. (1999). Crystal structure of the surfactin synthetase-activating enzyme sfp: a prototype of the 4'-phosphopantetheinyl transferase superfamily. *The EMBO journal* 18, 6823-6831.

Riley, M. A. & Wertz, J. E. (2002). Bacteriocin diversity: ecological and evolutionary perspectives. *Biochimie* 84, 357-364.

Roest, H. P., Mulders, I. H., Spaink, H. P., Wijffelman, C. A. & Lugtenberg, B. J. (1997). A *Rhizobium leguminosarum* biovar trifolii locus not localized on the sym plasmid hinders effective nodulation on plants of the pea cross-inoculation group. *Molecular plant-microbe interactions : MPMI* 10, 938-941.

Ruhe, Z. C., Low, D. A. & Hayes, C. S. (2013). Bacterial contact-dependent growth inhibition. *Trends in microbiology* 21, 230-237.

Russell, A. B., Hood, R. D., Bui, N. K., LeRoux, M., Vollmer, W. & Mougous, J. D. (2011). Type VI secretion delivers bacteriolytic effectors to target cells. *Nature* 475, 343-347.

Russell, A. B., Singh, P., Brittnacher, M. & other authors (2012). A widespread bacterial type VI secretion effector superfamily identified using a heuristic approach. *Cell host & microbe* 11, 538-549.

Russell, A. B., LeRoux, M., Hathazi, K., Agnello, D. M., Ishikawa, T., Wiggins, P. A., Wai, S. N. & Mougous, J. D. (2013). Diverse type VI secretion phospholipases are functionally plastic antibacterial effectors. *Nature* 496, 508-512.

Sadar, M. D., Williams, D. E., Mawji, N. R., Patrick, B. O., Wikanta, T., Chasanah, E., Irianto, H. E., Soest, R. V. & Andersen, R. J. (2008). Sintokamides A to E, chlorinated peptides from the sponge *Dysidea* sp. that inhibit transactivation of the N-terminus of the androgen receptor in prostate cancer cells. *Organic letters* 10, 4947-4950.

Sakakibara, H., Naganawa, H., Ono, M., Maeda, K. & Umezawa, H. (1974). The structure of althiomycin. *The Journal of antibiotics* 27, 897-899.

Salomon, D., Gonzalez, H., Updegraff, B. L. & Orth, K. (2013). *Vibrio parahaemolyticus* type VI secretion system 1 is activated in marine conditions to target bacteria, and is differentially regulated from system 2. *PloS one* 8, e61086.

Scholz-Schroeder, B. K., Soule, J. D. & Gross, D. C. (2003). The sypA, sypS, and sypC synthetase genes encode twenty-two modules involved in the nonribosomal peptide synthesis of syringopeptin by *Pseudomonas syringae* pv. syringae B301D. *Molecular plant-microbe interactions : MPMI* 16, 271-280.

Schwarz, S., West, T. E., Boyer, F. & other authors (2010). *Burkholderia* type VI secretion systems have distinct roles in eukaryotic and bacterial cell interactions. *PLoS pathogens* 6, e1001068.

Schwarzer, D. & Marahiel, M. A. (2001). Multimodular biocatalysts for natural product assembly. *Die Naturwissenschaften* 88, 93-101.

Schwecke, T., Aparicio, J. F., Molnar, I. & other authors (1995). The biosynthetic gene cluster for the polyketide immunosuppressant rapamycin. *Proceedings of the National Academy of Sciences of the United States of America* 92, 7839-7843.

Schwyn, B. & Neilands, J. B. (1987). Universal chemical assay for the detection and determination of siderophores. *Analytical biochemistry* 160, 47-56.

Seyedsayamdost, M. R., Cleto, S., Carr, G., Vlamakis, H., Joao Vieira, M., Kolter, R. & Clardy, J. (2012). Mixing and matching siderophore clusters: structure and biosynthesis of serratiochelins from *Serratia* sp. V4. *J Am Chem Soc* 134, 13550-13553.

Shalom, G., Shaw, J. G. & Thomas, M. S. (2007). In vivo expression technology identifies a type VI secretion system locus in *Burkholderia pseudomallei* that is induced upon invasion of macrophages. *Microbiology* 153, 2689-2699.

Shneider, M. M., Buth, S. A., Ho, B. T., Basler, M., Mekalanos, J. J. & Leiman, P. G. (2013). PAAR-repeat proteins sharpen and diversify the type VI secretion system spike. *Nature* 500, 350-353.

Silver, L. L. (2011). Challenges of antibacterial discovery. *Clinical microbiology reviews* 24, 71-109.

Silverman, J. M., Agnello, D. M., Zheng, H., Andrews, B. T., Li, M., Catalano, C. E., Gonen, T. & Mougous, J. D. (2013). Haemolysin coregulated protein is an exported receptor and chaperone of type VI secretion substrates. *Molecular cell* 51, 584-593.

Singh, P. & Cameotra, S. S. (2004). Potential applications of microbial surfactants in biomedical sciences. *Trends in biotechnology* 22, 142-146.

Sleigh, J. D. (1983). Antibiotic resistance in *Serratia marcescens*. *British medical journal* 287, 1651-1653.

Srikannathasan, V., English, G., Bui, N. K., Trunk, K., O'Rourke, P. E., Rao, V. A., Vollmer, W., Coulthurst, S. J. & Hunter, W. N. (2013). Structural basis for type VI secreted peptidoglycan DL-endopeptidase function, specificity and neutralization in Serratia marcescens. *Acta crystallographica Section D, Biological crystallography* 69, 2468-2482.

Stachelhaus, T., Huser, A. & Marahiel, M. A. (1996). Biochemical characterization of peptidyl carrier protein (PCP), the thiolation domain of multifunctional peptide synthetases. *Chemistry & biology* 3, 913-921.

Stachelhaus, T., Mootz, H. D., Bergendahl, V. & Marahiel, M. A. (1998). Peptide bond formation in nonribosomal peptide biosynthesis. Catalytic role of the condensation domain. *The Journal of biological chemistry* 273, 22773-22781.

Stachelhaus, T., Mootz, H. D. & Marahiel, M. A. (1999). The specificity-conferring code of adenylation domains in nonribosomal peptide synthetases. *Chemistry & biology* 6, 493-505.

Staunton, J. & Wilkinson, B. (1997). Biosynthesis of Erythromycin and Rapamycin. *Chemical reviews* 97, 2611-2630.

Strickland, K. C., Hoeferlin, L. A., Oleinik, N. V., Krupenko, N. I. & Krupenko, S. A. (2010). Acyl carrier protein-specific 4'-phosphopantetheinyl transferase activates 10-formyltetrahydrofolate dehydrogenase. *The Journal of biological chemistry* 285, 1627-1633.

Su, L. H., Ou, J. T., Leu, H. S. & other authors (2003). Extended epidemic of nosocomial urinary tract infections caused by *Serratia marcescens*. *Journal of clinical microbiology* 41, 4726-4732.

Suarez, G., Sierra, J. C., Erova, T. E., Sha, J., Horneman, A. J. & Chopra, A. K. (2010). A type VI secretion system effector protein, VgrG1, from *Aeromonas hydrophila* that induces host cell toxicity by ADP ribosylation of actin. *Journal of bacteriology* 192, 155-168.

Sunaga, S., Li, H., Sato, Y., Nakagawa, Y. & Matsuyama, T. (2004). Identification and characterization of the *pswP* gene required for the parallel production of prodigiosin and serrawettin W1 in *Serratia marcescens*. *Microbiology and immunology* 48, 723-728.

Thirlway, J., Lewis, R., Nunns, L., Al Nakeeb, M., Styles, M., Struck, A. W., Smith, C. P. & Micklefield, J. (2012). Introduction of a non-natural amino acid into a nonribosomal peptide antibiotic by modification of adenylation domain specificity. *Angewandte Chemie* 51, 7181-7184.

Thomson, N. R., Crow, M. A., McGowan, S. J., Cox, A. & Salmond, G. P. (2000). Biosynthesis of carbapenem antibiotic and prodigiosin pigment in *Serratia* is under quorum sensing control. *Molecular microbiology* 36, 539-556.

Toesca, I. J., French, C. T. & Miller, J. F. (2014). The Type VI secretion system spike protein VgrG5 mediates membrane fusion during intercellular spread by *pseudomallei* group *Burkholderia* species. *Infection and immunity* 82, 1436-1444.

Trokter, M., Felisberto-Rodrigues, C., Christie, P. J. & Waksman, G. (2014). Recent advances in the structural and molecular biology of type IV secretion systems. *Current opinion in structural biology* 27C, 16-23.

Tseng, C. C., Bruner, S. D., Kohli, R. M., Marahiel, M. A., Walsh, C. T. & Sieber, S. A. (2002). Characterization of the surfactin synthetase C-terminal thioesterase domain as a cyclic depsipeptide synthase. *Biochemistry* 41, 13350-13359.

Voelz, A., Muller, A., Gillen, J., Le, C., Dresbach, T., Engelhart, S., Exner, M., Bates, C. J. & Simon, A. (2010). Outbreaks of *Serratia marcescens* in neonatal and pediatric intensive care units: clinical aspects, risk factors and management. *International journal of hygiene and environmental health* 213, 79-87.

Vogel, J. & Luisi, B. F. (2011). Hfq and its constellation of RNA. *Nature reviews Microbiology* 9, 578-589.

Walsh, C. T., Gehring, A. M., Weinreb, P. H., Quadri, L. E. & Flugel, R. S. (1997). Post-translational modification of polyketide and nonribosomal peptide synthases. *Current opinion in chemical biology* 1, 309-315.

Walsh, C. T. & Fischbach, M. A. (2010). Natural products version 2.0: connecting genes to molecules. *J Am Chem Soc* 132, 2469-2493.

Wang, W. L., Chi, Z. M., Chi, Z., Li, J. & Wang, X. H. (2009). Siderophore production by the marine-derived *Aureobasidium pullulans* and its antimicrobial activity. *Bioresource technology* 100, 2639-2641.

Weissman, K. J., Hong, H., Oliynyk, M., Siskos, A. P. & Leadlay, P. F. (2004). Identification of a phosphopantetheinyl transferase for erythromycin biosynthesis in *Saccharopolyspora erythraea*. *Chembiochem : a European journal of chemical biology* 5, 116-125.

Weissman, K. J. & Muller, R. (2008). Protein-protein interactions in multienzyme megasynthetases. *Chembiochem : a European journal of chemical biology* 9, 826-848.

Whitney, J. C., Chou, S., Russell, A. B., Biboy, J., Gardiner, T. E., Ferrin, M. A., Brittnacher, M., Vollmer, W. & Mougous, J. D. (2013). Identification, structure, and function of a novel type VI secretion peptidoglycan glycoside hydrolase effector-immunity pair. *The Journal of biological chemistry* 288, 26616-26624.

WHO (2011). Disease and injury regional mortality estimates for 2000-2011. *World Health Organisation*.

WHO (2014). Antimicrobial resistance: global report on surveillance 2014. *World Health Organisation*.

Williams, G. J. (2013). Engineering polyketide synthases and nonribosomal peptide synthetases. *Current opinion in structural biology* 23, 603-612.

Williams, R. P. (1973). Biosynthesis of prodigiosin, a secondary metabolite of *Serratia marcescens*. *Applied microbiology* 25, 396-402.

Wu, N., Cane, D. E. & Khosla, C. (2002). Quantitative analysis of the relative contributions of donor acyl carrier proteins, acceptor ketosynthases, and linker regions to intermodular transfer of intermediates in hybrid polyketide synthases. *Biochemistry* 41, 5056-5066.

Yap, M. N. (2013). The double life of antibiotics. *Missouri medicine* 110, 320-324.

Yu, D., Xu, F., Zeng, J. & Zhan, J. (2012). Type III polyketide synthases in natural product biosynthesis. *IUBMB life* 64, 285-295.

Zarantonello, P., Leslie, C. P., Ferritto, R. & Kazmierski, W. M. (2002). Total synthesis and semi-synthetic approaches to analogues of antibacterial natural product althiomycin. *Bioorganic & medicinal chemistry letters* 12, 561-565.

Zheng, J. & Leung, K. Y. (2007). Dissection of a type VI secretion system in *Edwardsiella tarda*. *Molecular microbiology* 66, 1192-1206.

Zoued, A., Durand, E., Bebeacua, C., Brunet, Y. R., Douzi, B., Cambillau, C., Cascales, E. & Journet, L. (2013). TssK is a trimeric cytoplasmic protein interacting with components of both phage-like and membrane anchoring complexes of the type VI secretion system. *The Journal of biological chemistry* 288, 27031-27041.

Zoued, A., Brunet, Y. R., Durand, E., Aschtgen, M. S., Logger, L., Douzi, B., Journet, L., Cambillau, C. & Cascales, E. (2014). Architecture and assembly of the Type VI secretion system. *Biochimica et biophysica acta*.

Publications